Saline Water Conversion—II

Based on symposia
sponsored by the Division of
Water and Waste Chemistry
at the 139th and 141st Meetings
of the American Chemical Society
March 27, 1961 and March 27–8, 1962

ADVANCES IN CHEMISTRY SERIES 38

AMERICAN CHEMICAL SOCIETY
WASHINGTON, D. C. 1963

Library of Congress Catalog Card 60–53480

PRINTED IN THE UNITED STATES OF AMERICA

Advances in Chemistry Series

Robert F. Gould, *Editor*

AMERICAN CHEMICAL SOCIETY

APPLIED PUBLICATIONS

PREFACE

By the year 2000, the population of the United States will have about doubled. At the same time, the standard of living will have risen, with an accompanying increase of both industrial and agricultural activities. At the present time, the nation requires about 300 billion gallons of water daily; in only 20 years, the requirement may exceed 600 billion gallons per day. There is a serious question as to whether that much can be made available readily from conventional fresh water sources. The conversion of salt water to fresh water is a way to virtually unlimited new supplies and a way to supplement other sources.

Many groups and organizations in the United States, governmental and otherwise, are interested in saline water conversion research and development. The State of California has a sea water conversion project, with the research being carried out at the University of California. Other federal agencies having particular interest in saline water conversion include the Department of Defense, the Atomic Energy Commission, and the Office of Emergency Planning.

Also, there is world-wide interest. There has been extensive development in Europe, notably in the Netherlands, Great Britain, and France. Some research has been reported in Spain and Italy. There has been research and development activity in Russia, Japan, North and South Africa, Australia, and Israel.

Extensive U. S. congressional hearings in 1952 showed the need for a research and development program on saline water conversion and resulted in the Saline Water Act. The Department of the Interior, through the Office of Saline Water, carries out this program by means of federally financed contracts and grants, by research in federal laboratories, and by stimulating and cooperating with private and governmental organizations.

In September 1961, another law was enacted which increased the research and development program substantially by authorizing $75,000,000 over the next 6 years. It provides for a large increase in basic research and also in applied research and development. Funds must be obtained from the Congress by yearly appropriations. The new law also provides for recommendations to the Congress for the additional demonstration plants.

Scientific and technical activities in saline water conversion range from basic research to commercial plants. Now more than 25,000,000 gallons per day of fresh water from saline sources is being produced in large plants in various parts of the world. Most of this is produced from sea water, using several methods of distillation. The remainder is obtained by using electrodialysis processes on brackish waters. The largest sea water distillation capacities are in Kuwait, on the Persian Gulf, and in Aruba and Curaçao, in the Caribbean. Two of the newest plants, the largest sea water distillation plants in the United States, are the Office of Saline Water's million-gallon-per-day plants—one at Freeport, Tex., and the other at San Diego, Calif. Large electrodialysis plants for brackish waters are at Bahrein in the Persian Gulf, Welkom, South Africa, more recently Buckeye, Ariz., and the OSW plant at Webster, S.D.

Basic research is an important phase of the conversion effort and a source of needed new ideas. These investigations range from theoretical studies on behavior of ions in aqueous solutions through studies of phenomena having potential use for converting saline water.

Past research and development efforts have resulted in grouping saline water conversion processes as follows: distillation, including solar energy applications; membrane processes; separation by freezing; and other chemical, electrical, or physical conversion methods. There are a number of different processes in each of these major groups.

Several of the distillation processes are most advanced today. A number are in commercial use. Distillation processes are being used in three demonstration plants. However, development of both distillation and electrodialysis processes continues, in order to obtain new or improved methods for further reduction of costs. Attention is being given to solar energy applications in distillation. Freezing processes are relatively new. Some of them now have reached the pilot plant stage of development. The hydrocarbon hydrate process is an important example in the category of other processes; pilot plants are being designed. Use of solvent extraction is another method on which extensive laboratory work has been completed; it shows promise for certain brackish water applications.

Experience with saline water conversion has shown that testing and evaluating pilot plants on actual sea water at a sea coast site are necessary development steps for promising processes. A Research and Development Test Station for this use is being constructed at Wrightsville Beach, N. C.

Different processes will be developed having advantages for particular applications. For example, some types of processes will be more economical for treating brackish waters; some processes are expected to be particularly adaptable to use in household-type units or small installations; others will be best for multimillion gallons per day plants. Factors connected with location, such as fuel costs, weather conditions, and waste disposal conditions, can determine which of several conversion processes would be the most economical to use.

Five demonstration plants have been authorized. Three are now in operation. The processes and plants are:

Multiple-Effect, Long-Tube Vertical (LTV) Distillation Process. This is a sea water conversion plant at Freeport, Tex., producing 1,000,000 gallons per day of fresh water. It has 12 effects; the evaporators are of a falling film type.

Multistage Flash Distillation Process. This plant is near San Diego, Calif., and also has a capacity of 1,000,000 gallons per day; 36 flashing stages are used.

Electrodialysis Process. This plant at Webster, S. D., operates on brackish well water and has a capacity of 250,000 gallons per day.

Vapor-Compression Distillation Process. This plant will operate on a highly brackish water and will be located at Roswell, N. M. It will have a design capacity of 1,000,000 gallons per day. Construction is under way.

Freezing Process. Plans were to build a 250,000-gallon-per-day demonstration plant at Wrightsville Beach, N. C. However, the bids for the construction of that plant were reviewed recently by the Office of Saline Water. Following an evaluation of the current status of the development of freezing processes, it was decided that a plant of that size would not properly demonstrate economic potentials of freezing processes. Because of recent technical advances in these processes, it has been decided to build a large pilot plant in order to obtain engineering data to permit construction later of a freezing process demonstration plant in a 1,000,000- to 3,000,000-gallon-per-day size.

The demonstration plants will provide a great deal of important data. However, it is unlikely that the processes selected for these first plants are the best that can be developed. Further research will not only improve the processes but also may develop new methods that will give lower cost converted water than now can be reasonably predicted. Operation of demonstration plants also can be expected to uncover problems requiring additional research and development for solution.

All Office of Saline Water research and development are carried out in the expectation that results will lower conversion costs. There have been many saline water conversion costs published and quoted; however, almost all are estimates and have not been proved. The existence of the demonstration plant program attests to this lack of reliable cost information. It is generally agreed that the conversion of sea water to fresh by distillation processes in use 15 to 20 years ago produced fresh water in small quantities at costs of $4 to $5 per thousand gallons. Based upon the Office of Saline Water cost estimating procedure, it is estimated that the first two sea water conversion demonstration plants will produce water at about $1.25 per thousand gallons in the million-gallon-per-day size. Further research and development will lead to lower costs.

This volume includes papers from two symposia on saline water conversion sponsored by the American Chemical Society, one in St. Louis, Mo., in 1961, and the other in Washington, D. C., in 1962. For the 1962 symposium, papers on typical research efforts in saline water conversion were selected without limitation to Office of Saline Water work. The presentations included basic and applied research. Also, in order to present additional information on more recent saline water conversion research and development, several papers, not presented at the last symposium, were invited by the American Chemical Society for inclusion in this volume.

JOSEPH J. STROBEL, *Chairman*
Symposium on Saline Water Conversion

Office of Saline Water
U. S. Department of the Interior
Washington 25, D. C.

Review of Distillation Processes for the Recovery of Fresh Water from Saline Waters

BARNETT F. DODGE

Chemical Engineering Department, Yale University, New Haven, Conn.

This paper presents a general review and discussion of distillation (alternatively, evaporation) processes, including such topics as the many variants of processes of this general category, the thermodynamics of the processes and their energy requirement, properties of saline solutions of importance in distillation, heat transfer, scale formation and prevention, corrosion, processes and equipment, and U. S. government demonstration plants. It is primarily a highly condensed summary of published information in this field and not a critical review. The paper was originally presented in April 1961, but additional material has been added to bring it up to date.

Developments in distillation processes are summarized in this paper, written originally in 1961, but recently updated by the author. At the outset, it is desirable to make a few general statements about such processes, in order to put them in better perspective. For the purposes of this discussion, evaporation is considered to be synonymous with distillation. Although "evaporation" is the more common term in general chemical engineering practice, in the case of saline water conversion "distillation" seems to be the preferred term.

Three main characteristics of distillation processes should be noted:

They separate the water directly, using a liquid-vapor interface as a semipermeable membrane.

Either heat or work (mechanical and, indirectly, electrical) may be used.

The energy requirement bears no direct relation to the latent heat of vaporization. In other words, the heat to vaporize the water must be largely recovered if the energy requirement is to be kept within practical limits. If the energy is supplied in the form of heat, multistage operation is imperative; if in the form of work, it is used merely to pump the latent heat from one temperature level to a higher one. This divides all distillation processes into two general categories: single-stage with vapor compression and multistage with or without vapor compression. Any one of the distillation processes can be of either type, irrespective of the other features of the process.

The energy sources considered for distillation are: fossil fuels, uranium fission, waste heat from various industrial operations, ocean temperature difference, and radiation from the sun.

Fossil fuels are the only proved source for large scale operations at the present time, but the others are all still under active consideration. Solar energy is a special case that is not considered in this paper.

Distillation processes are the only ones that have been proved on a commercial scale up to the present time, at least for saline solutions as concentrated as sea water. For brackish waters the electrodialysis process using ion-permeable membranes is the only one in successful large scale use, but a distillation process will be used at the government demonstration plant at Roswell, N. M. The total capacity of sea water distillation plants now installed is of the order of 20,000,000 gallons per day. The largest plant is the one on the island of Aruba, which has a capacity of about 2,700,000 gallons per day in five units and produces water for something in the range of $1.25 to $2.00 per 1000 gallons, depending on the credit taken for power produced as a by-product.

Variants of Distillation Processes

Variants are due primarily to the use of different types of evaporators, to different methods of utilizing energy, and to the way in which heat is transferred. For example, one may use a boiling-type evaporator or a flash type, a submerged tube or film type, a stationary or rotating evaporating surface, forced circulation or natural convection, multiple effect or vapor compression, heat transfer through metal walls or by the use of immiscible liquids, etc. Many combinations of these variations are possible and we do not intend to consider all possible cases, but to confine the discussion to the following nine types, which are believed to be the most important at the present time.

1. Boiling-type, submerged-tube heating surface
2. Boiling-type, long-tube, vertical evaporator
3. Flash evaporation
4. Forced circulation, vapor-compression, flash evaporation
5. Rotating surface evaporator
6. Wiped-surface evaporator
7. Vapor-reheat process
8. Heat transfer using an immiscible liquid
9. Condensing-vapor heat transfer by use of a vapor other than steam

A "boiling type" of evaporation process is one in which the heat is transferred as latent heat to liquid boiling at a substantially constant temperature. It is to be distinguished from a "flash" process, in which heat is added to the liquid under nonboiling conditions and hence stored as internal energy. Upon subsequent reduction of the pressure, the stored internal energy supplies the latent heat to evaporate a portion of the stream.

Boiling Types. The first type has commonly been used with vapor compression in a large number of small units built mainly for military use, where compactness and portability are prime considerations, but it is also used in large multiple-effect systems. It is the type now used in the large plants on Aruba and Curaçao. In view of recent developments, this type of evaporator is essentially obsolete for large plants at the present time.

The second type is used in the process developed by W. L. Badger Associates, being used in the government demonstration plant at Freeport, Tex. It is a 12-effect system, with evaporation from a falling film in long tubes (LTV). Its direct energy source will be exhaust steam from turbines, so that electric power is a by-product of the water plant. A general review of the work done by Badger Associates on this process was given recently by Standiford and Bjork (*34*).

Flash Evaporation. The third type is already in wide use on both shipboard and land. The largest plant is the one in the sheikdom of Kuwait, with a capacity of about 2,500,000 gallons per day. It uses only four stages of flash evaporation and for this reason it also is essentially obsolete for large plants. A 26-stage plant is in operation at the Oxnard station of the Southern California Edison Co., and a 52-stage plant was determined as the optimum for a 50,000,000-gallon-per-day plant using a nuclear reactor as the steam source. The government demonstration plant at Point Loma, San Diego, Calif., will use this process with 36 stages.

Forced Circulation. The fourth is a process which was proposed by Dodge and Eshaya and extensively studied from an engineering and economic standpoint under Office of Saline Water auspices (*15*). A pilot plant was proposed (*14*), but no steps were taken to implement the proposal. The method involves heating of brine under nonboiling conditions at linear flow velocities of the order of 8 to 10 feet per second, followed by flash evaporation and compression of the flashed vapor for use as the heating medium. Dropwise condensation of the vapor was another feature of the process. A somewhat similar process has been selected for the government demonstration plant at Roswell, N. M. This plant will use vapor compression in conjunction with multiple-effect (two or three effects) evaporation, and as far as we are aware this is the first time that this combination has ever been used.

Rotating Surface Evaporator. The fifth type has been developed in several forms. The first was the Hickman still, which was single-stage with vapor compression. At least five different models have been built and extensively tested. One was on a pilot-plant scale, with a capacity of about 25,000 gallons per day and was tested by Badger Manufacturing Co. at Wrightsville Beach, N. C. At present, Aquastills, Inc., Rochester, N. Y., is working on the development of a unit for household use. Another form is the Glover still, which differs from the Hickman mainly in the fact that the vapor compressor is an integral part of the rotor, and this brings in other mechanical differences. One model, built by Mechanical Equipment Co., New Orleans, has been tested at the Denver laboratory of the U. S. Bureau of Reclamation.

Still a third modification is a rotating-surface multiple-effect evaporator conceived and built by L. A. Bromley and associates at the University of California, Berkeley, Calif. This is a 29-effect laboratory unit, 4 feet in diameter with $^{9}/_{16}$-inch plate spacing and a capacity in the range of 6500 to 9000 gallons per day. The entire unit rotates at a speed of about 1000 r.p.m.

Wiped-Surface Evaporator. The sixth is an experimental unit built and tested by the General Electric Co. under contract with the Office of Saline Water and the Bureau of Ships, U. S. Navy. The unit consists of a copper tube 6 inches in diameter and 50 inches long, the inside surface of which is wiped by blades of a rotor turning at about 200 r.p.m. to maintain a thin film of brine on the evaporation surface. The outside surface of the tube is grooved longitudinally to promote dropwise condensation. Recently the General Electric Co. was awarded a contract by OSW to construct a 37,000-gallon-per-day unit using this process.

Vapor-Reheat. The vapor-reheat process (type 7) is a flash-evaporation process in which heat is transferred directly from flashed vapor to brine without a separating metallic surface. The idea is to save energy by reducing temperature differences and to lower equipment costs by eliminating the need for conventional heat exchangers. The hope has been expressed that it may be possible to operate with brine temperatures above 250° F. and thereby gain increased efficiency through the use of a larger number of stages. Presumably this hope is based on

the expectation that the scaling problem which now limits the maximum temperature will be eased. The basis for this is not clear, since in this respect the process does not differ from the more conventional flash-evaporation process.

It seems to us that the existing descriptions of this process do not adequately describe it nor clearly show its relation to the more conventional flash-evaporation process. We will try to correct this with the following brief discussion:

The basic idea of the flash process is to evaporate the salt solution in a series of stages by means of heat previously stored in it, through its use as the cooling medium to condense the vapors generated in the flash evaporation. This transfer of latent heat of condensation of steam to sensible heat in the feed brine is the distinguishing characteristic of a flash process. The vapor-reheat flash process has the same heat-transfer problem, but some existing descriptions give the impression that this is accomplished by direct exchange of heat between fluids without an intervening metallic surface. This is not the case. Direct mass transfer (with simultaneous heat transfer) between evaporating brine and incoming feed is clearly out of the question, because the feed would be diluted. To get around this, the vapor-reheat process transfers vapor directly from hot brine to colder pure water and then transfers the heat stored in the cold water to the feed. This latter transfer of heat must be made either with a conventional exchanger or by the use of an immiscible fluid with two contact towers. In either case the vapor-reheat process seems to impose an additional heat-transfer step over that used in the conventional flash process or that in a process using an immiscible fluid as a transfer agent. The advantage of this is not very apparent to us.

The process is under study by Othmer and associates at the Brooklyn Polytechnic Institute (*29*). Few experimental results are available at this time. Process variables have been studied with the aid of a digital computer and two laboratory units have been assembled: a small five-stage unit to demonstrate the feasibility of the idea, and a larger single-stage unit with a capacity of about 100 gallons per day to study conditions in any one stage of a multistage system. Work has been continued with a single-stage unit of greater capacity to test on a pilot-plant scale the direct exchange between vapor from flashed solution and fresh water.

Heat Transfer Using Immiscible Liquid. The eighth type involves an experimental investigation of heat transfer in a spray column, with the objective of developing a cheaper way to transfer heat than in a tubular heat exchanger. The work has been done by Food Machinery and Chemical Corp. under contract with the Office of Saline Water, using 4-inch-diameter glass columns and transferring heat to and from brine or water by means of a saturated paraffin hydrocarbon. Recently this contract was renewed to extend the development of this form of heat exchanger.

Condensing-Vapor Heat Transfer. The ninth involves the use of a heat-transfer medium other than steam (ammonia and dichlorodifluoromethane are examples) in a vapor-compression cycle. The purpose is to reduce the size of the compressor by using a denser fluid, which will require smaller volumes to be compressed for the same plant capacity.

Topics of Importance to All Distillation Processes

Thermodynamics and Energy Requirements. Dodge and Eshaya (*13*) pointed out that the theoretical energy requirement is not a unique quantity but depends on certain variables and assumptions. There is an absolute minimum

requirement for a completely reversible process whether isothermal or not, which is independent of the mechanism or steps of the process but does depend on temperature, concentration, and yield. This quantity is close to 3.0 kw.-hr. per 1000 gallons of pure water from a 3.50% NaCl solution at 25° C. The usual assumption is that this concentration of pure NaCl is a close approximation to normal sea water. What data there are on the activity of water in normal sea water indicate that the minimum work is less for sea water than for a pure NaCl solution at the same per cent by weight of salts.

What many writers have not made clear—and which is worth emphasizing—is that this minimum figure is totally unrealistic for two reasons: It assumes zero driving forces at every point in the process, which means equipment of infinite size, and it assumes 0% yield of fresh water or the pumping of an infinite amount of sea water.

The driving forces, resulting in thermodynamic irreversibility, that are inherent in any distillation process are:

Pressure difference to overcome fluid friction
Force difference to overcome mechanical friction in pumps and compressors
Temperature differences in heat exchangers and between the system and its environment and in fluid mixing
Concentration differences for mass transfer and in mixing of fluids

An important point to keep in mind is that the losses in availability resulting from each individual irreversibility are multiplied together and hence it is not surprising that the over-all thermodynamic efficiency of even the most modern distillation process does not exceed 10% and many operate at much lower efficiency.

Another point which further confuses the issue is that most distillation processes operate with heat energy and not with mechanical or electrical work, and the figure of 3 kw.-hr. per 1000 gallons is not a proper basis for a thermodynamic efficiency in such cases. One must deal with the availibility of heat, which depends on two temperature levels, that of the heat source and that of the heat sink. The 3 kw.-hr. is directly converted to 10,245 B.t.u. using only the first law of thermodynamics. One can relate minimum work to minimum heat through the well-known relation based on the first and second laws of thermodynamics,

$$W_{\min} = Q_{\min} \frac{T - T_0}{T} \tag{1}$$

For a source temperature of 250° F. and a sink temperature of 70° F. $Q_{\min} = 3.94$ $W_{\min} = 11.8$ kw.-hr. per 1000 gallons or 40,300 B.t.u. per 1000 gallons. For a source which is changing state as in the case of steam, we can introduce the second law of thermodynamics in the form of the function "availability." Steam at 260° F. (about 20 p.s.i.g. for saturated steam) has an availability of 274 B.t.u. per pound with respect to 70° F. and so the minimum requirement under these conditions is 10,245/274 or 37.4 pounds of steam per 1000 gallons or 224 pounds of water evaporated per pound of steam. The best steam-using distillation processes that are now available might evaporate 13.65 pounds of water per pound of steam, and this corresponds to a thermodynamic efficiency of about 6.1%. This could be raised appreciably by generating high pressure steam and using it in a turbine to generate power before using it in the distillation plant.

Returning to the second reason why the absolute minimum figure of 3 kw.-hr. has little meaning, one can readily calculate the reversible work requirement as a

function of the yield of fresh water from sea water; as shown by Dodge and Eshaya (*13*), it increases with yield. Energy for pumping the feed decreases with yield and a minimum occurs at about 40% recovery.

One can devise various separation processes and then calculate the energy requirement if they were operated under ideal conditions—i.e., with all driving forces reduced to zero except those that are inherent to the process. Such an energy requirement is often referred to as a theoretical or ideal energy requirement, but it should not be confused with the minimum work for a completely reversible process. For example, one can calculate the theoretical work for the separation process shown in Figure 1 if one assumes phase equilibrium between the concentrated brine and the water. This implies a single-stage rather than a differential process, in which the water vapor is formed only from the 7.0% solution rather than from a series of solutions varying continuously in concentration from 3.5 to 7.0%. It is irreversible because of the mixing of solutions differing in concentration.

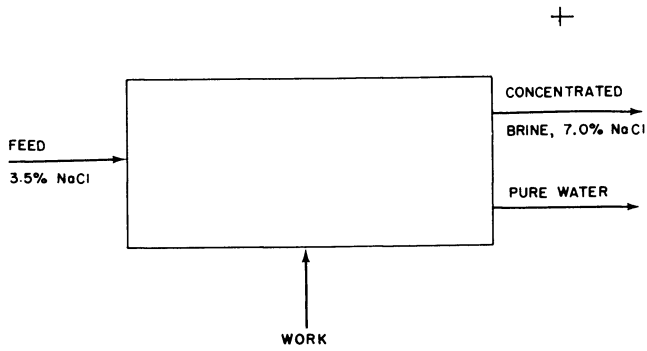

Figure 1. General separation process

The minimum energy requirement for a brackish water (say 4000 p.p.m. of salt) will be much less than for sea water, but it is doubtful if the practical requirement will be very different, because this will be determined largely by the irreversible effects which will not be very different for the two cases. Operating data on small household units published by Hickman *et al.* (*21*) show only minor differences in energy requirement between tap water of 170-p.p.m. solids and sea water.

Disregarding economics, there is a maximum number of effects in a multiple-effect system which is fixed by the boiling point elevation (BPE). The number depends on the over-all temperature range, the initial salt concentration, and the per cent yield. For the special case of a 35,000-p.p.m. NaCl feed, temperature range of 100° to 25° C., and 50% recovery, the maximum is about 107. Economics fixes a much smaller number and present indications are that the optimum number of effects will be somewhere between 10 and 20. This is for the case of boiling on the heat-transfer surface and not for flash evaporation, where the optimum number of stages is probably much greater.

The work required for vapor-compression distillation may be calculated from the equation

$$W = \frac{0.1345\ T_1(r^2 - 1)}{\epsilon r} \qquad (2)$$

where W = work, kw.-hr. per 1000 gallons
T_1 = compressor intake temperature, °R
r = compression ratio
ϵ = adiabatic efficiency of compressor

The pounds of water evaporated per pound of steam in a multiple-effect system may be approximated by the relation

$$\Sigma w = \frac{w_1(1 - w_1^n)}{1 - w_1} \tag{3}$$

where Σw = pounds evaporated per pound of steam in n effects
w_1 = pounds evaporated per pound steam in a single effect and assumed to be the same for all effects

Letting C_s = cost of steam in cents per 1000 pounds and C_E = cost of electric energy in cents per kw.-hr., one can derive from the above two equations the following:

$$n = \frac{\log\left[1 - \frac{61.8(1 - w_1)r\epsilon C_s}{w_1 T_1(r^2 - 1)C_E}\right]}{\log w_1} \tag{4}$$

where n = number of effects in a multiple-effect system that would have the same energy cost as a single-effect vapor-compression evaporator. Let us apply this to the following case: $w_1 = 0.90$, $\epsilon = 0.75$, $C_s = 55$, $C_E = 0.70$, $r = 1.39$ (corresponding to 1-atm. intake pressure to the compressor, Δt across the heating surface of the vapor-compression evaporator of 15° F., BPE of 2° F.).

For this case, $n = 21$, or the multiple-effect evaporator would need to have 21 effects to be equivalent to the vapor-compression still in energy cost. If w_1 were 0.97, all other conditions remaining the same, $n = 10$ (approximately). (It is estimated from the published data that w_1 for the Aruba six-effect plant is 0.95.)

In a recent report, Tribus and others (*36*) have presented a detailed study of some thermodynamic and economic considerations in the preparation of fresh water from sea water. From the three principles—first law of thermodynamics, second law, and conservation of mass—the following equation applying to a general, continuous-flow, separation process is obtained:

$$\frac{-\dot{W}}{\dot{n}_{w_2}} + \frac{\Sigma\dot{Q}_H}{\dot{n}_{w_2}}\left(\frac{T_H - T_0}{T_H}\right) = \frac{T_0\dot{S}}{\dot{n}_{w_2}} + (\bar{H} - T_0\bar{S})_{w_2} - (\bar{H} - T_0\bar{S})_{w_0} + \frac{\dot{n}_{w_3}}{\dot{n}_{w_2}}\left[(\bar{H} - T_0\bar{S})_{w_3} - (\bar{H} - T_0\bar{S})_{w_0} + \frac{\dot{n}_{s_3}}{\dot{n}_{w_3}}\left((\bar{H} - T_0\bar{S})_{S_3} - (\bar{H} - T_0\bar{S})_{s_0}\right)\right] \tag{5}$$

where W = work
n = pound-moles
Q = heat
T = absolute temperature
S = entropy
H = enthalpy

Subscripts 2 and 3 refer to fresh water and brine, respectively. S and W refer to salt and water, respectively. 0 refers to ambient conditions. H refers to a heat reservoir at an elevated temperature.

A bar over a property indicates that it is a partial molal property.

A dot indicates a time derivative.

This equation, along with the necessary properties, is applied to the calculation of energy requirements for various cases and some important conclusions are drawn, based on thermodynamics alone. Economic considerations are then introduced and combined with the thermodynamics to show the effect of a number of variables on cost. Vapor-compression systems and thermal-separation plants using

the ocean temperature difference are analyzed in some detail, using the various relations previously developed. One specific conclusion was that the lowest possible cost of recovering fresh water from sea water by a vapor-compression process is 34 cents per 1000 gallons.

It is, of course, impossible to review in a few paragraphs a long and highly mathematical report like this, but this brief discussion may at least whet one's appetite for further details.

It has long been recognized that the distillation process would be more efficient if higher temperatures could be used. The present upper limit of about 250° F. is fixed by the scaling problem. Assuming that this problem will eventually be solved, a group in the Institute of Engineering Research, University of California, Berkeley, is making a computational study to determine the temperature for maximum heat economy. Present indications are that this lies above the critical temperature. However, this will probably not be the temperature of minimum cost, because of the increased capital costs due to the higher operating pressure.

Properties of Saline Solutions. Certain properties are obviously essential for the study of distillation processes, but such data on naturally occurring saline solutions are rather meager. The report by Tribus *et al.* (*36*) contains extensive tabulations and graphs of the following properties for pure NaCl solutions over a range of concentration and temperature:

Partial molal volumes of salt and water
Partial molal heat capacities of salt and water
Relative partial molal enthalpies of both components
Activity coefficient of NaCl
Activity of water
Vapor pressure

For sea water at various total percentages of solids and various temperatures there are given

Activity of water
Density
Partial molal volume of water
Osmotic pressure

Some of these properties have been deduced from inadequate data and much more experimental work in this area is needed. Data of all kinds are lacking on typical brackish waters.

Clark, Nabavian, and Bromley (*11*) measured a heat of dilution of concentrated (7%) sea water and heat capacities of normal and concentrated sea water at room temperature. From these data and vapor-pressure data of Arons and Kientzler (*1*), with the aid of thermodynamic relations they calculated heats of concentration and boiling point elevations. Both of these properties are presented in graphs and tables over a temperature range of 77° to 302° F. and for salt concentrations up to 9%. Integral heat of concentration increases with the temperature up to about 180° F. substantially independent of concentration and then decreases. The maximum value for 7% salts is only about 1.0 B.t.u. per pound of original sea water and hence is negligible for most practical purposes.

They also presented data on boiling point elevation over the temperature range from 80° to 300° F. and up to 9% salt concentration. These values are appreciably lower than those reported by others—for example, at 7% salts and 1 atm., Clark *et al.* give 1.6° F., and Dodge and Eshaya give 2.3° F. The difference may lie in the fact that the values of Clark *et al.* are based on actual vapor

pressures of sea water, whereas the values given by others are calculated from the vapor pressure of water by the well-known thermodynamic relations but assuming 100% ionization. This assumption is open to question. Although we have not made a critical review of the methods and data used by Clark *et al.*, it should be noted that some doubt has been expressed about the reliability of the vapor-pressure data of Arons and Kientzler. Furthermore, Clark *et al.* found the specific heat of a 7.0% saline solution to be higher than that of normal sea water, which is contrary to results reported by others [see Frankel (*18*)] and to what one would predict.

Frankel (*18*) gives the specific heat of sea water at 70° F. as a function of concentration over the range from 0 to 80,000 p.p.m. of total solids. Sourirajan (*31*) investigated the pressure-temperature-composition relationships of the system NaCl-H_2O and more specifically the vapor pressure of saturated solutions from 250° to 700° C., the solubility of NaCl in steam in the temperature range 350° to 750° C. and pressures up to saturation, and composition of liquid and vapor phases in equilibrium at pressures up to 1200 bars. Experimental results are summarized in five graphs. The methods and results of this investigation have recently been given in greater detail by Sourirajan and Kennedy (*32*).

Heat Transfer. Rate of heat transfer determines the size and hence the cost of all equipment in which heat is transferred. The way in which the heat is transferred is also an important factor and three ways are under study: transfer from one fluid to another through a separating wall, direct transfer from vapor to brine without a separating wall, and indirect transfer through an intermediate liquid insoluble in water.

Most of the work has been done on the first method and in connection with the development of specific types of "hardware." Three ways have been tried for increasing the rate of transfer on the liquid side: increasing velocity of the liquid pumped through tubes, using rapidly rotating surfaces to maintain a thin film of evaporating liquid on the surface, and using wiper blades to maintain a thin film. Heat transfer on the condensing side can be improved in two ways: use of centrifugal force to remove the condensate instead of reliance on gravity and dropwise instead of film condensation. The use of a rotating surface can increase the rate of heat transfer on both the evaporating and the condensing side.

Sparrow and Gregg (*33*) have presented an interesting mathematical study of condensation on a rotating disk, based on application of the Navier-Stokes equation and mass- and energy-balance equations. Numerical solutions were obtained for Prandl numbers from 0.003 to 100 and for values of the ratio $C_p\Delta t/L$ (L is latent heat of vaporization) from 0.0001 to 1.0. Results are given for heat transfer, condensate thickness, torque-moment, temperature profile, and velocity profile. No comparisons of predicted with experimental values are given.

Some recent work has also been done on increasing the rate of transfer on the condensing-steam side by promoting dropwise condensation. This type of condensation results from surface-tension effects and is promoted in three ways:

Method 1. Addition to the steam of agents which adhere to a metal surface and are water-repelling
Method 2. Coating the metal surface with a water-repellent material
Method 3. Use of an axially grooved surface

Dodge and Eshaya (*14*) and Dodge (*12*) have recently reviewed some of the results of work using Methods 1 and 2. Lustenader *et al.* (*24*) have recently presented results based on all three methods. They tested chromium-plated tubes

and also about 10 organic compounds known to be dropwise promoters. The chromium plate gave over-all coefficients (see Equation 6) of about 5000. The promoters used were oleic acid, stearic acid, benzyl mercaptan (α-toluenethiol), and dodecanethiol; all gave excellent dropwise condensation. When the promoter was placed on the tube (copper and chromium-plated) prior to starting the tests, its effect wore off in a few hours or less and filmwise condensation returned, but when mercaptan was injected into the vapor, long life was achieved (no time stated).

Table I. Values of Over-All Heat

Equipment	*Size of Unit*	*Variables and Conditions*
Hickman still	25,000 gal./day	Rotor speed, 400 r.p.m. Temp. level, 105–40° F. Δt, 3.67–5.23° F.
Hickman still	Laboratory size 15-inch to $4^1/_2$-ft. diam. rotors	Shape of rotors, feed application, type of condensation, rotor speed
G.E. thin-film, wiped surface	6 inch diam. × 50 inch tube. 8000 gal./day	Blade design, feed rate, feed distribution, temp. level, Δt, dropwise cond. Wiper speed, 200 r.p.m.
Badger Assoc. LTV pilot plant	7 2-inch × 24 ft. tubes	Falling film, boiling temp. feed rate, steam rate, salt concn.
Glover rotary still	5 to 25 gal./day $25^1/_2$-inch diam. rotor	R.p.m. of rotor, condensing temp.
Bromley, rotating, multiple effect	4 ft. diam. $^9/_{16}$-inch plate spacing 8600 gal./day	29 effects, 970 r.p.m.
Exp. flash evaporator	About 10,000 gal./day	Velocity in condenser tubes varied from 1.3 to 7.0 ft./sec.

In Method 3 the tube surface was fluted longitudinally and film coefficients of about 10,000 were obtained or about four times the value for film condensation on a corresponding tube with smooth surface. Additions of a dropwise promoter actually caused a decrease in the coefficient.

This paper also presents a theoretical study of thin-film evaporation using a set of rotating wiper blades and experimental data showing the effect of wiper speed and temperature difference.

Acoustical vibration as a means of improving heat-transfer rates is under study by the Southwest Research Institute and results appeared in an OSW research and development report (*30*). Very briefly the results may be summarized as follows: Acoustic vibration effected a marked improvement in liquid-film coefficients at low Reynolds numbers in the viscous region, but the improvement decreased as Reynolds number increased. The only effective way of applying acoustic vibrations seemed to be transverse vibration of a pipe, with the water flowing in an annulus outside the pipe. Other methods of applying the vibrations produced no significant improvement. Vibration also improved the heat-transfer coefficient of condensing steam, especially when inert gas was present. Some flaking of scale deposits as a result of vibration was observed.

Results on heat transfer are usually presented as over-all coefficients of heat transfer defined by the simple relation

$$U = \frac{q}{A\,\Delta t} \tag{6}$$

where U = over-all heat-transfer coefficient, B.t.u./hr. sq. ft. ° F.
q = rate of heat transfer, B.t.u./hr.
A = area of heat-transfer surface, sq. ft.
Δt = temperature difference across transfer surface, ° F.

The values to choose for q, A, and Δt are not always clear and obvious and assumptions may be involved. The original papers will have to be consulted for these. Furthermore, U is affected by many variables and this paper is limited to presenting a few typical values, which are given in Table I. In all cases little, if any, scale was present.

Transfer Coefficients

U, B.t.u./ Hr. Sq. Ft. ° F.	*Notes*	*Reference*
1600–2600	Also referred to as No. 5 Badger-Hickman still. Actual capacity about 17,000 gpd. Presence of noncondensable gas lowered capacity	(*21*)
2400–5000	U of 3000 considered conservative for production-size units. U varies as $\sqrt{\text{r.p.m.}}$	(*6, 21*)
1200–8300	Additive for scale prevention. Developed for marine use. U of 2500 in 130-hr. test on sea water	(*19, 24*)
375–700	U for rising film about $^1/_2$ of that for falling film. Only variable with much effect was boiling temp. U increases with t	(*2, 4*)
Average of 2200	2000 p.p.m. solids in feed. U decreased with increase in r.p.m.	(*9*)
3000	Very few operating data available	(*10*)
250–1000		(*18*)

For comparison with the coefficients in Table I there are given in Table II calculated values of U for forced circulation of water at 212° F. in copper tubes 1 inch in outside diameter width 0.05-inch wall for two different steam-film coefficients.

Table II. Calculated Values of Over-All Coefficient of Heat Transfer for Steam Heating of Water in Forced Circulation

Velocity of Flow, Ft./Sec.	*Liquid film Coefficient, h_L, B.t.u./(Hr.) (Sq. Ft.) ° F.*	*Steam Film Coefficient, h_S*	*Over-all Coefficient, U, B.t.u./(Hr.) (Sq. Ft.) (° F.)*
6	2130	2500	1180
10	3200		1450
12	3700		1540
6	...	8000	1670
10	...		2260
12	...		2500

A comparison of the values in Tables I and II indicates that the rotary, thin-film type of evaporator is capable of giving appreciably higher coefficients of heat transfer than the usual multi-tubular type, even when forced circulation at good velocities is used in the latter. This is presumed to be one of the chief advantages of the rotating-surface and the thin-film, wiped-surface evaporators. It is still to be demonstrated that the corresponding reduction in heating surface more than compensates for the increased capital and maintenance costs. It is possible that these more exotic evaporator types will find their main use in relatively small units where compactness is important. They may also have some advantages where scale is a serious problem.

In the experiments with the use of an immiscible liquid reported by Woodward (*40*) of Food Machinery and Chemical Corp., 3-inch and 4-inch glass columns were used and the hydrocarbon was sprayed into the bottom through a nozzle. The results were expressed in the form of a volumetric coefficient, V_v, defined as B.t.u./(hr.) cu. ft.) (° F.), since the heat-transfer area was unknown. Values in the range of 6000 to 10,000 were obtained with single columns. In an actual application a double column will be necessary to transfer heat from one aqueous solution to another and it is expected that a realistic value of U_v for a double column would be about. 2500. Several variables were studied, but none of them had much effect on the coefficient. Assuming a U of 300 in a shell-and-tube exchanger, about 8 square feet of surface in such an exchanger would be equivalent to 1 cubic foot of column in the spray-column exchanger.

The statement has been made that a packed-column exchanger would be much cheaper than a conventional shell-and-tube type, but no figures have been presented to substantiate this. The work on the spray-column exchanger has been limited to the exchange of sensible heat and in any distillation process by far the greatest part of the heat exchanged is latent heat. There appears to be no reason why latent heat cannot also be exchanged in this manner.

A group at the Institute of Engineering Research, University of California, Berkeley, is also investigating heat transfer with an immiscible fluid, based on a cycle proposed by C. R. Wilke. This involves the transfer of sensible heat from the fluid (tetrachlorodiphenyl) to boiling solution in a co-current contactor and transfer of latent heat of the steam to sensible heat in the fluid after compression of the steam to raise its temperature. Equipment has been assembled to study the heat transfer in the boiling section of the cycle, but no results have been reported. Details of the flow diagram and the experimental setup are given in two progress reports (*38*, *39*).

A group at the Department of Engineering, UCLA (*25*), is investigating heat transfer in a single-tube, falling-film evaporator with dropwise condensation of the steam. No results on this work were available to us.

Scale Formation and Prevention. Scale in the distillation of sea water results from the reactions:

$$2HCO_3^- = CO_3^{-2} + CO_2\uparrow + H_2O \quad (7)$$

$$Ca^{+2} + CO_3^{-2} = CaCO_3\downarrow \quad (8)$$

$$H_2O + CO_3^{-2} = 2OH^- + CO_2\uparrow \quad (9)$$

$$Mg^{+2} + 2OH^- = Mg(OH)_2\downarrow \quad (10)$$

$$Ca^{+2} + SO_4^{-2} = CaSO_4\downarrow \quad (11)$$

The equilibrium conditions for these reactions have been reasonably well established over limited ranges. All the salts that can precipitate have inverted

solubilities, so that increase of temperature favors scale formation. (This may not be true for $CaCO_3$ but only appears to be because of the effect of increased temperature on the release of CO_2.) An increase in the concentration of H^+ ions will prevent Reaction 8 by converting CO_3^{-2} to HCO_3^- ions and will reverse Reaction 10. Consequently the hydroxide and carbonate scales can be prevented by pH control, using either an acid such as sulfuric or citric or a salt such as ferric chloride. This has been known for some time and practiced successfully, but the cost is a significant item and the lowered pH accelerates corrosion. Alkaline scales can also be controlled by additives such as Hagevap (trade-name for a compound containing a polyphosphate and a foam suppresser), but such compounds are useful only to an upper temperature limit of about 200° F.

$CaSO_4$ deposition can be controlled by keeping the concentration below the saturation value at any point in the system. This means control of the degree of concentration of the sea water in relation to the temperature. The situation is complicated by the fact that $CaSO_4$ exists in three different crystal forms that are stable in contact with solutions and by the fact that the crystal form actually deposited is more likely to be determined by kinetic considerations than by equilibrium. Thus anhydrite is the stable solid phase in all cases encountered in sea water distillation, but the actual phases found are either gypsum or hemihydrate.

As a rough indication of the temperature-concentration relation, the following facts from Standiford and Sinek (35) may be cited:

Below 185° F., sea water can be concentrated to four times normal strength without formation of sulfate scale.

At 252° F., the maximum allowable concentration factor is 1.7 to 2.0.

At 300° F., substantially no concentrating can be done without risk of scale formation. These limits apply only to the case of the sulfate scale.

Much of the work by W. L. Badger Associates, Inc., in the LTV pilot plant at Wrightsville Beach, N. C., was directed toward scale prevention; the results are presented in reports to the Office of Saline Water and in the paper by Standiford and Sinek (35). Prior to this work Badger Associates (3) made a comprehensive literature survey covering some 900 papers and reports; a critical review with 143 of the most significant references given, is available from the Office of Technical Services.

The use of seed crystals of $CaCO_3$ and $Mg(OH)_2$ suspended in the evaporating salt solution was found to be an effective means of preventing the formation of carbonate and hydroxide scales, at least up to 250° F. The concentration of seeds in this slurry should be somewhere between 0.1 and 0.5% by weight. Although this technique has been reasonably well proved in the pilot plant, it has yet to be demonstrated that it will work continuously in a full-scale plant such as the one at Freeport, Tex. No tests on this scale have been made to date.

Seed crystals of $CaSO_4$ were also tried, but the results on preventing of sulfate scale were inconclusive and further work must be done. In most cases sulfate scale was prevented, but in a few cases some did form. Subsequent work in the LTV pilot plant has demonstrated that the sludge recirculation method using a slurry of about 1% $CaSO_4$ was effective in preventing scale up to temperatures of 300° F. Tests are under way on flash evaporators, and so far this method has not been wholly successful in preventing scale. Tests on a forced-circulation evaporator proved that a $CaSO_4$ sludge was effective for scale control.

A related method of scale control, the contact-stabilization method, in which the evaporating brine is passed through a bed of crystals outside of the evaporator,

was reported by Langelier, Caldwell, and Lawrence (23), but no recent work appears to have been done on it.

Scale problems can be minimized by operating a multiple-effect evaporator with forward feed, so that the temperatures drop as the concentrations increase.

Figure 3 of Standiford and Sinek (35) shows the concentration factor (ratio of concentration of the brine to that of normal sea water) *vs.* temperature relation (dashed line) for the 12-effect evaporator of the pilot plant. On the same graph are shown the solubilities of the three forms of calcium sulfate and the limiting values of pH for the formation of the alkaline scales. The curve labeled 7.0 pH shows that at 160° F. scale will not form if the concentration factor is below 2.0. There is a margin of safety in using this graph, because it represents equilibrium conditions and a certain amount of supersaturation is necessary for deposition to proceed at an appreciable rate. The line representing the conditions in the 12-effect evaporator lies above the anhydrite solubility line. This means that anhydrite scale should form in all but the first two effects and probably would if infinite time (equilibrium) were allowed. In other words, in predicting conditions for scale formation we need to know something about rates as well as equilibria.

Banchero and Gordon (5), working under contract with the Office of Saline Water, are studying the mechanism and conditions of scale formation in an apparatus which permits visual observation of the deposition surface. This surface is a 3.8-inch-diameter copper cylinder with a helical groove cut on it, surrounded by a close-fitting glass tube. The brine solution flows through the groove and the tube is heated on the inside by means of hot water. Surface temperatures of the tube are measured by thermocouples. To summarize the result, one can do no better than to quote from the abstract of their paper.

Scale formation was followed visually in an apparatus which approximated conditions in evaporators producing potable water. The time required for appearance of scale was investigated with and without boiling under a variety of solution and surface temperatures, concentrations, and flow rates. Results with aqueous solutions of lithium carbonate, calcium sulfate, calcium hydroxide, and sodium sulfate, all of which possess inverted solubility curves, gave gentle curves when plotted as per cent supersaturation against the logarithm of the time for scale to appear with a parameter of concentration. For a given supersaturation a lower concentration (and necessarily higher wall temperature) resulted in more rapid formation of scale than a higher concentration. The time for scale formation was independent of liquid velocity between 2 and 10 feet per second and ranged from 2 to 360 minutes with supersaturations from 90 to 5%.

From a qualitative standpoint, this paper adds little to the information already available, but the quantitative data should be useful in interpreting the results from pilot and full-scale plants and other operating units. This investigation of conditions governing scale formation is being continued and includes work with actual saline waters as well as prepared solutions. Rate of scale deposition is being determined by measuring the change in thermal resistance.

A group at the University of California, Berkeley, working under the Sea Water Conversion Program, is determining the solubilities of $CaSO_4$, $CaCO_3$, and $Mg(OH)_2$ in sea water of various concentrations at temperatures from 60° to 200° C. This should provide much needed data to assist in the interpretation of results on scaling. More basic data of this kind should be obtained.

One of the supposed advantages of the rotary-type evaporator is the lower rate of scale formation. To date the results are too meager to permit any conclusions about this, and one can only state that this assumed advantage has not been demonstrated.

Frankel (18) presents results on scale prevention in a flash evaporator using

Hagevap LP (a mixture of sodium tripolyphosphate and lignin sulfonic acid derivatives). The concentration ratio of the sea water was not allowed to exceed 2 and therefore only the alkaline scales could form. As long as the maximum brine temperature did not exceed about 200° F., no evidence of scale deposition was obtained. At 210° to 215° F. there was definite indication of scale from the increase in terminal temperature difference (TTD). At the conclusion of a series of tests the inside surface of the tubes was examined and found to have a very thin layer of loose, powdery deposit (after drying) which rubbed off easily and would not be classed as scale.

In Equations 7 to 11, it is evident that the formation of either $CaCO_3$ or $Mg(OH)_2$ scale depends on the release of CO_2 and if the system were pressurized so that CO_2 could not escape, scale should not form. Silver (*18*, p. 332) mentions the use of such a method in connection with a flash-evaporation process. In this process, it is relatively easy to keep the brine under a pressure above the decomposition pressure of the bicarbonate ion all the way through the heaters. The CO_2 is then bled off from the first flash stage and the precipitated solids are carried through the rest of the system in suspension. In the boiling type of evaporator this would not be so easy.

A group in the Department of Engineering, UCLA (*25*), is looking into scale control by means of CO_2 absorbed from Diesel engine exhaust gases. This combines pH control with the recovery of waste heat in the gases.

W. R. Grace & Co. is working on a process for preparing a fertilizer from the calcium and magnesium in sea water. The scale-forming constituents would be removed in the form of a salable product. Ammonia, phosphoric acid, and sodium hydroxide or carbonate are added to the water to precipitate a mixture of phosphates, which when dried can be used as a fertilizer. The economics of such a process appear favorable in some circumstances, but it will take large scale tests to determine its feasibility.

Other schemes for simultaneous removal of scale formers and recovery of a salable product are being studied. One which may have promise involves recovery of the potassium either as a magnesium potassium phosphate or by chelation.

The Office of Saline Water in collaboration with the Bureau of Yards and Docks of the Navy has awarded a contract to the Dow Chemical Co., to investigate the use of ion-exchange resins for removal of scale-forming constituents from sea water using the concentrated blowdown from the distillation unit as the regenerant of the resin. The tests showed that Dowex 50W cation exchange resin removed about 50% of the calcium from sea water and this was sufficient to prevent accumulation of sulfate scale in the particular vapor-compression evaporator used. No regenerant except the blowdown brine was used. Similar results were obtained with a brackish water similar to the feed for the Roswell demonstration plant. The estimated cost of softening in a 10,000,000-gallon-per-day plant with four times the concentration of sea water was about 9 cents per 1000 gallons. Details on this process are given in a recently issued report (*26*). The removal of calcium and magnesium ions by ion exchange with polystyrene cationic resins and use of the waste brine as regenerant have also been investigated in the Sea Water Conversion Program at the University of California; 67% removal was achieved in a one-stage process and 77% in two stages.

Since all scale-forming constituents of saline waters have inverted solubility-temperature relationships, the scale problem can be alleviated, if not wholly solved, by evaporation at high vacuum and hence low temperature. Some small single-stage units for household and other uses boil the solution at a temperature as low

as 110° F. This has the added advantage of making possible the use of low-potential waste heat as the energy source.

The use of chelating agents to remove the hardness ions from sea water has been studied (*22*), but the results are unpromising from an economic point of view.

Corrosion. Fink (*16*) of Battelle Memorial Institute has presented the results of a literature study combined with views of experts on the corrosion of metals by sea water. The study revealed a paucity of data on corrosion at elevated temperatures. The Cl ion is the chief culprit in causing corrosion, but an important factor is dissolved oxygen and it is probable that oxygen-free sea water would have very little corrosive action, at least at ordinary temperatures. Natural sea water may have very different corrosion effects from synthetic sea water because of the organic content. Fouling of the surface by organic deposits can lead to severe pitting due to concentration-cell effects. Consequently corrosion by actual water is not readily simulated in the laboratory by synthetic sea water.

Many factors contribute to the over-all results known as corrosion. Some of the most important are: oxygen concentration, temperature, composition and concentration of solutions, contact of dissimilar metals, flow velocity, impingement, stress pattern in the metal, cavitation, fouling of the surface, pH, and pollution with compounds not present in normal sea water. Whereas the qualitative effects of most of these variables are recognized, much work remains to be done to obtain a better quantitative picture.

The specific metals most commonly used or considered for equipment exposed to sea water are: iron and steel, aluminum and its alloys, stainless steels, Monel, copper-base alloys, titanium, and Hastelloy C. The latter two are the most resistant but too expensive to use except for special parts subjected to severe corrosion. Mild steel can be used in many places and even for the tubes of an evaporator, if precautions are taken to control some of the more important factors affecting corrosion, especially the oxygen content. Even though the corrosion rate for steel is greater than for some other metals, its lower cost may still make it more desirable for use, if conditions for localized attack can be prevented.

Aluminum is a good material for sea water service, if no copper and nickel ions are present and if all galvanic couples with most other metals can be avoided.

Stainless steels are unpredictable in sea water. In some circumstances, certain grades have stood up well but in other cases rapid attack has occurred. Stainless steels are prone to stress-corrosion cracking and susceptible to attack due to crevices and deposits. The consensus seem to be that stainless steels may be excellent in certain cases but must be used with caution.

Monel is one of the best all-around metals for sea water service, but its high cost militates against widespread use.

Admiralty brass, high-tin bronzes, aluminum brass, and cupronickel have all given good service in sea water. The most generally useful material for sea water plants is considered to be cupronickel. The 90% Cu–10% Ni alloy with about 1.5% iron is the most widely used, but the 80% or 70% alloys may be preferred for the more severe conditions.

There seems to be some evidence that copper tubes are corroded in flowing salt solutions if the velocity exceeds about 2 feet per second. This undoubtedly is influenced by other factors and needs further study before acceptance as an established fact.

One of the most important conclusions that I draw from a study of the avail-

able information on corrosion in sea water is that much more basic research is needed to unscramble the effects of the many variables.

Experience with the Badger Associates LTV pilot plant at Wrightsville Beach, N. C., has yielded some useful practical information on corrosion which might be summarized as follows (*2*):

Evaporator tubes of aluminum brass, admiralty brass, copper, and 90/10 cupronickel were all almost completely resistant to corrosion and results with steel tubes were "encouraging." The tubes were insulated electrically from the tube sheets in order to avoid galvanic action. Severe pitting occurred with aluminum tubes.

Protective coatings, cathodic protection, and corrosion inhibitors are all potential methods for corrosion control, but they have apparently not been used to any extent in plants for processing sea water and little experience is available. These might be fruitful fields for further investigation, but it must be admitted that the economics are doubtful.

The use of deaeration to remove oxygen from solution is probably the most effective way of combating corrosion and will probably make possible the use of ordinary steels.

Nobe (*28*) is investigating photovoltaic effects in metal single-crystal electrolyte systems and also the effect of stress. A few experimental results are presented on electromotive force *vs.* stress for steel-NaCl solutions and on photovoltaic potentials *vs.* light intensity for copper in distilled waters and in NaCl solutions. The effect of light might have some importance in solar-distillation plants.

Processes and Equipment

Rotary Stills. Five models of the Hickman still have been built and tested under OSW auspices. Some of the features of these stills were:

1. Single, 15-inch-diameter, conical aluminum disk
2. Rotor with two opposed, 18-inch, conical aluminum disks
3. Single 18-inch conical copper rotor
4. $4^1/_2$-foot-diameter conical copper rotor
5. (Badger-Hickman) 8 conical copper rotors, 8-foot diameter

No. 4 was later modified to a flat rotor which gave better performance because of better spreading on the surface. No. 5 was a pilot-plant size with a total of 600 sq. feet of evaporating surface. The nominal capacity is generally stated to be 25,000 gallons per day, but this varies with conditions and especially with Δt (temperature difference). Assuming an over-all heat-transfer coefficient of 2500 in the usual units, the calculated capacities would be

Δt, ° F.	3	5	10
Capacity, gal./day	12,950	21,500	43,000

A typical range of operating data for the No. 5 Badger-Hickman still is shown in Table III (*21*).

Table III. Typical Ranges of Operating Data for Badger-Hickman Pilot-Plant Unit

Rotor speed, r.p.m.	400
Condensing temp., ° F.	105–140
Temp. difference (corrected for BPE), ° F.	3.67–5.23
Concentration factor (feed/distillate)	2.5–4.4
Over-all coefficient of heat transfer, B.t.u./(hr.)(sq. ft.) (° F.)	1600–2440
Total energy requirement, kw.-hr./100 gal.	51.4–84.0
% of total energy for compressor	77.7–70.0
% of total energy for rotor	17.9–27.4

Engineering design studies by Battelle Memorial Institute (*6*) based on pilot-plant results indicated that the optimum unit would have about sixty 8-foot-diameter rotors, and would operate at a speed of 400 to 600 r.p.m. with 150° F. evaporation temperature and a Δt of 8° F. With a U of 2500, such a unit would have a capacity of about 350,000 gallons per day and the estimated water cost would be $0.94 to $1.07 per 1000 gallons, depending on the life of the equipment. It was concluded that this still is competitive with other distillation processes at the same capacity. Further work to study scale formation and corrosion was recommended.

Aquastills, Inc., Rochester, N. Y., is working on the development of a small, automatic rotary still of the Hickman type for household use, with a capacity of about 500 gallons per day. Six models have been built to date. The still operates at a low evaporation temperature of about 120° F. and consumes about 60 kw.-hr. per 1000 gallons, when operating on city water, and about 80 on sea water. None of these units is ready for the market.

Before leaving the subject of the Hickman still it may be of interest to call attention to a paper by Bromley (*8*), in which the theory of the Hickman type of still is developed and applied to the prediction of the performance with fair success.

The Glover still (*9*) is a modification of the Hickman. Preliminary results with a unit having a 25-inch rotor were not very encouraging. Water quality was very poor, because of excessive entrainment. The salt content of the brine was reduced only by 60 to 70% at best and often less. Since the rotor carrying the evaporation surface is also the vapor-compressor, capacity depends greatly on speed of rotation. The higher the speed, the greater the compression ratio and hence the Δt across the evaporation surface. Capacity also depends considerably on the evaporation temperature since increase in temperature increases not only U but also Δt because of the higher vapor density. Rotor speeds are higher than for the Hickman still, varying in the tests from 150 to 3500. For some unexplained reason, U decreased as speed increased, contrary to prediction. Power requirements were extremely high. Even at the theoretically calculated production rate, energy requirement was 1500 kw.-hr. per 1000 gallons and the lowest figure cited (basis not clear) was 215 kw.-hr. per 1000 gallons. In spite of these fantastic power requirements and very low water purity, further tests were recommended after "limited modifications."

The evaporator developed by Clark and Bromley (*10*) at the University of California is, as far as I know, the first and only one of the rotary stills using the multiple-effect principle in one unit. Of course, individual rotary stills could be coupled together to make a multiple-effect system, but a much more compact unit is obtained by placing rotating evaporator plates in close proximity inside a shell. The evaporator in question has 29 evaporator plates, 4 feet in diameter and spaced 9/16 inch apart. The complete unit including evaporator plates, heat exchangers, and the housing is rotated at about 1000 r.p.m. The vapor evolved from the upper surface of an evaporator plate is condensed on the under surface of the plate above and is carried to the periphery by centrifugal force.

Equations were developed to predict the performance of such an evaporator under a variety of operating conditions, and solved by computer. A few of the predicted results are given, along with results of four test runs on city water and San Francisco Bay water. Operation was with steam at 209° F. and a steam economy of 21.5 to 23.3 pounds evaporated per pound of steam was achieved. This corresponds to a w_1 of 0.98 in Equation 3, which is remarkably high for any

multiple-effect evaporator. Agreement between predicted and measured performance was reasonably good. The power required to rotate the evaporator was about 34 kw.-hr. per 1000 gallons of product, which is about as much as the total energy requirement of a vapor-compression unit, but this can undoubtedly be reduced by careful design and also by reducing the speed of rotation. The economic optimum speed is probably considerably less than 1000 r.p.m. Production rates of 7000 gallons per day were achieved, compared to the design rate of 10,000. At the latter rate the product was contaminated by flooding of the waste stream into the product. A two-effect evaporator with 2-foot-diameter plates and some modifications in mechanical design is under construction.

As far as we know, no attempt has been made to scale up this evaporator or to predict costs for any capacity. Although the steam economy is much greater than that of a conventional multiple-effect system, it seems doubtful if this type of evaporator will be competitive on a large scale with other types, because of capital costs. Its main field of application would seem to be for relatively low capacity.

Long-Tube, Vertical (LTV) Multiple-Effect Evaporator. The results on heat transfer, scale prevention, and corrosion obtained from the pilot plant operation have been given above. A description of the pilot plant is available from other sources. Work at the pilot plant is being continued through a contract with W. L. Badger Associates, Inc., and will be directed toward further study of the prevention of scale and corrosion, especially at temperatures above 250° F.

We confine our discussion to reviewing some of the estimates made for large plants, though even these were made several years ago. Two basic flowsheets were considered. One used exhaust steam from a power plant to operate the multiple-effect system and the cost of this steam was estimated on the basis that the electric-energy cost should be the same whether the steam was exhausted at a high back-pressure or at the conventional high vacuum. Putting it another way, the loss in value represented by the lower quantity of electric energy generated was to be compensated for by the value of the bled steam.

This scheme assumes that all the electric energy developed, which might be of the order of 85 kw.-hr. per 1000 gallons of water product, could be sold at a reasonable price. The other flowsheet assumed that no electric energy could be sold and so the mechanical power of the turbine was used to drive a vapor compressor operating a vapor-compression evaporator. The turbine would still exhaust at a high enough back-pressure to operate a multiple-effect evaporator. The reason that the steam is not expanded to a high vacuum and the entire evaporation carried on by vapor compression is purely one of economics. Because of the high cost of the compressor, the combination plant is appreciably cheaper than one using vapor compression alone. Some estimated total costs of fresh water for plants of various sizes, based on the pilot plant results are:

Plant capacity, gal. per day	10^6	10^7	2×10^7
Cost, cents per 1000 gal.	1000	55	35

Flash Evaporation. This type of evaporation is probably the most widely used at the present time, at least for other than relatively small units where vapor compression may lead. Large land-based units are located in Kuwait, Bermuda, Bahama Islands, Virgin Islands, Oxnard, Calif., Isle of Guernsey, and Venezuela and there are also large shipboard units. The largest single unit has a capacity of about 1,250,000 gallons per day. The Guernsey unit has 40 stages with a capacity

of 500,000 gallons per day and a performance ratio of 11 (pounds of water produced per pound of steam).

From a purely thermodynamic point of view, this process is less efficient than ordinary evaporation and this is reflected in the fact that many more stages are required to obtain comparable steam economy. The reason for its low efficiency can be visualized by considering the simple diagram shown in Figure 2.

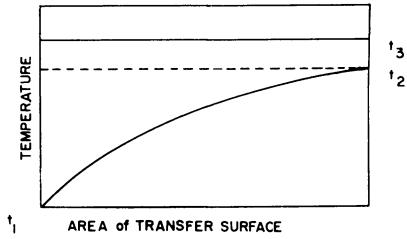

Figure 2. Temperature difference in evaporators

t_1. Temperature of feed entering stage
t_2. Temperature of boiling solution or final temperature of feed from stage of flash evaporator
t_3. Temperature of condensing steam

For a given minimum Δt for heat transfer in either a boiling or a flash stage ($t_3 - t_2$ in Figure 2) the mean Δt in the flash type is greater because the temperature of the brine is increasing, whereas in the boiling evaporator it remains constant. Therefore the thermodynamic irreversibility is inherently greater in the flash type. On the other hand, the greater irreversibility means a greater driving force for heat transfer for the same minimum Δt and hence less surface area required for the same over-all coefficient of heat transfer.

A flash evaporator can be analyzed to show the effect of variables on the economy, by writing heat and material balances around each stage. When done in a rigorous manner, the result is so complex because of the large number of stages that it becomes necessary to solve with the aid of a digital computer. This has been done by the Fluor Corp.; details of the development of the equations and their solution are given in a report to the Office of Saline Water (*17*). The variables considered were number of stages, terminal temperature difference (TTD), and concentration ratio. The relationship among performance ratio (pounds of product per pound of steam), terminal temperature difference, and number of stages for a concentration ratio of 2 and brine inlet and outlet temperatures–i.e., to the flash system–of 220° and 90° F., respectively, is shown in a graph (*7*).

Some other characteristic differences between flash and boiling evaporators may be of interest. In a boiling exaporator, if the Δt across the heating surface is fixed, the number of effects and hence the performance are fixed for a given over-all temperature range. This is not at all the case for the flash system, where for a given terminal temperature difference the number of stages can vary from 1 to infinity. [In the theoretical treatment of flash evaporation, an infinite number of stages is commonly used as a limiting case. This is not correct, because the number of stages is limited by boiling point elevation, just as is the number of effects in boiling evaporation. For example, Dodge and Eshaya (*13*) showed that for a certain range of temperatures the maximum possible number of effects was 107.

The argument is purely academic, of course, because the thermodynamic limit is well above the economic limit and from a practical standpoint the difference between the maximum possible and infinity is of no consequence.] This is easily seen from the Fluor data and also from curves published by Mulford (*27*) based on a simplified theory. For example, the Fluor calculations show that a given performance ratio of 10 can be obtained with 20 stages and a 2.5° F. TTD and also with 100 stages and a 7.5° F. TTD. The flash system is more flexible, in that the number of stages can be varied independently of the economy or, putting it another way, the economy of a flash system is much less dependent on the number of stages than that of a boiling evaporator. Another advantage of a flash evaporator over the boiling type is that a decrease in rate of heat transfer due to fouling of the surface, or possibly other causes, can be compensated for by an increase in brine circulation.

The Fluor Corp. report (*17*) contains a large amount of useful data on flash evaporators for sea water. It also is concerned with the optimization of a flash system for minimum total cost, and the calculations yielded the following optimum conditions for a 50,000,000-gallon-per-day plant:

Number of stages	52
Terminal temp. difference	4° F.
Concentration ratio	1.7

For a multiple-effect boiling evaporator the optimum number of effects would probably lie between 10 and 20. The absolute values naturally depend on the particular conditions and unit costs chosen, but the relative numbers for the two systems would probably not change very much.

By making certain simplifying assumptions, the mass and heat balance equations can be reduced to the following very simple form, which is a good approximation useful for many calculations:

$$P = \text{performance ratio} = \frac{\text{pounds of distillate}}{\text{pounds of steam}} = \frac{n(R - \Delta t)}{R + n\Delta t} \qquad (12)$$

where

n = number of stages
R = over-all temperature range or difference in temperatures of brine entering and leaving the flash system, ° F.
Δt = terminal temperature difference across the condensers, ° F.

This equation, or one very similar to it, was given by Mulford (*27*) without derivation. An equation involving similar simplifying assumptions has been given by Frankel (*18*), but only for the case of an infinite number of stages.

Using Equation 12 one can arrive at the following figures:

$$n = 20,\ R = 160\ (250 \text{ to } 90),\ \Delta t = 5,\ P = 11.0$$

Since Equation 12 assumes no heat loss, the comparable performance ratio for a 20-effect boiling evaporator would be 20. If $\Delta t = 0$, Equation 12 reduces to $P = n$, the same as for the boiling evaporator, but this would require an infinite heat-transfer surface. (Experimental flash evaporators have been successfully operated with a Δt as low as 1° F.) One can conclude that a boiling evaporator requires less steam than a flash evaporator if the comparison is made under reasonably comparable conditions, a conclusion already reached from general thermodynamic considerations.

Although a flash evaporator needs more stages than a boiling evaporator for

the same performance, it has a design advantage in that the various stages can be combined into a single unit, which gives a cheaper construction and also eliminates much of the external piping needed by the boiling type. Since the evaporation does not occur in contact with the heating surface, the flash type should give less trouble from scale than the boiling type. There appear to be no actual operating data in the literature to confirm this conclusion.

Frankel (*18*), in addition to a discussion of the simplified theory of flash evaporation, gives some data on the properties (boiling point elevation and specific heat) of saline solutions and a considerable amount of information on the design of this type of evaporator. He also discusses various development problems which were investigated in two test rigs, one for heat-transfer and scale-deposition studies and one for entrainment and water-purity studies. The first one had only two stages but corresponded in capacity to a fully staged evaporator producing about 50,000 gallons per day. Results with this rig have been given under the headings of heat transfer and scale prevention. The second rig, containing three flash chambers, was used to test the effect of several variables and the design of entrainment separators on the purity of the product. Very few results were presented, but those given for one type of separator showed that purities of the order of 10 p.p.m. were obtained.

Frankel believes that the majority of the large land-based plants built in the near future will be of the flash type.

Brice and Townsend (*7*) state that the practical limit, on the basis of current technology, to the size of flash-evaporation units is in the range of 25,000,000 to 30,000,000 gallons per day. They also give some information on mechanical design of units of this size.

An English firm has been awarded a contract by OSW to study the multistage flash-distillation process, with the objective of improving its efficiency by developing more economical designs of the flash chambers.

Vapor Compression. A group in the Department of Engineering (*25*) at UCLA is working on the improvement of existing commercial models of small vapor-compression stills and on the recovery of heat in the exhaust gases from a Diesel engine driving the compressor of a vapor-compression evaporator. The heat in the gases will be transferred to the feed water going to the evaporator. No results have been reported.

The most comprehensive published study of vapor compression is that of Dodge and Eshaya (*15*). This was an engineering and economic study of a forced-circulation, flash-evaporation process which also featured dropwise condensation of steam to increase the capacity of the equipment. Some of the most pertinent facts which emerged from this study were: The optimum brine velocity in the tubes of the main heat exchanger was in the range of 7.5 to 8.5 feet per second for the particular unit cost assumptions. The cost of energy for brine recirculation was only about 3 cents per 1000 gallons of product. The optimum Δt in this exchanger was around 5° F. The optimum fraction of the brine which is flashed to steam in one pass through the heater is about 0.004. Power requirement of the vapor compressor was about 45 kw.-hr. per 1000 gallons and for the brine recirculation pump it was 4.5 kw.-hr.

The use of exhaust steam from turbines driving the compressor to heat the feed would make a very significant reduction in the size of the auxiliary heat exchangers (those exchanging heat between feed, product water, and waste brine) and reduce the cost of water by about 7 cents per 1000 gallons. The cost of product from a 10,000,000-gallon-per-day plant was estimated to be in the range of

69 to 86 cents per 1000 gallons, depending on various circumstances. Corresponding capital costs ranged from $1.60 to $2.09 per gallon per day.

The size of vapor-compression units is probably limited by the size of compressors available. Some calculated figures on the relation among plant capacity, evaporation temperature, and intake volume to the compressor are given in Table IV.

Table IV. Relation of Compressor Capacity to Plant Capacity for a Vapor-Compression Process

Intake Vol., Cu. Ft./Min.	*Temp., ° F.*	*Plant Capacity, Gal./Day*
100,000	160	213,000
500,000	160	1,065,000
	212	3,180,000
1,000,000	160	2,130,000
	212	6,360,000

An axial compressor with a capacity of 1,000,000 cubic feet per minute or even larger seems to be entirely feasible at the present time and hence unit capacities of 2,000,000 to 6,000,000 gallons per day seem to be reasonable. The largest vapor-compression unit in operation that has come to our attention has a capacity of 250,000 gallons per day, but the Roswell, N. M., plant will have four times this capacity.

Some Process Comparisons. Let us make a rough comparison between vapor compression and multiple-effect boiling evaporation under the following assumed conditions:

1. Fuel oil is the energy source in both cases.
2. Steam is generated at 850 p.s.i.g. and 815 ° F. and costs 55 cents per 1000 pounds.
3. Steam is first used in turbines to generate power and for the multiple-effect system is exhausted at 20 p.s.i.g. from the turbines and for the vapor-compression system at 1 inch of mercury absolute.
4. Over-all turbine efficiency is 75%.
5. The multiple-effect system uses 12 effects and produces 10 pounds of water per pound of steam.
6. Temperature difference in vapor-compression evaporator is 5° F. (boiling-type evaporator).
7. Vapor to compressor at 1 atm. and 214° F.
8. Over-all efficiency of compressor is 75%.
9. Electric energy can be sold for 7 mills per kw.-hr.

On the basis of these assumptions the figures in Table V were calculated per 1000 gallons of product.

Table V. Comparison of Vapor-Compression and Multiple-Effect Boiling Evaporators

By-product electric energy from multiple-effect operation, kw.-hr.	56
Steam used by multiple-effect, lb.	833
Steam used by vapor-compression evap., lb.	275
Work of compression, kw.-hr.	33
Value of by-product energy, cents	39.1
Cost of steam to multiple-effect, cents	45.9
Net cost of steam for multiple-effect, cents	6.8
Cost of steam for vapor-compression, cents	15.1
Selling price of by-product energy for break-even, mills per kw.-hr.	5.5

As long as by-product electric energy can be sold for higher than 5.5 mills per kw.-hr., the energy cost for the multiple-effect system will be less than for vapor compression for the particular conditions chosen.

The over-all temperature range for multiple-effect is about 170° F. and subtracting 10° F. for boiling point elevation leaves 160° F. as the total Δt for heat transfer or 13.3° per effect. If the heat-transfer coefficients were the same in the two systems, the vapor-compression system would require about 13.3/5 or 2.65 times as much heating surface as the multiple-effect. In the process proposed by Dodge and Eshaya the over-all U was estimated to be about 2000 compared to about 500 to be expected for the LTV multiple-effect evaporators. A vapor-compression system using the Dodge and Eshaya process would require less heat-transfer surface but at the expense of increased power to pump the brine. Finally, the compressor is likely to cost nearly as much as the heating surface, and we are forced to conclude that a vapor-compression plant is not likely to be competitive with multistage evaporation, either boiling or flash type, if by-product electric energy can be sold at a reasonable figure. If the electric energy cannot be sold, it becomes advantageous to operate a vapor-compression plant in conjunction with multistage evaporation.

Gillam (*20*) compared costs of a 12-effect LTV evaporator and a 16-stage flash evaporator, both for a capacity of 1,000,000 gallons per day. Some rounded figures are given in Table VI.

Table VI. Cost Comparisons of Multiple-Effect Long-Tube Vertical, Film-Type, Boiling Evaporator and Multistage Flash Evaporator

	LTV	*Flash*
Capital cost for 10^6 gal./day	$915,000	$1,350,000
Cost per 1000 gal. of product (operating plus charges on investment)	$0.96	$1.19

He also noted that charges based on the investment for distillation plants vary from 40 to 58% of the total, energy costs from 20 to 50%, and operating costs from 9 to 29%. A capital cost of $1.00 per gallon per day is a good round figure for estimating cost of plants whose capacity is in the neighborhood of 1,000,000 gallons per day.

Wiped-Film Evaporator. The only reported work on this type of evaporator is by the General Electric Co. on a small experimental unit based on a copper tube 6 inches in diameter and 50 inches long with 0.05-inch wall. [Since this was

Table VII. General Information

Process	*Feed*	*Location*	*Capacity, Gal./Day*
LTV multiple-effect evaporator (12 effects)	Sea water	Freeport, Tex.	1,000,000
Flash evap., 36 stages	Sea water	San Diego, Calif. (Point Loma)	1,000,000
Forced-circulation vapor compression combined with multiple effect[a]	Brackish well water	Roswell, N. M.	1,000,000

[a] First case of which we are aware in which more than one effect has been used with vapor compression. 2, or at most, 3 effects will be used. The saving in energy over that for a single effect is not great but appears

written we have learned of work on a similar evaporator by the Department of Engineering, UCLA (37). Their work is with a wiped film on the outside of a 4-inch-diameter copper tube, thus allowing visual observation.] The following variables were investigated:

1. Shape of wiper blade and angle with tube wall
2. Material of wiper blade
3. Rate of feed
4. Method of feed distribution
5. Two different pitches of grooves on outside wall of tube
6. Over-all temperature difference (5° to 25° F.)
7. Temperature level (170° and 195° F.)

The wiper had four blades, 90° apart, and was rotated at 200 r.p.m., in all tests. The feed was jetted onto the wall just above the wiper blades and about 40% of it was evaporated. Hagevap was added to the extent of 2 p.p.m. to control scale. Noncondensable gases were removed from the feed by flashing it into a packed-column deaerator.

The grooves on the outside surface of the copper tube, which had a height of 0.026 to 0.040 inch and a pitch of 0.04 to 0.06 inch, evidently promoted dropwise condensation, since in some tests the steam-film coefficient was estimated to be as high as 10,000 in the usual units. The power requirement for the wiper was estimated to be $^1/_4$ hp. for an 8000-gallon-per-day still, so that the cost of the power is negligible. The total energy requirement will depend mainly on the power to compress the steam and this would be no different than for any other vapor-compression process. This statement was made because a recent news report claims that this evaporator requires only one fourth as much energy as other conversion systems.

Results of the tests with this unit have been reported in a research and development report of the Office of Saline Water.

No cost data are available on this evaporator and no information on how it might be scaled up to a large unit. It might find special uses where compactness is very important but is not likely to be generally competitive with other distillation methods, at least for large capacities. Recently the General Electric Co. has been awarded a contract by OSW to build and operate a 37,000-gallon-per-day pilot plant to develop this type of evaporator further.

Demonstration Plants of Office of Saline Water. Three of the five demonstration plants planned by the Office of Saline Water use distillation processes. Some general information on these three plants is given in Table VII.

on Demonstration Plants

Designer	*Constructor*	*Present Status*
W. L. Badger Associates	Chicago Bridge and Iron Co. Plant cost $1.26 per gpd	In operation since June 1962
Fluor Corp.	Westinghouse Electric Corp. contract price of $1.61 per gpd	In operation since February 1962
Catalytic Construction Co.	Chicago Bridge and Iron Co. contract price $1.79 per gpd	Under construction

to be significant. Although the steam is re-utilized by the multiple effects, the pressure difference against which the compressor must operate is correspondingly increased and this partly offsets the gain from steam re-use.

Literature Cited

(1) Arons, A. B., Kientzler, C. F., *Trans. Am. Geophys. Union* **35,** No. 5 (1954).
(2) Badger Associates, Inc., W. L., "Operation of Pilot Plant LTV Evaporator at Wrightsville Beach, North Carolina," Final report under Contract No. 14-01-001-93 (Sept. 30, 1960).
(3) Badger Associates, Inc., W. L., Office of Saline Water, Research and Development Progr. Rept. **25** (July 1959).
(4) *Ibid.*, **26,** PB 161,290 (1959).
(5) Banchero, J. T., Gordon, K. F., ADVAN. CHEM. SER., No. **27,** 105–14 (1960).
(6) Battelle Memorial Institute, Office of Saline Water, Research and Development Progr. Rept. **43** (September 1960).
(7) Brice, D. B., Townsend, C. R., ADVAN. CHEM. SER., No. **27,** 147–55 (1960).
(8) Bromley, L. A., *Ind. Eng. Chem.* **50,** 233 (1958).
(9) Bureau of Reclamation, Saline Water Demineralization Laboratory, U. S. Dept. Interior, Denver, Colo., Rept. **R-SWD-5** (June 6, 1960).
(10) Clark, R. L., Bromley, L. A., *Chem. Eng. Progr.* **57,** 64–70 (January 1961).
(11) Clark, R. L., Nabavian, K. J., Bromley, L. A., ADVAN. CHEM. SER. No. **27,** 21–6 (1960).
(12) Dodge, B. F., *Am. Scientist* **48,** 476–513 (1960).
(13) Dodge, B. F., Eshaya, A. M., ADVAN. CHEM. SER., No. **27,** 7–20 (1960).
(14) Dodge, B. F., Eshaya, A. M., "Development of a Pilot Plant for a Forced-Circulation and Dropwise Condensation Vapor-Compression Evaporator and an Experimental Program," Rept. to OSW under Contract 14-01-001-172 (September 1959).
(15) Dodge, B. F., Eshaya, A. M., "Economic Evaluation Study of Distillation of Saline Water by Means of Forced-Circulation Vapor-Compression Distillation Equipment, Office of Saline Water, Research and Development Progr. Rept. **21.**
(16) Fink, F. W., ADVAN. CHEM. SER., No. **27,** 27–39 (1960).
(17) Fluor Corp., Ltd., Whittier, Calif., Office of Saline Water, Research and Development Progr. Rept. **34,** PB 161,010 (1959).
(18) Frankel, A., *Proc. Inst. Mech. Engrs.* (*London*) **174,** 321–24; discussion 325–61 (1960).
(19) General Electric Co., Final Report under Contract Nobs –78202, "Evaluation of a Thin-Film, Sea-Water Distillation Unit for Marine Application," July 1960.
(20) Gillam, W. S., Annual Meeting, A.I.M.E., New York, February 1960.
(21) Hickman, K. C. D., Hogan, W. J., Eibling, J. A., Hogan, W. J., ADVAN. CHEM. SER., No. **27,** 128–46 (1960).
(22) Lacey, R. E., Lang, E. W., Feazel, C. E., Office of Saline Water, Research and Development Progr. Rept. **42** (March 1961).
(23) Langelier, W. F., Caldwell, D. H., Lawrence, W. B., *Ind. Eng. Chem.* **42,** 126–30 (1950).
(24) Lustenader, E. L., Richeter, R., Neugebauer, F. J., *J. Heat Transfer* **81,** 297–306 (November 1959).
(25) McCutchan, J. W., *et al.*, Univ. California, Los Angeles, Dept. Engineering, Rept. **60–70,** 27–33 (1960).
(26) McIlhenny, N. F., Office of Saline Water, Saline Water Research and Development Progr. Rept. **62** (May 1962).
(27) Mulford, S. F., Proceedings, Symposium on Saline Water Conversion, Natl. Acad. Sci.–Natl. Research Council, Pub. 568, 91–102 (1957).
(28) Nobe, K., Univ. California, Los Angeles, Dept. Engineering, Rept. **60–70,** 91–103 (1960).
(29) Othmer, D. F., Beneati, R. F., Goulandris, G. C., *Chem Eng. Progr.* **57,** 47–51 (January 1961).
(30) Ruben, I. A., Commerford G., Dretert R., Office of Saline Water Research and Development Progr. Rept. **49** (March 1961).
(31) Sourirajan, S., Univ. California, Los Angeles, Dept. Engineering, Rept. **60–70,** 77–89 (1960).
(32) Sourirajan, S., Kennedy, G. C., *Am. J. Sci.* **260,** 115–41 (1962).
(33) Sparrow, E. M., and Gregg, J. L., *J. Heat Transfer,* **81,** 113–19 (1959).
(34) Standiford, F. C., Jr., Bjork, H. F., ADVAN CHEM. SER., No. **27,** 115–27 (1960).
(35) Standiford, F. C., Jr., Sinek, J. R., *Chem. Eng. Progr.* **57,** 58–63 (January 1961).
(36) Tribus, M., *et al.*, "Thermodynamic and Economic Considerations in the Preparation of Fresh Water from the Sea," UCLA Rept. **59–34** (September 1960).
(37) University of California, Los Angeles, Calif., Repts. **61–26, 61–37** (1961).
(38) Wilke, C. R., *et al.*, Univ. of California, Institute of Engineering Research, Progr. Rept. **75–23** for year ending June 30, 1960, pp. 9–11.
(39) *Ibid.*, Rept. **75–24** for year ending June 30, 1961.
(40) Woodward, T., *Chem. Eng. Progr.* **57,** 52–7 (January 1961).

RECEIVED June 18, 1962.

Recovery of Minerals from Sea Water by Phoshate Precipitation

MURRELL L. SALUTSKY and MARIA G. DUNSETH
Washington Research Center, W. R. Grace & Co., Clarksville, Md.

The oceans contain practically every element and could be an inexhaustible source of many minerals. Only salt, magnesia, and bromine are now recovered. Future recovery of other minerals will be enhanced by the need for fresh water, making the processing of large volumes of sea water necessary. Many elements in sea water are precipitated with ammonium (and sodium) phosphate. Almost complete removal of calcium and magnesium eliminates scale, which seriously handicaps some water recovery processes. The precipitate (essentially magnesium ammonium phosphate containing calcium and trace elements) is an excellent fertilizer and has commercial value. When the scale-forming elements are precipitated with sodium phosphate in the absence of ammonia, potassium is precipitated as magnesium potassium phosphate. Treatment with ammonium bicarbonate solution converts this compound to magnesium ammonium phosphate and a potassium bicarbonate solution, from which various potassium chemicals are made. Other minerals may be recovered from the phosphate precipitates.

The dissolved solids present in sea water contain practically every known element. This aqueous mine contains an immense quantity of material. The dried solids in the oceans would form a layer approximately 500 feet thick over the entire land area of the earth. Obviously, the total amounts of even the trace elements are tremendous. For example, a ton of sea water contains only milligram quantities of uranium, but the total uranium content in the oceans is several hundred billion tons. If methods of extraction were economically feasible, the oceans would serve as an inexhaustible source of many substances.

One factor of utmost importance is that the oceans are so accessible; of even more consequence, the constituents are in solution. Much effort and cost are often involved in dissolving solids prior to further processing and ultimate recovery of desired products. So the fact that sea water is a solution, admittedly dilute, has

definite technological importance. Because of the great dilution, it has not been economical in the past to recover most minerals from sea water. It did not seem reasonable to pump the tremendous quantities of water necessary to recover these minerals. Today the picture is changing rapidly. It will be necessary to pump large quantities of water for the desalinization of sea water.

The quantities of chemicals produced from the major mineral constitutents of the sea will be extremely large. Fortunately, there are several large chemical industries which could probably consume significant proportions of these quantities. Two examples are the fertilizer industry and the chlor-alkali industry. Currently, 25,000,000 tons of fertilizer are sold each year (9) in the United States, containing 7,600,000 tons of major plant nutrients (2,800,000 tons of N, 2,600,000 tons of P_2O_5, and 2,200,000 tons of K_2O). It has been estimated (4) that by 1965 the chlor-alkali industry will sell 19,000,000 tons of products per year, including 5,700,000 tons of chlorine, 4,700,000 tons of caustic soda, 6,100,000 tons of soda ash, and 1,300,000 tons of hydrochloric acid.

Composition of Sea Water

The composition of sea water is shown in Table I. Sea water is approximately 96.5% water and 3.5% dissolved salts. Sodium chloride amounts to about 3% of the sea water, and the remaining constituents—primarily Mg, S, Ca, K, Br, C, Sr, and B—are present to the extent of 0.5%. All other elements represent only 0.0005%. Obviously, some elements are present at extremely minute concentrations.

Table I. Composition of Sea Water

	%		%
Salts	3.5	K	0.039
Cl	1.9	Br	0.0065
Na	1.1	C	0.002
Mg	0.13	Sr	0.001
S	0.09	B	0.001
Ca	0.041	Others	0.0005

Unlike river water, sea water contains considerably more magnesium than calcium (Table I). Calcium is precipitated in the sea as carbonates and used by various forms of sea life to form shells. Another interesting fact about sea water is that the potassium content is nearly equivalent to the calcium content.

Current Products from Sea Water

The products currently produced from sea water are listed in Table II. Solar salt (sea salt) is produced by evaporating sea water until the sodium chloride crystallizes. The resultant salt is separated from the bittern (primarily magnesium and potassium salts), washed with fresh water, and dried. Solar salt is used largely by the chemical industry in coastal areas, but in some parts of the world it is a source of salt for human consumption.

Magnesia is currently produced from sea water by adding lime to the sea water in the form of either dolomite or calcined oyster shells. The lime precipitates magnesium hydroxide, which is filtered, washed, and calcined to magnesia. Bromine is separated from sea water by displacement with chlorine or by adding both chlorine and aniline to the water to produce tribromoaniline. Iodine is produced indirectly from sea water by extraction from various forms of seaweed.

Table II. Products from Sea Water

Current	*Future*
Salt	Fertilizer
Magnesia	Potassium chemicals
Bromine	Chlorine
Iodine (indirect)	Caustic soda
Fresh water	Various metals

Increasing population and industrial requirements have made it necessary in some parts of the world to recover fresh water from sea water. The total world production of fresh water from sea water today, produced mostly by distillation processes, amounts to more than 25,000,000 gallons per day. A rather rapid increase in water production is anticipated. For example, Israel plans to integrate its coastal power plants with sea water conversion units in order to produce 50 billion gallons of water per year to supplement its natural water resources (*11*).

Future Products from Sea Water

Some of the future products which may be separated from sea water are also listed in Table II. One of these is fertilizer. For several years research has been carried out on a new type of high analysis, nonburning fertilizer based on magnesium ammonium phosphate and other metal ammonium phosphates (*3*). Precipitation of metal ammonium phosphates is illustrated by Equation 1:

$$MeCl_2 + H_3PO_4 + 3NH_3 + xH_2O \rightarrow \underline{MeNH_4PO_4.xH_2O} + 2NH_4Cl \qquad (1)$$

where $x = 0$, 1, 3, or 6

and Me = Mg, Fe, Mn, Cu, Zn, Co, Ni, Cd, Be, or UO_2.

The metal ammonium phosphates are a group of compounds of low solubility consisting of a divalent metal, ammonium, and phosphate ions with 0, 1, 3, or 6 moles of water of crystallization (*2*). Magnesium ammonium phosphate, the best known compound of the series, exists in two hydrated forms—i.e., with either 1 or 6 moles of water.

Extensive agricultural tests with magnesium ammonium phosphate have shown that this compound has unusual and highly desirable properties as a fertilizer or fertilizer ingredient. In addition to the major plant nutrients, N and P_2O_5, magnesium ammonium phosphate contains the important secondary nutrient Mg, which is a constituent of chlorophyll. In granulated form it is nonburning to plants (seeds have been germinated and plants have been grown in the pure fertilizer containing no soil), it is long-lasting (after a year under vegetables granules of the compound were still present in the soil), and, because of its low solubility, which is believed to be about optimum for efficient consumption by plants (about 0.02 gram per 100 ml. of water), the compound does not leach from sandy soils, as do most other nitrogen-containing fertilizers. Magnesium ammonium phosphate has shown considerable promise in the fertilization of a large variety of plants, including tree seedlings, ornamentals, grasses, and vegetables. This compound is currently produced from conventional raw materials (*5*). Its production directly from sea water offers an inexpensive and inexhaustible source of magnesium and various trace elements.

Some potassium chemicals are currently separated from sea water by fractional crystallization of the bittern from solar salt production. Several years ago the Dutch operated a process which utilized dipicrylamine to precipitate potassium from sea water, but this reagent is rather costly. We are developing a

process which seems promising for recovery of potash from sea water by precipitation of an insoluble magnesium potassium phosphate. The process is discussed in more detail below.

It would seem that the concentrated brine from the evaporators of a distillation plant could be utilized for the production of chlorine and caustic soda in a diaphragm cell. If the sea water had been originally stripped of calcium, magnesium, and other heavy metals (by phosphate precipitation as discussed below), the brine should be suitable for the chlor-alkali industry. It is necessary to remove calcium and magnesium from natural salt before preparing a charge for the diaphragm cells.

It can be anticipated that various other metals will eventually be separated either from sea water or from the waste evaporator brine. Many metals are concentrated from sea water by phosphate precipitation during production of the magnesium ammonium phosphate fertilizer. Future metal recovery processes may utilize the fertilizer as a raw material. Because the evaporator brine contains a high concentration of chloride, a number of metals will be present in it as chloride complex anions (7). Many of these complex anions may be removed from the brines on an anion exchange resin such as Dowex 1 and then recovered from the resin simply by washing the column with fresh water.

Descaling Sea Water and Producing High Analysis Fertilizer

One of the most serious problems encountered in the recovery of fresh water from sea water (and other saline waters) is the formation of scale within the equipment used in some of the processes. The scale consists of insoluble compounds of calcium, magnesium, iron, and other metals which are gradually deposited on the vessel walls. After a time, the scale formation builds up to a point where the operation must be interrupted so that the deposit may be removed. This is costly in both labor and loss of production.

The scale is primarily a mixture of calcium carbonate, magnesium hydroxide, and calcium sulfate. The first two are alkaline compounds, formed as a result of the loss of carbon dioxide from the water. The formation of this type of scale can be eliminated by addition of sufficient acid to maintain a pH too low for its precipitation. However, the addition of acid does not prevent the formation of calcium sulfate (gypsum). Currently, distillation equipment is operated at temperatures and concentrations such as to minimize the formation of gypsum—i.e., avoiding conditions under which the solubility product of calcium sulfate is exceeded or operating for a short time under the metastable condition of supersaturation. Generally, only about 1 gallon of fresh water is recovered from 2 gallons of sea water. The brine concentration factor (or blowdown ratio) is 2 to 1.

If the scale problem did not exist, more water could be recovered by distillation. A concentration factor of 4 to 1 and possibly higher has been postulated. The scale decreases the efficiency of the distillation equipment. If it did not form, the equipment could be operated at higher temperatures and could be smaller, with considerable savings on capital costs. If the scale problem did not exist, electrodialysis equipment could be operated more efficiently, because the scale (particularly the gypsum) tends to foul the membranes.

One method of solving the scale problem is to remove calcium and magnesium from sea water completely or to lower their concentration to a point at which the solubility products of the scale compounds [$CaCO_3$, $Mg(OH)_2$, and $CaSO_4 . 2H_2O$]

are not exceeded. This could be done by precipitation and removal of insoluble magnesium and calcium compounds, but the method would be practical only if the cost of the precipitating agents was low or the value of the precipitated compounds was high. Because of the very large quantities of materials involved, a large market for the resulting by-products would be necessary. Research has been carried out (supported partly by the Office of Saline Water) to determine the feasibility of preparing a high analysis fertilizer from elements removed in the pretreatment of raw sea water (*6*, *8*).

The flowsheet of the process for descaling sea water and simultaneously producing a high analysis fertilizer is shown in Figure 1. Wet process phosphoric acid (or sodium phosphates obtained from reaction of wet process phosphoric acid and sodium hydroxide or soda ash) and anhydrous ammonia are added continuously to the raw sea water to precipitate the scale-forming elements as metal ammonium phosphates and other phosphates. The precipitated solids are removed from the sea water by settling and the descaled sea water is pumped to the saline water conversion plant.

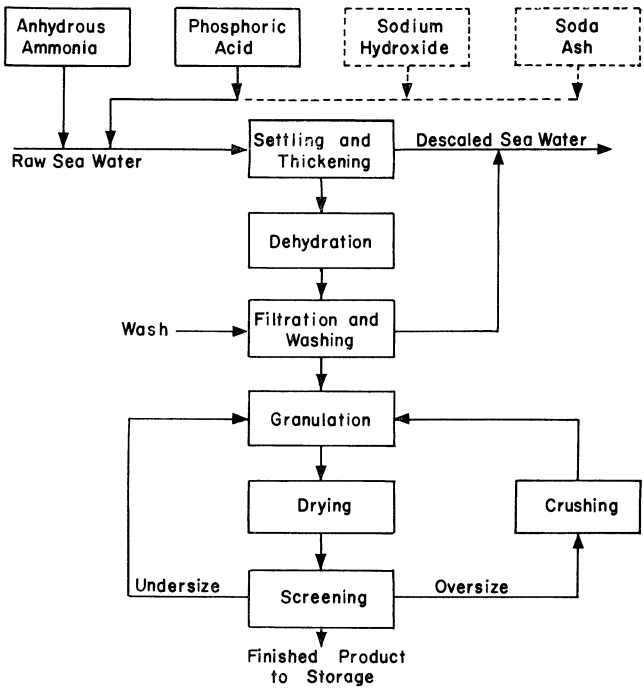

Figure 1. Process flowsheet for descaling sea water and producing fertilizer

The settled slurry containing about 17 to 20% solids is then heated to 90° C. to convert the magnesium ammonium phosphate hexahydrate to the monohydrate. After dehydration, the slurry is filtered. The filter cake is washed, mixed with recycled fines, and granulated. The granules are dried, screened, and then conveyed to product storage. It is necessary to wash the filter cake only if the chloride content of the dried product must be less than 1%—for the few crops that are sensitive to chloride, such as tobacco.

The fertilizer produced from the scale-forming elements is a mixture of magnesium ammonium phosphate, calcium hydrogen phosphate, and trace metal phosphates including iron, zinc, copper, manganese, cobalt, and nickel. The fertilizer contains approximately 7% nitrogen, 43% phosphoric acid(P_2O_5), 21% magnesium oxide, and 5% calcium oxide. For each million gallons of sea water descaled, about 37 tons of fertilizer would be produced.

The residual magnesium and calcium content in descaled sea water, determined by emission spectroscopy, is shown in Table III. The residual magnesium and calcium concentration decreases with increasing pH of precipitation. For comparison, the average concentration of magnesium and calcium in raw sea water is also given. At pH 8.5 only about 0.25 and 5% of the magnesium and calcium, respectively, remained in the treated sea water. Chemical analyses of the phosphate precipitates obtained at pH 8.5 gave a magnesium and calcium recovery of approximately 100 and 97%, respectively.

Table III. Residual Mg and Ca in Descaled Sea Water

Pptn. pH	*Mg, P.P.M.*	*Ca, P.P.M.*
7.2	174	92
7.9	25	56
8.5	3	20
Sea water	1200	400

Magnesium ammonium phosphate hexahydrate contains approximately 60% magnesium ammonium phosphate monohydrate by weight and 40% additional water of crystallization. From an economic viewpoint, it is desirable to convert the hexahydrate to the monohydrate, thereby greatly increasing the percentage of plant foods in the fertilizer. Comparative analyses of the phosphate precipitate and the dehydrated fertilizer product are given in Table IV. Dehydration cannot be carried out by heating the dry hexahydrate because ammonia is also lost during the drying (*1*). Figure 2 shows the effect of slurry concentration on dehydration when batch samples are digested for 1 hour at 90° C. The P_2O_5/N weight ratio should remain constant during conversion from the hexahydrate to the monohydrate. Loss of ammonia is indicated by an increase in ratio. Above 25%

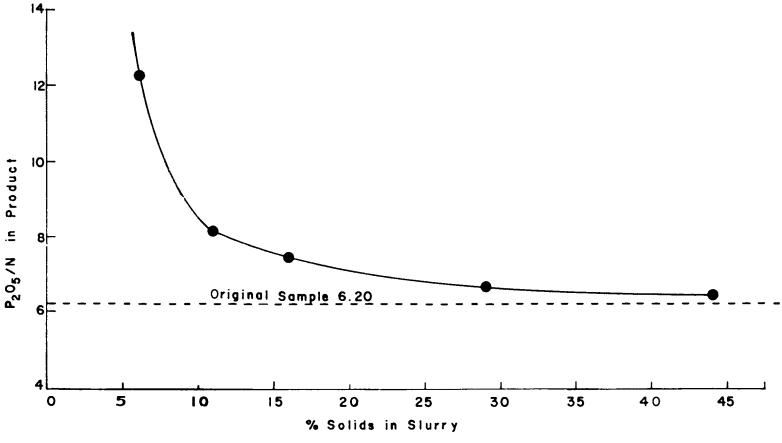

Figure 2. Effect of slurry concentration on decomposition during dehydration

solids in the slurry only a very small amount of nitrogen is lost during dehydration and the P_2O_5/N weight ratio approaches that of the original sample.

Table IV. Enrichment by Dehydration

Phosphate Precipitate	*Fertilizer Product*
92% $MgNH_4PO_4.6H_2O$	87% $MgNH_4PO_4.H_2O$
8% $CaHPO_4.2H_2O$	13% $CaHPO_4.2H_2O$
29% P_2O_5	43% P_2O_5
5% N	7% N
15% MgO	21% MgO
4% CaO	5% CaO

The loss of ammonia was reduced when the dehydration was carried out in a continuous manner. The slurry from the settler of the descaling step was continuously pumped into a reactor vessel fitted with a stirrer, thermometer, and heater in which the phosphates were dehydrated. The overflow was discharged by gravity into a filter or a settler. When this method of dehydration was used on a slurry containing 17% solids in sea water, the product was equivalent in composition to that obtained by the best batch procedures—i.e., with the more concentrated slurries.

A thermogram of the fertilizer produced from sea water is shown in Figure 3. The depression in the curve at 200° C. probably corresponds to the dehydration of the dicalcium phosphate dihydrate to the anhydrous form. Between 200° and 400° C. magnesium ammonium phosphate monohydrate decomposes, with the loss of both water and ammonia. Above 400° C. water of constitution is lost, with the final formation of pyrophosphate at 700° C. Thermograms of both

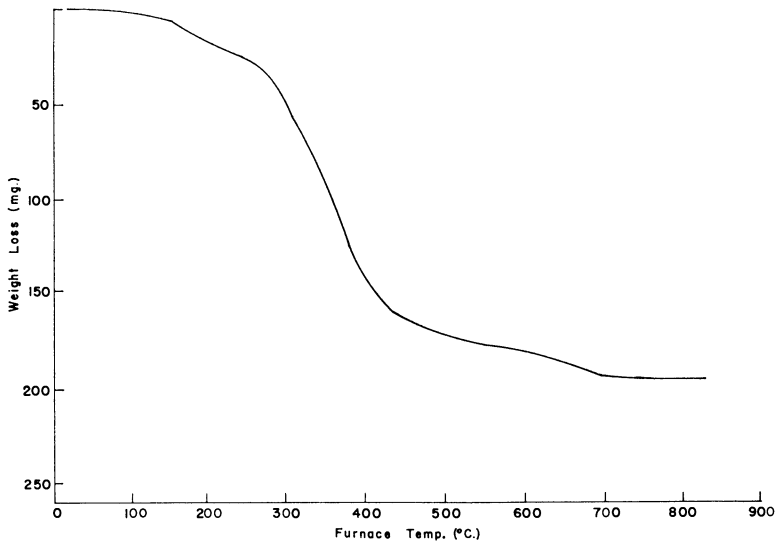

Figure 3. Thermogram of fertilizer from sea water

hydrates of pure magnesium ammonium phosphate are shown in Figure 4. The thermogram of the monohydrate is similar to that of the fertilizer in Figure 3. Magnesium ammonium phosphate monohydrate is considerably more stable than the hexahydrate (*10*). Some ammonia is lost in heating the hexahydrate even

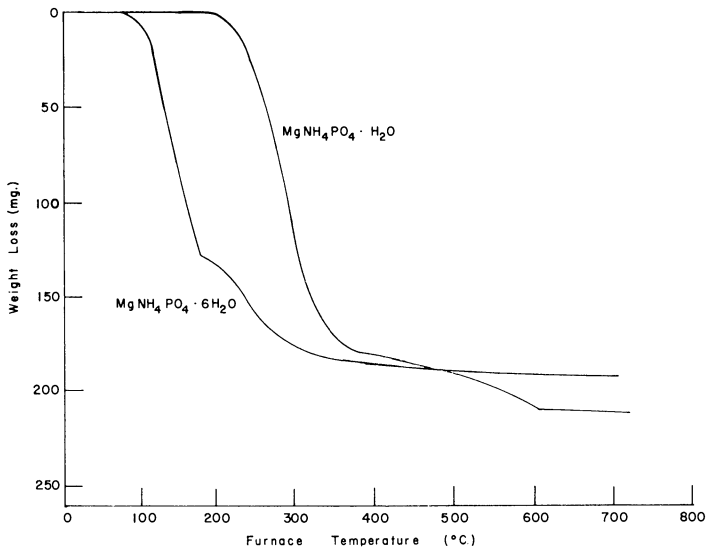

Figure 4. Thermograms

before it is dehydrated to the monohydrate. Greater stability and higher analysis are the reasons for converting the hexahydrate to the monohydrate.

For a plant descaling 1,000,000 gallons of sea water per day, on the basis of current market prices for the raw materials (phosphoric acid and ammonia), and taking no credit for the increased value of the descaled water, the fertilizer produced by the preceding process would have to command a price greater than that of conventional farm fertilizers and be marketed as a premium fertilizer. This could probably be accomplished because of its premium quality and the growing markets for such fertilizers. However, for large descaling plants—i.e., greater than 10,000,000 gallons per day—it would be necessary to compete with conventional fertilizers for farm markets. Large scale production will reduce processing costs. However, the most important cost of the fertilizer is raw materials, with phosphoric acid and ammonia amounting to roughly $^2/_3$ and $^1/_3$, respectively. Substantial reduction in raw material costs will be necessary, if the fertilizer is to compete with conventional fertilizers. This might be accomplished by technological improvements, using cheaper raw materials in the process. For plants descaling 10,000,000 gallons or more of sea water per day it may be economical to build a phosphoric acid plant. Such a plant could be constructed without facilities for concentrating the acid, thus reducing its capital cost.

Producing Sodium Phosphates from Sea Water

The simplest method for precipitating the scale-forming elements (used in preceding process) is to add phosphoric acid to the sea water and neutralize with ammonia. The precipitation reactions for magnesium and calcium (assumed present in the sea water as chlorides) are shown by Equations 2 and 3.

$$MgCl_2 + H_3PO_4 + 3NH_3 + 6H_2O \rightarrow \underline{MgNH_4PO_4.6H_2O} + 2NH_4Cl \quad (2)$$

$$CaCl_2 + H_3PO_4 + 2NH_3 + 2H_2O \rightarrow \underline{CaHPO_4.2H_2O} + 2NH_4Cl \quad (3)$$

In both equations 2 moles of ammonia are consumed to neutralize the acid and

these 2 moles remain in the descaled sea water as ammonium chloride. Although there is a slight chemical advantage in the precipitation of metal ammonium phosphates to neutralize the acid with ammonia, because of the common ion effect on solubility, this may not be the least expensive route. If an inexpensive method could be developed for producing disodium phosphate or monosodium phosphate, the metal ammonium phosphates could be precipitated more economically according to Equations 4 and 5, where Me is any metal capable of forming a metal ammonium phosphate:

$$MeCl_2 + Na_2HPO_4 + NH_3 \rightarrow \underline{MeNH_4PO_4} + 2NaCl \quad (4)$$

$$MeCl_2 + NaH_2PO_4 + 2NH_3 \rightarrow \underline{MeNH_4PO_4} + NH_4Cl + NaCl \quad (5)$$

In Reaction 4 there is no waste or loss of ammonia, whereas in Reaction 5 half the ammonia (1 mole) remains in the descaled sea water as ammonium chloride and hence must be considered as lost. In either case (Reaction 4 or 5) the cost of the alkali must be less than the cost of an equivalent amount (mole basis) of ammonia.

The simplest method for producing sodium phosphates involves the neutralization of phosphoric acid with either sodium hydroxide or carbonate, but, unless some waste source of alkali is found, it may not be the most economical. For this reason other methods of producing sodium phosphates were investigated. The two most promising methods involve conversion of monocalcium phosphate (or normal or triple superphosphate fertilizer) to sodium phosphate by ion exchange, and neutralization of phosphoric acid with dilute sodium hydroxide produced electrolytically from brine.

Normal superphosphate or triple superphosphate (common commercial fertilizers) are cheap sources of water-soluble phosphate. Normal superphosphate is primarily a mixture of monocalcium phosphate and calcium sulfate (gypsum), while triple superphosphate is essentially all monocalcium phosphate. Monosodium phosphate was prepared from superphosphate by first leaching superphosphate with sea water until a saturated solution of monocalcium phosphate was obtained. Then the monocalcium phosphate solution in sea water was percolated through a column of Dowex 50 (strongly acidic type resin) in the sodium form. The effluent from the column was a solution of monosodium phosphate in sea water and the resin was converted to the calcium form as shown by Equation 6.

$$2R\text{—}Na + Ca(H_2PO_4)_2 \rightarrow R_2\text{—}Ca + 2NaH_2PO_4 \quad (6)$$

The resin is regenerated to the sodium form with evaporator brine—i.e., 6% sodium chloride solution—producing a waste effluent of calcium chloride.

$$R_2\text{—}Ca + 2NaCl \rightarrow 2R\text{—}Na + CaCl_2 \quad (7)$$

The use of normal or triple superphosphate as a raw material for phosphate should have a distinct economic advantage over phosphoric acid. Because the procedure yields monosodium phosphate, additional savings would be realized from the decreased ammonia consumption.

One of the most common industrial methods for the production of sodium hydroxide depends on the electrolysis of brine in a diaphragm cell. The products of the electrolysis are chlorine, hydrogen, and cell liquor, which is a solution of sodium hydroxide and sodium chloride. A large fraction of the cost of commercial sodium hydroxide results from the concentration, separation, and purification of the alkali. The sodium hydroxide required in the sea water descaling process need

not be of high purity or concentration. The unconcentrated cell liquor could be used for neutralization of phosphoric acid (or monosodium phosphate) and the resulting brine containing disodium phosphate added to sea water (along with ammonia) as a precipitant. The electrolysis method for producing a dilute sodium hydroxide solution would be even more attractive if the raw material for the electrolysis was raw sea water, descaled sea water, or the concentrated waste brine from the evaporators.

Halogens from Sea Water

It is important in the chlor-alkali industry for economical operation of the diaphragm cells to balance sales of chlorine and caustic soda. Frequently, the demand for chlorine exceeds that for caustic soda. Production of a low-cost caustic soda (for use in the descaling process) in a diaphragm cell from evaporator brine would simultaneously generate chlorine, for which there is a market. The evaporator brine produced from descaled sea water could be used as raw material, because it would be free of calcium and magnesium salts which normally foul a cell and the product cell liquor (dilute caustic soda–sodium chloride solution) would need no additional processing for use in the descaling process. These considerations plus the large scale of operation should be reflected in the price of the chlorine. Bromine and iodine could also be recovered from the evaporator brine either during the electrolysis or by replacement with part of the chlorine.

Recovery of Potassium Chemicals from Sea Water

In the precipitation of the scale-forming elements with the stoichiometric amounts of disodium phosphate and ammonia, the recoveries of calcium, magnesium, phosphate, and ammonia were found to depend on pH. The effect of pH is shown in Figure 5. Above pH 7.5 recovery of both magnesium and phosphate is high. A pH of 8.5 is necessary for good calcium recovery. The ammonia reaches a peak recovery of about 88% and then drops off rapidly as an excess is used to achieve a higher pH. Low ammonia recovery led to the interesting observation that potassium was coprecipitating with the magnesium ammonium phosphate.

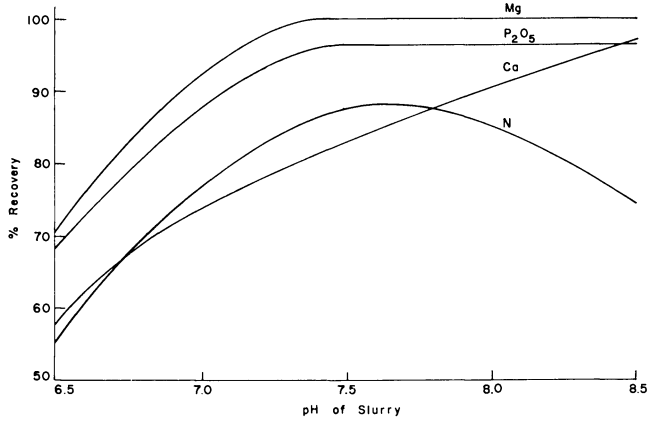

Figure 5. Effect of pH on recovery

Chemical analyses indicated the presence of water-insoluble potassium, presumably as magnesium potassium phosphate coprecipitated with magnesium ammonium phosphate. From this observation the question arose as to the possibility of producing potassium chemicals from sea water by direct precipitation—a thought not new, but one which has challenged the imagination of chemists for many years. Because most of this nation's potash deposits are in the West, production of potassium chemicals (particularly for agricultural use) from sea water might have some economic advantage in the eastern part of the United States. If this could be accomplished during the descaling operation, the values gained from the potash might influence the economic picture of the saline water project.

To enhance the formation of the potassium compound, precipitations were carried out with sodium phosphate in the absence of ammonium ion:

$$MgCl_2 + KCl + Na_3PO_4 + 6H_2O \rightarrow \underline{MgKPO_4.6H_2O} + 3NaCl \quad (8)$$

Recovery of the potassium in sea water was 90% (see Table V) when phosphate was added equivalent to the calcium and magnesium content of the sea water and the final pH was adjusted to 9.5. The hydrated product, probably a mixture of magnesium potassium phosphate diluted with other magnesium and calcium phosphates, contains approximately 3% K_2O (or an estimated 4 to 5% K_2O after dehydration).

Table V. Recovery of Potassium and Other Minerals from Sea Water by Precipitation with Trisodium Phosphate

	% Recovered			
pH of Pptn.	*K_2O*	*MgO*	*CaO*	*P_2O_5*
7.5	15	45	88	45
8.5	61	84	89	74
9.5[a]	90	96	98	91

[a] Precipitate contains 3% K_2O by weight.

Experiments were then carried out to determine the possibility of separating the potassium from the phosphate mixture and thereby making manufacture of potassium chemicals from sea water more feasible. The method investigated involved the treatment of magnesium potassium phosphate monohydrate with ammonium bicarbonate solution. The magnesium potassium phosphate was converted to magnesium ammonium phosphate, leaving a solution of potassium bicarbonate as indicated by Equation 9.

$$MgKPO_4.H_2O + NH_4HCO_3 \rightarrow \underline{MgNH_4PO_4.H_2O} + KHCO_3 \quad (9)$$

In Table VI are given the analyses of the original magnesium potassium phosphate used in this experiment and of the treated cake. The data indicate that 98% of the K_2O present in the $MgKPO_4.H_2O$ was extracted as soluble potassium bicarbonate, which could serve as raw material for production of various potassium chemicals.

Concentration of Trace Minerals from Sea Water by Phosphate Precipitation

The material precipitated from sea water during descaling was analyzed by emission spectroscopy (Table VII). The precipitate contains trace amounts of a variety of elements, many of which are important agronomically. Many other

Table VI. Conversion of Magnesium Potassium Phosphate to Magnesium Ammonium Phosphate with Ammonium Bicarbonate Solution

	Original $MgKPO_4.H_2O$	*Product* $MgNH_4PO_4$[a]
Wt. of sample, g.	17.64	15.1
% P_2O_5	38.70	39.70
% K_2O	25.87	0.62
% MgO	23.59	23.20
% N	...	5.25
% water-sol. N	...	0.65
Wt. of K_2O, g.	4.56	0.09
% K_2O extracted	...	98.0

[a] Probably mixture of hydrates, because sample was dried at room temperature.

elements are undoubtedly present, but were not picked up by the spectrographic method utilized. The concentration of some of the trace elements—e.g., copper—reported is higher than would be expected from the amounts of these elements in sea water. Apparently, the additional material came from other reagents and the equipment.

Table VII. Spectrographic Analysis of Phosphates Precipitated from Sea Water

	%		%
P_2O_5	30	V_2O_5	<0.003
MgO	16	TiO_2	0.04
CaO	3.4	Na_2O	0.01–0.05
Fe_2O_3	0.01	SiO_2	0.05
SrO	0.05–0.1	B_2O_3	<0.02
CuO	0.006	MnO	0.008
Al_2O_3	0.02	Cr_2O_3	<0.003

Some of the metals might be recovered by treatment of the phosphate precipitate with ammonia or ammonium carbonate as in the recovery of potassium from these precipitates. Metals which form complex ammonium ions–e.g., copper, zinc, nickel, and cobalt–would be extracted and could be recovered from the ammoniacal solution.

Conclusions

Most sea water conversion plants now in operation are outside the United States. Many countries are not only water-short but also fertilizer-short. Water alone does not solve an agricultural problem. Fertilizers are usually necessary too. Combining fertilizer production with sea water conversion may have particular value in these countries, which are not necessarily have-not nations. Those which can economically support sea water conversion as a source of fresh water could probably support a premium quality fertilizer. Its low solubility, nonburning, nonleaching in sandy soils, and trace element content make it more valuable than ordinary fertilizers and could be of great merit in the future development of these nations.

The descaling method would have particular value in desalination processes involving distillation. Some advantage in electrodialysis is also anticipated. Scale formation is not a problem in processes involving hydrate formation and freezing.

In a research program on the descaling of sea water and the recovery of minerals from sea water many questions arise. How far would it be economical to go in removing fresh water from sea water, if scale were not a problem? Would

it be economical to concentrate to a saturated sodium chloride solution? If not, to what degree of saturation would it be feasible? What is the value of the descaled sea water to various desalinization processes? What fraction of the scale-forming elements needs to be removed? If, for example, 50% removal could be tolerated, the quantity of phosphate now used could be utilized to treat twice the volume of water. What can we extract from the waste evaporator brines of economic value? What of economic value can we extract from the phosphate precipitate (or fertilizer), and how? What large uses can we find for the phosphate precipitate in addition to fertilizers—e.g., construction materials? If markets were not available for the phosphate precipitate, how could all or part of the P_2O_5 be economically recycled?

Answers to these and other intriguing questions can be supplied by sustained research unrestrained by the thought that it cannot be done.

Acknowledgment

The authors are indebted to G. L. Bridger for many helpful suggestions. The laboratory phase of the research was ably assisted by Manuel Eisenstadt and Bruce L. MacEwen. Credit is due David E. Kramm for analytical support. The thermogravimetric measurements were made by Saul Gordon, 12 Brookfield Way, Morristown, N. J.

Literature Cited

(1) Auger, V., Ivanoff, N., *Compt. Rend.* **204,** 434 (1937).
(2) Bassett, H., Bedwell, W. L., *J. Chem. Soc.* **1933,** 865.
(3) Bridger, G. L., Salutsky, M. L., Starostka, R. W., *J. Agr. Food Chem.* **10,** 181 (1962).
(4) *Chem. Eng. News* **39,** 24 (May 29, 1961).
(5) *Ibid.,* **39,** 83 (Sept. 11, 1961).
(6) *Ibid.,* **40,** 52 (Jan. 22, 1962).
(7) Krause, K. A., Nelson, F., Paper 837 (U.S.A.), International Conference on Peaceful Uses of Atomic Energy, Geneva, Switzerland, August 1955.
(8) Salutsky, M. L., Dunseth, M. G., Eason, W. E., "Removal of Scale-Forming Compounds from Sea Water," W. R. Grace & Co. Summary Rept. 6 to Office of Saline Water for year ending June 1, 1961, Contract No. 14-01-001-202; *Ibid.,* Report 10, June 1, 1962.
(9) Scholl, W., Davis, M. M., Wilker, C. A., *Agr. Chem.* **16,** 36 (1961).
(10) Vol'fkovich, S. I., Remen, R. E., Rozenberg, T. S., *Zhur. Priklad. Khim.* **22,** 448 (1949).
(11) *Water Newsletter,* June 20, 1961.

Received May 28, 1962. Work supported in part by the Office of Saline Water, U. S. Department of the Interior, under Contract 14-01-001-202.

3

Minimizing Scale Formation in Saline Water Evaporators

W. F. McILHENNY

Texas Inorganic Research, The Dow Chemical Co., Freeport, Tex.

Temperatures and concentrations of saline water evaporators are now limited by the potential calcium sulfate scale. Partial ion exchange softening has been demonstrated to be effective in minimizing scale formation. Sea water was softened in a novel fluidized bed, and the ion exchange resin regenerated by the concentrated evaporator blowdown brine. No additional regenerant was required. The rate of scaling during a 1000-hour pilot plant test on softened sea water was less than one thirteenth that found when raw sea water was fed. The ion exchange equilibria in the Ca^{+2}—Mg^{+2}—Na^{+} system are presented and a method of calculation for the ternary system is indicated.

The formation of scale has always been a problem in the production of fresh water from sea water. As water is removed, the dissolved salts concentrate in the brine until the limit of solubility is reached for some compounds. These precipitate and form scale, especially on any heat transfer surfaces, rapidly causing a loss in thermal efficiency, and if they are not removed, eventually result in deterioration of the equipment.

No entirely satisfactory method has been proved for the control of all scales. $CaCO_3$ and $Mg(OH)_2$ may be controlled by addition of acid, or by a sludge recycle. $CaSO_4$ scale limits the design of virtually all sea water conversion equipment as well as equipment designed for many other saline or brackish waters. The only proved method has been to halt the concentration before $CaSO_4$ becomes insoluble.

When magnesium and calcium are removed from sea water, a softer sea water is produced. When used as a feed to a sea water evaporator in place of ordinary raw sea water, this can be evaporated at higher temperatures to greater concentrations. Evaporator thermal efficiency and on-stream time can be increased and evaporation capital can be reduced.

The incoming raw sea water can be softened by a cation resin, and the concentrated evaporator blowdown liquor can be used as the sole regenerant for the ion exchange resin. No additional regenerant is ordinarily required.

A pilot plant embodying these ideas, in an unusual method of softening, was designed and constructed by the Texas Division of The Dow Chemical Co. Two 4000-gallon-per-day vapor compression evaporators were furnished for the testing program by the Bureau of Yards and Docks, United States Navy. The Office of Saline Water furnished, under a research contract, the operating funds for a 9-month testing program.

The estimated cost of softening the evaporator feed at a rate of 10,000,000 gallons per day is 9.4 cents per thousand gallons.

Scale Formation

Scales found in sea water evaporators are of two types: that formed when the bicarbonate breaks down and that produced when the limit of solubility of the dissolved compounds is exceeded.

The alkalinity in sea water is almost entirely due to bicarbonate. When the sea water is heated, the bicarbonate breaks down to produce carbon dioxide and carbonate ion. The carbonate can further disproportionate to produce carbon dioxide and hydroxyl ion. The carbonate can react with the dissolved calcium to precipitate calcium carbonate when the solubility is exceeded at the concentrations, temperatures, and pressures at which the evaporation is conducted. Dissolved magnesium can react with the hydroxyl ion to precipitate magnesium hydroxide.

$CaCO_3$ scales predominate below 185° F. and $Mg(OH)_2$ scales above this temperature.

Calcium sulfate scale can form when the solubility limit is exceeded in the sea water evaporator. This scale is formed only by the concentration of the brine as distillate is removed and by the decrease in solubility as the temperature of the solution is raised.

W. L. Badger and Associates have published a review of literature on the formation and prevention of scale (*2*). Little is known about the solubilities of the scale-forming components and the crystal phases usually encountered are not those expected on the basis of equilibrium considerations (*1*).

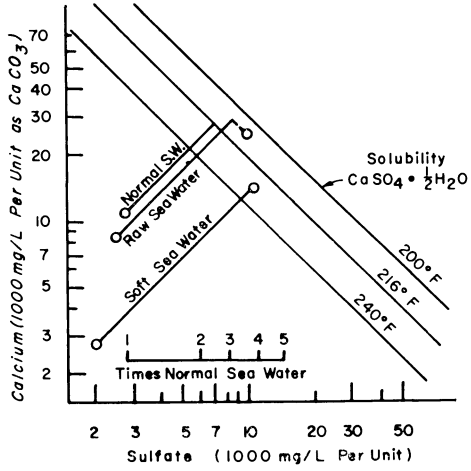

Figure 1. Stability diagrams and evaporation paths of $CaSO_4$ in sea water

Calcium sulfate has several crystal forms, but only three can exist in solutions. Gypsum ($CaSO_4 . 2H_2O$) is the stable form at lower temperatures, and anhydrite ($CaSO_4$) at higher temperatures. However, anhydrite is so difficult to crystallize that alpha-hemihydrate ($CaSO_4 . {}^1/_2H_2O$) can exist for long periods and is the form ordinarily encountered in sea water evaporators.

The stability diagram for $CaSO_4 . {}^1/_2H_2O$ is shown in Figure 1. Plotted are the solubility lines at 200°, 216°, and 240° F. Normal sea water can be concentrated to its original concentration without hemihydrate precipitation at the atmospheric boiling point.

The potential scale concept of Standiford and Sinek is very useful (7). If it is assumed that hemihydrate is the stable $CaSO_4$ phase, and that the HCO_3^- alkalinity has broken down completely into CO_3^{-2} or OH^-, then the amount of the scaling compounds that cannot be carried in solution can be calculated as the concentration is increased. Figure 2 is the potential scale expected when normal sea water is concentrated.

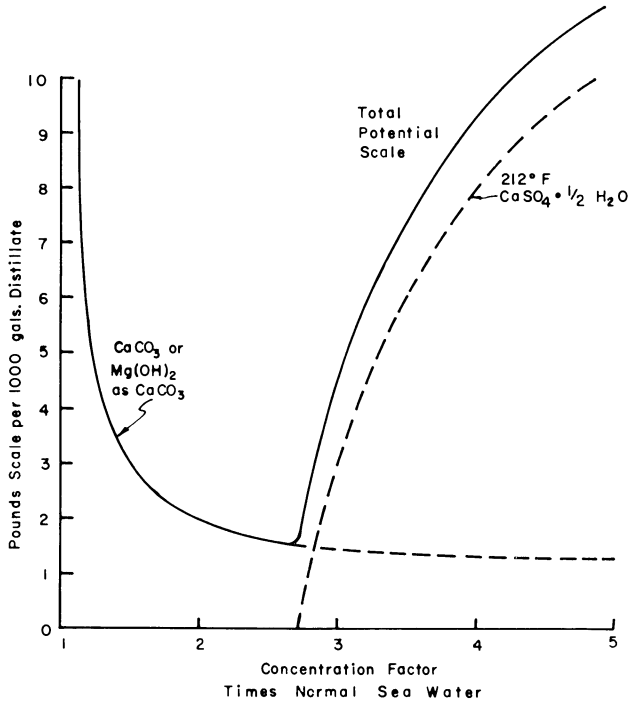

Figure 2. Potential scale from normal sea water

Redrawn from (1)

Proved methods are available for preventing the formation of $Mg(OH)_2$ and $CaCO_3$ (those scales due to alkalinity) on heat transfer surfaces. Acid will neutralize the alkalinity and by pH control prevent the alkaline scales from forming (2, 3, 7, 8). Contact stabilization has been used to minimize alkaline scale formation (4, 6). A sludge recycle process has been successful in preventing $Mg(OH)_2$ formation (2, 7).

The present work utilizes two concepts. If the concentration of either Ca^{+2} or SO_4^{-2} can be decreased, the resultant solution can be concentrated until the

solubility product is reached at the temperatures and pressures of the evaporation. It is neither necessary nor desirable to remove all of the calcium, only that portion required to maintain less than saturation conditions after evaporation.

The calcium may be removed from sea water by chemical methods which leave relatively intact the nontroublesome magnesium content (5). An ion exchange removal of the calcium can use the evaporator blowdown brine as a regenerant, if there is sufficient difference in selectivity between the resin and the solution at the concentrations of the incoming feed water and outgoing brine solution.

Because the sea water obtained in Freeport, as in many other estuarial locations, varies in salinity, a standard must be set against which the concentrations are measured both in the diluted sea water and in the concentrated brine.

"Normal sea water" as prepared by the Hydrographic Laboratories of Copenhagen is used whenever a standard sea water is designated. It is slightly more concentrated than other standard sea waters, having a total solids concentration of 35,175 p.p.m. Calcium is 408 p.p.m.; magnesium 1298; sulfate 2702; and bicarbonate 142 p.p.m.

Pilot Plant

An over-all view of the pilot plant is shown in Figure 3. The two Cleaver Brooks 200-gallon-per-hour vapor compression stills are on the left and the ion exchange softening columns on the right. The large round tank is the soft sea water buffer storage tank and the square tank in the foreground is the evaporator brine storage tank. In Figure 4 is shown the ion exchange softening equipment.

The softening was operated in a batch cycle and the evaporators were operated continuously. Enough soft sea water was produced during a softening cycle to feed the evaporator during the pumping, washing, draining, and regeneration portion of the cycle.

The manner of softening and regeneration, and the type of resin, were chosen to give maximum efficiency during each part of the cycle and to allow engineering of very large equipment with a minimum of anticipated difficulty.

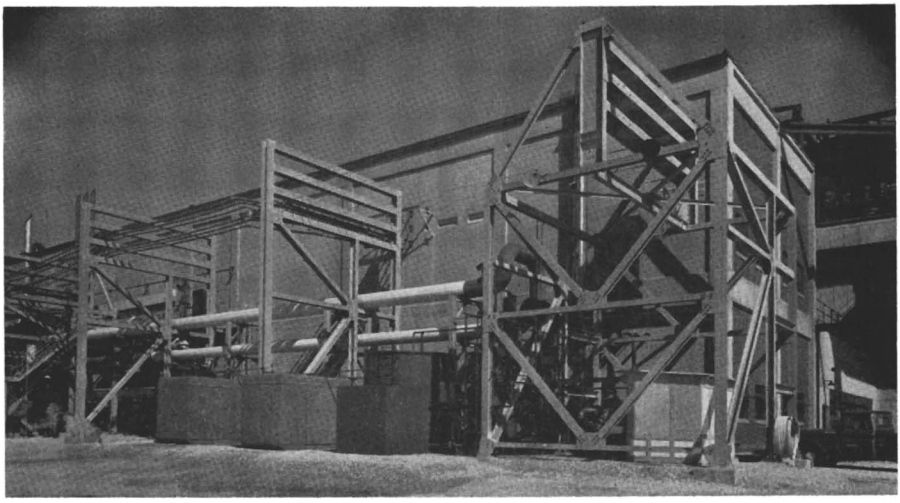

Figure 3. Over-all view of soft sea water pilot plant

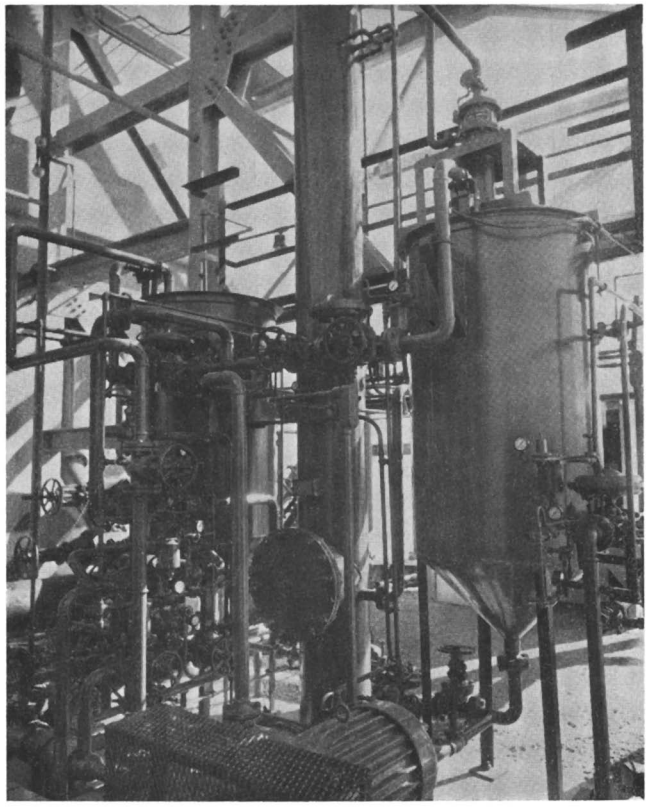

Figure 4. Ion exchange softening
Soft sea water pilot plant

A flowsheet of the pilot plant is shown in Figure 5.

The plant was charged with 15 cu. feet of Dowex 50W 50–100-mesh cation exchange resin. During softening, the raw sea water is fed into a 15-inch I.D. by 15-foot contact column at the same time as a 60 volume % resin slurry. The

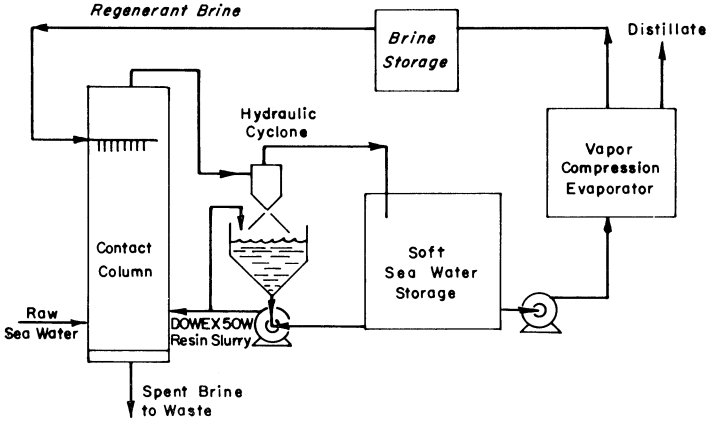

Figure 5. Flowsheet of soft sea water pilot plant

sea water and resin flow concurrently through the contact column into a 4-inch hydraulic cyclone, where they are separated, the resin is returned to softening, and the softened sea water is forwarded for storage before evaporation. The columnar flow is 30 to 40 gallons per minute per square foot, much above the carryover velocity of the resin, and much above the flow rates used for conventional water softening. The cyclone removes more than 99% of the resin fed.

Softening is continued for a specified time (usually 35 minutes). The spent resin slurry is then pumped into the contact column and the column drained to bed level. Regenerant from the evaporator is fed through a sparger and removed at the bottom through a porous bonded coke resin filter support. Regenerant flows are low, about 1 to 1.5 gallons per minute per square foot, the hydraulic head furnishing the only drive. The regeneration time averaged 100 minutes. After regeneration, the bed is washed downflow with raw sea water until the brine is displaced. The resin is slurried and pumped into the storage tank for the next softening. The total cycle time was about 4 hours.

A typical softening profile is shown in Figure 6. At the end of softening, the resin still has the ability to remove calcium, but the time and flows are balanced to give an average water of the desired degree of calcium removal. Although not necessary for scale prevention, some magnesium is removed by the resin from the incoming sea water. Because of the greater selectivity of the resin for calcium, the proportional removal of the calcium fed is larger.

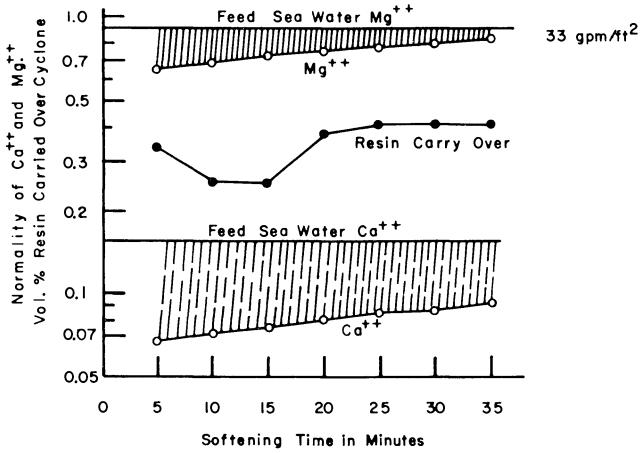

Figure 6. Typical softening profile

A fluidized resin-liquid contact was chosen for several reasons. Turbidity in the incoming sea water presents no problem, because the suspended material is carried over with the softened sea water. It is difficult, if not impossible, to force raw sea water through an ion exchange resin bed at reasonable flow rates because of the rapid buildup of a sludge blanket in the top few inches of the bed, which results in a rapid increase in pressure drop.

A fixed bed downflow regeneration was chosen because the amount of regenerant is limited to that produced by the evaporation of the softened sea water. A fixed bed gives the maximum possible contact and the use of fine-mesh resin gives a large number of transfer units and allows a close approach to the equilibrium. A low flow rate was used in the pilot plant.

A typical regeneration wave is shown in Figure 7. Because the resin is well mixed during the softening and pumping, the adsorbed calcium is evenly dispersed

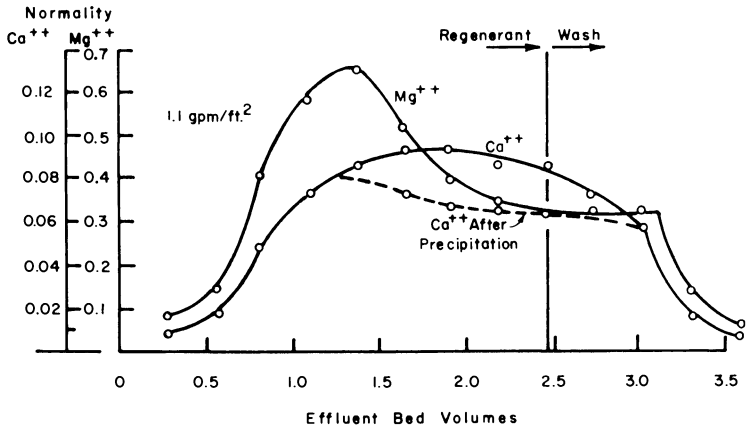

Figure 7. Typical regeneration wave

in the bed at the beginning of regeneration. When the regeneration wave moves downflow through the bed, the calcium is continually being eluted in the waste stream and does not peak in as high a concentration as it would if the calcium were concentrated in a portion of the bed. Such an elution is desirable because of the high sulfate content of the regenerant brine, which leads to supersaturation of the effluent wave with calcium sulfate. Since the regenerant effluent calcium is spread more evenly in the waste, the local supersaturation is not as high as would be encountered in more conventional fixed bed elution, either upflow or downflow.

At the peak removal of calcium, the effluent is supersaturated with gypsum, which will precipitate after removal from the bed. The dashed line in Figure 7 shows the calcium level reached after standing for one week. Undisturbed samples became opalescent, indicating precipitation, about an hour after sampling. In spite of the gypsum supersaturation, no trouble was ever experienced with precipitation in the bed, in the porous carbon bed support, or in the effluent piping from the pilot plant.

Dowex 50W Resin Stability

The pilot plant was initially charged with 15 cu. feet of Dowex 50W 50–100-mesh Na^+ form cation exchange resin. During the 9 months of operation, 10 cu. feet were added.

Resin was sampled daily and the particle size was followed microscopically. Figure 8 is a plot of the 50% by count particle diameter as a function of cycle number. There was no significant change in either average particle size or number of broken beads during the period of pilot plant operation.

The resin, which is initially light in color, became dark brown in service as iron was picked up from the mild steel equipment and incoming sea water and retained. However, calcium removal capacity did not appreciably decline during the testing period. The iron is readily stripped by HCl and the resin returned to its original color.

Some resin was lost to drain when the crackerjack filter cracked and lost the seal to the metal column. This was repaired and no further resin was lost to waste. The greater majority of resin was lost through the packing of the Wemco pump. By the end of the 1000-hour run, the pump shaft was grooved and leaked continuously in spite of being repacked daily. Most of the spilled resin was

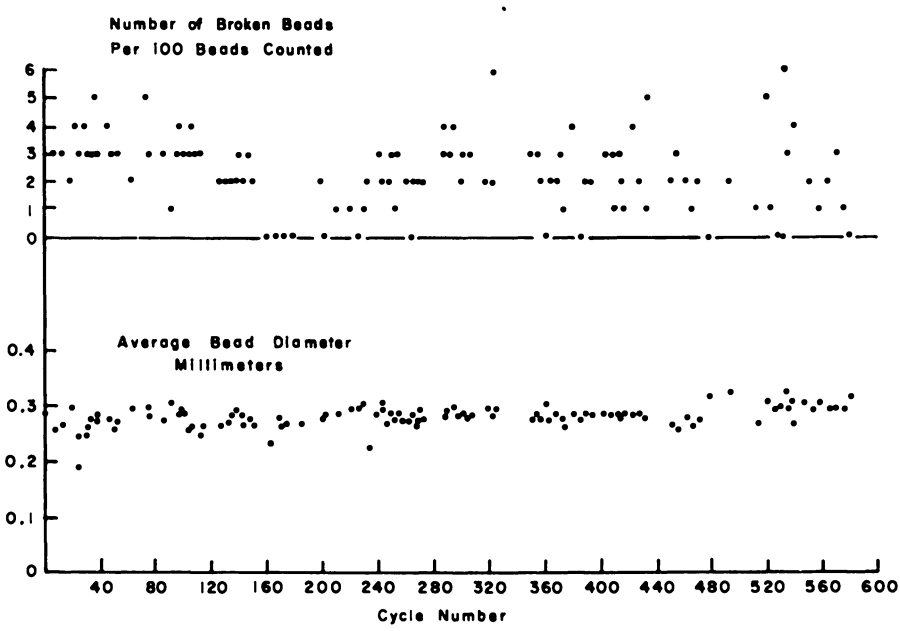

Figure 8. Dowex 50W particle size during pilot plant operation

picked up, washed, screened, and returned to the system. Pump leakage would account for almost all of the resin lost from the system.

Both the new and used ion exchange resins were analyzed for operating capacity, leakage, sphericity, and particle size (Table I). The resin showed no apparent physical degradation in the 9 months of use.

Table I. Ion Exchange Resin Properties

	New	*Used*
Operating capacity, kgr./cu. ft.	30.5	29.8
Leakage, grains	0.77	0.76
Wet volume total capacity, H^+, meq./ml.		1.95
Dry weight capacity, H^+, meq./dry gram		4.90
Sphericity	99.0	95.0

The finer mesh resin was chosen because the fine beads are sulfonated without strains and the resin is physically more stable to attrition than is a standard water softening mesh size resin. The ion exchange kinetics are also more rapid, 70-mesh resin reaching 90% of calcium equilibrium in 1 minute as compared with almost 10 minutes for a 20-mesh resin.

Ion Exchange Equilibria

The ternary ion exchange system of interest is:

$$\tfrac{1}{2}\,MgS + NaR \leftrightarrows \tfrac{1}{2}\,MgR + NaS$$

$$\tfrac{1}{2}\,CaS + NaR \leftrightarrows \tfrac{1}{2}\,CaR + NaS$$

$$\tfrac{1}{2}\,CaS + \tfrac{1}{2}\,MgR \leftrightarrows \tfrac{1}{2}\,CaR + \tfrac{1}{2}\,MgS$$

$$K_{Na}^{Ca} = \left[\frac{(X_R^{Ca})}{(X_S^{Ca})}\right]^{1/2} \frac{(X_S^{Na})}{(X_R^{Na})}$$

where X_R = equivalent fraction ion on the resin $\Sigma X_R = 1$
X_S = equivalent fraction ion in the solution $\Sigma X_S = 1$
K_{Na}^{Ca} = selectivity coefficient (superscript is the preferred ion on the resin)

Each of the three ions is competing for sites on the resin and none can be ignored when an equilibrium is to be calculated. Selectivity coefficients of the type shown are used to calculate equilibriums. The resin and solution activities are included in the coefficient, as are the solution concentration, which varies widely, and the total ionic concentration on the resin, which varies slightly on a volume basis. The sum of equivalent fractions of ions on the solution and on the resin is equal to unity in each case.

The variation of the equilibria in the system Dowex 50 resin–Ca-Mg-Na is shown in Figure 9. The two divalent-monovalent exchanges are concentration-dependent. The divalent-divalent exchange is not.

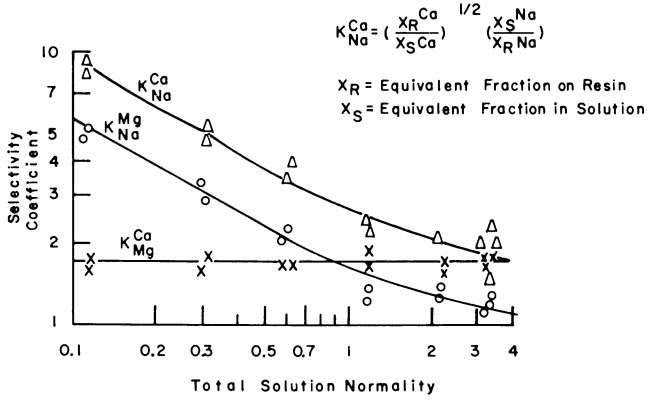

Figure 9. Ion exchange equilibria
Ca^{+2}–Mg^{+2}–Na^{+}–Dowex 50W

If either the solution composition or the resin composition is known and the total solution concentration is given, the composition of the other phase may be calculated.

Using Na as the base ion: $\Sigma X_R = 1$

$$X_R^{Na} + K_{Na}^{Ca2}\left[\frac{X_R^{Na}}{X_S^{Na}}\right]^2 X_S^{Ca} + K_{Na}^{Mg2}\left[\frac{X_R^{Na}}{X_S^{Na}}\right]^2 X_S^{Mg} = 1$$

Then: $X_R^{Na} = \dfrac{-1 + \sqrt{1 + 4A}}{2A}$

where $A = (K_{Na}^{Ca})^2 \dfrac{(X_S^{Ca})}{(X_S^{Na})^2} + (K_{Na}^{Mg})^2 \dfrac{(X_S^{Mg})}{(X_S^{Na})^2}$

and $X_R^{Ca} = (K_{Na}^{Ca})^2 \dfrac{(X_S^{Ca})}{(X_S^{Na})^2} (X_R^{Na})^2$

$$X_R^{Mg} = (K_{Na}^{Mg})^2 \frac{(X_S^{Mg})}{(X_S^{Na})^2} (X_R^{N})^2$$

The equilibrium diagram for the sea water–resin-evaporator brine system constructed from the above data is shown in Figure 10, in which the calcium equivalent fraction on the resin is plotted against the calcium equivalent fraction in

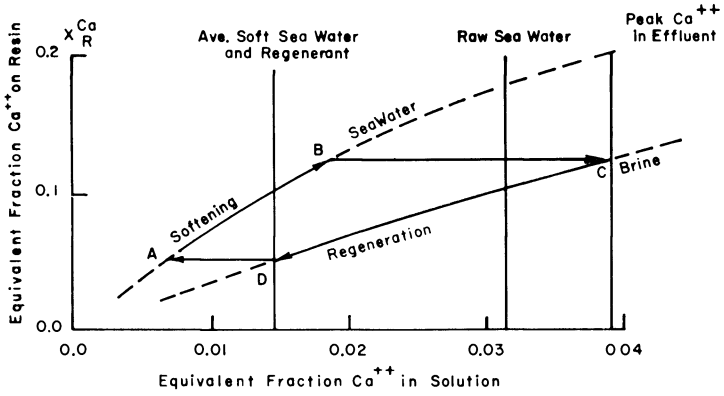

Figure 10. Equilibrium diagram of sea water softening

solution. During softening the resin picks up calcium from point *A* to point *B*. The resin is then exposed to the concentrated brine blown down from the evaporator at point *C* and gives up calcium to the regenerant to point *D*. Because there is no precipitation in the evaporator, the soft sea water and influent regenerant have the same ionic ratios. When equilibrium is reached between the softening ability of the resin and the removal ability of the brine, the ratio of calcium to total ions in the effluent solution at point *C* must equal or exceed the ionic ratio in the incoming raw sea water. Flows must be balanced, since no additional regenerant is used and the amount removed from the water by the resin must equal the amount removed by the brine from the resin.

Operating Results

The pilot plant was designed and operated to remove about 50% of the calcium from the sea water when the evaporator was operating at a blowdown concentration four times that of normal sea water.

This chosen calcium removal level was sufficient to keep the calcium concentration below that needed to prevent hemihydrate precipitation at the evaporator temperature. The evaporator was operated to maintain a constant vapor head pressure at zero-pound gage, which kept the brine at the atmospheric boiling point.

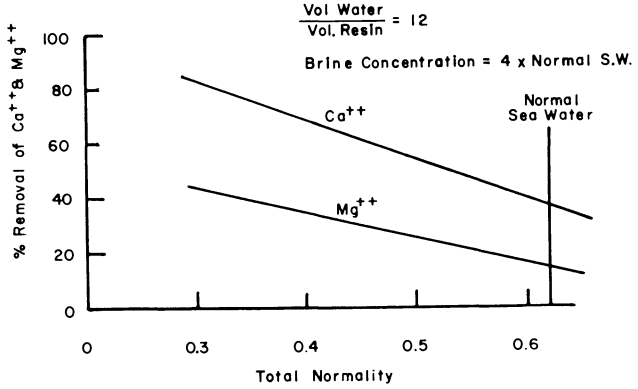

Figure 11. Removal of calcium and magnesium from sea waters

The flows and cycle timing were arranged to use all of the evaporator blowdown brine to regenerate the resin. During the entire 9 months of operation, additional salt was added only twice, both times to prepare a synthetic brine to start up the system.

The most important single variable determining the calcium removal is the salinity of the incoming sea water. In Figure 11 is shown the removal of calcium and magnesium as the sea water concentration is varied. During the testing period, the total normality of the received sea water varied from 0.3 to 0.5, which meant that, at times, the evaporator was concentrating the feed sea water as much as 7 times to reach the desired brine concentration.

Three long-term test runs were made with the pilot plant, all at a brine concentration of about four times normal sea water. The first run was with raw sea water, the second with softened sea water with no acid addition, and the third with softened sea water treated with acid to remove alkalinity. These are shown in Figure 12.

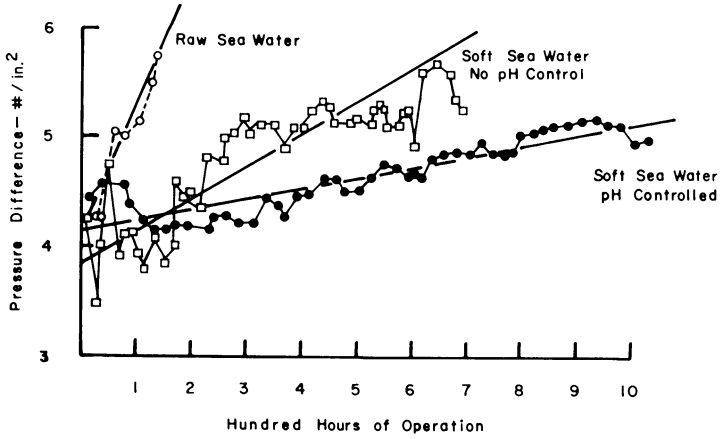

Figure 12. Increase in evaporator pressure difference with time of operation

When raw sea water was fed to the vapor compression evaporators the 6-p.s.i. cutoff pressure differential was exceeded in 150 hours. $Mg(OH)_2$ and $CaSO_4 \cdot {}^1/_2H_2O$ were found by x-ray analysis in the tube scale samples. The evaporation path for raw sea water as shown in Figure 1 indicated that $CaSO.{}^1/_2H_2O$ precipitation was expected and did occur.

When softened sea water was fed to the evaporators without acid to neutralize the alkalinity, $Mg(OH)_2$ was expected and was found. The rate of scaling was one quarter that found with raw sea water.

When softened sea water was fed to the evaporators with the addition of hydrochloric acid to remove the alkalinity, the rate of scaling was one thirteenth that found with raw sea water. There was some increase in pressure differential, but tube scale samples showed no $Mg(OH)_2$ or $CaSO_4$ in any form.

During the raw sea water run, the evaporator foamed very badly and antifoam had to be added almost continuously to allow operation of any sort. No foaming was encountered with soft sea water, although, except for softening, the feeds were identical.

A cost estimate indicates that at 1961 equipment and labor prices, the softening would cost 9.4 cents per 1000 gallons of distillate at a rate of 10,000,000 gallons per day. All of this cost is capital, maintenance, and labor. A minimum resin make-up is the only chemical requirement for the ion exchange softening. The cost of softening does not include the acid feed necessary to control deposition of $Mg(OH)_2$.

For a reduction in the total cost of fresh water from sea water, the cost of the sea water softening would, of course, have to be balanced by a decrease in evaporator capital or a decrease in operating cost by increasing on-stream time, or by decreasing evaporator efficiency by the higher allowable evaporative temperatures.

Some saline waters have calcium sulfate scaling problems even more difficult than those of sea water. The partial ion exchange softening should allow operation at temperatures and pressures that up to now have not been possible.

Literature Cited

(1) Badger Associates, Inc., W. L., Office of Saline Water, U. S. Dept. Commerce, R and D Rept. **26,** OTS Publ. **161290** (1959).
(2) *Ibid.*, **PB 161399** (December 1959).
(3) Hillier, H., Ling, F. B., U. S. Patent **2,733,196** (Jan. 31, 1956).
(4) Langelier, W. F., *et al.*, *Ind. Eng. Chem.* **42,** 126 (1950).
(5) McIlhenny, W. F., *et al.*, U. S. Patent **2,772,143** (Nov. 11, 1956).
(6) Spaulding, C. H., Lindsten, D. C., Office of Technical Services, U. S. Dept. Commerce, **PB 111569** (1953).
(7) Standiford, F. C., Sinek, J. R., *Chem. Eng. Progr.* **57,** 59 (1961).
(8) Williams, J. S., Rept. R-011, U. S. Naval Civil Engineering Laboratory, Port Hueneme, Calif.

RECEIVED June 18, 1962.

4

Saline Water Distillation–Scaling Experiments Using the Spray Evaporation Technique

L. S. HERBERT and U. J. STERNS

Chemical Research Laboratories, Division of Chemical Engineering, Commonwealth Scientific and Industrial Research Organization, Melbourne, Australia

During a study of the applicability of "spray" or "fog" evaporation to sea water desalination, it was found that this technique was particularly useful for scale deposition studies. Thus, test conditions are reproducible and heat transfer coefficients are very high, so that the effect of scale formation is readily apparent. Three novel methods for the control of scale deposits on the evaporating surfaces of a spray evaporator were explored. One involves the addition of small quantities of low molecular weight polyacrylic acid to the feed water, which prevents the formation of adherent scale. The methods are applicable under certain conditions to scales formed from sea water containing substantial amounts of calcium sulfate in addition to alkaline scale-forming substances. While spray evaporation appears to be of limited application in water desalination, the scale-control methods developed are probably applicable to other types of evaporator, particularly of the long-tube type.

In 1959 a study of methods for saline water conversion was commenced in the Division of Chemical Engineering, Commonwealth Scientific and Industrial Research Organization in Australia. In view of the obvious importance of distillation to Australian conditions, an experimental program into thermal distillation methods was begun. Preliminary studies (*5*) underlined the importance of high heat transfer coefficients and of high brine boiling temperatures in the production of distilled water at low cost. In view of the high heat transfer coefficients known to be achieved in "spray" evaporation (*10*), it was decided to base the investigations on this technique. At this time it was thought possible that the low residence time of the evaporating liquid on the heat transfer surface, which is a characteristic of this type of evaporator, would lead to a marked reduction in the rate of scaling when distilling sea water and similar hard waters.

Preliminary runs on sea water gave the expected high heat transfer coefficients, but the high initial value was very rapidly reduced by scaling; thus, the heat transfer coefficients dropped from an initial 4000 B.t.u./sq. ft. hr. ° F. to around 800 in 8 hours. Changes in evaporation conditions made little difference to the rapid rate of scaling, and test results showed a high degree of reproducibility.

These two characteristics made spray evaporation a convenient technique for the study of scale formation and of methods of overcoming the deleterious effects of scale, although the question of the applicability of the results to conventional evaporators must be taken into account. Standard conditions were used throughout in scaling experiments to facilitate comparison of test data.

Spray Evaporation

The technique of "spray" or "fog" evaporation involves the evaporation of a two-phase steam-water mixture moving very rapidly over the heat transfer surface, and may be regarded as an extension of the climbing film regime. The two-phase steam-water mixture is fed to the evaporator instead of preheated liquid feed as used—e.g., in long-tube (climbing film) evaporators. In this way, the indeterminate regimes of "slug" and "froth" flow (*3*) in the evaporator are avoided and the spray evaporation regime is established throughout the evaporator. At high velocities with two-phase flow it is known that annular flow can occur, in which the shear resulting from the high speed vapor core causes the liquid to pass up the wall as a thin film. At still higher velocities the spray regime sets in, and although a wall film is still present, the liquid phase in this case appears to be transported mainly by entrainment. Thus, the film is continuously stripped from the wall by the vapor core, while other droplets are deposited on the wall to maintain film continuity. Consequently, the liquid moves at a speed approaching that of the bulk two-phase stream, and the residence time of any given particle of liquid is very small. In view of the reported influence of residence time on rate of scaling of hard waters (*1*), it appeared that this feature of spray evaporation could be important in reducing scale formation. The thin film and interchange of droplets between the wall and the bulk stream, together with the high velocities existing in the spray evaporation regime, appear to account for the high observed values of heat transfer coefficients.

Experimental

Equipment. Figure 1 gives a simplified flow diagram for the atmospheric pressure spray evaporation test apparatus.

The heat transfer section comprises a vertical length of $^3/_4$ inch o.d. 18 s.w.g. drawn copper tube, steam jacketed for a length of 2 feet. Preheated feed water is mixed with entrainment steam in a Venturi-type mixer and the resultant two-phase mixture passes through the evaporator tube to a cyclone separator. Steam passes to a condenser, and brine to a vessel containing an electronic capacitance-type level control device which discharges the brine via a valve to atmosphere.

The steam jacket is supplied with steam at a controlled pressure and the flow of jacket condensate is measured to allow calculation of the heat transferred in the test section. Jacket condensate may also be passed to a measuring tank and a continuous record of level in the tank used to estimate the average heat transfer rates over hourly or longer periods.

Method of Operation. The experimental procedure is standardized to avoid gross errors due to variations in surface condition of the evaporator test section. Each tube (of commercially available drawn copper) is degreased overnight by

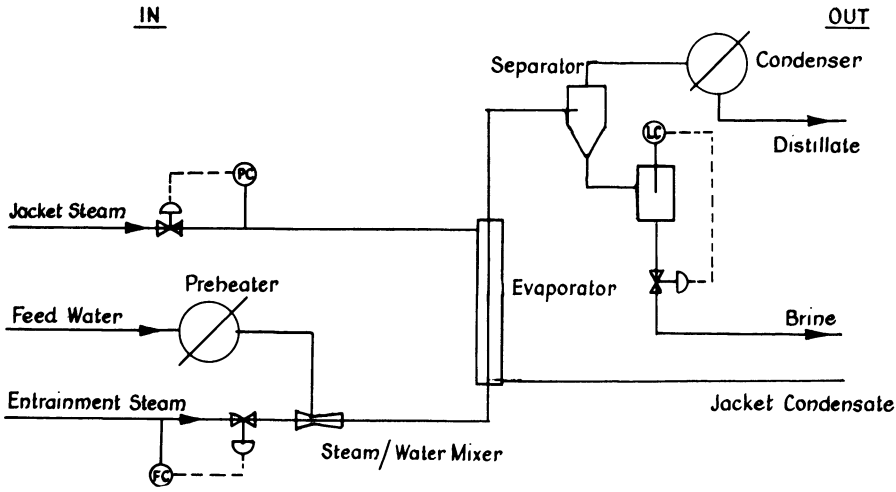

Figure 1. Simplified flow diagram for spray evaporation plant

immersion in liquid trichloroethylene, the outside of the tube burnished with steel wool, and the dropwise condensation promoter wiped onto the outside of the tube with a soft cloth. The tube is inserted into the jacket and the experiment started as soon as possible. When untreated feed water is used, the required evaporation conditions are established on Melbourne tap water (total solids ca. 40 p.p.m.) before the test water is turned on. Where additives are used in the feed water, the cold treated water is allowed to run through the apparatus for a few minutes and the required evaporation conditions are established using the feed water.

The duration of each run is normally 6 to 8 hours, although several longer runs of up to 50 hours' duration have been made with effective antiscale additives. At the end of a run, the feed water is turned off and tap water is allowed to flow through the evaporator while evaporation is still proceeding. Steam is then turned off and the apparatus allowed to cool, thus ensuring that the evaporator tube is never allowed to run dry while still hot. The tube is removed when cool and cut in half, lengthwise, while still wet, to enable the scale to be examined.

During the run, standard evaporation conditions are maintained, and top and bottom evaporator test section pressures are recorded at regular intervals, together with jacket condensate delivery rates. Unusual behavior—e.g., pressure gage fluctuations, appearance of brine effluent, etc.—is noted. In early runs, mass and heat balances were established.

Calculation of Over-all Heat Transfer Coefficient. The rate of production of jacket condensate is used to calculate the heat transferred across the evaporator test section. The calculated value is adjusted for known heat losses and a value of over-all heat transfer coefficient is derived from the equation

$$Q = uA(T_J - T_{av})$$

where Q = heat transferred, B.t.u./hr.
u = over-all heat transfer coefficient, B.t.u./sq. ft. hr. ° F.
A = heat transfer area, sq. ft.
T_J = saturation temperature of jacket steam, ° F.
T_{av} = saturation temperature of steam at average of inlet and outlet evaporator test section pressures, ° F.

Although this value of u has limited value for precise heat transfer calculations, it is considered to be a satisfactory measure of the effect of scaling in the comparative studies reported. Values of u *vs.* time are plotted for all experiments.

Promotion of Dropwise Condensation. Preliminary heat transfer experiments, using distilled water as feed, gave values of over-all heat transfer coefficient around 1000 B.t.u./sq. ft hr. ° F. and analysis indicated that the jacket condensate film provided the main resistance to heat transfer, due to filmwise condensation of the jacket steam. Following reports by Garrett (*4*) of successful tests using dropwise condensation promoters, it was decided to use oleic acid for this purpose in the present experiments. The resulting improvement in jacketside coefficients enabled over-all heat transfer coefficients in excess of 5000 B.t.u./sq. ft hr ° F. to be achieved.

The usual method of promotion was to wipe the oleic acid onto the cleaned outside of the tube before the experiment commenced, although it was also found possible to add the promoter to the jacket steam line via a two-valve arrangement. Tests showed that the original wiped-on film remained effective for at least 8 hours, but some improvement in over-all heat transfer coefficient resulted from the use of additional promoter after 30 to 40 hours' operation.

Supply of Sea Water. Sea water was collected from Port Phillip Bay at Frankston, Victoria, some 30 miles from Melbourne, the nearest point to the laboratories at which clean sea water of salinity approximating that of standard sea water (*1*) could be regularly obtained. The water was transported in 3000-gallon batches by road tanker and delivered into two large rubber-lined tanks at the laboratories. Analyses of the batches over a period of two years gave the results reported in Table I.

Table I. Analysis of Frankston Sea Water

Average of 20 samples	
Chlorosity, g./l.	19.2 ± 1.0
Phosphorus, mg./l.	<0.2 as P_2O_5
Total alkalinity, g./l.	Approx. 0.120 as $CaCO_3$
Typical single sample	
Chlorosity, g./l.	20.00
Ca^{+2}, g./l.	0.41
Mg^{+2}, g./l.	1.41
SO_4, g./l.	0.28
Total alkalinity, g./l.	0.116 as $CaCO_3$

Standard Operating Conditions. During preliminary experiments, it was found that, although the value of the over-all heat transfer coefficient varied with rate of flow and other operating conditions, the variation due to high rate of scale formation predominated under all conditions. Standard conditions for the scaling experiments were selected as shown in Table II. These were chosen in such a way that at least 20 pounds per hour of jacket condensate was produced (to permit accurate measurement) and the initial wetness of steam was adequate to initiate the spray evaporation regime at the bottom of the tube.

Table II. Standard Evaporation Conditions

Feed water rate, lb./hr.	300
Entrainment steam rate, lb./hr.	96
Jacket steam pressure, p.s.i.g.	40 (287 ° F.)
Evaporator test section	2 ft. × 3/4 inch o.d. × 18 s.w.g. (0.37 sq. ft.)
Average tube side pressure, p.s.i.g.	8 to 12
Average tube side velocity, ft./sec.	200
Feed water preheated temp., ° F.	200
Approx. concentration factors	Initially 1.3, falling to 1.1 as scale deposited on heating surface

The pressure inside the evaporator tube was not controlled, and resulted from back-pressure in the separator, condenser, and associated piping. Since the condenser was vented to atmosphere, the evaporator pressure varied with the degree of evaporation, diminishing from the highest value at the start of the experiment to the lowest at the end.

The average tube side pressure of 10 p.s.i.g. corresponded to a saturation temperature of 240° F., which was considerably greater than the usual limiting temperature of 190° to 200° F. achievable in practice with conventional anti-scaling additives.

Results Obtained

Complete experimental data are not presented, but significant results are summarized below.

Untreated Sea Water. During approximately 18 months about 50 runs were made with untreated sea water. Consistent scaling behavior was noted and sets of results selected at random are given in Table III.

Table III. Typical Experimental Results for Untreated Sea Water

Date	*Batch No.*	*Over-all H.T.C. at Time from Start*				
		1 hr.	*2 hr.*	*4 hr.*	*6 hr.*	*8 hr.*
1961						
Jan. 13	70/1	1100	760	470	360	...
Feb. 20	70/2	1400	850	540	380	340
March 9	70/3	1800	1600	1020	880	...
April 10	71	1300	900	1740	980	700
April 14	71	1420	1280	930	620	530
May 31	72	1100	760	460	350	...
Aug. 1	74	1490	1330	920	530	...
Sept. 12	77	770	700	620	530	...
1962						
Feb. 1	83	960	930	480	360	...
April 10	85	1750	2140	1580	1170	850
July 12	87	800	1210	820	700	...

As the initial over-all heat transfer coefficient was approximately 4000 B.t.u./sq. ft hr. ° F. in all cases, the effect of scaling in first hour reduced the initial coefficient by a factor in excess of 2.

Figure 2 shows the decrease of over-all heat transfer coefficient with time; two curves are given, one showing a typical continuous decline curve and the other a discontinuous curve. The discontinuity is considered to be caused by self-stripping of part of the scale from the heat transfer surface. An immediate rise in over-all heat transfer coefficient results, accompanied by large fluctuations in evaporation conditions—e.g., in pressure gage readings—but as more scale is deposited on the surface, the continuous decline curve is once more established. The discontinuity normally occurs within the first 2 or 3 hours of operation and is probably associated with variations in surface condition of the evaporator tubes. For both types of curve an over-all heat transfer coefficient of less than 1200 B.t.u./sq. ft. hr. ° F. is always obtained at the end of an 8-hour run on untreated sea water. Practically all the experimental data lie within the region between these two curves.

The scale generally formed is a brown gelatinous layer, which extends throughout the length of the tube and is similar in appearance and thickness in both heated and nonheated sections of the evaporator tube. Chemical analysis showed the oven-dried material to comprise approximately 90% $Mg(OH)_2$, 3%

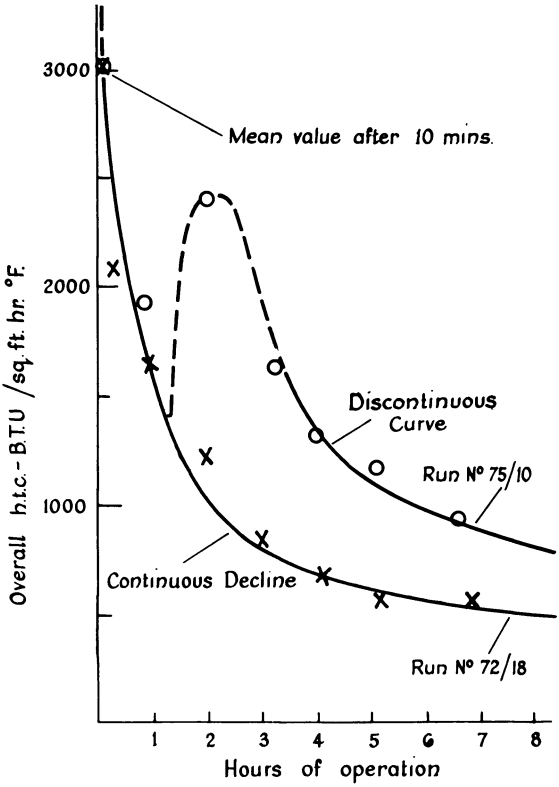

Figure 2. Over-all heat transfer coefficient vs. time for untreated sea water

$CaSO_4$, with smaller amounts of Fe, Na, and Cl. This scale begins to dry immediately on exposure to air, and, as drying proceeeds, considerable shrinkage occurs until the scale becomes a powder, completely detached from the surface and occupying only a small fraction of its wet volume. There is some evidence that the wet scale is strongly hydrated $Mg(OH)_2$ in amorphous form, although rigorous chemical and physical examination has not been made.

In a few tests a white crystalline $Mg(OH)_2$ scale has been produced, which remains on the tube surface as an attached layer when dry. It is thought that the presence of suitable crystal nuclei in the feed water may account for this result. In tests on one batch of sea water a scale containing approximately 30% $CaCO_3$ [remainder largely $Mg(OH)_2$] was produced. Analysis of this batch of sea water showed only minor deviations from standard sea water for the major constituents and no explanation can be offered for this unusual result.

Drying Technique for Scale Removal. The observed shrinkage on drying of the gelatinous scale suggested a new method of scale removal *in situ*. The method (7) adopted involved turning off the feed water at approximately 1-hour intervals for a short period, generally 60 to 90 seconds, while all other evaporation conditions were maintained unchanged. On resumption of the feed water flow, the over-all heat transfer coefficient returned almost to the initial clean tube value. It was presumed that this behavior resulted from partial dehydration and shrinkage of the scale, which disengaged from the surface.

High average over-all heat transfer coefficients were obtained over several runs, but, in view of the rapidly changing rate of heat transfer due to alternate scale formation and stripping, it was impossible to calculate instantaneous values of over-all heat transfer coefficient. However, it would appear that the curve of over-all heat transfer coefficient against time takes the form shown as broken lines in Figure 3.

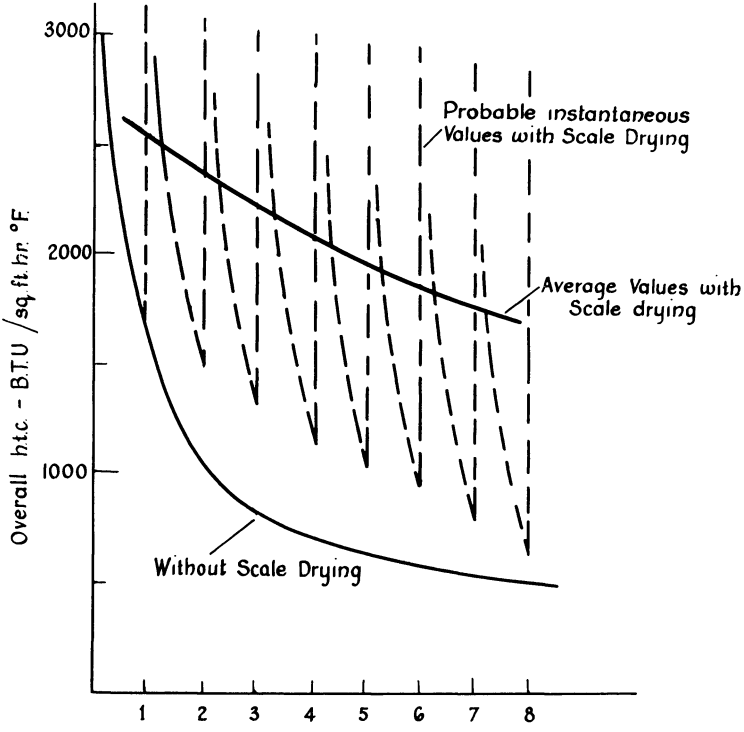

Figure 3. Over-all heat transfer coefficient for untreated sea water with scale drying

Reagent Entrainment Technique of Scale Control. When the scale-drying technique was used, the over-all heat transfer coefficient did not quite recover to the initial clean tube value. After several scale-drying operations a residual white crystalline deposit was found adhering to the heat transfer surface, which consisted mainly of $Mg(OH)_2$ and was readily soluble in weak acid. A method has been evolved (*6*) in which a solution of a suitable descaling agent is introduced with the entrainment steam into the evaporator, allowing effective and rapid descaling without appreciable interruption of evaporation. In the case of residual scale from sea water evaporation, a descaling solution consisting of approximately 0.5% HCl in sea water was found satisfactory. When descaling is complete, the acid feed is replaced by untreated sea water. When this technique is used, particularly in conjunction with scale drying, only small amounts of acid are required to dissolve the scale and considerable acid economy is achieved.

Application of Scale-Drying Technique to $CaSO_4$-Enriched Sea Water. A scaling test was carried out with sea water enriched with $CaSO_4$ to give a concentration of 1150 p.p.m. of calcium and 4330 p.p.m. of sulfate. The scale-

drying technique described above was employed, the feed being interrupted at hourly intervals. The over-all heat transfer coefficient was 1950 B.t.u./sq. ft. hr. ° F. after 7 hours' operation, compared with 800 after 2 hours' operation without scale drying. Hence the scale-drying technique is applicable to saline water containing much higher concentrations of $CaCO_4$ than standard sea water.

Acidified Sea Water. Runs were carried out with sea water acidified with HCl to neutralize all the bicarbonate alkalinity completely. The feed water was adjusted to pH of between 4.0 and 4.5, giving a value of around 7.0 for the brine concentrate. No scaling was observed during a 50-hour run, although the heat transfer surface was discolored, possibly by iron in the surface oxide film. A slight diminution in over-all heat transfer coefficient also occurred, probably due to thickening of the oxide film. Partial acidification was not effective in preventing scale; even with 90% of complete acidification, the over-all heat transfer coefficient was significantly reduced in an 8-hour run.

Preheating of Sea Water. Sea water was preheated to about 300° F. in a pressure vessel, with a noncondensable gas vent, having a holdup time of about half an hour. The preheated feed water was then passed to the spray evaporator, where evaporation took place at the usual temperature of approximately 240° F. A white $Mg(OH)_2$ scale formed fairly rapidly in the evaporator, producing a rate of fall of over-all heat transfer coefficient similar to that for untreated sea water.

Evaporation at Higher Pressure. Sea water has been evaporated at temperatures up to 300° F. in a similar unit designed to operate at elevated pressure. Preliminary experiments show that under these conditions a very thick $Mg(OH)_2$ scale is formed very quickly.

Sea Water with Conventional Additives. Experiments were made with several commercially available additives in sea water, to test their effectiveness for scale prevention in the spray evaporator. Figure 4 shows graphically the results obtained with three of the more successful additives. In all cases scale was formed, although often there was a marked change in its physical nature. The high temperature of evaporation was probably responsible for the failure of these additives to prevent scale in these experiments.

Use of Polyacrylic Acid for Scale Control. Several experiments were made with additives used previously on a laboratory scale by workers interested in crystallization phenomena. McCartney and Alexander (*9*) had used several materials as crystal growth-retarding agents and samples of some of these agents, including low molecular weight polyacrylic acid, were tested. The effect of 5 p.p.m. of the low molecular weight polyacrylic acid (molecular weight approximately 20,000) in reducing sea water scaling was most remarkable and a further larger sample was obtained from another source (*11*). Further tests with this material confirmed the initial result and prolonged run of 50 hours' duration using sea water pretreated with 3 p.p.m. gave over-all heat transfer coefficients varying from an initial 4200 to a final value of 2500 B.t.u./sq. ft. hr. ° F. During the test violent fluctuations occurred in the readings of the pressure gages connected to the bottom and top of the heat transfer tube.

Following the 50-hour polyacrylic acid run, the evaporator tube was opened for examination while still wet, and showed an apparently clean bright surface over practically the whole length of the tube. Almost immediately, thin flakes or "whiskers" of a translucent blue film appeared, detaching from the tube to leave a highly polished copper surface. The flakes appeared to be formed by air drying of a plastic film coating the surface.

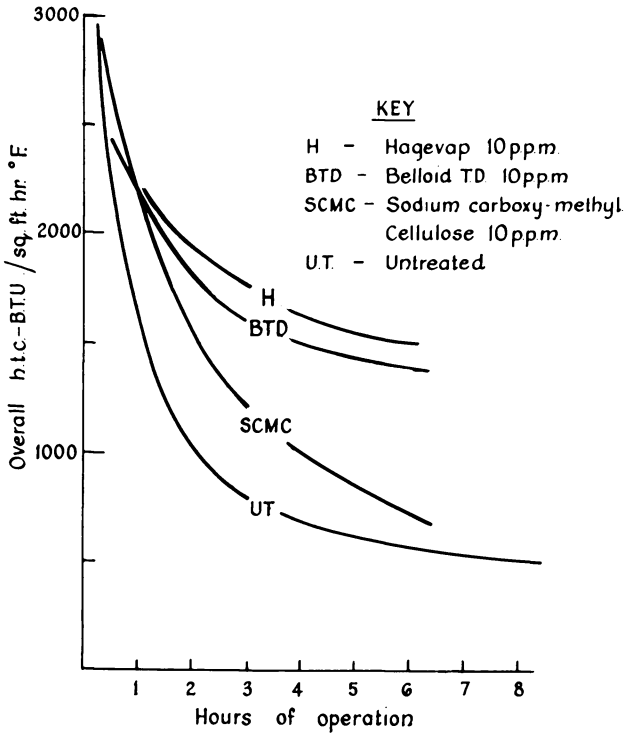

Figure 4. Over-all heat transfer coefficient vs. time for sea water plus commercial additives

It is thought that, during evaporation, a thin film containing polyacrylic acid, possibly combined with some of the cations present in sea water, forms on the surface of the copper tube. As the film thickens, shear stresses cause some portions to break away from the surface, before the film thickens sufficiently to cause significant decrease of the heat transfer coefficient, and the film is regenerated on the newly exposed tube surface. Prevention of scale formation may be due to either nonadherence of the normal scales to the surface of the film or to continuous stripping of film together with adhering scale. The final clean copper surface may be the result of mild chemical reaction with polyacrylic acid.

In one run, sodium sulfate and calcium chloride were added to a 200-gallon batch of sea water to give a sulfate concentration of 5200 p.p.m. and a calcium concentration of 640 p.p.m. An addition was made of 5 p.p.m. of low molecular weight polyacrylic acid and the treated sea water was evaporated under standard conditions. The over-all heat transfer coefficient averaged 3600 B.t.u./sq. ft. hr. ° F. for a 5-hour period, with no detectable falloff during the period, and the tube was found to be clean, except for the plastic film. In contrast, evaporation of a similar batch of calcium sulfate-enriched sea water, with no polyacrylic acid, resulted in a marked decrease in heat transfer coefficient to less than 800 B.t.u./sq. ft. hr. ° F. after 2 hours.

The possibilities of scale prevention by this "regenerating film" technique seem very promising. Considerable research appears to be justified, in order to elucidate the mechanism by which the film is produced, and the reasons for scale prevention. The principle may have applications in many scaling problems

other than desalination, and other organic polymers may find application for various scaling constituents (8).

Tests were made with commercially available polyacrylic acid having a molecular weight of around 100,000. Using 5 p.p.m. in sea water, an unusual scale was formed which was tacky when wet and which adhered in lumps to the evaporator tube and connecting pipelines. It is therefore apparent that molecular weight is an important variable in the selection of polymers for this method of scale control.

Miscellaneous Tests with Synthetic Scaling Solutions. Figure 5 shows graphically the results obtained using the following synthetic hard waters, prepared from Melbourne tap water (ca. 40 p.p.m. of total dissolved solids).

Saturated $CaSO_4$ solution, prepared by adding stoichiometric amounts of $CaCl_2$ and Na_2SO_4 to tap water.

$Ca(HCO_3)_2$ solution, prepared by adding $CaCl_2$ and $NaHCO_3$ to tap water to give 300 p.p.m. $Ca(HCO_3)_2$.

$Mg(HCO_3)_2$ solution, prepared by adding $MgCl_2$ and $NaHCO_3$ to tap water to give 300 p.p.m. $Mg(HCO_3)_2$.

As will be seen from Figure 5, the $Mg(HCO_3)_2$ solution had the most marked effect on the heat transfer coefficient, producing an almost immediate reduction of the over-all value to around 1200 B.t.u./sq. ft hr. ° F. The $Ca(HCO_3)_2$ solution scaled immediately on mixing with steam in the Venturi mixer. After about 4 hours' running, the evaporator piping was almost blocked with $CaCO_3$ scale, which was deposited most thickly in the divergent cone of the Venturi mixer.

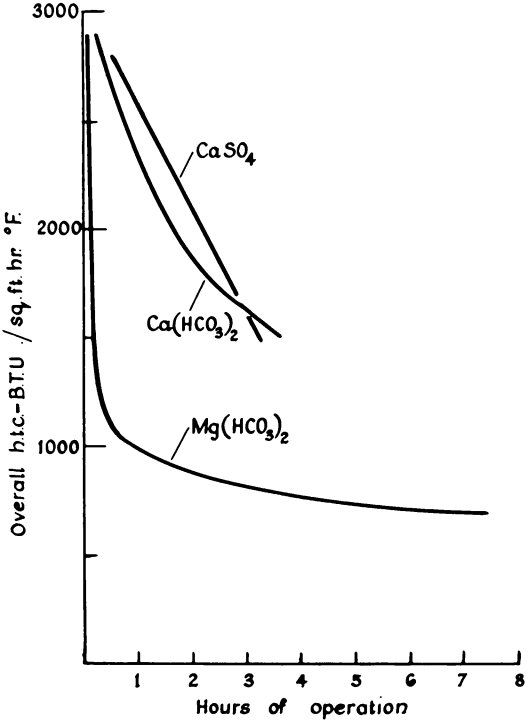

Figure 5. Over-all heat transfer coefficient vs. time for synthetic scaling solutions

While most marked with the $Ca(HCO_3)_2$ solution, it is significant that scaling occurs at all in such an evaporator system, where the total time of residence may be measured in milliseconds; even if the residence time in the preheater is included, the feed water is in the apparatus for less than 10 seconds. It would appear that scale deposition from sea water is a function of local conditions of evaporation in a given apparatus and that reported delays in crystallization (*1*) are specific to the apparatus rather than to physical characteristic of scaling solutions.

However, in the evaporation of thermally sensitive liquids, where scale is known to result from degradation products produced by slow reactions—e.g., evaporation of fruit juices, sugar solutions, etc.—spray evaporation may be one method of reducing or avoiding scale.

Discussion

The present results indicate that the spray evaporation technique provides a rapid and sensitive method for the investigation of scale formation on evaporator surfaces. Very high heat transfer rates are obtainable, especially when dropwise condensation promoters are used on the steam side, so that the effect of a thin film of scale becomes rapidly apparent.

Three new methods for the control of scale have been proposed: scale drying, dissolution by entrained reagent, and the use of strippable films of polymeric materials such as polyacrylic acid. The first two methods are particularly applicable to spray evaporation, in view of the very low liquid holdup under these conditions, so that the process of cleaning can be carried out in a matter of a minute or so by automatic time cycle control. There is evidence that scale drying is restricted to a comparatively limited temperature range of evaporation, over which $Mg(OH)_2$ is deposited in gelatinous form. The dissolution method is of much wider applicability, and, if dilute mineral acid is used as the reagent, the acid consumption is much less than that required if it were added to the sea water feed to destroy the bicarbonates. The quantity is likely to be so low, in fact, that more expensive reagents—e.g., citric acid—could be used.

Although the foregoing methods of scale control are particularly effective with the alkaline scales, there is evidence that calcium sulfate scale can also be controlled by codeposition with the alkaline scales. This is particularly true of the first two methods, and cases might well arise where small amounts of compounds such as sodium or magnesium bicarbonate might be added to waters containing high concentrations of calcium sulfate in order to control deposition of the latter.

As regards the applicability of spray evaporation to large scale water desalination, it is necessary to take into account the fact that at atmospheric pressure, or below, the high heat transfer rates are obtained at the expense of a relatively high pressure drop, so that the temperature difference available for evaporation is reduced. Since in addition a proportion of the heating steam must be bypassed through the evaporator for entrainment purposes, it is apparent that spray evaporation is unlikely to be suitable for this purpose under these conditions. However, for higher pressure operation, as in the case of high temperature stages preceding a conventional evaporator, the effect of pressure drop is less and the low temperature differences obtainable between stages as a result of the high heat transfer coefficient would minimize losses resulting from the use of entrainment steam, so that the process shows more promise.

Although the methods proposed for scale control relate specifically to spray evaporation, the strippable film technique may well be applicable to other types of evaporator, and this requires further investigation. The other two methods are practicable as a result of the very low liquid holdup in spray evaporation, so that interruption of the feed leads to elimination of the holdup in a matter of seconds. The same process should be applicable to conventional evaporators of low holdup—e.g., long-tube climbing and falling film types—if entrainment steam were admitted at the same time as the feed is interrupted, and this possibility would well repay further investigation.

Conclusions

The spray evaporation technique provides a rapid method of producing scale during the evaporation of scaling solutions. The scales deposited are chemically similar to those deposited in conventional sea water evaporators, although their physical characteristics, particularly as regards $Mg(OH)_2$ scales, appear very different.

The gelatinous $Mg(OH)_2$ scale formed during spray evaporation can be substantially removed by an intermittent "scale-drying" technique of short duration. Thin residual scale may be removed *in situ* when necessary by dispersing a suitable cleaning solution—e.g., acid—in the entrainment steam.

Both the above scale-removal techniques may be applicable to long-tube and other low holdup evaporators by the injection of steam, with or without cleaning solution, at predetermined time intervals.

Tests with commercial antiscaling additives, while producing some changes in the physical nature of the scale, have shown no prolonged effectiveness in scale prevention under the evaporation conditions used in this work.

A new additive, low molecular weight polyacrylic acid, has shown promise as an antiscale additive. It is suggested that scale prevention in this case is due to protection of the surface by a polymeric film, which alternately breaks away from the surface and regenerates, resulting in only slight resistance to heat flow.

Although the foregoing scale removal techniques were developed originally for the alkaline scales, there is evidence that calcium sulfate scales can be similarly removed by deposition in admixture with alkaline scale components.

Acknowledgment

The authors express appreciation to H. R. C. Pratt and D. F. Kelsall for their help in the initiation and direction of this work. They also record their appreciation to A. E. Alexander of the University of Sydney and to G. H. Segall of Canadian Industries, Ltd., for providing the low molecular weight polyacrylic acid used in these experiments. Thanks are also due to E. S. Pilkington for assistance with the chemical analyses.

Literature Cited

(1) Badger & Associates, Inc., W. L., Ann Arbor, Mich., "Critical Review of Literature on Formation and Prevention of Scale," Office of Saline Water, Rept. **25** (July 1959).
(2) Bennett, J. A. R., Collier, J. G., Pratt, H. R. C., Thornton, J. D., *Trans. Inst. Chem. Engrs.* **39**, 113 (1961).
(3) Collier, J. G., Lacey, P. M., *Nucl. Power* **5**, 68–73 (August 1960).
(4) Garrett, D. E., *Brit. Chem. Eng.* **3**, 498 (1958).

(5) Herbert, L. S., Procedures of Arid Zone Technical Conference, Melbourne, Paper 39 (1960).
(6) Herbert, L. S., Sterns, U. J., Australian Prov. Pat. Application **13303/62.**
(7) *Ibid.*, **13304/62.**
(8) *Ibid.*, **21150/62.**
(9) McCartney, E. R., Alexander, A. E., *J. Colloid Sci.* **13,** 383 (August 1958).
(10) Pratt, H. R. C., Thornton, J. D., Proc. 2nd Intern. Conf. Peaceful Uses of Atomic Energy, Geneva, 15/P 1451, 1958.
(11) Segall, G. H., Canadian Industries, Ltd., McMasterville, Quebec, private communication.

RECEIVED September 19, 1962.

Effect of Vibration on Heat Transfer and Scaling in Saline Water Conversion

IRWIN A. RABEN, GEORGE COMMERFORD, and GALE E. NEVILL, Jr.
Southwest Research Institute, San Antonio, Tex.

Heat transfer from the inner tube to water in forced axial flow through an annulus was investigated at Reynolds numbers of 5000 to 28,000. Transverse vibration of the inner tube significantly increased heat transfer rates. Improvement due to vibration was highest percentagewise at low flow Reynolds numbers, but showed increasing economic advantage with increasing Reynolds numbers. A qualitative explanation of the heat transfer mechanisms active in combined axial and oscillating cross flow is presented, with a new data correlation. Acoustic vibrations in the water at frequencies of 1000 to 5000 cycles per second improved heat transfer less than vibrations of the heat transfer surface. The effect of vibration of the heat transfer surface on steam condensation outside vertical tubes, nucleate boiling, and scale deposition was also studied. Typical results are discussed.

The objective of this investigation was to determine the effects of vibration on heat transfer and scaling mechanisms related to saline water conversion processes. During the initial phases of this study the effect of both vibration of the heat transfer surface and resonant acoustic vibrations in water on forced convection heat transfer was explored. Forced convection heat transfer was considerably more influenced by a vibrating heat transfer surface than by a standing acoustic wave in the flow medium. The major portion of this study was therefore concentrated on forced convection heat transfer from a vibrating heat transfer surface.

The other studies, which included the effect of vibration on steam condensation, nucleate boiling heat transfer, and scale deposition, investigated the relation of frequency and amplitude of vibration of the heat transfer surface to increases in these heat transfer mechanisms. The study of the effect of acoustic vibrations in water on forced convection heat transfer investigated the influence of frequency and amplitude of the standing waves on increasing heat transfer rates and the flow Reynolds numbers at which increases could be obtained.

In general, improvements sought were increased water film coefficient, promotion of dropwise steam condensation, and increased boiling heat flux at the same differential temperature and reduced scale deposition.

Previous work involving heat transfer from vibrating surfaces, such as the studies of Fand and Kaye (3) and Lemlich (6), has largely been concentrated on natural convection heat transfer in air. Martinelli and Boelter (7), and more recently Deaver (1), have studied natural convection heat transfer from a vibrating surface in water. Raben (8) reported on forced convection heat transfer from a vibrating surface to water in laminar flow. The purpose of the present study was to extend the range of Raben's investigations to turbulent forced convection, steam condensation, boiling, and scale deposition.

Experimental

A schematic diagram of the apparatus for the study of heat transfer from a vibrating pipe is shown in Figure 1.

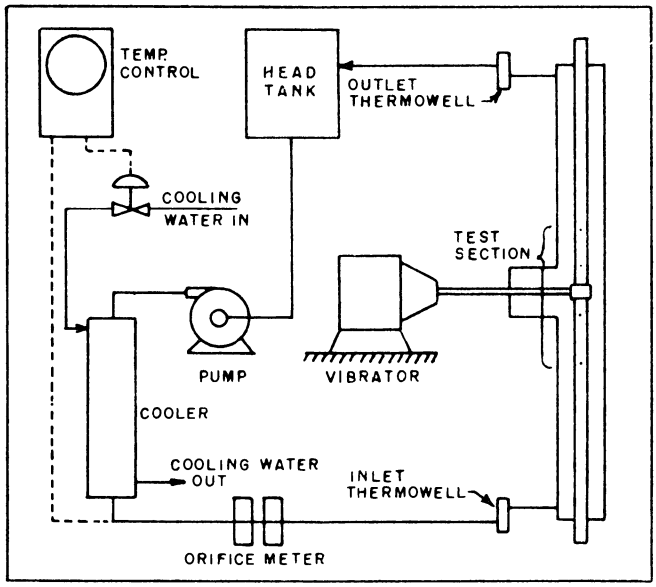

Figure 1. Schematic diagram of apparatus

Two test sections were used: an electrically heated stainless steel tube, 1-inch O.D. (38.5 inches long) installed inside the 2-inch I.D. glass pipe ($d_2/d_1 = 2$), and a 1-inch O.D. tube installed in a 3-inch I.D. glass pipe ($d_2/d_1 = 3$). The heat transfer area was the same for both (0.84 sq. foot). A Ling vibrator (25-pound force) was used for all experiments.

Thermocouples were installed in the tube wall to measure the ΔT from tube surface to the inlet water temperature and strain gages were used to measure the force applied to vibrate the tube and amplitudes of vibration.

Distilled water was used for all experiments and flow rate and heat flux were maintained constant throughout each experiment. For the annulus ratio of $d_2/d_1 = 2$, the flow Reynolds numbers, $(\mathrm{Re})_f$, studied were 5000, 6770, 10,000, 15,000, 20,000, and 28,000; for $d_2/d_1 = 3$, they were 5000, 6740, 10,000, 15,000, 20,000, and 24,000. The inlet water temperature was controlled at approximately 100° F. for all experiments.

The power from the amplifier to the Ling vibrator was maintained at 84 watts. The range of frequencies, F, studied was 30 to 100 c.p.s. The resonant frequency for the $d_2/d_1 = 2$ annulus ratio was 37 c.p.s.; for the $d_2/d_1 = 3$, 40 c.p.s. Amplitudes, H, of vibration varied from 0.02 to 0.5 inch. Force and phase angle measurements were made at each test condition, so that power required for vibration could be calculated.

An experiment consisted of the following set of steps:

1. The flow rate was set at a given value for the $(\mathrm{Re})_f$ to be studied.
2. The heat rate was set at an input level resulting in a 2° to 3° F. water temperature rise through the test unit.
3. After steady-state conditions had been reached, heat transfer data were taken without vibration.
4. The power amplifier to the vibrator was set at 84 watts and study with vibration begun. After equilibrium had been reached, heat transfer data were taken. Temperature data included ΔT from tube surface to the inlet water temperature, and dT from inlet to outlet water temperature.

Discussion and Analysis of Results

To verify the reliability of the instrumentation and gain assurance that the results obtained were typical of annular flow, it was deemed desirable to compare the heat transfer data without vibration with those of others. The equation of Wiegand (*10*)

$$\mathrm{Nu} = 0.023\,(\mathrm{Re})_f^{0.8}\,(\mathrm{Pr})^{0.4}\,(d_2/d_1)^{0.45} \qquad (1)$$

was selected as a satisfactory correlation of a large number of independent results involving heat transfer from the inner tube to water flowing steadily through a surrounding annulus. With the average water temperature taken as 100° F., the Nusselt numbers predicted by this equation for various values of the product $(\mathrm{Re})_f(d_2/d_1)^{0.45}$ are shown as the solid line in Figure 2 (Prandtl number remains constant). For comparison with these predictions of the Wiegand equation the

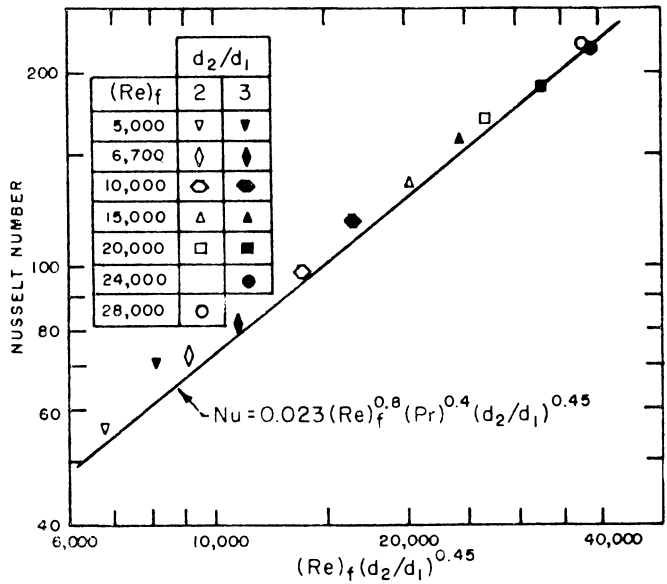

Figure 2. Heat transfer without vibration

experimentally determined Nusselt numbers for various values of $(\mathrm{Re})_f$ and d_2/d_1 for the system without vibration are also plotted in Figure 2. The experimental results fall slightly above the predicted values, with a maximum deviation of 5%, and the agreement indicates that data produced by the apparatus are reliable. Complete elimination of inlet turbulence was not attempted and the slightly higher experimental values are believed due to this turbulence and turbulence generated at the tee and shaft connection in the center of the test section.

Preliminary analysis of heat transfer from a vibrating surface indicated that the Nusselt and Reynolds numbers, with the amplitude and frequency of the impressed vibration, were the significant parameters. Since the flow when vibration is present is definitely a superposition or combination of the axial flow and vibration influences, it was considered appropriate to consider some combination parameter rather than separate parameters to represent the flow with vibration. It was therefore necessary to define a Reynolds number having significance for the combined axial and oscillatory cross flow envisioned.

The idealized model used is shown schematically below.

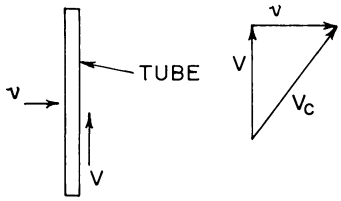

WHERE
v = OSCILLATORY CROSS FLOW VELOCITY
V = STEADY AXIAL FLOW VELOCITY
$V_c = \sqrt{V^2 + v^2}$

Thinking of a linearized model in which V and v are perpendicular, a combination velocity parameter, $V_c = \sqrt{V^2 + v^2}$, was chosen. Here the simplest possible approximation to the time-varying lateral velocity component, v, was made. v was defined as equal to the average velocity, 2 FH (twice the frequency times the double amplitude), or the total distance traveled per unit time.

With this combination velocity parameter it is possible to define a combination Reynolds number, having significance in the case where vibration is present, as

$$(\mathrm{Re})_c = \frac{d_e \rho V_c}{\mu} \tag{2}$$

The experimental data were then plotted on log-log paper (in anticipation of an exponential functional relationship) in the form h_v/h_o *vs.* $(\mathrm{Re})_c/(\mathrm{Re})_f$, where h_o and $(\mathrm{Re})_f$ represent the heat transfer coefficient and Reynolds number, respectively, without vibration and h_v represents the heat transfer coefficient with vibration as defined by the combination Reynolds number, $(\mathrm{Re})_c$. The data are adequately represented by a single straight line (see Figure 3) and it may be concluded that the slopes of the straight lines representing the data are dependent on flow Reynolds number $(\mathrm{Re})_f$ and that the intercepts (on the $h_v/h_o = 1$ line) are dependent on the annular ratio d_2/d_1.

Next, to compensate for the two d_2/d_1 ratios ($d_2/d_1 = 2$ and $d_2/d_1 = 3$), the data were replotted as h_v/h_o *vs.* $[(\mathrm{Re})_c/(\mathrm{Re})_f]\ [d_2/d_1]^{0.45}$. Since the Wiegand equation employs the factor $(d_2/d_1)^{0.45}$ for this compensation, it was used here and proved satisfactory. Single straight lines, satisfactorily representing the data for both $d_2/d_1 = 2$ and $d_2/d_1 = 3$, have been drawn for each $(\mathrm{Re})_f$ in Figure 4.

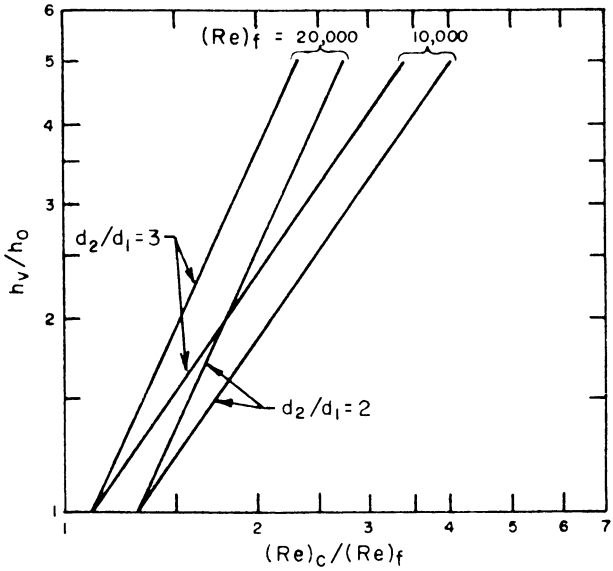

Figure 3. Heat transfer with vibration

These lines have approximately the same intercept (on the line $h_v/h_o = 1$) and their slopes increase with increasing $(\mathrm{Re})_f$.

A plot of the slopes of the lines representing the data for $(\mathrm{Re})_f$ values *vs.* $(\mathrm{Re})_f$ (Figure 5) falls very nearly on the straight-line approximation shown.

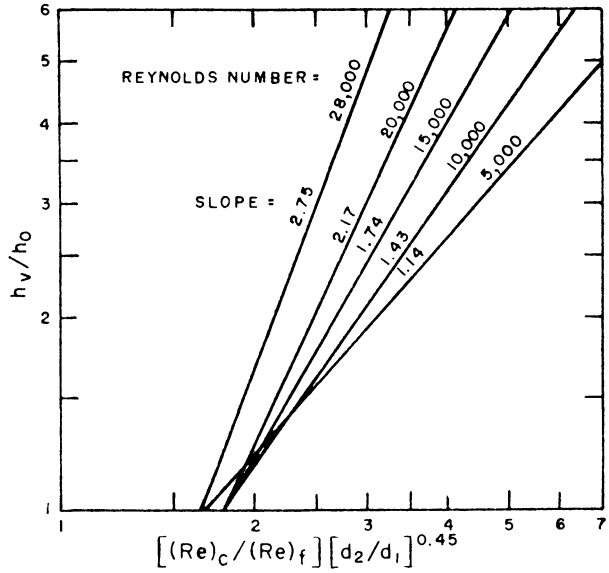

Figure 4. Heat transfer with vibration

Therefore, it was possible to correlate the data for all the values of $(\mathrm{Re})_f$ and for both d_2/d_1 ratios on the same plot, in the following way. Assuming that an exponential relationship of the form

$$\frac{h_v}{h_o} = Y\left[\frac{(\mathrm{Re})_c}{(\mathrm{Re})_f}\left(\frac{d_2}{d_1}\right)^{0.45}\right]^X \tag{3}$$

exists, we may solve for X and Y. First, the value of X may be determined from Figure 5 to be

$$X = 0.8 + 0.65(\mathrm{Re})_f \times 10^{-4} \tag{4}$$

Next, taking the logarithm of both sides of Equation 3 yields

$$\log \frac{h_v}{h_o} = \log Y + X \log\left[\frac{(\mathrm{Re})_c}{(\mathrm{Re})_f}\left(\frac{d_2}{d_1}\right)^{0.45}\right] \tag{5}$$

From Figure 4, it is seen that the intercepts at $h_v/h_o = 1$ of the lines representing the data are all close to 1.8. If this value is used, Equation 5 becomes

$$\log 1 = \log Y + X \log 1.8 \tag{6}$$

Solving for Y yields

$$Y = 10^{-0.243X} \tag{7}$$

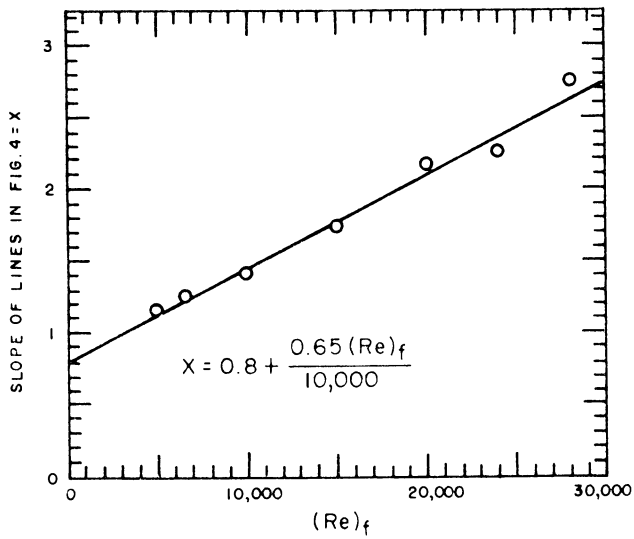

Figure 5. Change of slope with $(Re)_f$

It is seen in Figure 6 that the above correlation technique allows a satisfactory composite presentation of the experimental data for $(\mathrm{Re})_f$ values from 5000 to 28,000 and for $d_2/d_1 = 2$ and 3. Detailed data are given by Raben, Commerford, and Nevill (9).

A qualitative explanation of the above results is based on fluid dynamics and other heat transfer results. First, a relationship of the form $h_v/h_o = [(\mathrm{Re})_c/(\mathrm{Re})_f]^X$ would be expected. The fact that this exponent X is composed of a constant term plus a term dependent on $(\mathrm{Re})_f$ is not surprising, in light of the results of others—for example, Eckert and Drake (2). For axial flow, having no flow separation, the rate of increase of heat transfer coefficient with Reynolds number remains essentially constant; for cross flow, at Reynolds numbers such that flow separation occurs, it increases with increasing Reynolds number. The

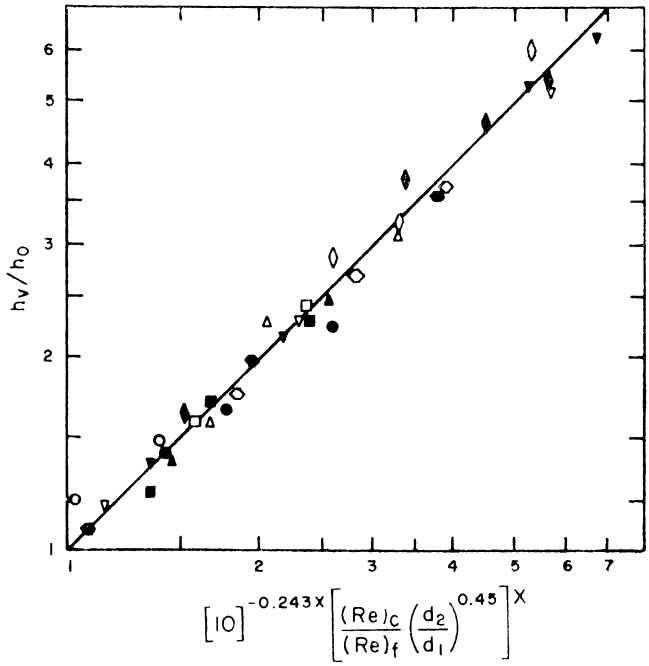

Figure 6. Final correlation
Symbols same as in Figure 2

constant and Reynolds number–dependent parts of the exponent are therefore felt to reflect the effects of axial flow and cross flow phenomena, respectively.

The changes in heat transfer coefficient due to vibration are strongly dependent on the initial flow Reynolds number. This means that the effects of vibration are strongly influenced by the initial turbulence level of the liquid. Therefore, subsequent studies of the effects of vibration on convective heat transfer phenomena should give close attention to initial or residual turbulence levels in the fluid.

The existence of a threshold value of $(\mathrm{Re})_c/(\mathrm{Re})_f$ for significant improvement is believed due to flow separation with its attendant rapid increase in heat transfer coefficient which would not take place until $\mathrm{Re}_c/\mathrm{Re}_f$ reaches some particular level.

Reductions in heat transfer coefficients (up to 25%) were found at low values of average vibrational velocity, $v = 2FH$. However, in every case as the vibrational velocity was increased heat transfer coefficients increased significantly. Since the goal of this study was to investigate possible improvements in heat transfer using vibration, it was considered appropriate to concentrate on the improvements. Results and analyses, presented previously, neglected data below the threshold values of vibrational intensity required for significant improvement in heat transfer rate. These reductions may be unique to the experimental apparatus utilized; however, since others such as Jackson (5) have reported such decreases, this is not felt to be the case. Rather, it seems likely that some not yet identified fluid flow phenomena are involved.

Extension of the results presented here is important in utilizing these findings for the design of commercial heat exchangers. The extension to prediction of results for considerably increased products of frequency and amplitude of vibra-

tion or for significantly increased $(Re)_f$ should be made with caution, since the incidence of cavitation might produce radical changes in behavior. It is, however, considered feasible to predict response for annulus diameter ratios varying significantly from $d_2/d_1 = 2$ and 3 here studied. The confidence in this extension is based on the wide range of applicability of the Wiegand equation, which utilizes the same compensation factor, $(d_2/d_1)^{0.45}$, for steady axial flow heat exchange. Finally, quantitative extensions of these results to other geometries, such as bundles, are not yet considered possible, though it is hoped that future work will allow such extensions.

Economics

The feasibility of using vibrations to improve heat transfer will eventually reduce to a question of economics. Comparisons for commercial heat exchangers have not been attempted. Rather, comparisons have been limited to those based on experimental data for the particular test apparatus used. Operation at or very near the resonant frequency of the vibrating system is desirable, since, for a given maximum exciting force, this allows a maximum amount of energy to be put into the system.

The only meaningful economic comparison considered possible for the experimental apparatus relates the relative cost in additional power to produce a certain increase in heat transfer coefficient by vibration to the cost of increasing the over-all flow velocity. Table I summarizes the power requirements of the experimental apparatus both without vibration and with vibration at resonance for several values of $(Re)_f$. Heat transfer coefficients are also shown.

Table I. Power Requirements for Experimental Apparatus

$(Re)_f$	*Pumping Power, Watts*	*No Vibration, h_o, B.t.u./Hr. Sq. Ft. ° F.*	*Power to Vibrating Tube, Watts*	*Resonance*		*Resonance, h_v, B.t.u./Hr. Sq. Ft. ° F.*
				F, c.p.s.	*H, in.*	
		$d_2/d_1 = 2$				
5,000	0.20	245	60	37	0.39	1552
10,000	0.73	429	53	37	0.50	1753
20,000	4.8	730	38	37	0.48	1751
28,000	18.3	957	47	37	0.45	1945
56,000 (calcd.)	147	1690	..	..	..	..
		$d_2/d_1 = 3$				
10,000	0.94	255	40	39.5	0.416	1044
20,000	7.0	414	41	39.5	0.414	1073
24,000	13.3	468	39	39.5	0.408	1039
48,000 (calcd.)	106.4	865	..	..	..	..

It is seen that the pumping power required rises very rapidly with flow Reynolds number, $(Re)_f$. At low $(Re)_f$ values, increases in heat transfer coefficient are obtained with relatively small increases in pumping power alone. At the higher $(Re)_f$ values, however, pumping power requirements increase very rapidly and the use of vibrations becomes economically advantageous. For example, without vibration, a heat transfer coefficient of 957 B.t.u./hr. sq. ft. ° F. was found at a $(Re)_f$ of 28,000 for the $d_2/d_1 = 2$ test apparatus. Increasing this heat transfer coefficient to 1690 B.t.u./hr. sq. ft. ° F. by increasing pumping power would require an estimated 129 additional watts of power, whereas only 47 watts of vibrational power increased the coefficient to 1945 B.t.u./hr. sq. ft. ° F. (without increasing pumping power required, since pressure drop was not affected). Pressure drop data obtained are presented in Table II.

Table II. Pressure Drop Data from Experimental Heat Transfer Unit

($d_2/d_1 = 2$)

$(Re)_f$	ΔP, Inches Water	
	Without vibration	*With vibration*
5,000	3.1	3
10,000	7	7
20,000	24	24
28,000	53	53

Results for the $d_2/d_1 = 3$ apparatus were similar. For example, without vibration, a heat transfer coefficient of 468 B.t.u./hr. sq. ft. ° F. was found at $(Re)_f$ 24,000. Increasing this coefficient to 865 requires 93.1 additional watts of pumping power, whereas only 39 watts of vibrational power increases the coefficient to 1039 B.t.u./hr. sq. ft. ° F. Quantitative generalization of the results here presented to other configurations is not believed justified; however, it appears that the use of vibrations to increase heat transfer coefficients has significant advantages over increasing over-all flow rate at the higher $(Re)_f$ values of interest. Further studies with other geometries such as tube bundles are necessary to define further the economics of using vibration to improve heat transfer.

When vibrations are used, the energy is applied directly to producing turbulence at the heat transfer surface, whereas increasing over-all flow rate requires additional pumping energy distributed throughout the entire system. The use of vibration of the heat transfer surface increases not only forced convection heat transfer, but also steam condensation and boiling heat transfer rates. In addition, since the use of vibrations tends to reduce scaling problems, whereas other turbulence-promoting devices tend to accentuate such problems and require additional pumping energy, these factors will weigh heavily in any economic comparison involving applications to saline water conversion equipment.

The use of vibrations to improve heat transfer and reduce scaling in saline water conversion and other equipment shows promise of significant economic advantage. Further study is required to develop its practical application to saline water conversion processes.

Effect of Resonant Acoustic Vibrations in Water on Forced Convection Heat Transfer

The effect of resonant acoustic vibrations in water on forced convection heat transfer was investigated at flow Reynolds numbers (defined as d_i V ρ/μ where d_i is the inside tube diameter, V is the average axial velocity, and ρ and μ are as previously defined) from 1400 to 10,000. The experimental apparatus consisted of a 0.67-inch I.D. horizontal tube, 8 feet long, with an unheated entrance section 4 feet long and a heated test and an exit section each 2 feet long. Water was circulated through the tube while the wall of the test section was maintained at 211° F. by condensing steam. Experiments were carried out at three resonant frequencies, 2500, 5000, and 7500 c.p.s., where standing waves are set up in the tube. Heat transfer increased significantly at Reynolds numbers of 1400, 2000, and 2350; above 2350, no significant increase was found. The maximum increase in over-all heat transfer coefficients was 20% at a Reynolds number of 2000 and a frequency of 5000 c.p.s. A summary of data obtained is presented in Table III.

Similar results were found by Jackson (*4*), who reported a maximum increase of 20% in over-all heat transfer coefficients at a Reynolds number of 2100, when

Table III. Effect of Resonant Acoustic Vibration in Water on Forced Convection Heat Transfer

Reynolds No.(Re)	h, B.t.u./Hr. Sq. Ft. ° F., Freq., C.p.s.				% Improvement $(h_v/h_o - 1)$ 100			Press. Ampl., Inches H_2O		
	0	2500	5000	7500	2500	5000	7500	2500	5000	7500
1,400	180	189	190	189	5.0	5.6	5.0	2	1	0.5
2,000	192	200	206	199	4.2	7.3	3.6	2	1	0.5
2,350	206	222	247	224	7.8	20.0	8.7	2	1	0.5
4,000	289	312	314	309	8.0	8.7	6.9	4	2	1.0
10,000	508	504	472	507	..	..	..	..	..	..

acoustic resonant vibrations were imposed in an air stream flowing through a horizontal heated tube.

Effect of Vibration of Heat Transfer Surface on Nucleate Boiling Heat Transfer

This experimental study investigated the effect of vibration of the heat transfer surface on nucleate boiling heat transfer over the heat flux ranges of 2300 to 15,200 and 50,000 to 250,000 B.t.u./hr. sq. ft.

The experimental unit for the low heat flux study consisted of an electrically heated 1-inch O.D. stainless steel tube inside a 2-inch I.D. pipe with water flowing through the annular space at velocities of 1 and 2 feet per second. Increases in boiling heat transfer coefficients as high as 130% were obtained at a heat flux of 4000 B.t.u./hr. sq. ft. when the inner tube was vibrated at its resonant frequency of 38 c.p.s. and an amplitude of 0.35 inch.

The experimental apparatus for the high heat flux study consisted of a $^3/_8$-inch O.D. tube inside a 1-inch I.D. pipe with water flowing at 2 feet per second through the annular space. Increases in boiling heat transfer coefficients as high as 80% were obtained at a frequency of 150 c.p.s. and an amplitude of 0.15 inch. The improvement in boiling heat transfer due to vibration decreased with increasing heat flux.

A summary of typical boiling heat transfer data with and without vibration of the heat transfer surface is given in Table IV.

Table IV. Summary

Amplitude, Inch	Q/A, B.t.u./Hr. Sq. Ft.	h_b	% Improv. $\left(\frac{h_v}{h_o} - 1\right)$ 100
Tube Diameter 1 Inch. Resonant Frequency 38 C.p.s. Area 0.84 Sq. Foot			
0	2300	449	...
0.30	2300	979 (h_{bv})	117.4
0	4000	496	...
0.35	4000	1143 (h_{bv})	130
0	6250	595	...
0.30	6250	1218 (h_{bv})	104.7
0	15,200	832	...
0.30	15,200	1505 (h_{bv})	80.9
Tube Diameter $^3/_8$ Inch. Resonant Frequency 150 C.p.s. Area 0.0327 Sq. Foot			
0	50,700	2409	...
0.15	50,700	4419 (h_{bv})	83.4
0	74,900	2535	...
0.145	74,900	3760 (h_{bv})	48.3
0	100,600	3116	...
0.14	100,600	4003 (h_{bv})	28.5
0	248,000	6672	...
0.08	248,000	6858 (h_{bv})	2.8

Effect of Vibration on Steam Condensation

Steam condensation on the outside of a tube oscillating laterally at frequencies from 25 to 150 c.p.s. was investigated.

The experimental units consisted of aluminum tubes, $^1/_2$-inch and 1-inch O.D. installed inside a 3-inch I.D. glass pipe. Cooling water was circulated through the aluminum tube and steam at atmospheric pressure flowed downward through the annular space at feed rates of 65 to 200 pounds per hour. The maximum increase in heat transfer for the vibrating 1-inch tube was 122% at a frequency of 40 c.p.s., an amplitude of 0.4 inch, and a steam feed rate of 200 pounds per hour. Improvements as high as 82% were found using the $^1/_2$-inch tube vibrating at a frequency of 25 c.p.s. and an amplitude of 0.5 inch for the same steam feed rate.

Steam feed rate appeared to have only slight effect on heat transfer coefficients. Improvement in steam condensation heat transfer due to vibration was, in general, a function of the product of frequency and amplitude.

Table V summarizes heat transfer data with and without vibration.

Table V. Effect of Vibration on Steam Condensation outside Vertical Tubes

Tube Diameter, Inch	*Freq., C.p.s.*	*Amplitude (H), Inch*	*Steam Coeff.*	*% Improvement, $(h_v/h_o - 1)$ 100*
$^1/_2$	0	0	917	...
	25[a]	0.50	1405	82.1
	70	0.13	1308	63.5
	100	0.05	1192	42.8
	150	0.025	1112	29.6
	0	0	1256	...
	30[a]	0.44	2400	87.0
	40	0.40	2860	122.0
	80	0.07	1460	16.0
	100	0.025	1370	9.0
	150	0.01	1304	3.8

[a] Resonance.

A limited study was also carried out to determine the effect of lateral vibration on steam condensation inside a 0.37-inch I.D. tube at steam feed rates of 30 to 50 pounds per hour. Two frequencies were studied—30 and 170 c.p.s. Increase in heat transfer due to vibration was found to be 25% at a frequency of 30 c.p.s., amplitude of 0.45 inch, and steam rate of 46 pounds per hour. At the higher frequency, vibration at an amplitude of 0.08 inch produced somewhat less improvement at the same steam rate.

Effect of Vibration of Heat Transfer Surface on Scale Reduction

The study of scale deposition with and without vibration was limited to determination of the feasibility of scale prevention and removal by vibration of the heat transfer surface. Calcium sulfate solutions and sea water were used as scaling liquors: calcium sulfate because of the difficulty of preventing its deposition (due to its inverse solubility), and sea water so that this vibration technique could be evaluated using a typical feed to a saline water conversion unit.

The experimental apparatus consisted of a vertically mounted tube with liquor flowing in the surrounding annular space and steam condensing inside. The tube was vibrating in a transverse direction. Initial heat transfer coefficients without vibration for calcium sulfate solutions averaged 580 B.t.u./hr. sq. ft. ° F.

After the tube was completely covered with scale, the coefficient was reduced to 335 B.t.u./hr. sq. ft. ° F., a reduction of 40%. Scaling experiments using calcium sulfate solutions with the inner tube vibrating laterally at frequencies of 33 and 94 c.p.s. and amplitudes of 0.35 and 0.045 inch, respectively, showed reductions in heat transfer coefficients of only about one half those experienced without vibration.

Similar results were obtained in experiments conducted on a typical sea water.

Conclusions

The rate of heat transfer by forced convection, steam condensation, and boiling is significantly improved by vibrating the heat transfer surface.

Scale deposition is reduced by vibration.

The heat transfer mechanisms active in combined axial and oscillating cross flow are qualitatively explained, with a new and satisfactory correlation of the data.

The use of vibration to improve heat transfer shows promise of significant economic advantage.

Acknowledgment

The authors acknowledge the contract support of the Office of Saline Water, U. S. Department of the Interior. The work was done under the technical cognizance of C. F. McGowan, Director, and W. S. Gillam, Chief of Research Division.

Nomenclature

A = heat transfer area, sq. ft.
d_1 = outside diameter of inner tube of annulus, feet or inches
d_2 = inside diameter of outer pipe of annulus, feet or inches
d_e = equivalent diameter of annulus, feet or inches = $d_2 - d_1$
d_i = inside diameter of tube, feet or inches
dT = change of temperature from inlet to outlet, ° F. = $T_2 - T_1$
F = frequency of vibration or sound, cycles per second
H = peak to peak amplitude of vibration, inches or feet
h = film heat transfer coefficient, B.t.u./hr. sq. ft. ° F.
h_o = film heat transfer coefficient without vibration, B.t.u./hr. sq. ft. ° F.
k = thermal conductivity of water, B.t.u./hr. sq. ft. (° F./ft.)
T = temperature, ° F.
T_1 = inlet water temperature, ° F.
T_2 = outlet water temperature, ° F.
ΔT = differential temperature across film, ° F.
V = flow velocity of water, feet per second
V_c = combined velocity of flow and vibration, feet per second $= V^2 + v^2$
v = average velocity of vibration, inches or feet per second = $2FH$ or total distance traveled ($2H$) per unit of time
Y = variable function
μ = viscosity of water, lb./ft.-second
ρ = density of water, pounds per cu. foot
Nu = Nusselt number = hd_e/k
Pr = Prandtl number = $C_p\mu/k$
(Re) = Reynolds number = $d_iV\rho/\mu$
$(\mathrm{Re})_c$ = combined Reynolds number for water flow with vibration = $d_eV_c\rho/\mu$
$(\mathrm{Re})_f$ = flow Reynolds number for water without vibration = $d_eV\rho/\mu$
Q = heat transferred, B.t.u./hr.

Literature Cited

(1) Deaver, F. K., ASME 1961 Meeting, New York, N. Y., Paper 61-WA-178.
(2) Eckert, E., Drake, R., "Heat and Mass Transfer," 2nd ed., McGraw-Hill, New York, 1959.
(3) Fand, R., Kaye, J., "International Development in Heat Transfer, A.S.M.E.," p. 490, 1961.
(4) Jackson, T., Spurlock, K., Oliver, C., Paper 57, 1961 International Heat Transfer Conference, ASME, p. 483, 1961.
(5) Jackson, T., Spurlock, K., Purdy, K., Progress Report 4, Contract AF 33(616)-5742, Project A-383, Georgia Institute of Technology, June 1959.
(6) Lemlich, R., *Ind. Eng. Chem.* **47**, 1175 (1955).
(7) Martinelli, R., Boelter, L., Proc. 5th Intern. Congr. Appl. Mechanics, 1938, p. 578, Stanford Univ. Press.
(8) Raben, I. A., Proc. 1961 Heat Transfer and Fluid Mech. Inst., p. 90, Stanford Univ. Press.
(9) Raben, I. A., Commerford, G. E., Nevill, G. E., Jr., Final Report (Contract No. 14-01-001-188), Project 2-919-1, Office of Saline Water, Dept. of Interior, February 1962.
(10) Wiegand, J. H., *Trans. A.I.Ch.E.* **41**, 147 (1945).

RECEIVED May 28, 1962.

6

Saline Water Conversion Using Wiped Thin-Film Distillation

CHARLES W. LOTZ

Distillation Equipment Program, Missile and Armament Department, General Electric Co., Burlington, Vermont

The chief advantages of thin films of distilland and condensing steam in the distillation of sea water is that significantly higher heat transfer rates are obtained. The wiped film process uses a rotating wiper blade to form the thin distilland film, and a corrugated surface to drain condensate, resulting in a thin condensate film. Using this method, several laboratory models and prototypes have been built and tested. The results have been a net increase in output for a specific expenditure of energy and use of surface. Durability of results has been obtained by the addition of phosphate-based chemicals or sulfuric acid to the sea water feed.

The deterrent to large scale conversion of saline water to fresh water has been the economics of the various conversion processes. Costs of energy and capital equipment have been too high. Distillation is still believed by many to hold the greatest promise of an economical process (*1*). However, there must still be developed means of using low cost materials of construction and of increasing the output from the amount of heat transfer apparatus used.

Much is being learned of the role of dissolved oxygen, pH, and other properties of saline water as they affect the life of materials of construction. We are fast approaching the time when carbon steel, cast iron, and plastics can be used for saline water distilling plants.

To obtain higher output from the heat transfer surfaces of the still, the resistance to the flow of heat along the path through the surface must be reduced. Numerous investigators have shown that generally the fluid boundary layer or film immediately adjacent to the heat transfer surface represents the major portion of over-all resistance. In fact, the use of high fluid velocities and turbulence inducers to minimize these fluid films is well known.

F. J. Neugebauer and E. L. Lustenader of the General Electric Co. studied mechanically removing the boundary layer of evaporating water in 1957. Included in this work was the optimization of a series of drainage grooves to break up the fluid film on the condensing side of a steam-heated evaporator surface. The result

(3) was a remarkable improvement in over-all heat transfer coefficient. This investigation led to the development of the wiped thin-film distillation process (2).

The distilling unit consists of an outer shell and an inner heat transfer tube or bundle of tubes. Figure 1 shows such a distilling unit in cross section. The heat transfer tube is made of copper and is about 6 inches in diameter. On the inside of each tube is an assembly of rotating wiper blades fixed to a hollow shaft driven at low speed by a subfractional horsepower motor.

The raw feed, previously heated in counterflow to distillate and brine, enters at the bottom of the hollow drive shaft. Flowing upward in the drive shaft, the feed exits near the top through small distribution ducts and pours onto the inside surface of the heat transfer tube. The wiper blades continuously spread the feed in a thin unbroken film on the inside wall of the tube. The feed gravitates toward the bottom. Feed in excess of the thin film is carried along in front of the blades. No heavy boundary layer is permitted to form.

Steam at higher temperature and pressure is admitted to the distilling unit shell and condenses, giving up heat on the outside wall of the tube. This heat provides the energy to vaporize part of the thin film. The vapor, which is later condensed separately, is drawn off the top of the tube, the concentrated brine is drawn off the bottom, and the condensate is removed from the bottom of the shell.

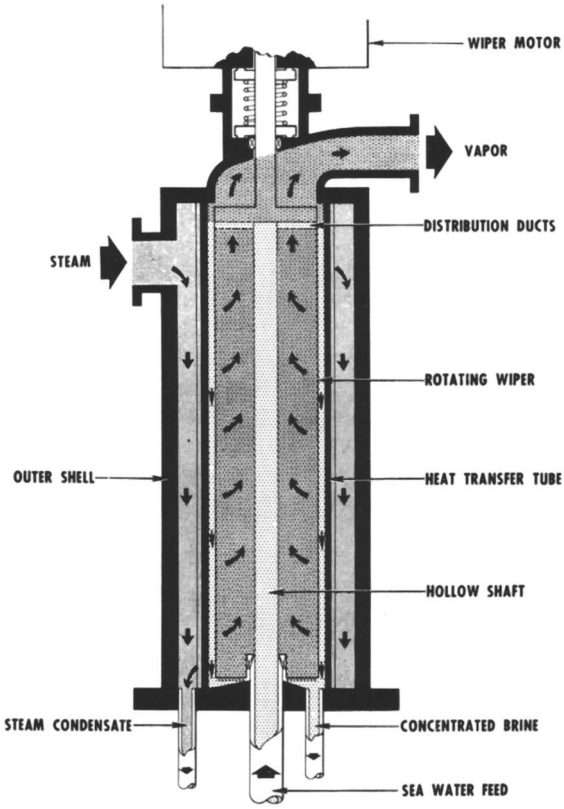

Figure 1. Schematic diagram of distilling unit

Figure 2, an end view of the same distilling unit, shows more clearly the arrangement of the rotating wiper blades. The wave of excess feed water formed in front of each blade is composed of the raw feed plus concentrated brine from the

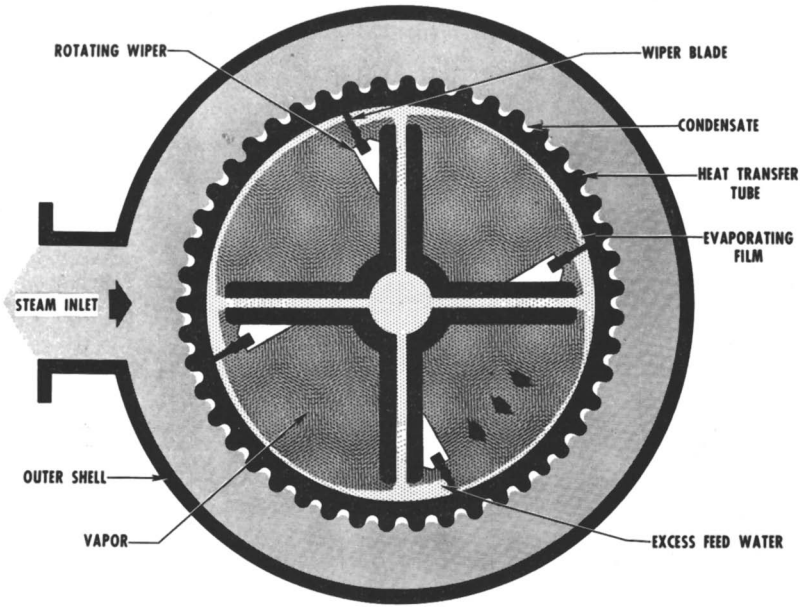

Figure 2. Operation of thin-film distilling unit

passage of the preceding blade. From top to bottom the wave and film of water become progressively concentrated in dissolved solids as evaporation takes place.

The pattern of the wave and film was studied using a glass tube and a stroboscopic light source. Figure 3 shows the turbulence in the wave, and the outstanding clarity of the transparent thin film.

The path of heat flow in this distilling unit is through the layer of condensate and the tube wall and into the evaporating film. The over-all resistance to the flow of heat is equal to the sum of the resistances of these three elements. High over-all performance is obtained in the distilling unit by the reduction of all of these series resistances. As in an electric or hydraulic series circuit, one high resistance in the path could choke the entire flow. They are reduced in the three elements as follows.

Since it proved impractical to rotate wiper blades about the outside surface of the tube, small vertical drainage grooves in the outside surface of the copper tube were used to lower the resistance in the layer of condensate. These grooves minimize the film of condensate which forms on the intervening surfaces, providing areas of low resistance. The shape, relative size, and pitch of the grooves determine the effectiveness of this extended surface to drain off the condensate. The grooves tend to overflow and become less effective toward the bottom of the tube, if the vertical length of the condensing surface is too great. A drainage groove, designed to provide ample condensing surface after adequate cross section for downward flow, proved satisfactory in actual tests.

Low resistance to heat flow was obtained in the wall of the tube by using oxygen-free copper for the tube. This material possesses high conductivity and excellent corrosion resistance in most saline water environments. For special applications where copper is not suitable, bronze or aluminum brass could be used. Low conductivity material such as Monel and copper-nickel is not suitable.

The thermal resistance of the evaporating wiped film is governed by its

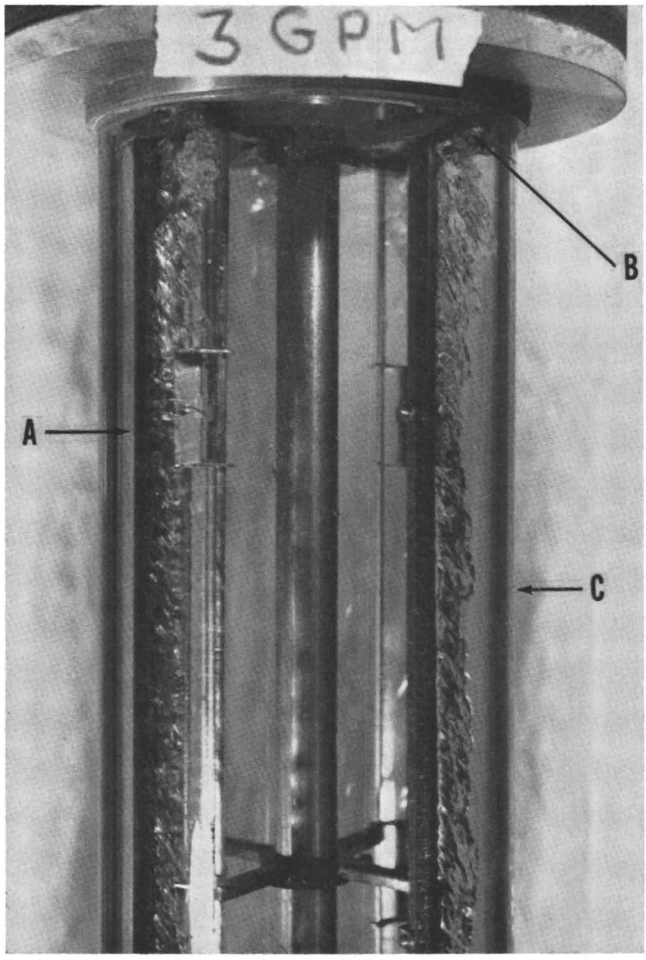

Figure 3. High speed strobe light photograph of wiper assembly in operation

A. Wiper, 200 r.p.m.
B. Water distributor discharge, 3 gallons per minute feed
C. Glass tube simulating fluted heat transfer surface

average thickness, which depends on the initial thickness immediately behind the rotating blade, the rate of evaporation, and the rate of renewal of the film.

All of these factors are easily controlled in the design of such apparatus. Initial film thickness is controlled by hydrodynamic action of the blade, defined as that resulting from the balance of centrifugal force, water resistance, and a journal bearing type of lift. Rate of evaporation is controlled by the selection of the operating temperature difference across the heat transfer tube and the rate of film renewal is controlled by choice of output speed of the gear motor which drives the blade.

The manner in which these factors affect thermal resistance of the evaporating film can be seen in Figure 4. Increasing the operating temperature difference and therefore the rate of film evaporation improves performance at a selected wiper

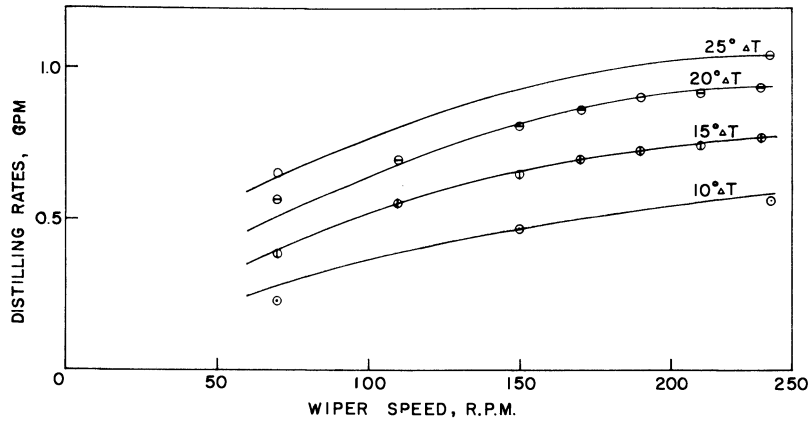

Figure 4. Marine tube performance
Evaporating temperature level 170° F.

speed, since it reduces the average film thickness. For a given temperature difference, increasing wiper speed increases the rate of renewal of the feed film and also causes the hydrodynamic action of the blade to spread a film of smaller initial thickness. This again results in a smaller average film thickness. The result is an increase in performance up to about 250 r.p.m.

As a result of this development for low path resistance, a heat path with an over-all heat transfer coefficient five times higher than in conventional distillation equipment was obtained. Coefficients on the order of 2500 B.t.u./hr./° F./sq. ft. were easily obtained in the operation of the units. Depending on the cost factors of a particular application, this fivefold increase in productivity of the heat transfer surface can be used to decrease the temperature difference and the energy required to distill a given quantity of water, or to reduce the square footage of heat transfer surface required to distill a given quantity of water. Ideally, benefits from the fivefold increase should be distributed between the energy and the square footage

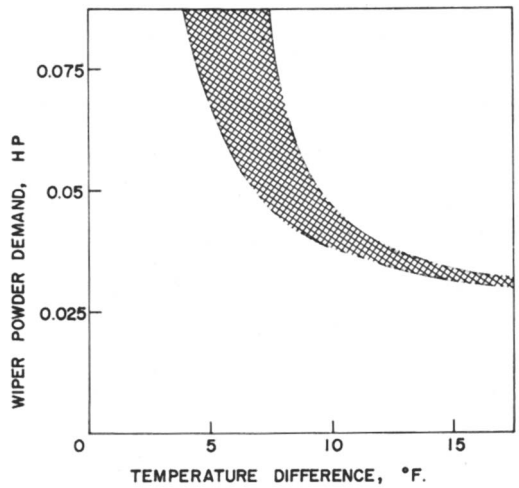

Figure 5. Wiper power demand

of heat transfer surface in whatever way will realize the greatest cost savings (*4*, *5*).

Rotating parts have been utilized, consisting of the shaft assembly pieces set in water-lubricated Rulon bearings. The power required for rotation under actual operating conditions was found to be about 1/20 hp. per shaft, as can be seen in Figure 5. The blades encounter very little drag or wear, because they ride on a film of water, and this no doubt accounts for the low power expenditure. An additional shaft seal similar to those used in the plant pumps is also required. These component parts are all subject to low stress and wear. Present wiped thin-film plants have an excellent machinery history on these rotating parts.

Scaling has always presented a problem in distilling brackish and sea water. High heat transfer rates will deteriorate very rapidly if scale is allowed to accumulate on the tube surface. Early in this development program it was feared that the gains being made in heat transfer could not be sustained because of scaling.

During several thousand hours of tests with full strength sea water while injecting phosphate-based chemicals for scale control, it was found that the action of the rotating blades discourages a buildup of heavy scale. Only a thin layer forms, which interferes very little with the transfer of heat. This thin layer was

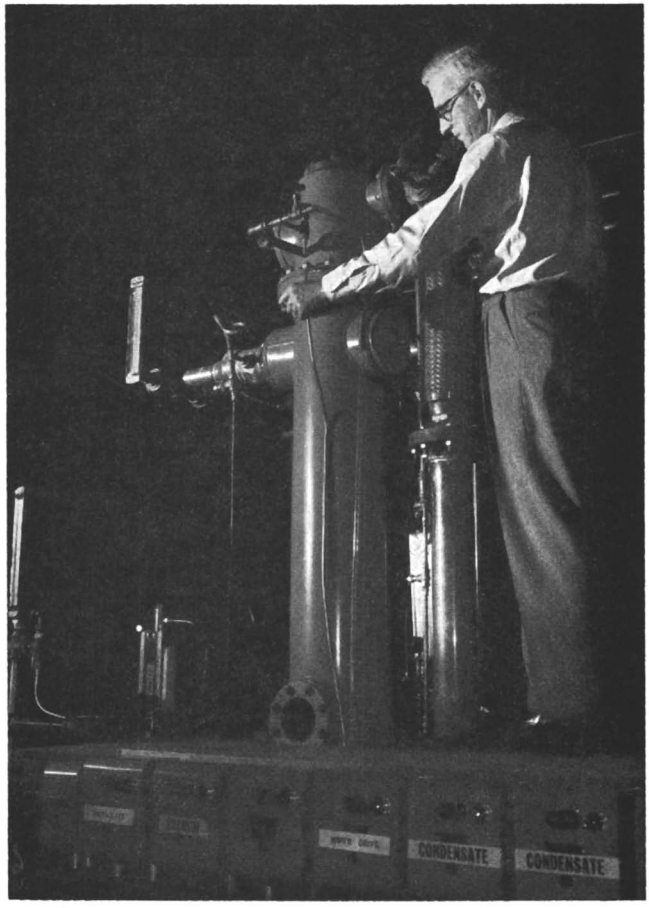

Figure 6. Wiped thin-film distilling unit

easily cleaned off with inhibited sulfamic acid. In other runs, sulfuric acid was 100% effective in preventing scale formation.

The purity of the distillate is one of the most important measures of performance in distillation equipment. Evaporation from wiped thin films was not accompanied by violent flashing or boiling, which would propel droplets into the vapor. Consequently, no special separating or drying equipment is needed to meet distillate purity requirements for most applications. But if high heat fluxes or low evaporating temperatures are required, as in the marine distilling units built to date using the thin-film process, the resulting high vapor velocity inside the tube will cause particles of feed water to be stripped from the film and carried into the vapor stream. In this case Monel mesh is installed in a vertical section of the vapor pipe to strain out the droplets in the vapor. Such a marine distilling unit is shown in Figure 6 on test. The mesh is contained within the section on which the drive motor is mounted.

The stability of performance was demonstrated by several thousand hours of laboratory testing, including one 1100-hour test at the Navy's Engineering Experiment Station at Annapolis. These tests showed that the average over-all heat transfer coefficient of 2500 B.t.u./hr./° F./sq. ft. can be maintained over long periods of operation. Figure 7 is a plot of a week's running at Annapolis. Phosphates were added to the sea water feed for scale control in these runs. The same equipment was used throughout the tests.

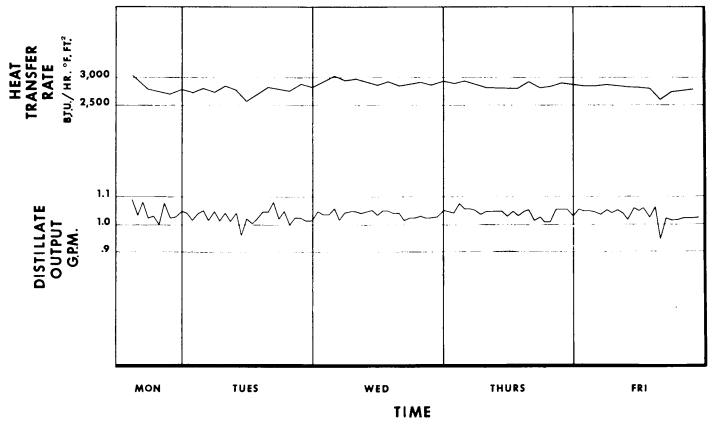

Figure 7. *Data from navy evaluation test*

The resulting net increase in productivity demonstrated in these tests has led to the design of a pilot plant now under construction for the Office of Saline Water. A model of this plant is shown in Figure 8.

The OSW pilot plant is conceived as a test model composed of the building blocks for a 15-effect 250,000-gallon-per-day plant, to be installed at OSW's new sea water test facility at Wrightsville Beach, N. C. It will consist of two effects of thin-film evaporators, with all heat exchangers, pumps, vacuum, and deaeration equipment. The pilot plant capacity will be 37,000 gallons per day when operating at 10° F. temperature difference per effect. The pilot plant will be tested as two adjacent effects of the 15-effect 250,000-gallon-per-day plant on which it is based. Operating range will be from the design conditions of effects 1 and 2 to those of effects 14 and 15. Test variables will include operating temperature dif-

ference and feed-distillate ratio. This pilot plant program will develop the data from which optimum designs of large wiped thin-film distillation plants will evolve. Operation is planned to start in April 1963.

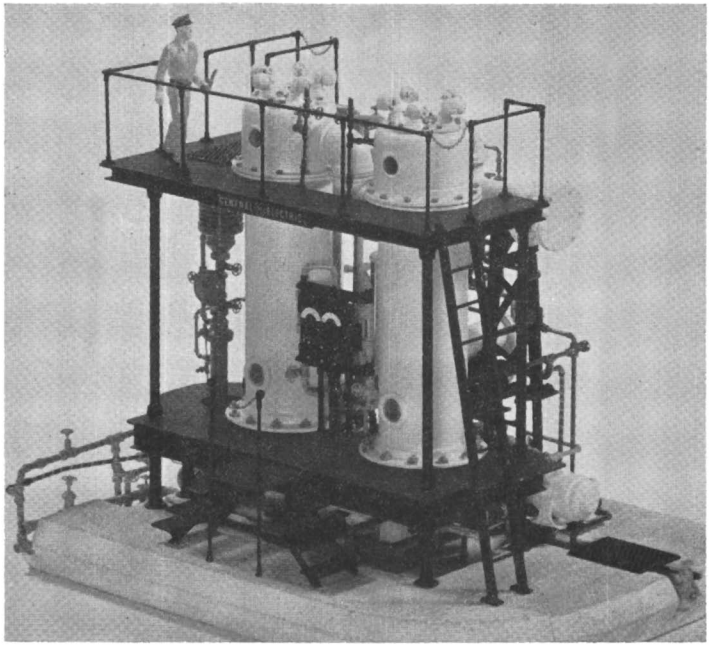

Figure 8. Distillation pilot plant

Office of Saline Water, 37,000 gallons per day

Literature Cited

(1) Ellis, C. B., "Fresh Water from the Ocean," Ronald Press, New York, 1954.
(2) Lotz, C. W., "Wiped Thin Film Distillation. New Process for Purification of Water," American Power Conference, 1962.
(3) Lustenader, E. L., Richter, R., Neugebauer, F. J., *J. Heat Transfer* **81**, 297–307 (1959).
(4) Miller, E. H., "Economic Factors Affecting Integration of Sea Water Distillation and Steam Power Generation Cycles," National Power Conference, 1961.
(5) Murphy, G. W., "Minimum Energy Requirements for Sea Water Conversion Processes," Office of Saline Water, Progr. Rept. 9 (1956).
(6) Sonderman, G. E., "Economics of Salt Water Conversion for the Power Industry," American Power Conference, 1961.
(7) Whistler, R. E., "Operation of the Sea Water Distillation Pilot Plant, Mandalay Station," American Power Conference, 1960.

RECEIVED September 24, 1962.

7

Saline Water Conversion by the Diffusion Still

E. L. LUSTENADER

General Engineering Laboratory, General Electric Co., Schenectady 5, N. Y.

The purification of saline water by a rotating disk diffusion still has been investigated. A multistage diffusion cycle arrangement has been tested in which partial pressure gradients are used to achieve multistaging in a single container with no internal partitions. Evaporation and condensation take place at atmospheric pressure. The cycle is similar to a conventional multiflash-recirculation arrangement and theoretically can achieve the same performance ratios (distillate produced per unit of heat input) and thermal efficiencies as the multiflash evaporator at the same temperatures. For a given capacity, the diffusion still, because of its lower condenser performance, requires more condensing surface area than a multiflash unit. However, the requirements for a vacuum container, partitions between stages, an air ejection system, and means for vapor-liquid separation are eliminated. The diffusion still appears most suitable where capacity does not exceed 500 gallons per day or increased condenser area is of minor importance, as in household or light commercial use.

There are surprisingly few areas in the world where natural fresh water (ground water) is so low in mineral content as not to be a candidate for softening or demineralization. In this country, only the New England states, part of the eastern seacoast, and a few central southern states fit this category. In most other areas, ground water hardness is well above 200 p.p.m. In many areas, the ground and surface waters are distinctly brackish, with mineral content of over 1000 p.p.m. In these areas, the usefulness of a demineralizer may be considered essentially the same as that of a water softener in moderately hard water areas. In addition, demineralization is useful for the conversion of saline and other brackish waters to fresh, and for producing the equivalent of distilled water where that is desirable. There are many applications for a small demineralizer. In practice, demineralization can be accomplished in a variety of thermal cycles and mechanical configurations. Trade-offs in equipment size and complexity for thermal efficiency and operating cost can be made in almost any proportion.

This paper describes a development effort made in the small demineralizer area (less than 500 gallons per day). The concept discussed is a rotating disk diffusion still capable of being multistaged yet remaining fundamentally simple.

Diffusion Still Concept

The principle of operation of the diffusion still is first described as a single-stage device. This is illustrated in Figure 1, in which the system is shown comprised of two parallel heat transfer surfaces—one supplied with heated feed water, the other cooled. The surfaces are closely spaced. The heated water is supplied to surface *a* for evaporation.

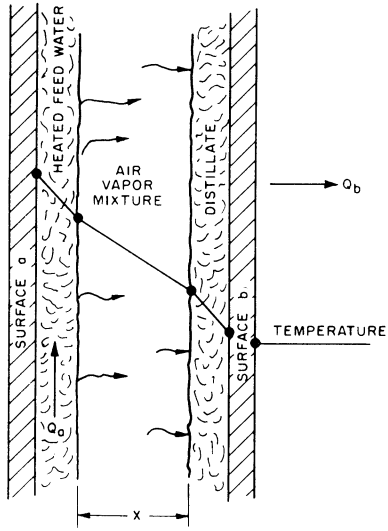

Figure 1. Basic principle of diffusion

As in a flash distillation system, the heat of vaporization is supplied as sensible heat in the incoming liquid. When vaporization occurs at surface *a*, the water molecules leave the evaporating liquid, diffuse through the air-water vapor mixture between the plates, and condense on the adjacent surface, *b*, where pure water is formed. By maintaining the condensing surface, *b*, at a temperature lower than the evaporating surface, *a*, partial pressure and temperature gradients are established which maintain the mass transfer process.

The basic rate equation for mass transfer is given (*1*) as:

$$G = -\frac{DP_o}{XR_vT_o} \ln \frac{P_o - P_{va}}{P_o - P_{vb}} \tag{1}$$

where

$$D = 0.982 \frac{(14.22)}{P_o} \left(\frac{T_o}{460}\right)^{1.8} \tag{2}$$

Equation 1 is valid for diffusion through a stationary gas. It has been successfully used to describe the experimental results which follow, thereby indicating that at close spacing between the condenser and evaporation surface, the air gap is diffusion-controlled with little or no convection effect.

From a number of possible configurations utilizing this diffusion concept, the configuration shown in Figure 2 was selected (3) on the basis of being mechanically simple.

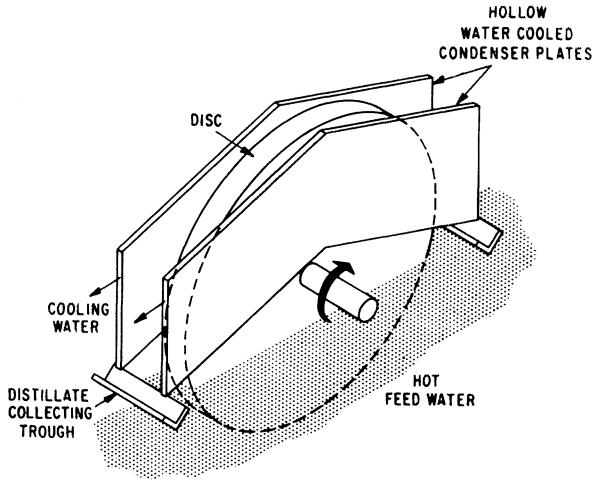

Figure 2. Schematic diagram of diffusion still

A number of vertical flat disks, one of which is shown, are secured to a horizontal rotating shaft. The bottom half of the disk is immersed in a reservoir of heated feed water; the top half passes between fixed condenser plates.

As the shaft turns at a speed of about 60 r.p.m., a film of feed water is picked up by the disk (5) and passes approximately $^1/_8$ inch from the condenser plates. Water vapor transfers by diffusion through the air from the hot feed water film on the disk surface to the colder condenser surface. The residual water film on the disk is cooled by the evaporation and its salinity is increased. The disk surface then returns to the reservoir, where the cool concentrated film is washed off and the film is renewed with hot feed water.

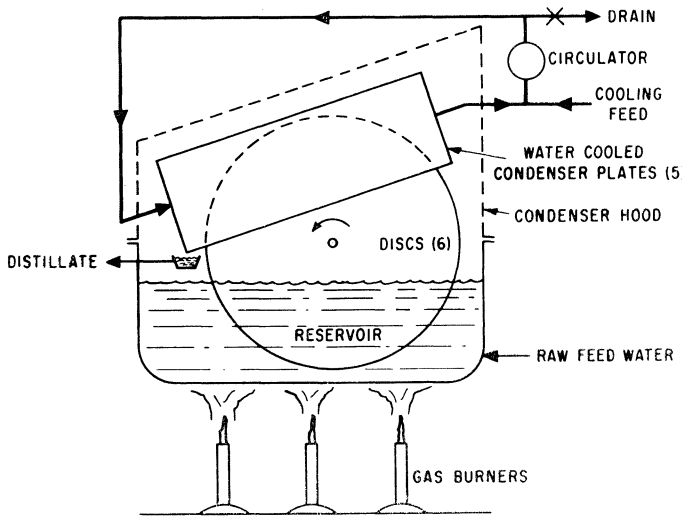

Figure 3. Single-stage bench model

The bottom edge of each condenser plate is sloped at an angle of approximately 30 degrees from the horizontal, from the center line of the condenser to each outer edge. Surface tension between the condensate and the condenser plate allows the condensate to adhere to the condenser surface and then to drain to the outer edge, where the condensate is accumulated in a collection trough.

Development Program

As a first step in the development program, a single-stage bench model of the device as shown in Figure 3 was evaluated.

It consisted of a single-pass, five-plate, water-cooled condenser capable of independent flow and temperature control. Heat was supplied to the evaporator reservoir, so that it could be operated at selected temperature levels. The rotating assembly, consisting of a shaft with spacers capable of accepting six disks 12 inches in diameter, of varying thickness and composition, was equipped with a variable speed drive. With the arrangement shown, approximately 2 sq. feet of disk-condenser surface area was available for mass transfer. Tests were performed on this unit at atmospheric pressure, using city water (125 p.p.m. of dissolved solids) as feed, to determine the effect on distillation rate of: (1) reservoir temperature level, (2) reservoir-condenser temperature difference, (3) disk rotational speed, (4) disk condenser spacing, (5) disk material, and (6) reservoir salinity. A few short tests were made using a simulated sea water solution.

The results of these tests can be summarized as follows:

Reservoir Temperature Level. The rate of diffusion of water vapor across the disk-condenser gap is a function of the partial pressure of air at the liquid surfaces a and b, by the ratio

$$\ln \left[\frac{\text{partial pressure of air at } a}{\text{partial pressure of air at } b} \right]$$

Increasing the reservoir temperature while holding a constant disk to condenser temperature difference decreases the partial pressure of air at a more than at b, giving a net increase in the rate. Furthermore, combining Equations 1 and 2 to eliminate the term D yields an equation explicit in $T^{0.8}$. The increase in reservoir temperature increases the rate by increasing the diffusion coefficient as well as the partial pressure gradient.

Reservoir-Condenser Temperature Difference. As the temperature difference is increased, the water vapor partial pressure gradient across the disk condenser gap steepens, which increases the rate of mass transfer for constant values of reservoir temperature.

Disk Rotational Speed. For all temperature conditions, the distillation rate was found to be very low when the disks were stationary, typical of condenser performance in the presence of noncondensable gases (2). However, when the 12-inch-diameter disks were rotated in the range of 5 to 60 r.p.m., distillation rate increased by a factor of 10 or more, depending on temperature level. Maximum speed of rotation was established by the point of carry-over (due to slinging of feed water into the condensate collection troughs). Excessively low disk speeds were found to result in a low heat transfer coefficient between the submerged disk surface and the water in the reservoir. Because of the relatively high temperature depression of the disk surface which is required to replace the heat removed from the disks by the water film during evaporation, the mean evapora-

tion temperature level of the disk surface is reduced, with consequent reduction in performance.

Disk-Condenser Spacing. Water vapor mass transfer varies inversely with the width of the gap which must be traversed by diffusion. Minimum gap width was established by mechanical interference considerations and balanced against costs of dimensional control. Tests indicated that gaps of $^3/_{32} \pm {}^1/_{32}$ inch gave good performance without requiring excessive mechanical precision. At this spacing, distillation rates were sufficiently high that surface area requirements, essential to provide output capacity compatible with small device applications, were within reason.

Disk Material. Disk materials with varying heat capacities including copper, brass, aluminum, and Transite were tried with no detectable effect on output at 60 r.p.m. Later analysis (*4*) showed that, for a disk with a high thermal diffusivity, most of the energy for vaporization is derived from the disk material. The minimum film temperature is thus determined by the temperature difference between the water in the reservoir and the submerged disk required to "replace" the heat removed from the disk by the film. For a disk with a low thermal diffusivity, a larger portion of the heat of vaporization is removed from the liquid film, so that less heat is removed from the disk, because the low diffusivity of the disk increases the thermal resistance. However, about the same temperature difference between the water reservoir and the submerged disk surface is required as for a high thermal diffusivity disk material. Theoretical considerations thus predict the effect of disk material on performance correctly. These considerations suggest the possibility that disk thickness can be made less than $^1/_8$ inch.

Reservoir Salinity. The test equipment was operated for extended periods with no blowdown from the reservoir. Salinity in the reservoir was allowed to build up approximately an order of magnitude, with no detectable effect on unit output or product purity. Short tests were made using a simulated sea water solution containing approximately 35,000 p.p.m. of dissolved sodium chloride. The distillate produced contained less than 1 p.p.m. of total dissolved solids.

Figure 4 shows a typical set of performance data recorded at a constant reservoir temperature level of 150° F. The effects of reservoir-condenser tempera-

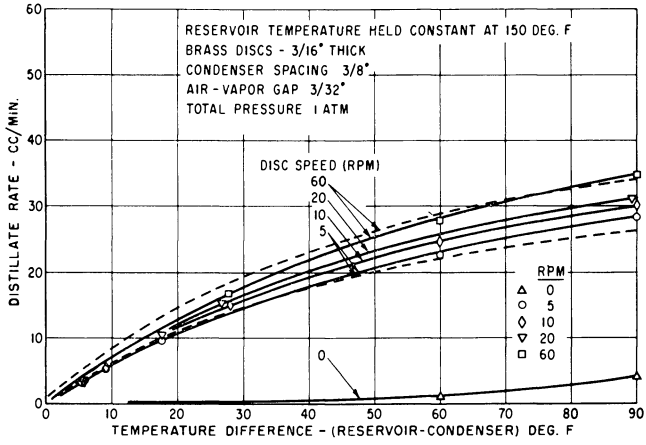

Figure 4. Single-stage diffusion still performance

—— Test
— — — Theory (2)

ture difference and disk speed are visible. A set of predicted curves are shown for comparison with test.

The net results of this first single-stage evaluation are summarized in Figure 5 in the form of condenser performance *vs.* reservoir temperature level and reservoir-condenser temperature difference. The curves shown are valid for distillation at atmospheric pressure, a constant disk speed of 60 r.p.m., and an air-vapor gap of $^{3}/_{32}$ inch. Since the test condenser was water-cooled at high flow rates, the over-all heat transfer coefficients shown are considered to be maximum values controlled by the resistance on the diffusion side.

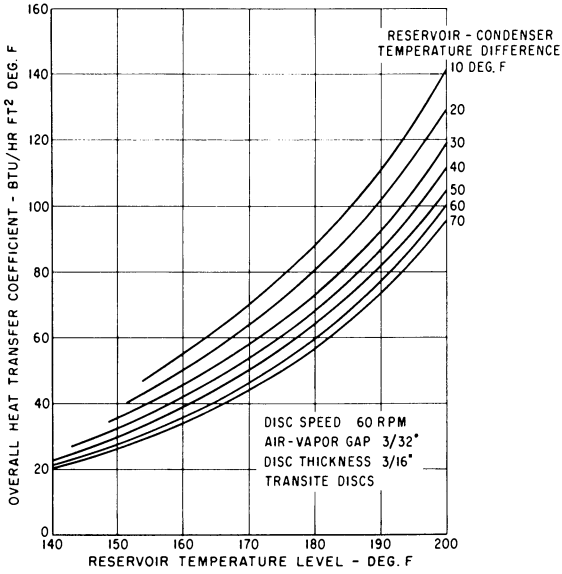

Figure 5. Condenser component performance

As the reservoir temperature level approaches 212° F., the saturation temperature corresponding to 1 atm., the over-all performance of the condenser should approach a value in the order of 500 to 700 B.t.u./hr. sq. ft. ° F.

Multistage Concept

A multistage arrangement of the basic diffusion still component (Figure 2) is possible, as shown schematically in Figure 6.

The unit is comprised of a set of stationary condenser plates, an atmospheric container with reservoir, a heater, a cooler, a set of rotating disks, and a recirculation pump.

The condenser plates, previously water-cooled in a parallel flow arrangement in the single-stage device, are now arranged in a series flow pattern to recover the heat of vaporization. A mixture of cold feed water and warm reservoir discharge water enters the first condenser plate. As the mixture flows through each condenser plate in series, its temperature is increased by the latent heat received from the condensation which occurs on the outside of the condenser plates. Upon discharging from the condenser unit, the flow enters a heater where its temperature is further increased. (The source of energy for the heater can be a resistance heating element, combustion of gas or oil, waste heat, or the condenser of a heat pump.)

The flow then enters the high temperature end of the reservoir, where a temperature difference has now been established between the last condenser plate and the water film on its adjacent rotating disk. As the water flows through the reservoir, raw water is picked up as a thin film by rotating disks and passed between the cold condensing surfaces. Both heat and mass are transferred from the reservoir to the condenser. This results in a lowering of reservoir temperature in the direction of flow. The evaporation which takes place on the disk surface is similar to that which exists in a flash distillation system, since the heat of vaporization has been partly stored as sensible energy in the film on the rotating disk (part of the energy for vaporization is stored in the disk material). Flashing will not occur, however, since the liquid is always below its boiling point.

The temperature drop of the liquid as it flows through the reservoir is approximately equal to the temperature rise of the liquid flowing in the condenser. A small part of the reservoir discharge flow is drained to control reservoir salinity. The remaining part of the flow enters a recirculation pump, and is pumped through a cooler, and the cycle is repeated. Under certain design conditions, cycle cooling can be obtained by the cold feed water. The difference in sensible energy between the warm distillate removed and the cold feed water supplied provides the necessary heat sink.

As shown in Figure 6, the entire unit is vented to atmospheric pressure and operates with a total pressure of 1 atm. The temperature of the liquid in the reservoir varies from one end to the other. The partial pressure of water vapor above the liquid will also vary in accordance with this temperature gradient. At each location along the length of the reservoir, the sum of the partial pressure of the air and the partial pressure of the vapor is constant and equal to 1 atm.

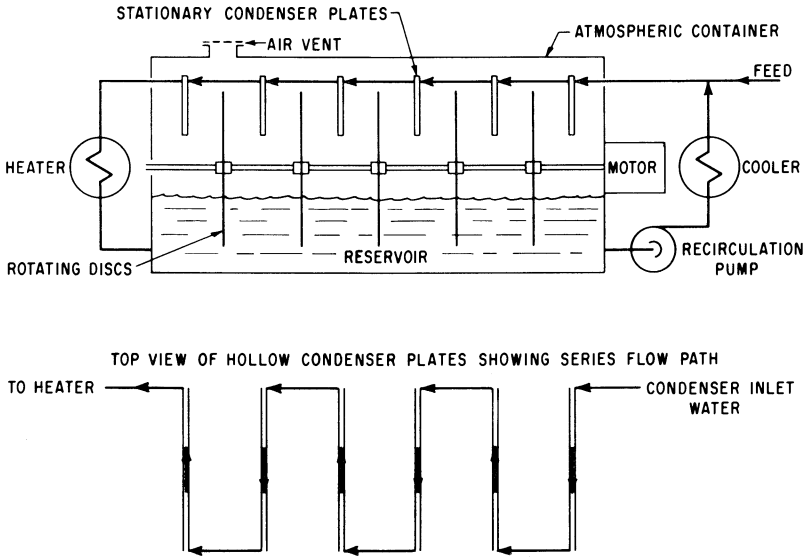

Figure 6. Schematic diagram of multistage cycle

Figure 7 shows a typical cycle diagram for a 200-gallon-per-day distilling unit operating on city water.

Two hundred and ten gallons per day of feed water, containing 125 p.p.m. of dissolved solids, are fed to the unit at 70° F. The feed water is mixed with the recirculated water from the reservoir and enters the condenser at 90° F. As the water flows through the condenser plates, the latent heat from the distillate increases the water temperature to 200° F. The water then flows through the

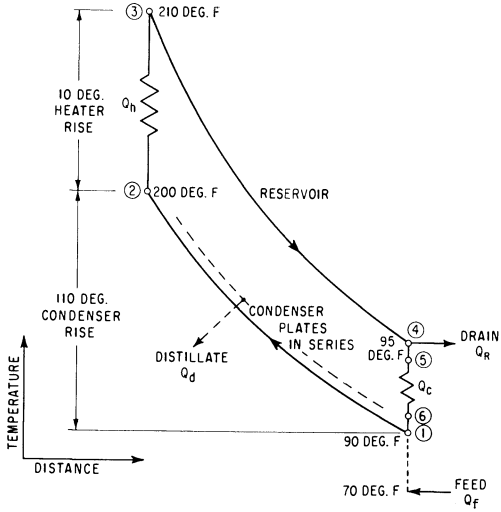

Figure 7. Diagram of multistage cycle

heater, where its temperature is increased to 210° F., and enters the reservoir. As it flows through the reservoir, the latent heat of distillation and the mass of distillate are removed, and this cools the remaining liquid down to approximately 95° F. Ten gallons per day are then discharged to the drain. The balance of the flow enters the cooler. The liquid leaving the cooler is then mixed with the feed and the cycle is repeated.

The distillate, formed on the condenser, leaves the unit at a temperature approximately equal to the average of the condenser inlet and discharge temperatures.

The amount of distillate formed is proportional to the temperature rise through the condenser $(t_2 - t_1)$. The amount of heat that must be supplied to the cycle is proportional to the temperature rise through the heater $(t_3 - t_2)$. When the rise through the condenser is greater than the rise through the heater, the cycle will produce more pounds of distillate than the equivalent energy supplied to the heater. For example, in the cycle shown, the temperature rise through the condenser is 110° F., and the rise through the heater is only 10° F. The "performance ratio" of this unit will then be 11 pounds of distillate produced for approximately every 1000 B.t.u. supplied to the heater. Based on this cycle, the following equations can be written:

The sensible heat of the distillate leaving the unit:

$$\dot{Q}_d = \dot{w}_d c_p \frac{(t_2 + t_1)}{2} \tag{3}$$

The sensible heat entering the unit with the feed water:

$$\dot{Q}_f = \dot{w}_f c_p t_f \tag{4}$$

A heat balance on the condenser:

$$w_1 c_p(t_2 - t_1) = \dot{w}_d[(h_{fg})_s + c_p(t_s - t_d)] \tag{5}$$

The energy supplied at the heater:

$$\dot{Q}_h = \dot{w}_1 c_p(t_3 - t_2) \tag{6}$$

The sensible heat of the water entering the reservoir:

$$\dot{Q}_3 = \dot{w}_1 c_p t_3 \tag{7}$$

The energy removed from the reservoir:

$$\dot{Q}_s = \dot{w}_d[(h_{fg})_s + c_p t_s] \tag{8}$$

The sensible heat of the liquid leaving the reservoir:

$$\dot{Q}_4 = \dot{Q}_3 - \dot{Q}_s = \dot{w}_1 c_p t_3 - \dot{w}_d[(h_{fg})_s + c_p t_s] \tag{9}$$

The temperature of the liquid leaving the reservoir can be expressed as:

$$t_4 = t_3 - \frac{(h_{fg})_s}{c_p\left[\frac{\dot{w}_1}{\dot{w}_d} - \frac{1}{2}\right]} \tag{10}$$

The energy lost to the drain:

$$\dot{Q}_R = (\dot{w}_f - \dot{w}_d) c_p t_4 \tag{11}$$

The sensible heat in the fluid entering the cooler:

$$\dot{Q}_5 = (\dot{w}_1 - \dot{w}_f) c_p t_4 \tag{12}$$

The sensible heat of the liquid as it leaves the cooler:

$$\dot{Q}_6 = \dot{Q}_5 - \dot{Q}_c \tag{13}$$

The sensible heat of the liquid entering the condenser:

$$\dot{Q}_1 = \dot{w}_1 c_p t_1 \tag{14}$$

A heat balance at the condenser inlet:

$$\dot{w}_f c_p t_f + c_p(\dot{w}_1 - \dot{w}_f) t_4 - (\dot{w}_1 - \dot{w}_f)(t_4 - t_6) c_p = \dot{w}_c c_p t_1 \tag{15}$$

will provide an expression for the temperature leaving the cooler:

$$t_6 = \frac{t_1 - \frac{\dot{w}_f}{\dot{w}_1} t_f}{1 - \frac{\dot{w}_f}{\dot{w}_1}} \tag{16}$$

If the flow of concentrate to the drain is zero, then

$$\dot{w}_f = \dot{w}_d$$

The amount of heat rejected to the cooler:

$$\dot{Q}_c = (\dot{w}_1 - \dot{w}_f)(t_4 - t_6) \tag{17}$$

An over-all heat balance on the cycle gives:

$$\dot{Q}_h + Q_f = \dot{Q}_d + \dot{Q}_R + \dot{Q}_c \tag{18}$$

Cycle conditions can be determined by assuming values of t_1, t_2, t_3, $\dot{w}_d$, $\dot{w}_f$, and t_f. The required circulation rate in the unit can then be determined from Equation 5 and the ratio of $(\dot{w}_1/\dot{w}_d)$ and $(\dot{w}_f/\dot{w}_1)$ can be calculated. The reservoir outlet temperature, t_4, can be found from Equation 10; the cooler outlet temperature, t_6, from Equation 16.

The various quantities of heat entering and leaving the cycle can then be found from Equations 3, 4, 6, 11, and 17. A final heat balance on the cycle is obtained from Equation 18.

These equations satisfy the thermodynamics of the cycle, but do not consider the condensing surface area required or the heat transfer performance of this area.

The single-stage performance shown in Figure 5 was next used to determine the condenser surface area requirements for a 150-gallon-per-day multistage unit. Additional analysis indicated the type of performance that could be expected. To confirm the effect of the many variables involved, a laboratory prototype unit was constructed (Figure 8).

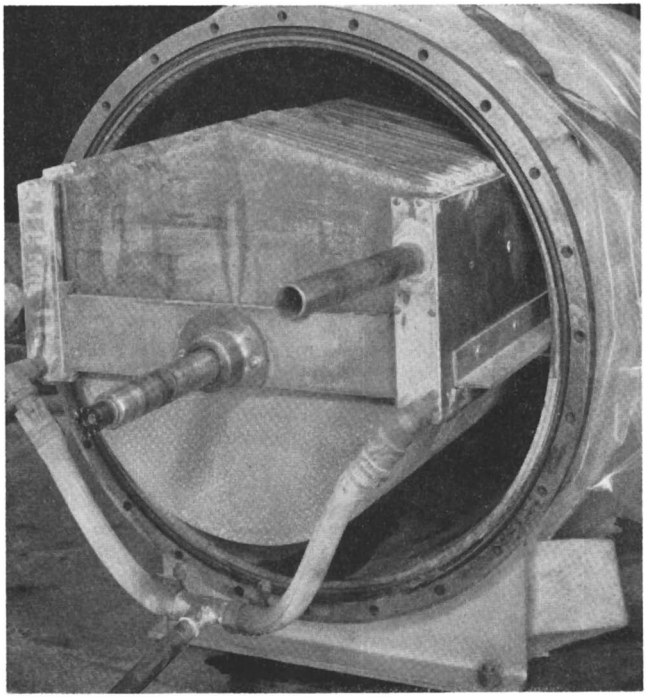

Figure 8. Flat plate condenser and rotating disk assembly in multistage test unit

It contained 34 disks, 12 inches in diameter of $^1/_8$-inch-thick Transite. The hollow flat condenser plates, 35 in number, were roll-bonded from sheet copper. The unit was housed in a pressure vessel designed to allow the effect of total pressure level of air and other inert gases to be evaluated.

All measurements of temperatures in the system, including temperature distributions in the reservoir, were made at a constant disk speed of 60 r.p.m. The unit was vented to atmospheric pressure. The effects of condenser recirculation rate, $\dot{w}_1$, maximum cycle temperature, t_3, and heater temperature rise, $(t_3 - t_2)$, were investigated.

Figure 9 shows a performance map produced from test data taken on the multistage unit. Product output is plotted against the condenser recirculation rate for a parameter of heater temperature rise. Superimposed on the plot are parameter curves of performance ratio, expressed in pounds of distillate produced per unit of heat input. A performance ratio of 1.0 would roughly correspond to a single-stage distillation device in which the heat of vaporization is utilized only once. Performance ratios greater than 1 indicate a re-use of the heat of vaporiza-

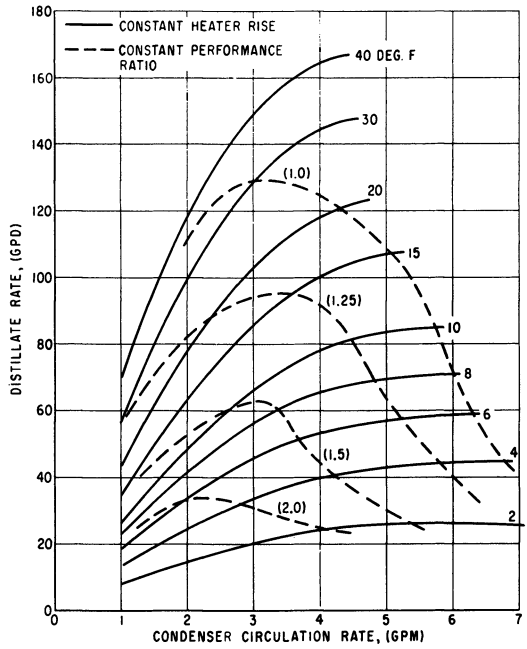

Figure 9. Multistage diffusion still performance

tion and show the multistaging effect. The curves are valid for t_3 equal to 210° F.

As the condenser recirculation rate is decreased at a given heater temperature rise, the product output is decreased. A lower recirculation rate reduces the water-side condenser coefficient, lowers the average condenser temperature and diffusion rate, and increases the performance ratio.

The test results show the feasibility of controlling product output by varying the power input to a fixed multistage diffusion design operating at constant disk speed. Further analysis has shown that by design changes in the condenser plates —i.e., multipass within each plate—for a fixed condenser area, performance ratio can be traded for capacity.

Conclusions

The purity of the product water is high, since the mass transfer occurs at temperatures below the boiling point. The absence of nucleate boiling eliminates one of the major causes of carry-over in distillation equipment. Evaluation of the multistage unit on a simulated sea water solution has produced distillate containing less than 1 p.p.m. of total dissolved solids.

By storing the energy for evaporation both in the liquid film and in the disk material, the diffusion still operates in a manner similar to a flash evaporator. It does not rely entirely on the transfer of energy through a heat transfer surface. As a result, the scaling problems encountered are similar to those with flash equipment. Scale formation on the disk surface has no measurable effect on performance. Formation of scale within the condenser results in a slight decrease in performance. However, this reduction is small, since the over-all condenser performance is initially low in the diffusion still.

The thermodynamics of the system are similar to a multiflash distillation system.

The laboratory unit has yielded performance ratios in the vicinity of 2.0. Higher performance ratios are possible with condenser design changes.

The concept of operating a multistage cycle in air in a single container without partitions is feasible. The vapor partial pressure gradients allow a multistage effect.

Nomenclature

G = mass transfer rate, lb./hr. sq. ft.
P = pressure, pounds per sq. foot
X = distance between plates, feet
R = gas constant, feet per ° R.
T = temperature, ° R.
t = temperature, ° F.
P = pressure, pounds per sq. foot
D = diffusion coefficient, sq. feet per hour
$\dot{w}$ = flow rate, pounds per hour
$\dot{Q}$ = rate of heat transfer, B.t.u. per hour
c_p = specific heat at constant pressure, B.t.u./(lb.) (° F.)
h_{fg} = latent heat of vaporization, B.t.u. per pound

Subscripts

1 = condenser inlet
2 = condenser outlet
3 = reservoir inlet
4 = reservoir outlet
5 = cooler inlet
6 = cooler outlet
s = average of reservoir
d = distillate
f = make-up feed
R = reject to drain
c = cooler
h = heater
v = water vapor
a = evaporating surface
b = condensing surface
o = mixture total, air plus water vapor

Acknowledgment

The author gratefully acknowledges the support provided by L. G. Kropacek in the design, construction, and evaluation of the experimental units, by F. J. Neugebauer and D. H. Brown in their contribution to understanding and applying the diffusion principle to a practical distillation device, and by F. W. Staub in his analytical work which has led to a better understanding of the diffusion process and predictions of multistage performance.

Literature Cited

(1) Eckert, E. R. G., "Introduction to the Transfer of Heat and Mass," McGraw-Hill, New York, 1950.
(2) Jacob, M., "Heat Transfer," Vol. I, Wiley, New York, 1955.

(3) Lustenader, E. L., "Development of the Diffusion Still," General Electric Tech. Inform. Ser. **61GL214** (November 1961).
(4) Staub, F. W., "Analysis of Single Stage Diffusion Still Performance," *Ibid.*, **62GL144** (September 1962).
(5) Van Rossum, J. J., *Appl. Sci. Res.* **7**, 121 (1957–8).

RECEIVED July 25, 1962.

Saline Water Conversion by Flash Evaporation Utilizing Solar Energy

DONAT B. BRICE

Department of Water Resources, State of California, Sacramento, Calif.

In the application of solar energy to saline water conversion, the combination of a solar heat collector with a process that is capable of energy re-use may be economically more attractive than direct solar distillation. A combination plant consisting of a solar heat collector and a multistage flash evaporator was designed to produce 345 × 10^7 gallons of water annually when collecting slightly more than 4 trillion B.t.u. of heat. The conversion economics were based on the insolation received in Southern California. A large collector area was selected, so that the economics would be representative for supplying a populous area. The maximum plant output of 16,500,000 gallons per day occurred in July. The water produced was estimated to cost approximately $1.10 per thousand gallons.

In applying solar energy to saline water conversion, the combination of a solar heat collector with a process capable of energy re-use may be economically more attractive than direct solar distillation. The multistage flash evaporation process can utilize the relatively low temperature saline water produced in a flat-plate solar heat collector more efficiently than most other conversion processes. A combination plant was designed to produce annually 345 × 10^7 gallons of water when collecting slightly more than 4 trillion B.t.u. of heat.

A coastal location in Southern California was assumed for the site of this combination plant; consequently, solar insolation and other meteorological data for that area were used in making calculations for the solar heat collector. The results, however, should be generally applicable to other geographical areas, if corrections are applied for the amount of insolation received.

The primary purpose of this study was to optimize the cost of water produced in a multistage flash evaporator supplied by brine heated in a solar heat collector. It was therefore not possible to select both plant capacity and the solar collector area and still permit optimization. In addition, the brine temperature limitation would be set by an economic evaluation of the multistage flash

evaporator and the solar heat collector. Evaporator capital and operating cost estimates from a previous study (*4*) were used extensively in this evaluation.

Because plant output varies with the time of year, the monthly average of the insolation received at a site along the Southern California coast was used as a basis for calculation. With this known, it was possible to determine the net heat that could be captured by a solar heat collector with a given number of glazing layers. The cost of installing the solar collector was estimated. Then, the relative cost of the solar energy on a monthly average basis for several selected brine temperatures could be determined and the plant could be optimized for a given assumed brine temperature and assumed stage terminal temperature difference in the flash evaporator. It was first necessary to determine the approximate plant size. By optimizing the water cost by month for the minimum solar energy cost for several selected brine temperatures, it was possible to determine the point of minimum operating cost for the several assumed evaporator plant capacities, and to calculate the area of solar collector required for each condition.

As expected, the optimization was heavily weighted in terms of summer operation when insolation is at a maximum and for the higher brine temperatures when the plant output is relatively greater.

Description of Process

Figure 1 represents the general flow diagram of the multistage flash evaporation process and the solar heat collector system. The process conditions shown are typical for operation with a brine temperature of 140° F., as would be the case during May, June, and August.

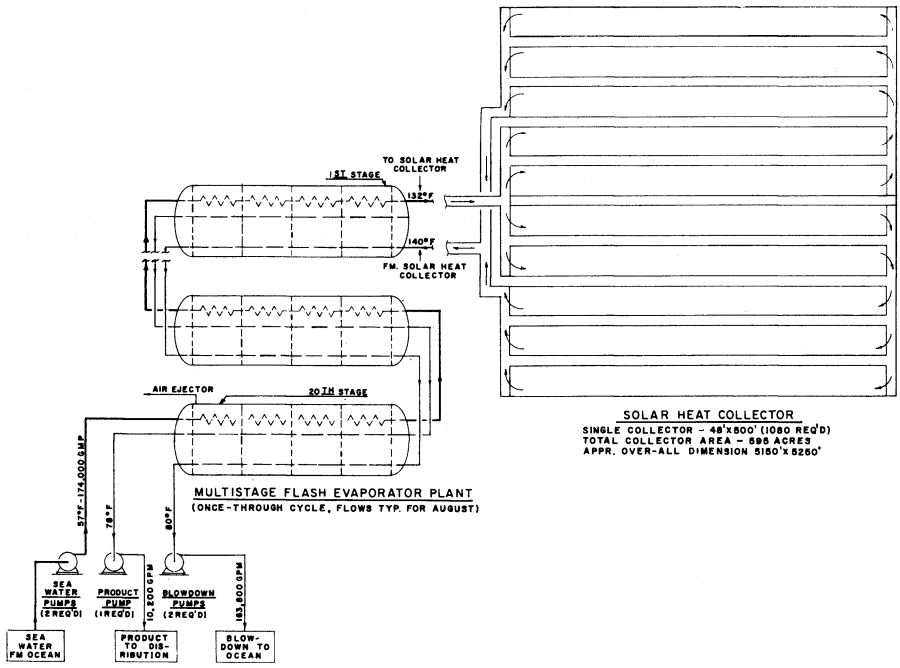

Figure 1. Schematic flow diagram
3° F. terminal temperature difference

The sea water is pumped from the inlet sump to the evaporator plant, where it flows through the tubes of the 20-stage evaporator, and is gradually heated to 132° F. as a result of the vapor condensing on the outside of the tubes. As it leaves the first stage of the evaporator at 132° F., it is discharged into a canal system and allowed to flow by gravity to the solar heat collector. The sea water then flows through the solar heat collector, as shown in Figure 1. This flow arrangement down the entire length and return permits the flow to take place by gravity without piping and with a minimum amount of channels. The sea water travels approximately 2 miles in about 36 hours. During August the sea water is returned to the evaporator at 140° F. It is introduced into the shell side of the first stage of the evaporator vessel, which is under a partial vacuum. The flashing process starts at this point.

The heated sea water enters the shell side of the first stage with 33,600 p.p.m. of salt. Since some of the water is flashed off in each stage, by the time the sea water reaches the lowest temperature stage the salt concentration is increased by approximately 6%. Two pumps are required in the sea water sump to supply the volumetric flow of 174,000 gallons per minute at the head required. Approximately 164,000 gallons per minute are returned to the ocean as blowdown. The difference (about 10,000) is the product, which is also pumped from the system and delivered to the distribution system.

This flow system is known as a "once-through system." When operating at higher brine temperatures, the brine is usually recirculated several times and the blowdown concentration is perhaps twice that of normal sea water. The primary reason for recycle is to reduce the cost of chemicals required to prevent scale when operating at higher temperature. In the combination with the solar heat collector the economics are different. The economic life of the plastic glazing material is longer when operating at relatively lower temperatures. Operation much above a 150° F. brine temperature requires the addition of chemicals for scale control. For higher brine temperatures to be advantageous, it would be necessary to increase the temperature of the solar collector operation substantially, thus more than compensating for the cost of the scale control chemicals. With the increased heat loss at higher temperatures and the reduced life of the glazing, higher temperature operation of the solar collector is not economically justified.

The tube-side brine is discharged from the first stage of the evaporator vessel into a concrete-lined and covered channel which permits the brine to flow into the solar heat collector. The collector is composed of concrete curbing on 48-foot centers in one direction and 500-foot centers in the other direction, and is covered with multiple layers of glazing. The sea water flows parallel to the 48-foot sides—that is, the flow path is along the 500-foot dimension. These 500-foot curbings represent a common wall from one collector to the next. Slots in the curbs permit the brine to flow continuously through the entire mile of collector before reversing direction. Once the brine has reached the end of the solar collector away from the evaporator, it flows into a concrete-lined channel and is diverted back through another series of collectors, emerging finally into a concrete-lined channel at the evaporator end of the collector. The heated sea water then returns to the evaporator plant and is introduced into the shell side of the first stage of the evaporator through a siphon leg. No pump is required at this point. Actually, as can be seen from Figure 1, pumps are required only to move the sea water through the tubes and to remove the blowdown and the product from the last stage.

The thickness of the multiple-layer glazing covering was selected as follows:

Top layer	4 mils
Inside layers	1 mil
Bottom layer	3 mils

The bottom layer floats on the surface of the sea water. A cross section of a five-layer glazing covering in the inflated condition is shown in Figure 2.

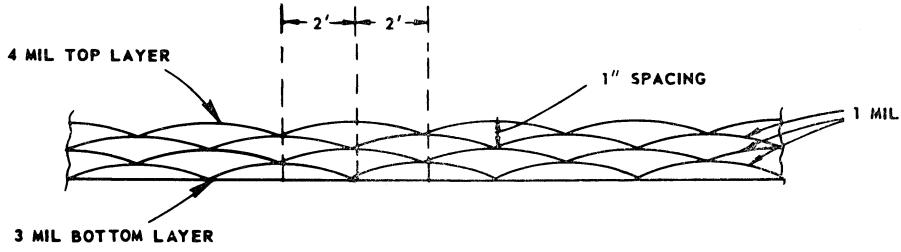

Figure 2. Cross section of five-layer glazing covering in inflated condition

The layers are heat-sealed every 4 feet and air pressure is used to hold the layers apart. The air space between layers imparts desirable heat-insulation properties to the covering. The primary purpose of the bottom floating layer is to prevent evaporation and condensation between the water surface and the glazing.

Table I. Summary of Process Conditions[a]

(3° F. terminal temperature difference)

No. of stages	20
Maximum sea water temp., ° F.	140
Sea water temp. to solar heater, ° F.	132
Temp. rise in solar heater, ° F.	8
Blowdown temp., ° F.	80
Product temp., ° F.	78
Sea water flow, gal./min.	174,000
Product, gal./min.	10,200
Sea water salt concentration, p.p.m.	33,600
Blowdown salt concentration, p.p.m.	35,700
Velocity of sea water in tubes, feet/second	6
Solar collector area, acres	595
No. of layers of glazing	5
Solar collector heat duty, B.t.u./hr. $\times 10^{-6}$	680
Solar collector net heat gain, B.t.u./(sq. ft.)(day)	630
Sea water velocity in collector, foot/second	0.06 to 0.1
Residence time of sea water in collector, hours	36

[a] Typical for operation during August.

The process conditions summarized in Table I are typical of operation only, since the output from day to day depends upon the amount of solar insolation received. A slightly higher output at a higher brine temperature would be expected in July, and lower operating temperatures and output during the remaining months, a minimum occuring during December and January, when the minimum amount of solar insolation is captured by the still.

Solar Collector Selection

The most complete information on radiation received in Southern California is available from the U. S. Weather Bureau in Los Angeles. Therefore, the

monthly average of solar radiation received in the Los Angeles area during a 10-year period was used as a basis for determining the insolation available in the San Diego area. Cloudless day radiation was calculated from the relationship:

$$Q = Q_0 (a + bS) \quad (1)$$

where Q = quantity of solar energy received on a unit area of horizontal plane at the earth's surface per unit of time
Q_0 = cloudless day radiation, quantity of solar energy received on a unit area of horizontal plane at the earth's surface per unit of time during cloudless days
S = number of hours of sunshine instrumentally recorded, divided by the number of hours of possible sunshine
a, b = constants

The expected radiation received in San Diego was then calculated, using sunshine data published by the Weather Bureau in San Diego. The mean solar radiation received in Los Angeles varies from a low of 856 B.t.u./sq. ft. (day) in December to a high of 2370 in July. Corresponding figures calculated for San Diego are 843 and 2155.

Since the angle of incidence of radiation changes continuously with relation to a horizontal surface, it is necessary to determine the amount of heat captured

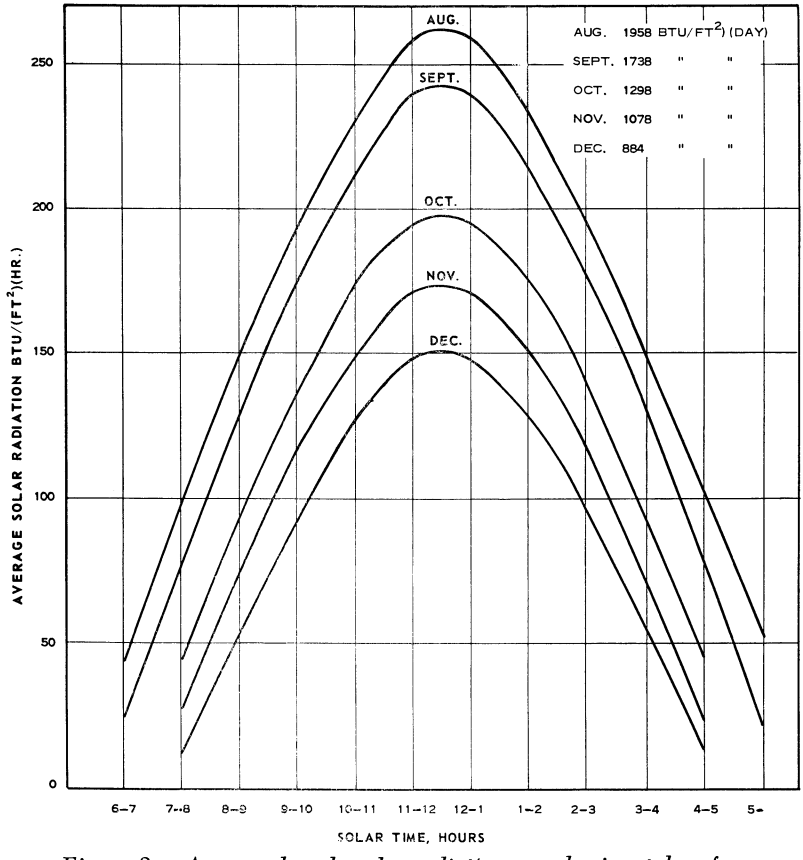

Figure 3. Average hourly solar radiation on a horizontal surface
August through December, Southern California coastal area

by a solar collector on an hourly basis. The data of Löf (*12*), which present the fraction of total daily radiation received on a horizontal surface each hour by month, were used in this study.

The effect of the latitude difference between Los Angeles and San Diego on the insolation received was negligible during the summer months; however, correction of several per cent was indicated for the six winter months from October through March. The results of these calculations are shown graphically in Figure 3 for August through December. The other months have curves of similar shape.

The solar energy received on a horizontal surface, as shown Figure 3, is composed of direct and diffuse radiation. The weather bureau measurements were made with an Eppley pyrheliometer (*6, 11*), which measured the total radiation falling on a horizontal surface. Since the incident angle of diffuse radiation does not vary with time of day and year as it does with direct radiation, it was necessary to determine each component separately.

Several estimates of the per cent of diffuse radiation were found (*1, 7, 10, 12*). Typical values for three solar times in July are:

Time from Solar Noon, Hours	*Diffuse Radiation, %*
0.5	17.5
2.5	18
4.5	20.5

Values used in this study for each month by hourly solar time can be derived from data presented in Table II.

With the total insolation determined and the per cent of diffuse radiation established, it was possible to calculate the quantity of direct and diffuse solar radiation available on a monthly average basis for each hour of solar time (Table II). The next step was to determine how much of this available energy could be captured by a solar heat collector.

Preliminary calculations of the transmittance of solar radiation through multiple layers of glazing (glass and plastics) indicated the superiority of Tedlar (Du Pont) over the others; consequently, the detailed calculations were made assuming a Tedlar glazing. The transmittance of the surface was calculated from the following equation developed by Hottel and Woertz (*9*):

$$\tau_n = \frac{1 - r}{1 + (2n - 1)\, r}$$

where τ_n = over-all transmittance of n layers of nonabsorbing glazing
r = surface reflectivity of glazing
n = number of layers of glazing material

The transmittance of a single layer of Tedlar as a function of the incident angle of the sun was obtained from a chart presented by Edlin (*5*). This measured value is the net amount of energy transmitted by the glazing, taking into account both reflection and absorption losses.

The absorptivity of a blackened surface is a function of the angle of incidence, and was based on data presented by Hottel (*9*) and Yellott (*15*). The product of the transmittance and absorptivity of the glazing as a function of the number of layers of glazing and incidence angle is shown in Table III for three, four, and five layers of Tedlar glazing. Figure 4 shows the transmittance-absorption variation with the angle of incidence for one to seven layers of Tedlar glazing. Values read from Figure 4 were used to calculate the direct and diffuse solar radiation captured by the solar heat collector. The angle of incidence

Table II. Hourly Summary of Direct and Diffuse Radiation

(Monthly average basis)

Month	Solar Time 11–12 12–1	10–11 1–2	9–10 2–3	8–9 3–4	7–8 4–5	6–7 5–6	Total B.t.u., Sq. Ft./Day
	Insolation, B.t.u./(Sq. Ft.)(Hr.)						
January							
I_d[a]	42	37	29	20	9	..	274
I_D[b]	107	94	71	38	9	..	638
I_T[c]	149	131	100	58	18	..	912
February							
I_d	53	48	39	27	16	..	366
I_D	142	127	99	63	24	..	910
I_T	195	175	138	90	40	..	1276
March							
I_d	43	39	33	25	17	6	326
I_D	197	178	144	99	51	9	1356
I_T	240	217	177	124	68	15	1682
April							
I	40	38	32	25	19	9	326
I_D	193	171	147	109	63	24	1414
I_T	233	209	179	134	82	33	1740
May							
I_d	46	41	35	27	19	10	356
I_D	216	192	159	120	76	29	1584
I_T	262	233	194	147	95	39	1940
June							
I_d	44	40	35	29	22	16	372
I_D	208	190	161	127	89	49	1648
I_T	252	230	196	156	111	65	2020
July							
I_d	45	41	37	31	26	19	398
I_D	215	196	170	139	99	59	1756
I_T	260	237	209	170	125	78	2154
August							
I_d	45	40	35	28	21	12	362
I_D	215	191	161	121	77	33	1596
I_T	260	231	196	149	98	45	1958
September							
I_d	43	39	33	26	19	8	336
I_D	197	175	146	106	59	18	1402
I_T	240	214	179	132	78	26	1738
October							
I_d	35	33	26	21	12	..	254
I_D	160	145	113	71	33	..	1044
I_T	195	178	139	92	45	..	1298
November							
I_d	47	42	35	23	13	..	320
I_D	124	109	84	47	15	..	758
I_T	171	151	119	70	28	..	1078
December							
I_d	41	37	28	20	7	..	266
I_D	107	93	67	35	7	..	618
I_T	148	130	95	55	14	..	884

[a] Diffuse insolation.
[b] Direct insolation.
[c] Total insolation.

is a function of time of day and year for the direct radiation. Appropriate values were used to read the transmittance-absorption product from Figure 4. The product for the diffuse component of the radiation is a value corresponding to a 58° angle of incidence (*8, 12*).

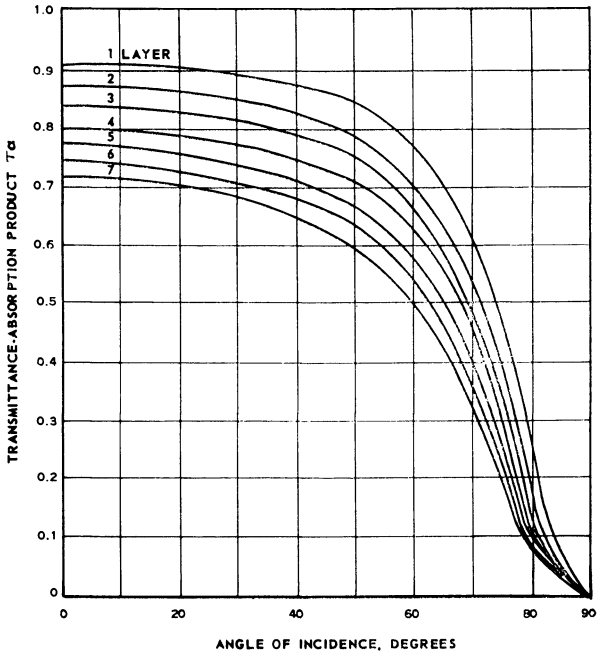

Figure 4. Transmittance-absorption product for Tedlar glazing and black-bottom surface with respect to angle of incidence

Table III. Transmittance-Absorption Product for Tedlar and Blackened Collector Bottom

No. of Layers	*Incidence Angle, Degrees*	*Transmittance*	*Absorptivity of Bottom*	*Product*[a]
3	0	0.876	0.960	0.833
	20	0.871	0.958	0.826
	40	0.832	0.939	0.773
	60	0.755	0.880	0.658
	80	0.182	0.657	0.118
4	0	0.840	0.960	0.798
	20	0.836	0.958	0.793
	40	0.788	0.939	0.733
	60	0.703	0.880	0.612
	80	0.143	0.657	0.093
5	0	0.810	0.960	0.770
	20	0.803	0.958	0.762
	40	0.749	0.939	0.696
	60	0.659	0.880	0.574
	80	0.119	0.657	0.077

[a] Reduced 1% for dirt on glazing surface.

The total insolation captured by five layers of Tedlar glazing was calculated to be 1439 B.t.u./sq. ft. (day) in July and 465 in December. Intermediate values were determined for the other months.

The heat transmitted through the glazing surface and absorbed by the collector is available for heating the brine. The useful amount depends on the fraction that is not lost to the atmosphere or ground.

Heat losses from solar collectors have been calculated by several investigators (3, 9, 13, 14). In this study the equation developed by Hottel (9) was used. The relationship, although somewhat complicated, can be solved directly and has been demonstrated by Hottel to give reliable values over the range commonly encountered in solar collector design.

$$q_L/A = \frac{T - T_a}{\dfrac{n}{C\left(\dfrac{T - T_a}{n + f}\right)^{1/4}} + \dfrac{1}{h_w}} + \frac{\sigma (T^4 - Ta^4)}{\dfrac{1}{\epsilon_C} + \dfrac{2n + f - 1}{\epsilon_G} - n} \qquad (2)$$

where q_L = rate of heat loss through top of collector, B.t.u./hour.
A = area, sq. feet
T = absolute temperature of brine, ° R.
T_a = absolute temperature of outer air, ° R.
n = one less than total number of glazing surfaces (one layer of glazing floating on water was not considered as contributing to heat retention except as it affects C)
C = constant [Figure 15, (9)]
f = effective thermal resistance of outer glazing relative to others
h_w = forced convection coefficient due to wind on top plate, B.t.u./sq. ft. (hr.) (° F.)
σ = Stefan-Boltzmann constant, 0.173×10^{-8} B.t.u./sq. ft. (hr.) (° R.^{4})
ϵ_C = emissivity and absorptivity of blackened collector
ϵ_G = emissivity and absorptivity of glazing

Calculations were based on an average wind velocity of 6.4 miles per hour, which is typical for the San Diego area. The solution of the equation for four, five, and six layers of Tedlar glazing at three brine temperatures (100°, 125°, and 150°) and two ambient temperatures (55° and 70°) is presented in Table IV. Ground losses of 1 B.t.u./sq. ft. (day) (° F.) were based on the results obtained in the deep basin still (2) operated by the Battelle Memorial Institute for the Office of Saline Water in Florida.

Table IV. Solution of Equation 2

Heat loss, B.t.u./(Sq. Ft.)(day)

No. of Layers	Temp., ° F.		1st Term,[a] Eq. 2	2nd Term,[b] Eq. 2	Heat Loss		
	Brine	Ambient			Atmos.	Ground[c]	Total
4	100	55	5.32	12.72	434	45	479
		70	3.22	9.07	295	30	325
	125	55	9.22	21.8	745	70	815
		70	6.82	18.14	598	55	653
	150	55	13.40	31.3	1072	95	1167
		70	10.87	27.7	925	80	1005
5	100	55	3.80	9.85	327	45	372
		70	2.30	7.04	224	30	254
	125	55	6.58	16.9	564	70	634
		70	4.87	14.1	456	55	511
	150	55	9.59	24.3	814	95	909
		70	7.76	21.5	700	80	780
6	100	55	2.91	8.06	263	45	308
		70	1.76	5.75	181	30	211
	125	55	5.02	13.8	452	70	522
		70	3.73	11.5	366	55	421
	150	55	7.35	19.8	652	95	747
		70	5.95	17.5	586	80	666

[a] c = 0.195. n = one less than number of layers. f = 0.48. h_w = 2.95 B.t.u./sq. ft.)(hr.)(° F.).
[b] c_C, c_G = 0.95. σ = 0.173×10^{-8} B.t.u./(sq. foot)(hr.)(° R.^{4}).
[c] Based on loss of 1 B.t.u./(sq. ft.)(day)(° F.).

Since heat losses are affected by change in ambient temperature, Equation 2 was solved for several assumed ambient temperatures between 55° and 70°, which is a typical range for the area. The heat loss increases approximately 6 B.t.u./sq. ft. (hr.) when the ambient temperature changes from 70° to 55° F. (Table IV). The net heat gain is the difference between heat captured from the available solar radiation and the sum of heat lost to the atmosphere and ground. Figure 5 summarizes the net heat gain by month for assumed collector temperatures from 100° to 150° F. This varies considerably with time of year (Figure 6). The curves are not smooth; their exact shape is largely dependent on meteorological conditions. The deviation from a smooth curve during the spring months can be explained by the variation in the cloud cover during that time of year along the Southern California coast.

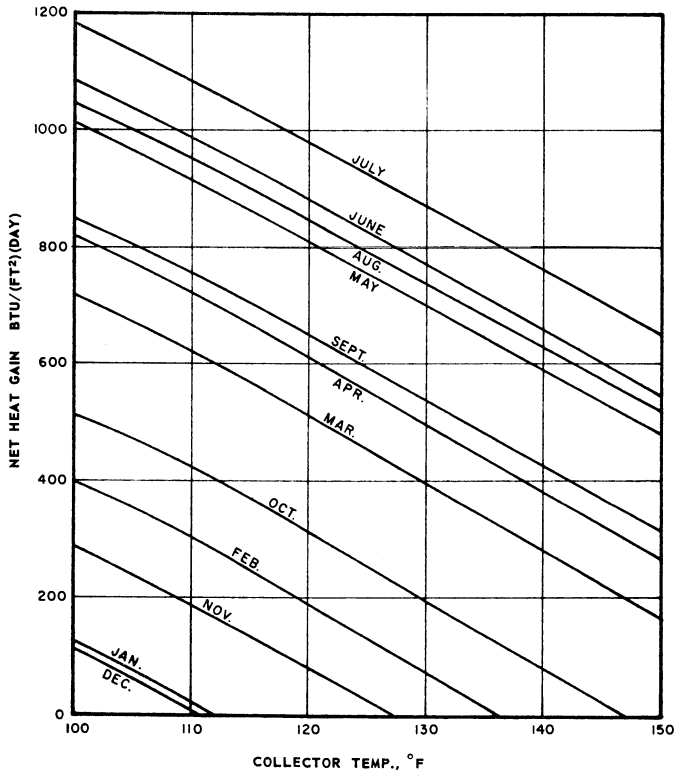

Figure 5. Net heat gain for five layers of Tedlar glazing

Solar Energy Cost

A preliminary calculation indicated that a solar collector area of approximately 25,000,000 square feet would be required to capture sufficient heat to operate the multistage flash evaporator shown in Figure 1. Since a large number of collector units would be required, the cost of installing 1000 units containing 24,000,000 square feet of collector surface was estimated, so that the cost per unit area and the amortized cost per unit area could be determined. For a variation of no more than 10% in the collector area the unit cost would remain the same.

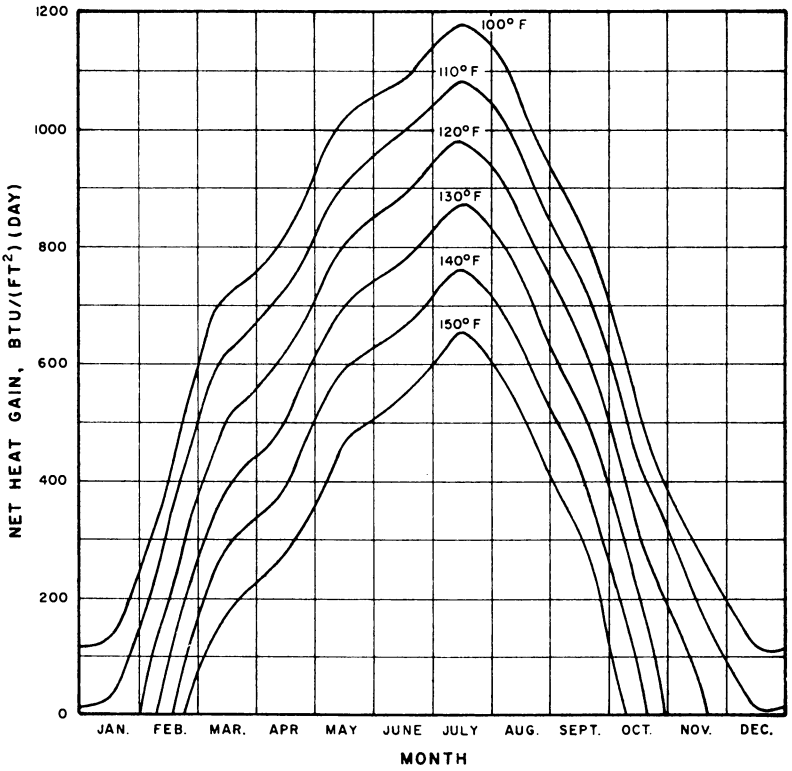

Figure 6. Variation in net heat gain for five layers of Tedlar glazing

Thus, the optimization could be made without making separate estimates of each assumed collector installation. Tables V to VII list the items of the solar collector and the installed cost of each. The total daily operating cost is summarized in Table VIII.

Before the cost of water from a multistage flash evaporator utilizing solar-heated brine could be estimated, an estimate of the cost of the recovered energy was required. This was determined in cents per million B.t.u. (Table IX). The net heat available for each selected condition is also listed in Table IX.

Table V. Installed Cost of Solar Collector[a]

(1000 units, 48 × 500 feet)

	Installed Cost, $	*Estimated Life, Years*	*Capital Cost, $/Unit*	*Amortized[b] Cost, Cents (Unit)(Day)*
Excavation	280,000	48	280	5.50
Concrete and paint[c]	1,370,000	48	1370	26.93
Plastic inserts and glazing holddown	200,000	8	200	12.38
Buggies[d]	60,000	24	60	1.64
Piping[e]	100,000	24	100	2.73
Total	2,010,000			49.18

[a] Does not include plastic ground cover or glazing.
[b] Money at 4% per annum.
[c] Amortized over plant life of 48 years, annual painting part of operating expense.
[d] Required to span collector for washing glazing and general maintenance work.
[e] Fresh water system for washing glazing.

Table VI. Cost of Bottom Covering[a]

	Collector[b]
Material cost[c]	$ 600
Heat sealing cost[d]	40
Installation cost[e]	700
Total	$1340
Unit cost, cents/sq. ft.	5.58
Amortized cost[f], cents/(unit)(day)	82.92

[a] Blackened polyethylene.
[b] One collector unit is 48 × 500 feet.
[c] 10-mil polyethylene, $0.50 per lb.
[d] 2000 lineal feet at $0.02 per foot.
[e] Includes cost of sealing bottom to plastic inserts (500 inserts per collector).
[f] 8-year life, 4% per annum, equivalent to 14.853% per annum.

Table VII. Installed Cost of Tedlar Glazing

No. of Layers	*Material*, $	*Fabrication*, $	*Installation*, $	*Fabricated Total*, $	*Amortized[a], Cents/ (Unit)(Day)*
2	3597	212	225	4034	249.62
3	4111	382	225	4718	291.95
4	4625	828	225	5678	351.34
5	5138	1083	225	6446	398.88
6	5652	1784	225	7661	474.06
7	6166	2124	225	8515	526.91

[a] 8-year life, 4% per annum.

Table VIII. Total Daily Operating Cost of Solar Collectors[a]

(Unit collector 48 × 500 feet)

No. of Layers	*Tedlar Glazing Cost, Cents (Unit)(Day)*	*Other Collect Costs, Cents (Unit)(Day)*	*Total Daily Collector Cost* $/(unit)	*Cents/sq. ft.*
2	249.62	203.03[b]	4.53	0.0189
3	291.95	203.03	4.95	0.0206
4	351.34	203.03	5.54	0.0231
5	398.88	203.03	6.02	0.0251
6	474.06	203.03	6.77	0.0282
7	526.91	203.03	7.30	0.0304

[a] Money at 4% per annum.
[b] 49.18 from Table V; 82.92 from Table VI, plus 45.93 for real estate and 25.0 for operation and maintenance labor.

At constant temperature, for some of the conditions presented, the quantity of heat captured actually decreases with an increase in the number of glazing layers—for example, at 110° F. brine temperature in July, the maximum heat is captured with five layers of glazing (Table IX). This simply means that the incremental heat loss due to reflection and absorption by the added layer of glazing is greater than the heat saved as a result of one more layer of glazing to act as an additional heat insulator.

The solar heat cost in cents per million B.t.u. is graphically presented in Figure 7. At 3° F. terminal temperature difference the brine temperature for minimum water cost is between 130° and 150° F. As can be seen from Figure 7, during the six months from April through September, the optimum falls within the domain of five layers of glazing. Since most plant output occurs during this period, the optimization will be heavily weighed in favor of five layers of glazing.

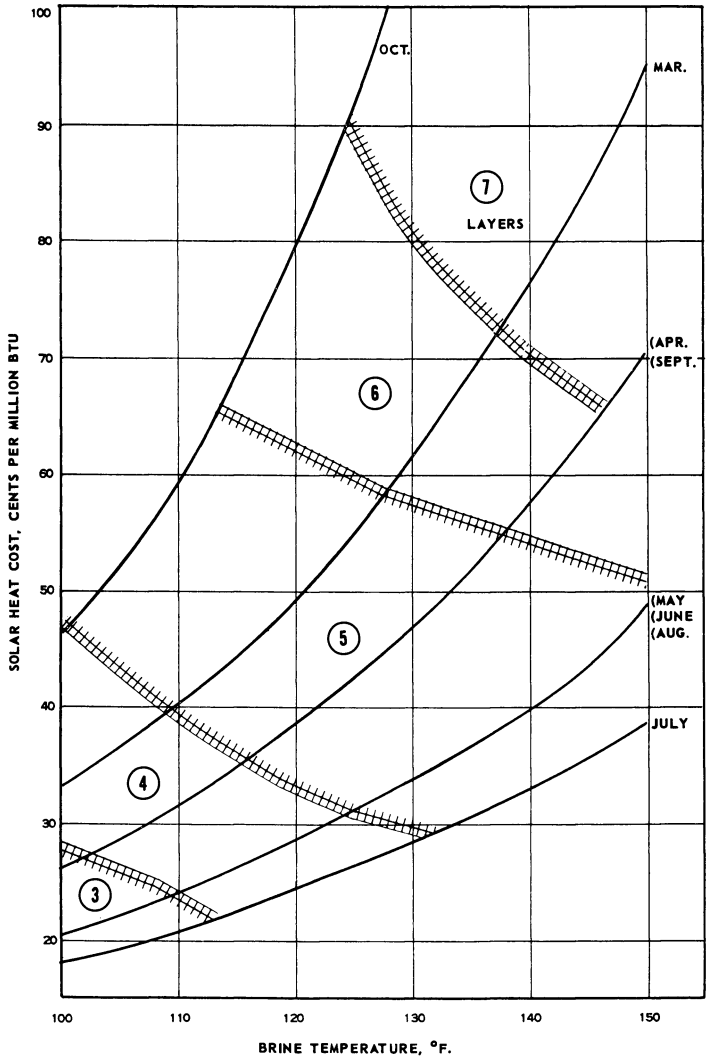

Figure 7. Domains of glazing layers for solar heat cost

Evaporator Cost

Data developed in a previous study (*4*) of evaporator economics were largely used in this analysis. The multistage flash evaporator heat and flow conditions for several terminal temperature differences are summarized in Table X. The estimated capital costs are presented in Table XI.

The variations in evaporator output and evaporator heat requirement with brine temperature are presented in Figures 8 and 9. The flash evaporator operating costs are summarized in Table XII.

Water Cost

To the evaporator cost must be added the cost of collecting the energy in the solar heat collector. The variation in the water cost for the time of year and

Table IX. Cost of Col

Month	Total Layers	Amort. Cost[a]	150° F. [b]	150° F. [c]	140° F. [b]	140° F. [c]
July	3	0.0206	166	124	370	55.7
	4	0.0231	515	44.9	660	35.0
	5	0.0251	653	38.4	760	33.0
	6	0.0282	693	40.7	792	35.6
	7	0.0304	738	41.2	815	37.3
May, June, August[d]	3	0.0206	32	644	225	91.5
	4	0.0231	374	61.8	515	44.9
	5	0.0251	522	48.2	630	39.9
	6	0.0282	571	49.4	668	42.2
	7	0.0304	621	49.0	700	43.4
April, September[e]	3	0.0206	...	...	...	...
	4	0.0231	163	142	308	75.0
	5	0.0251	318	79.0	430	58.4
	6	0.0282	370	76.2	468	60.2
	7	0.0304	435	69.9	515	59.0
March	3	0.0206	...	...	...	...
	4	0.0231	...	...	145	159
	5	0.0251	174	144	285	88.1
	6	0.0282	268	105	362	77.8
	7	0.0304	321	94.7	400	76.0
October	3	0.0206	...	...	...	...
	4	0.0231	...	...	...	...
	5	0.0251	...	...	85	296
	6	0.0282	54	522	155	182
	7	0.0304	117	260	195	156

[a] Cents/(sq. foot) (day).
[b] Net heat available, B.t.u./(sq. ft.)(day).
[c] Cost of collected solar heat, cents/10^6 B.t.u.

Table X. Summary of Flash Evaporator Heat and Flow Conditions for Several Terminal Temperature Differences

(20-stage plant)

TTD[a], ° F.	Brine Temp.[b], ° F.	Solar Heater Duty, B.t.u./Hr. × 10^{-6}	Plant Capacity,[c] Gal./Day × 10^{-6}
1.5	100	305	4.9
	110	365	7.35
	120	430	9.8
	130	490	12.25
	140	553	14.7
	150	612	17.1
3.0	100	335	4.9
	110	425	7.35
	120	510	9.8
	130	595	12.25
	140	680	14.7
	150	765	17.1
4.5	100	335	4.0
	110	431	6.0
	120	515	8.0
	130	585	10.0
	140	660	12.0
	150	735	14.0

[a] Stage terminal temperature difference.
[b] Inlet temperature to first stage.
[c] Capacity same for TTD of 1.5° and 3.0° F., since number of condenser tubes is same for each.

lected Solar Energy

Brine Temperature							
130° F.		120° F.		110° F.		100° F.	
b	c	b	c	b	c	b	c
575	35.8	775	26.6	970	21.3	1145	18.0
800	28.9	940	24.6	1075	21.5	1199	19.3
870	28.9	980	25.6	1085	23.1	1180	21.3
892	31.6	990	28.5	1075	26.2	1151	24.5
896	33.9	973	31.2	1048	29.0	1118	27.2
435	47.4	640	32.2	835	24.7	1002	20.6
658	35.2	800	28.9	935	24.7	1052	22.0
740	34.0	850	29.6	950	26.4	1046	24.0
765	36.9	860	32.8	950	29.7	1023	27.5
778	39.1	855	35.6	927	32.8	998	30.5
210	98.0	410	50.3	605	34.1	777	26.5
450	51.4	595	38.8	730	31.7	850	27.2
540	46.5	650	38.6	755	33.3	848	29.6
568	49.7	665	42.4	750	37.6	829	34.0
594	51.2	674	45.2	750	40.5	814	37.3
...	...	190	108	385	53.5	567	36.3
285	81.1	425	54.4	565	40.9	693	33.3
400	62.8	515	48.8	622	40.4	720	34.9
460	61.3	555	50.8	640	44.1	720	39.2
478	63.5	555	54.7	630	48.2	698	43.5
...	...	...	...	165	125	375	54.9
90	257	235	98.3	380	61.8	493	46.8
200	126	315	79.7	424	59.3	512	49.0
255	111	355	79.5	440	64.1	516	54.7
275	110	356	85.3	430	70.7	496	61.3

[d] August net heat values used.
[e] September net heat values used.

Table XI. Flash Evaporator Capital Cost and Power Requirements

(20-stage plant)

TTD[a], ° F.	1.5	3.0	4.5
Capital cost × 10^{-6}, $	20.7	15.5	11.3
Condenser area, sq. ft.	4,150,000	2,620,000	1,580,000
Pumping horsepower[b]	22,700	18,300	13,450

[a] Stage terminal temperature difference.
[b] Total of all installed pumps including pump and motor efficiencies. Based on velocity of 6 feet/second in condenser tubes for sea water pump.

Table XII. Flash Evaporator Operating Costs

(Dollars per stream day)

	TTD, ° F.		
	1.5	3.0	4.5
Electrical energy	4410	3310	2420
Supplies and maintenance material	175	88	70
Operating labor	191	191	191
Maintenance labor	130	66	52
Payroll extras	48	39	36
Overhead	43	43	43
Amortization	4152	3109	2267
Insurance	60	45	33
Evaporator total	9209	6891	5112
Interest on working capital	64	48	36

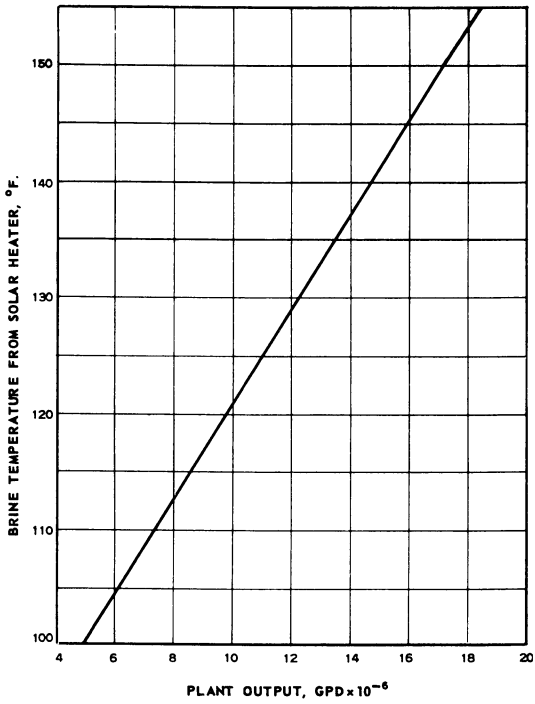

Figure 8. Variation in flash evaporator output with brine feed temperature

3° F. terminal temperature difference

brine temperature is shown graphically in Figure 10 for a 3° F. terminal temperature difference, which was established to be about optimum for this design. The curves in Figure 10 represent all costs associated with both the evaporator and solar heat collector. The weighted average cost of water is $1.10 per 1000 gallons.

Recommendations

The ideal glazing would transmit all the solar energy into the collector and, at the same time, reflect the long-wave reradiation from the collector. Research with glazing materials to improve the transmittance and reduce reradiation losses could improve the economics of a solar heat collector. It is, therefore, recommended that these two avenues of investigation be considered by researchers in this field.

Summary and Conclusions

The economics of a combination sea water evaporator–solar heat collector have been examined on the basis of current technology, using 1960 construction costs. A multistage flash evaporator was selected. A Tedlar-covered solar heat collector was selected to heat the brine.

Approximately 10,600 acre-feet of potable water could be produced during a 10-month operating year, utilizing nearly 1 square mile of solar heat collector surface.

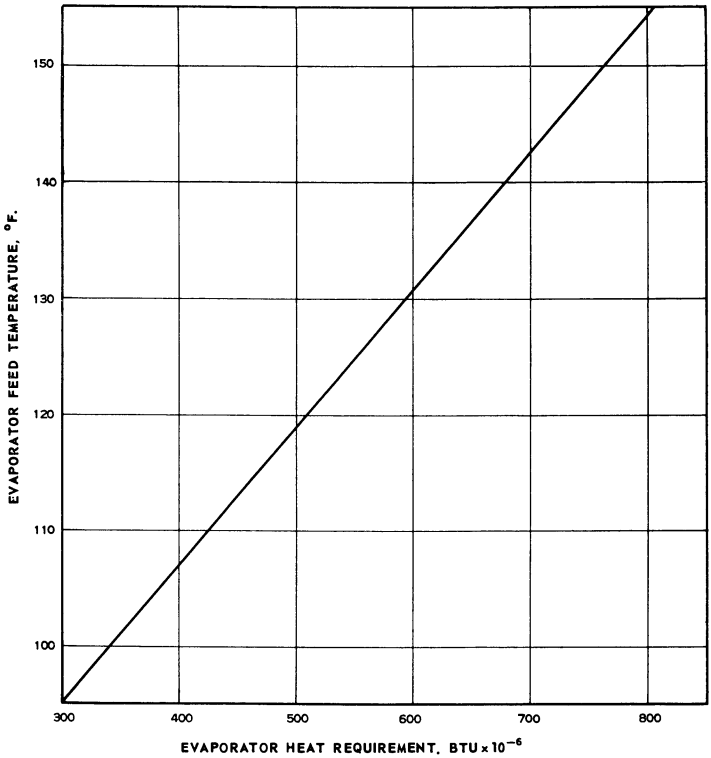

Figure 9. Variation in heat requirements of flash evaporator with brine feed temperature

3° F. terminal temperature difference

The total capital cost of the plant was estimated to be approximately $26,000-000, 60% of which was the cost of the evaporator and its auxiliaries. The 40% for the solar heat collector was divided into 26% for the glazing, 6% for the plastic bottom, and 8% for the collector installation.

During a 10-month operating year the average water cost for the plant was estimated to be approximately $1.10 per thousand gallons.

During a 10-month operating year the solar heat collector would capture slightly more than 4 trillion B.t.u.

Considerable improvement in the materials used for glazing will be required before the reflection and reradiation losses can be reduced sufficiently to make this means of obtaining heat generally economically attractive.

Literature Cited

(1) American Society of Heating and Ventilating Engineers, New York, "Heating, Ventilating and Air Conditioning Guide," 30th ed., 1952.
(2) Battelle Memorial Institute, "Study and Field Evaluation of Solar Sea Water Stills," Office of Saline Water, Quart. Progr. Repts. 1–7 (1959–60).
(3) Bliss, R. W., Jr., *Solar Energy* 3, 55 (December 1959).
(4) Brice, D. B., Townsend, C. R., ADVAN. CHEM. SER., No. 27, 147 (1960).
(5) Edlin, F. E., "New Materials for the Utilization of Solar Energy," International Colloquim on Thermal Applications of Solar Energy in Fields of Research and Industry, Montlouis, Pyrenees — Orientales, France, June 1958.
(6) Eppley Laboratory, Inc., Newport, R. I., Bull. 2.

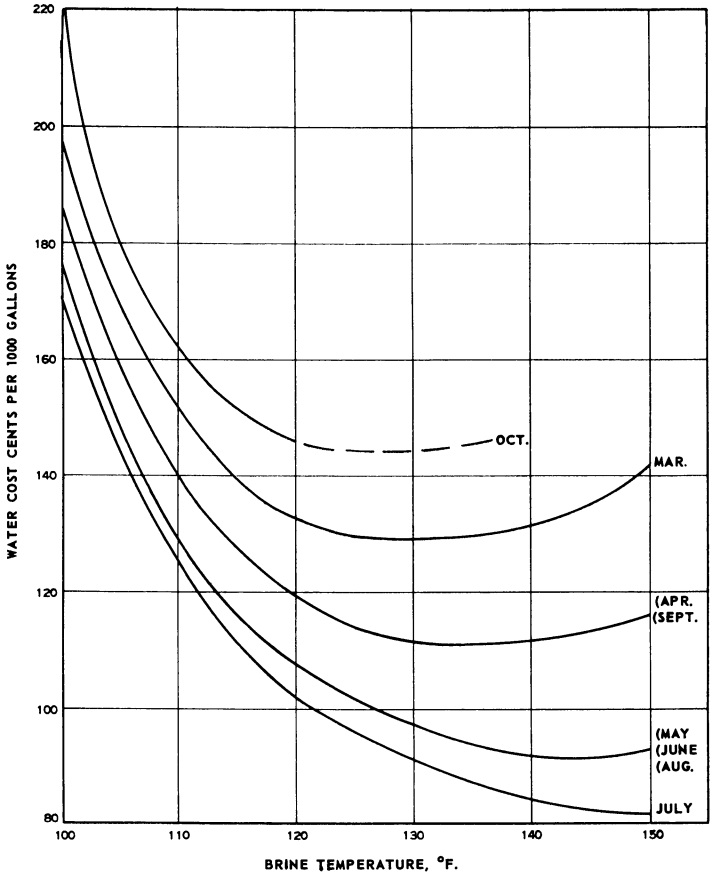

Figure 10. Water cost vs. brine temperature for 3° F. terminal temperature difference

(7) Hand, I. F., *Heating and Ventilating* **47**, 92 (January 1950).
(8) Hottel, H. C., Whillier, A., Transactions of Conference on Use of Solar Energy, Scientific Basis, Vol. II, Thermal Processes, Part 1, Section A, Flat-Plate Collectors, "Evaluation of Flat-Plate Solar-Collector Performance," Tucson, Ariz., **78** (Oct. 31–Nov. 1, 1955).
(9) Hottel, H. C., Woertz, B. B., *Trans. Am. Soc. Mech. Eng.* **64**, 91 (1942).
(10) Jordon, R. C., Threlkeld, J. L., *Heating, Piping, Air Conditioning* **25**, 111 (December 1953).
(11) Kimball, H. H., "Pyrheliometers and Pyrheliometric Measurements," Solar Radiation Investigations Section, U. S. Dept. Agriculture, Weather Bureau, Circ. **Q** (W. B. No. 1051), (November 1931).
(12) Löf, G. O. G., "Design and Evaluation of Deep-Basin, Direct Solar Heated Distiller for Demineralization of Saline Water," Office of Saline Water, Contract No. 14-01-001-74 (April 1959).
(13) Parmelee, G. V., Aubele, W. W., *Heating, Piping, Air Conditioning* **23**, 120 (November 1951).
(14) Threlkeld, J. L., Jordon, R. C., *Ibid.*, **26**, 193 (January 1954).
(15) Yellott, J. I., *Trans. Am. Soc. Mech. Engr.*, **79**, 1349 (1957).

Received May 14, 1962.

Sea Water Demineralization by Means of an Osmotic Membrane

SIDNEY LOEB

Department of Engineering, University of California, Los Angeles, Calif.

SRINIVASA SOURIRAJAN

Division of Applied Chemistry, National Research Council, Ottawa, Ontario, Canada

An osmotic membrane has been developed for demineralizing saline brines such as sea water. The major attractions of the process from an economic standpoint are its simplicity and relatively low energy consumption. The membrane is capable of producing a flux of 5 to 11 gallons of 0.05% NaCl water per sq. foot per day from a brine containing 5.25% NaCl, under a pressure of 1500 to 2000 p.s.i.g. The membrane is fabricated from a casting solution of cellulose acetate and acetone, to which is added an aqueous magnesium perchlorate solution. Key operations in the membrane fabrication process include immersion of the membrane in ice water within a prescribed period after casting, and subsequent heating of the membrane.

This process for demineralizing saline waters depends upon the use of an osmotic membrane—i.e., one which allows water to pass through at a much higher rate than the dissolved salts.

Microscopically the process can be considered one of "reverse" osmosis (Figure 1). An osmotic membrane allows the solvent, but not the solute, to pass through it. The solvent continues to pass through the membrane until the pressure difference across the membrane is equal to the osmotic pressure (350 p.s.i. for a fresh water–sea water interface). In the reverse osmosis desalinization process, a pressure greater than the osmotic pressure applied to the sea water causes fresh water to flow through the membrane from the sea water side.

The method has the salient advantage of containing no inherent irreversibility. Hence it can theoretically be operated as close as desired to the required thermodynamic minimum energy input. The reversible process would consist of operating at a pressure infinitesimally greater than the osmotic pressure; however, to obtain appreciable desalinized water fluxes, a greater operating pressure is necessary.

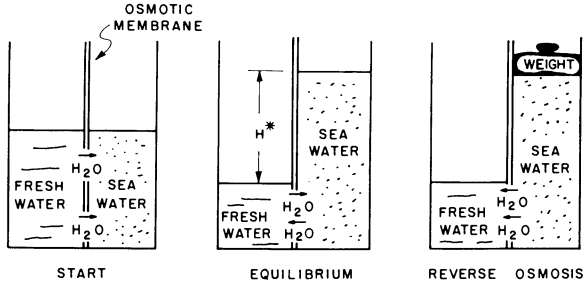

Figure 1. Principle of osmotic desalinization

Osmotic membrane allows passage of solvent but not solute. H (osmotic pressure) 350 p.s.i.*

Other inherent advantages of the process are: It is carried out at ambient temperature, thus minimizing corrosion and scale problems. Because of its simplicity, little operational maintenance is required.

Very little work has been reported on the use of osmotic membranes for desalinization of sea water or similar concentrations of strong electrolytes. The difficulties are associated with the problems of finding a membrane adequately semipermeable to these electrolytes and capable of operation for considerable periods at the operating pressures required. Breton (*1*) has reviewed the available literature.

Work at the University of California at Los Angeles has been directed toward the development of suitable plastic osmotic membranes and the design and fabrication of equipment to utilize these membranes. A narrow air gap may also be considered as an osmotic membrane. UCLA developments on an air gap membrane are discussed by Hassler and McCutchan (3). A suitable membrane is considered to be one which:

Is capable of producing potable water (less than 500 p.p.m. of dissolved solids) from a sea water brine containing solids in considerably greater concentration than in sea water.

Permits appreciable desalinized water fluxes (volumetric flow rate per unit area of membrane) at reasonable pressures.

Possesses these characteristics for several months.

Initial Work

Tentative Mechanism. The fundamental Gibbs adsorption equation can be written in the form:

$$u = -\frac{1}{2RT}\left(\frac{\partial\sigma}{\partial \ln a}\right)_{TA}$$

where u = adsorption of solute in moles per sq. cm. of surface
R = gas constant
T = absolute temperature
σ = surface tension of solution
a = activity of solute
A = area of surface of solution

This equation predicts the existence of a monolayer of fresh water on the surface of an aqueous solution of sodium chloride at the air-solution interface. The practical possibility of demineralizing sea water by the continuous "skimming"

of the surface layer of fresh water was first suggested by Yuster (7), and this suggestion was the starting point of these investigations.

While the mechanism of the process may itself be considered as an open question, this has not prevented the successful development of suitable membranes for sea water demineralization.

Experimental Equipment. Various demineralization techniques were investigated. The one that proved successful consisted of placing the saline water under pressure and in contact with a porous membrane.

Most of the experiments were carried out in a small desalinization cell, a disassembled view of which is shown in Figure 2, which also includes some modifications instituted at a later time. The feed solution passes into the cell solution reservoir and over the membrane while remaining within the confines of the high pressure O-ring. The fresh water passes through the membrane, into and through the porous plate, and to the desalinized solution outlet.

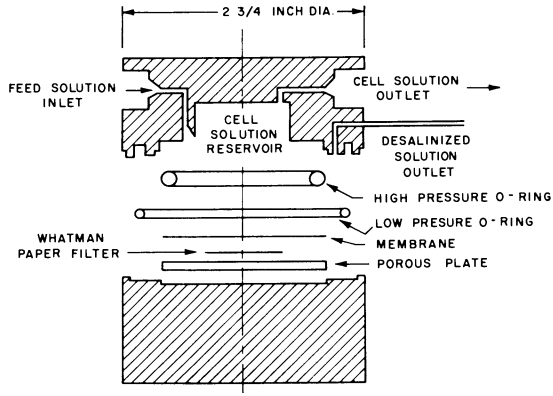

Figure 2. Diassembled view of small desalinization cell

The earliest experiments were carried out under static conditions, using a Carver laboratory press to pressurize the saline water. Since these early experiments, the flow system has undergone various modifications. The flow diagram of the system now in existence is shown in Figure 3. It is beneficial to maintain adequate circulation of the brine over the surface of the membrane. The circulating pump maintains a linear velocity of 4 feet per minute over the membrane surface.

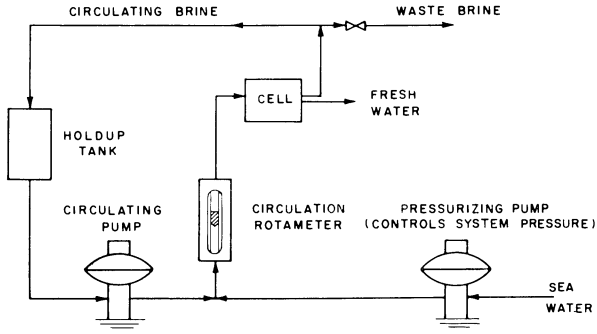

Figure 3. Flow diagram of system

Tests with Relatively Nonporous Films. First a set of experiments was carried out on ordinary untreated cellophane film. A 3.5% NaCl brine, under a hydraulic pressure of 1250 p.s.i.g., was used as the feed solution. Product water flux was on the order of 0.3 gallon per day for 1 sq. foot of membrane (gallons per square foot per day). However, no measurable desalinization occurred (experiment 1, Table I).

The effect of treating the surface of the cellophane membranes with various silicone fluids or Dow Corning Antifoam emulsions was then investigated (experiments 2, 3, 4, and 5, Table I). As high as 32.2% salt removal from a 3.5% NaCl brine, at a product flux of 0.122 gallon per sq. foot per day, was obtained by the use of cellophane films treated with Dow Corning Antifoam B emulsion. In general, product water flux increased as the degree of desalinization decreased.

These results clearly showed that saline water could be demineralized by pressure filtration through porous membranes, and the demineralization characteristics are a function of the chemical nature of the membrane in contact with the saline water.

Table I. Experiments with

Expt. no.	*Nature of Film and Film Treatment*	*Pressure Applied for Filtration P.S.I.G*	*Concn. of Na In feed water*
1	Plain unmoistureproof cellophane (Grade 300, PT-62, Du Pont)	1250	3.56
	Cellophane film		
2	Superficially treated with (I) 10% solution of Drifilm silicone 9987 in toluene, (II) 10% solution of Linde-Y-1001 silicone thermosetting resin in acetone, or (III) Linde-Y-1045 silicone elastomer solution	1250	3.57
3	Superficially treated with Dow Corning Antifoam A emulsion, silicone	1250	3.51
4	Superficially treated with Dow Corning Antifoam B emulsion	1250	3.59
5	Pressure-treated with Dow Corning Antifoam B emulsion	1250	3.51
6	Cellulose acetate film, Du Pont	1250	3.72
7	Treated with Dow Corning 200 Fluid, viscosity grade 12,500 at 25° C.	1500	3.72
8	Pressure-treated with Dow Corning Antifoam B emulsion	2000	3.72
9	Cellulose acetate-butyrate film, Eastman Kodak Co.	4000	3.59
10	Plain ethylcellulose film (0.001 inch thick)	1900 4000	3.52 3.52
11	Cellulose triacetate film (Kodapack IV) Eastman Kodak Co., 0.0008 inch thick	3800 4600 5000	3.52 3.52 3.52
12	Commercial porous Teflon (density 1.7 g./cc.), compressed at 4800 p.s.i.g., then heated at 625–30° F. in mold under mechanical compression, to give final density of 2.20 g./cc.	7000–7500	3.52

The next set of experiments involved the testing of two types of cellulose ester membranes—i.e., cellulose acetate and cellulose acetate-butyrate (experiments 6 to 9, Table I). A high degree of desalinization was obtained with these membranes [determined independently by Breton (*1*) at the University of Florida]. As high as 94.4% salt removal at a flux of 0.03 gallon per sq. foot per day was obtained by using an untreated cellulose acetate film. A cellulose acetate-butyrate membrane gave 99.2% desalinization. However, the flux was only 0.0076 gallon per sq. foot per day and a pressure of 4000 p.s.i.g. was required.

This set of experiments was significant, in that it demonstrated that potable water could be produced from 3.5% NaCl brine by a single pass through a pressure-activated membrane.

The suitability of several other membranes for demineralizing saline waters was then investigated. Commercially available membranes of polystyrene, poly(ethylene terephthalate), copolymer poly(vinyl chloride)–poly(vinyl acetate), rubber hydrochloride, cellulose triacetate, and ethylcellulose were tested. Only the cellulose triacetate and ethylcellulose gave high degrees of desalinization

Relatively Nonporous Films

Cl, Wt. %		*Rate of Production*	
In demineralized water	*Extent of Demineralization, %*	*of Demineralized Water, Gal./Sq. Ft. Day*	*Efficiency*
3.56	0	0.30	
3.21	10.0	0.34	Decreased rapidly with time
2.89	17.7	0.19	
2.39	18.4	0.17	Decreased rapidly with time
2.38	32.2	0.12	Decreased slowly with time
0.21	94.4	0.030	Decreased rapidly with time
0.20	94.7	0.027	Remained stable for 7 days of continuous service, then decreased slowly
0.13	96.4	0.014	Remained nearly stable throughout experimental period of 30 days of continuous service
0.03	99.2	0.0076	Remained completely stable throughout experimental period of 30 days of continuous service
0.32	91	0.0029	
0.25	93	0.0046	
1.23	65	0.0080	
0.70	80	0.0086	
0.14	96	0.010	
2.92–2.75	17–22	0.014	

(experiments 10 and 11, Table I). Desalinization as high as 95 and 93% was obtained by using a cellulose triacetate and an ethylcellulose membrane, respectively.

Tests were then carried out on porous Teflon (polytetrafluoroethylene) (experiment 12, Table I). Commercially available membranes were procured, 10 microns in pore diameter. These pores were reduced in size by various combinations of application of heat and pressure to the membrane. A desalinization of 10 to 24% with a flux of 0.032 gallon per sq. foot per day was the best result obtained by this method.

In view of the partial success obtained by treating cellophane films with various silicone fluids, a glass fiber–reinforced silicone film was also tested. There was some flow through this film, but no demineralization.

Screening tests were then conducted on three rubberlike materials: Buna N, neoprene, and a soft natural rubber. No flow was obtained with any of these materials.

As a result of these tests it appeared reasonable to give considerable attention to membranes fabricated from cellulosic derivatives.

None of the commercial films employed, except porous Teflon, were intentionally made porous. A considerable number of pores of optimum size in the membrane would have been completely fortuitous.

Commercially Available Porous Membranes of Cellulosic Derivatives

In view of the above considerations, membranes fabricated from cellulosic derivatives and having a high concentration of very fine pores were sought. It was found that Schleicher and Schuell Co., Keene, N. H., produced cellulose acetate membranes known as Ultrafine filters. Membranes of the finest grade which contained pores measuring allegedly 50 A. or less were procured. The filtering rate for this grade was stated to be about 700 gallons per sq. foot per day at a pressure differential of 15 p.s.i. The membranes as received were immersed in a dilute alcohol solution and were 0.003 to 0.005 inch thick.

These membranes gave no measurable desalinization. It was possible, however, to obtain appreciable desalinization from them by a simple expedient: heating them in hot water, which apparently contracted the pores. The linear shrinkage of the membrane varied directly with the temperature to which it was heated within the range of 80° to 90° C., where the linear shrinkage was 7 to 18%, respectively. By use of this technique it was possible to obtain fluxes on the order of a factor of 10 greater than previously obtained at comparable degrees of desalinization. Figure 4 displays the desalinization characteristics of these membranes. The flux is approximately inversely proportional and the degree of desalinization is directly proportional to the percentage of linear shrinkage of the membrane. While the degree of desalinization is relatively insenitive to the pressure differential across the membrane, the flux increases with increasing pressure differential up to what appears to be a limiting pressure differential of about 5000 p.s.i.

After the data of Figure 4 were taken, the desalinization cell was modified to permit more adequate circulation of the brine over the surface of the membrane. This resulted in improved membrane desalinization. Figure 4 shows the lowest salt concentration in the desalinized solution to be 0.7%. However, after the cell modifications, desalinized solution was obtained containing as low as 0.14% salt–i.e., 96% desalinization–at comparable fluxes.

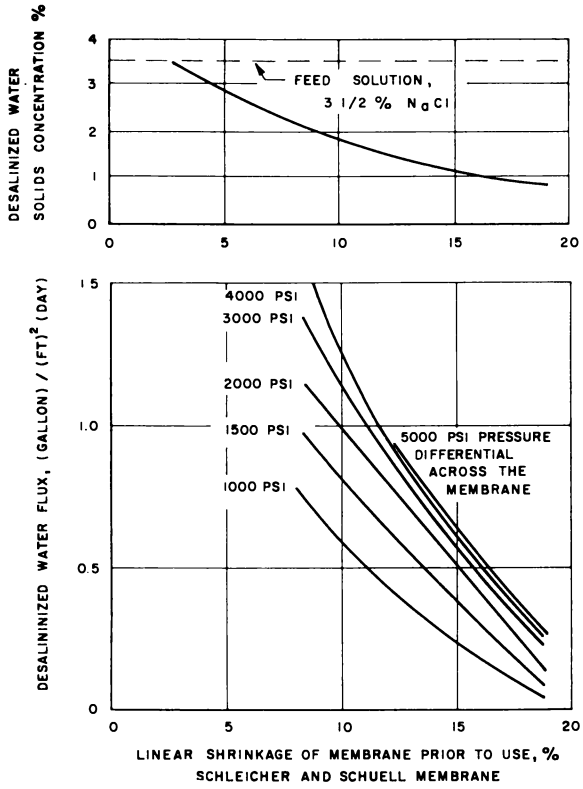

Figure 4. Effect of shrinkage and pressure differential on desalinization characteristics

During the following 6 months efforts were made to improve the flow and desalinization characteristics of the Schleicher and Schuell membrane.

Differential Heating of Films. At an early period in testing Schleicher and Schuell membranes, it was observed that the membrane had a "rough" and a "smooth" side and that desalinization could be obtained only if the rough side was placed in contact with the saline water. It was postulated that the membrane consisted of a fine layer of pore structure at the surface of the rough side, that the remainder of the cross section was a region of spongy, relatively large pores which did not contribute to the desalinization capacity of the membrane and possibly caused resistance to flow, and that by heating only the rough side of the membrane the small pores could be made to contract without shrinking the spongy bulk of material; hence the total resistance to flow through the membrane would be less. Differential heating was accomplished by keeping the smooth side cool with wet filter paper while heating the rough side by bringing it in contact with boiling water or steam. No net shrinkage of the membrane occurred where steam was used. Fair desalinization was obtained by both methods; however, no increase in flux resulted.

Drying of Films. The membranes are received from the vendor in a moist condition. If allowed to dry, the film shrinks appreciably. Since shrinkage also occurs as a result of the thermal treatment, films were subjected to various degrees of drying, including combinations of heating in water and drying. In all cases desalinization was inferior to that from the standard thermal treatment. It is believed that drying constitutes a rougher treatment, which ruptures some of the fine pores.

Silicone Treatment of Surface of Film. Because of the improvement in desalinization obtained by treating the early cellophane membranes with silicone compounds, the effect of silicone treatment on the Schleicher and Schuell membranes was investigated. No improvement in desalinization resulted.

Variation of pH of Heating Solution. In an attempt to determine the optimum pH of the heating solution, tests were made on films heated in water adjusted to various pH's with sulfuric acid. Within the pH range 1.1 to 10, both the product salt content and the flux were proportional to the pH of the heating solution—the flux characteristics are improved with increasing pH, but at the expense of desalinization capacity of the membrane.

Thermal Shrinking of Membranes under Pressure. Experiments were conducted on membranes heated under pressures of the order of 1500 p.s.i.g., to fix the film in a compressed condition while at testing temperature. No improved desalinization resulted.

In addition, a life test was carried out, to determine membrane stability. The Schleicher and Schuell membrane remained active under the laboratory test conditions (0.8% NaCl feed, 1500 p.s.i.g.) during continuous running for 6 months—i.e., it remained active throughout the whole test.

In view of the high degree of desalinization obtained with the early films made of cellulosic derivatives and the more recent success with commercial porous cellulose acetate films, experiments were carried out on commercial porous cellulose nitrate membranes containing pores with diameters of 50 A. or less. It was possible to obtain up to 11% shrinkage by heating the cellulose nitrate films in boiling water. However, unlike the commercial cellulose acetate membranes, no desalinization resulted. Since it was possible to desalinize by drying the commercial cellulose acetate membranes, the results of drying on the commercial cellulose nitrate membranes were also investigated. By the technique of drying it was possible to obtain only a 15% reduction of the original 3.5% salt in the input brine, at a flux of 0.3 gallon per sq. foot per day. It appeared that the cellulose nitrate membrane was either intrinsically inferior to the cellulose acetate membrane, or would not respond properly to the treatment developed for the cellulose acetate membrane.

After a number of relatively unsuccessful attempts with commercial cellulose acetate membranes, potable water (0.05% or less salt concentration) had never been obtained from a brine containing salts in the concentration found in sea water (3.5%). The lowest product salt was less than 1 gallon per sq. foot per day. Some of the best results (qualitatively taking into account both demineralization and flow rate) are shown in Figure 5. By using the Schleicher and Schuell membrane, potable water could be obtained only if the feed brine contained considerably less salt than sea water and even then the flux was only on the order of 2 gallons per sq. foot per day. Although the Schleicher and Schuell membranes constituted a significant improvement over previous membranes, flux or desalinization capabilities were not as high as desired. For this reason, casting of membranes was undertaken by project personnel.

Laboratory-Cast Membranes

From experience gained with commercially available films, the following approach was decided on for the laboratory fabrication of films (*4*).

Cellulose acetate would be used as the film matrix.
Acetone or some other solvent would be used for the casting solution.
Some means for making the film permeable to water would be employed.

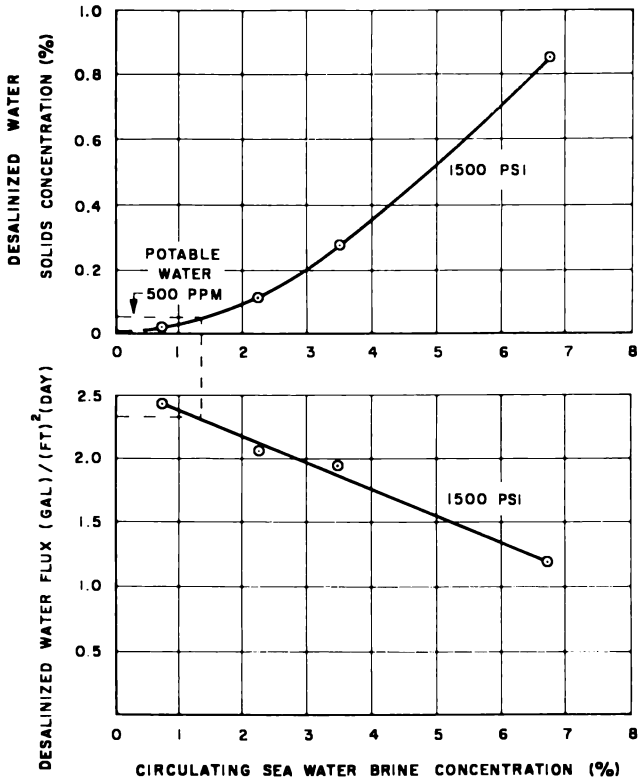

Figure 5. Effect of sea water solids concentration on desalinization characteristics

Schleicher and Schuell membrane

In the search for an adequate means of making the membrane water permeable, an article by Dobry (2) was found, which suggested the use of aqueous magnesium perchlorate in the fabrication of cellulose acetate films for general-purpose ultrafiltration. By incorporating aqueous magnesium perchlorate in the casting solution and instituting a large number of novel changes from the original Dobry method (patent being sought) it was possible to fabricate membranes whose desalinization and flux characteristics were of a considerable order of magnitude better than those of the commercial membranes tested.

By use of these membranes a flux of potable water of 5 to 11 gallons per sq. foot per day at 1500 to 2000 p.s.i. pressure differential was obtained from a brine containing as high as 5.5% sodium chloride.

Fabrication. The casting solution is a mixture of cellulose acetate, acetone, water, and magnesium perchlorate (22.2, 66.7, 10.0, and 1.1%, respectively).

The solution is cast at 0° to 10° C. onto a cold glass plate having 0.010-inch side runners to give this thickness to the as-cast film. Uniformity of film thickness is obtained by passing an inclined knife, resting on the side runners only, across the top of the plate. The knife forms the back wall of an integral frame, which containes an excess of casting solution.

The acetone is allowed to evaporate from the film in the cold box for 3 to 4 minutes, after which the film (and plate) are immersed in ice water for at least an hour.

After immersion in ice water, the membrane is removed from the glass plate and heated in hot water. The membrane is heated, for at least 1 hour, to 75° to 82° C., with the higher temperature favored.

After heating, the membrane is ready for use. The side of the membrane away from the glass during casting must be toward the brine solution in operation (recall results with Schleicher and Schuell films). For best results, the operating pressure should be applied in stages. Thus if the final pressure is to be 1500 p.s.i.g., a pressure of 1000 p.s.i.g. is applied first, for one-half hour.

Casting Solution Composition. The acetone in the casting solution used as a solvent for the cellulose acetate provides the proper viscosity. If the ratio of acetone to cellulose acetate was too low, very viscous casting solutions resulted and could not be used for casting uniform films. Conversely, if this ratio was too high, thin, films which became jellylike upon immersion in water resulted. An acetone–cellulose acetate ratio of about 3 has been found satisfactory.

The water and magnesium perchlorate contents were varied relatively independently. The range of variation covered thus far includes two conditions:

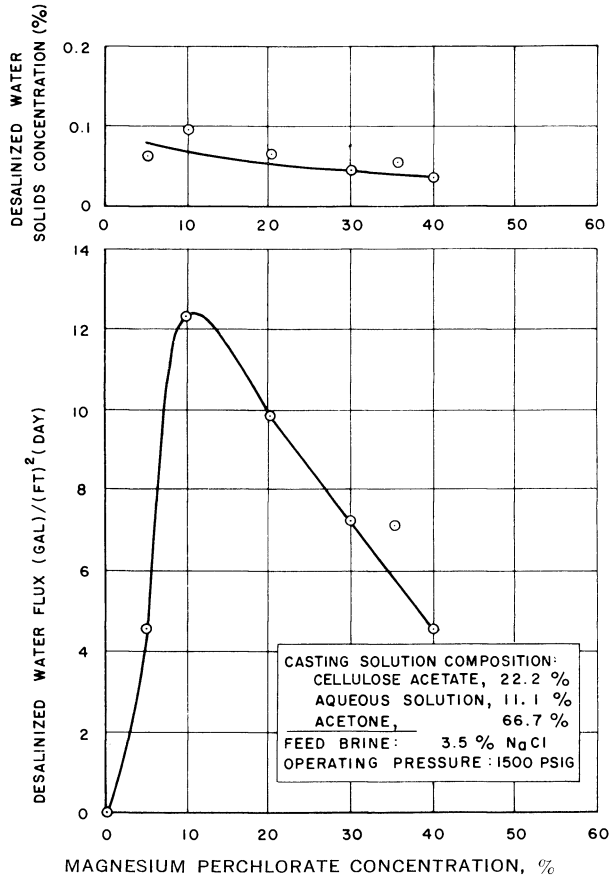

Figure 6. Effect on film performance of percentage of magnesium perchlorate in aqueous solution

Laboratory-cast film

Using a saturated $Mg(ClO_4)_2$ solution [50% $Mg(ClO_4)_2$] films were made from solutions containing various ratios of saturated $Mg(ClO_4)_2$ solution to cellulose acetate. The optimum ratio is 1 to 2.

With a 1 to 2 ratio of magnesium perchlorate solution to cellulose acetate, the amount of $Mg(ClO_4)_2$ in the aqueous solution was varied. As is seen in Figure 6, the highest water fluxes were obtained when aqueous solutions containing on the order of 10% $Mg(ClO_4)_2$ were used. When water alone was added to the casting solution—i.e., 0% $Mg(ClO_4)_2$—no water flowed through the membrane.

Film Casting Technique. After the membrane is cast on the glass plate, the acetone is allowed to evaporate from the films for a short time before immersion in water. If evaporation of the acetone were allowed to proceed to completion before the film was immersed in water, the desalinization capacity of the film would be seriously impaired. The proper time interval between casting and immersion depends on the rate of evaporation of acetone from the membrane and hence is a function of the temperature at which the membrane is cast and allowed to remain, prior to immersion. At room temperature, this time interval is relatively short, which made it difficult under these conditions to fabricate membranes which would give satisfactory, reproducible data. For this reason the membranes are cast in a freezer, with all components at about 0° C. It is also

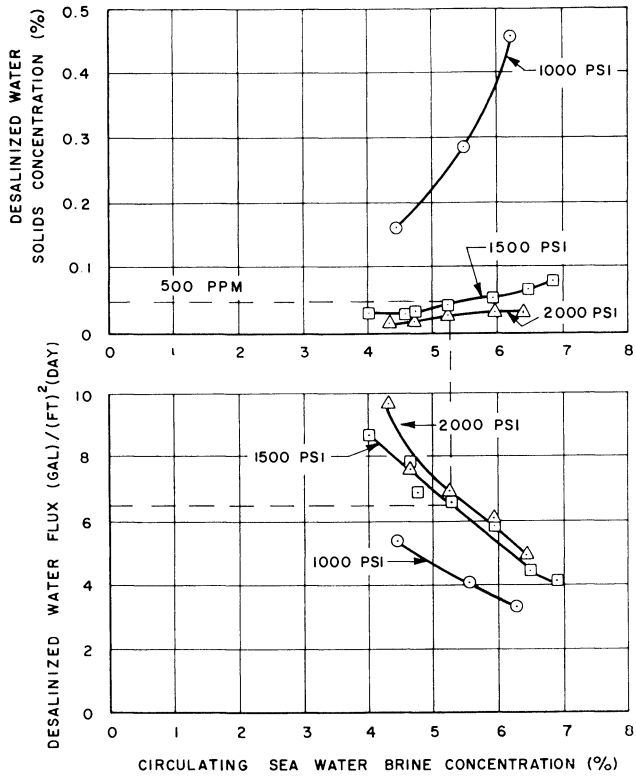

Figure 7. Effect of sea water concentration on desalinization characteristics

Laboratory-cast film

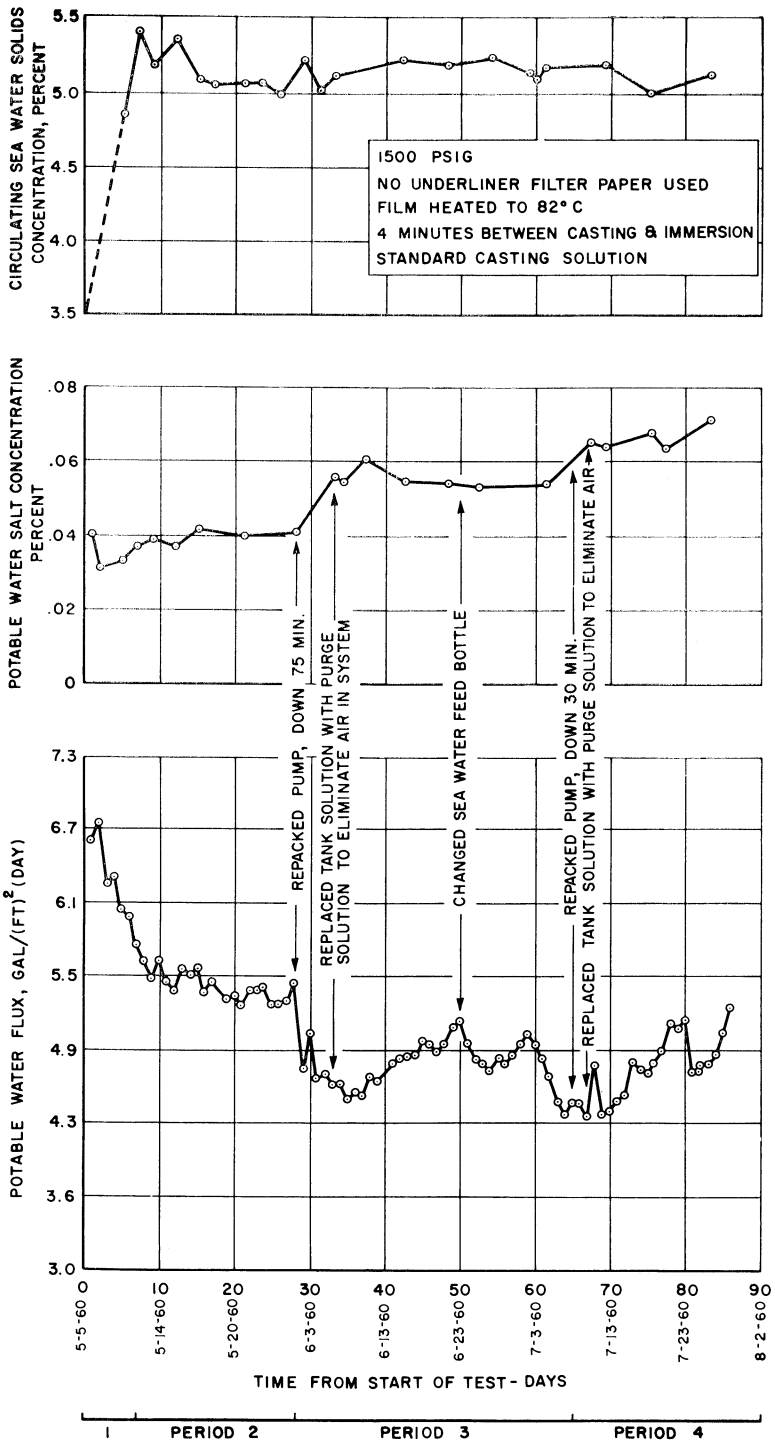

Figure 8. Life test of laboratory-cast film

desirable to immerse the membranes in water at a temperature just slightly over 0° C. An interval of about 3 or 4 minutes between casting and immersion has been found satisfactory, for casting carried out at 0° C.

Heating of Membranes. As with the commercial cellulose acetate membranes, it is necessary to heat the laboratory-made films in hot water to obtain desalinization. The optimum heating temperature is 75° to 82° C. Below 75° C. desalinization is poor, and above 82° C. the water flux drops off rapidly with an increase in temperature.

Typical results obtained with the membranes, fabricated and utilized as described above, are shown in Figures 7 and 8. It is perhaps instructive to compare the results of the laboratory-cast membranes in Figure 7 to those of the commercial cellulose acetate membranes in Figure 5.

Four-Inch Cell

The development work on films has been done primarily with the small cell of Figure 2. The effective area of this cell is 0.012 sq. foot. It is envisioned that a commercial desalinization unit utilizing these membranes would somewhat resemble a plate and frame filter press with a "close stacking" arrangement of membranes. To test the feasibility of this concept a larger cell (effective film area 0.2 sq. foot), capable of multiple film arrangement, was designed and fabricated.

A simplified view of the internal flow arrangement, which illustrates the "close stacking" concept, is shown in Figure 9. The basic unit (or package-frame assembly), as shown in Figure 10, consists of a porous collector plate with a film on each side and a frame which provides the volume for the brine to pass over the film. The frame "backs up" an O-ring which gives the system its external seal. The internal seal is maintained by means of an Epocast coating, a rubber gasket,

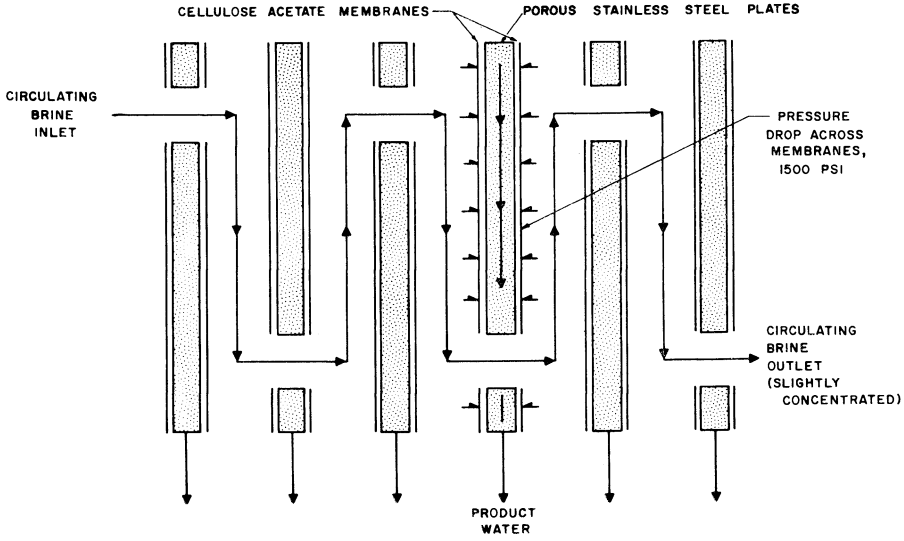

Figure 9. Flow through film packages

4-inch desalinization cell

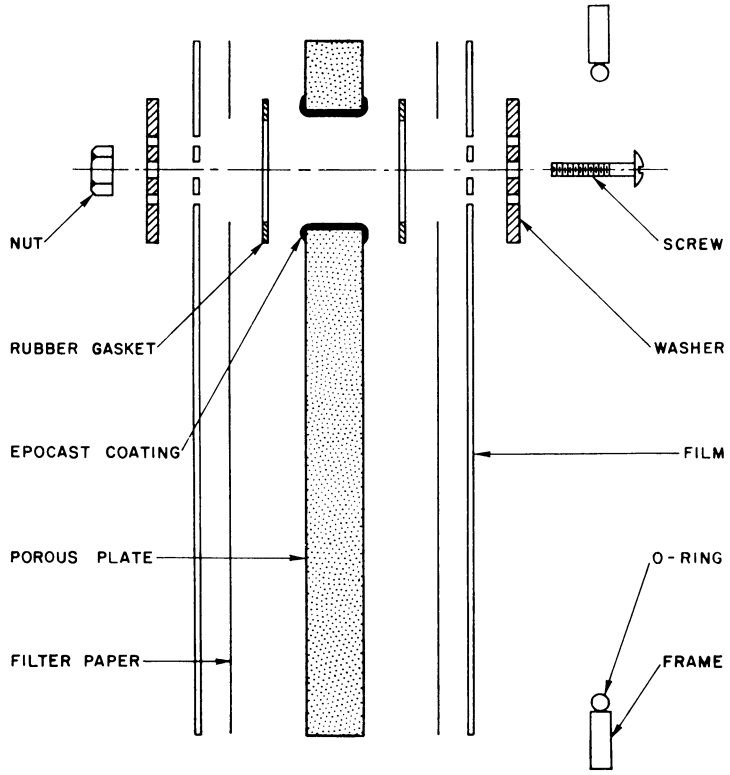

Figure 10. Dissassembled package-frame assembly of 4-inch desalinization cell

and a washer. The external flow system is similar to that of the small desalinization cell (Figure 2).

This larger cell was operated with as many as 12 films (six packages) at a time. Results were satisfactory, although performance was not as good as with the small cell. The discrepancy may be due to the fact that the brine circulation was not as good in the larger cell as in the small cell.

Preliminary Cost Analysis

A preliminary cost analysis was made on the process. Since it is based on small scale operation, it is not significant in determining a large scale cost figure, but it might reveal salient advantages and present weaknesses of the process.

The method of analysis used was that given by the Office of Saline Water, U. S. Department of the Interior (*6*). The estimates were based on 10,000,000 gallons of product water per stream day. The following assumptions were made:

The total cost of the desalinization cells could be approximated by the cost of the plate and frame filter presses.

The cost of a fabricated membrane would be ten times the cost of bulk cellulose acetate.

The expected life of a membrane would be 6 months.

Based on the above assumptions, two cost estimates were made:

The first assumed a product flux of 5 gallon per sq. foot per day, a waste brine salt concentration of 7%, a pressure of 1500 p.s.i.g., and a complete loss of the energy in the concentrated waste brine. Based on these conditions, the total cost was $1.00 per 1000 gallons of fresh water.

The second was based on a water flux of 11 gallons per sq. foot per day, a waste brine concentration of 5.25%, and a pressure of 2000 p.s.i.g. It was assumed that 70% of the energy in the concentrated brine would be recovered by using it to pressurize the entering sea water. In this case, the cost was $0.60 per 1000 gallons of fresh water.

The plant investment cost, which is the most important single item, is most strongly influenced by the water flux. By the second method, in which the flux is 11 gallons per sq. foot per day, the cost is considerably less than for the first, in which the flux is 5 gallons per sq. foot per day. These differences are shown in Table II.

Table II. Plant Investment Cost

	First Estimate		*Second Estimate*	
	%	*$/1000 gal.*	%	*$/1000 gal.*
Films, 6-month life	4.75	0.048	3.66	0.022
Labor	7.13	0.073	6.70	0.040
Amortization of plant investment	50.50	0.516	41.80	0.250
Taxes and insurance	13.52	0.138	11.03	0.073
Power	16.42	0.167	29.60	0.178
Supplies, overhead interest, etc.	7.68	0.078	7.21	0.043
	100.00	1.02	100.00	0.60

Summary

This process has two major attractions: It is very simple, as exemplified by the flow diagram of Figure 11, which shows a plant with a capacity of 10,000,000 gallons per day. It requires a relatively low energy consumption. A membrane has been developed for which the energy consumption is on the order of 13 times the free energy of separation [2.9 kw.-hr. per 1000 gallons as calculated by Murphy (5)].

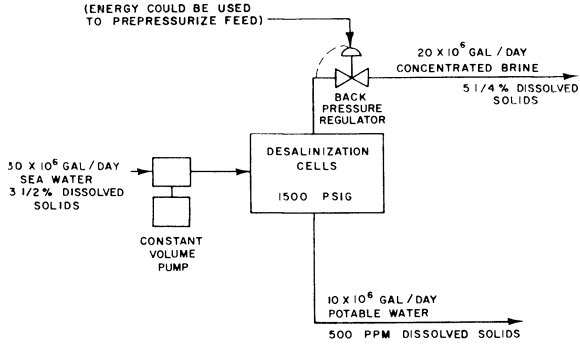

Figure 11. Proposed flow diagram of 10,000,000-gallon-per-day plant

The membrane can produce fresh water at a flux of 5 to 11 gallons per sq. foot per day. The capital cost of the plant is an inverse function of flux. The

fluxes attained are high enough to encourage the belief that potable water costs attributable to capitalization might not be excessive. Under these conditions the process may become competitive with other saline water conversion processes.

Literature Cited

(1) Breton, E. J., Jr., "Water and Ion Flow through Imperfect Osmotic Membranes," Office of Saline Water Research and Development, Progr. Rept. **58–26.**
(2) Dobry, A., *Bull. Soc. Chim. France* **3,** 312–18 (1936).
(3) Hassler, G. L., McCutchan, J. W., ADVAN. CHEM. SER., No. **27,** 192-205 (1960).
(4) Loeb, S., Sourirajan, S., "Sea Water Demineralization by Means of a Semipermeable Membrane," UCLA Rept. **60–60** (1960).
(5) Murphy, G., U. S. Dept. Commerce, Office of Tech. Services, Rept. **PB 161384** (1956).
(6) Office of Saline Water, U. S. Dept. Interior, "Standardized Procedure for Estimating Costs of Saline Water Conversion," March 1956.
(7)) Yuster, S. T., Sourirajan, S., Bernstein, K., "Sea Water Demineralization by the Surface Skimming Process," UCLA Rept. **58–26** (1958).

RECEIVED May 16, 1962. Research carried out at the University of California, Los Angeles, under sponsorship of the Statewide Water Resources Center Program in Sea Water Conversion Research. Activities of the University of California in this program coordinated by E. D. Howe. Project initiated by S. T. Yuster, project leader through 1957. Work covers developments through August 1960.

Operating Experience on a Large Scale Electrodialysis Water-Demineralization Plant

O. B. VOLCKMAN[1]

Process Development Division, National Chemical Research Laboratory, Council for Scientific and Industrial Research, Pretoria, South Africa

An electrodialytic water demineralization plant, with multiple units using the "sheet-flow" principle, was designed to produce 2,880,000 gallons per day of water with 525 p.p.m. of total dissolved solids from a 3100-p.p.m. TDS mine water in South Africa. The plant operated for over 18 months, but at not greater than 71% of rated capacity, and then only with a 2843-p.p.m. TDS feed water and 71.4% TDS removal. The low capacity was mainly due to excessive polarization and intercompartmental leakage. Extensive trials on full scale units showed that these difficulties could be eliminated. Desalting costs ranged from an actual $0.426 (U. S.) per 1000 gallons at 71.4% TDS removal and 1,540,000-gallon-per-day output to an estimated $0.297 (U. S.) per 1000 gallons at 82.1% TDS removal and 2,880,000-gallon-per-day output.

Work on saline water conversion using the electrodialysis process in South Africa was outlined by the author in 1957 (7), including plans for a 2,880,000-gallon-per-day (U. S. gallons) desalting plant at Welkom, Orange Free State, to desalt a highly saline mine water of approximately 3100 p.p.m. total dissolved solids (3000 p.p.m. NaCl) to 535 p.p.m. total dissolved solids (500 p.p.m. NaCl) (Figures 1, 2, and 3). Experience gained from operation of that plant is reported here.

The reasons for erecting the plant, and the design basis, have been described in detail (*1*, *2*, *4*, *5*, *9*). The decision to construct the large plant was taken by the mining companies with full knowledge that the urgency of the water-disposal situation at that time would permit only very limited prototype tests. This meant that the large plant would probably have to be operated, for the first 2 years at least, largely as a development plant, since many factors in the design and operation of large electrodialysis plants had not been fully investigated. Some of the operating expenses would be met by the sale of the desalted water produced, but it was thought unlikely that the venture would make a profit in the earlier stages.

[1] Present address, Department of Chemical Engineering, University of the Witwatersrand, Johannesburg, South Africa

Figure 1. Free State Geduld electrodialysis plant

Dam for 1,000,000 gallons of raw water
Right. Filter plant building
Rear. Electrodialysis plant building

The plant was principally an insurance against loss of mining production from an inability to dispose of large volumes of saline water.

As events developed, severe engineering difficulties were experienced, while the magnitude of the water-disposal problem progressively decreased.

Whereas in 1956, when the project was first considered, the salinity of the mine water from some mines was as high as 4000 p.p.m. TDS, the average value of the water to be treated by the Free State Geduld plant had fallen to 3100 p.p.m. TDS in 1958 and to 2700 by early 1961.

Up to October 1960 the output from the plant of desalted water per unit had not exceeded 71.4% of design and this output was only achieved with a product water of 813 p.p.m. TDS. The reasons for low production per unit were high electrical resistance due to polarization, sludge formation on the membranes (not scaling), and leakage from the diluting to the concentrating streams. The polarization difficulties were eventually overcome (*10*). Considerable work was done in the plant and in the laboratories at Pretoria to overcome the leakage problem (*11*). It was shown that this problem could be overcome, but because of the additional capital investment required and the fact that the water-disposal problem was rapidly becoming less serious, it was not possible to confirm the findings by long-scale tests on the plant.

In February 1961, the mining companies decided to suspend operations of the Free State Geduld Mine plant pending further work by the South African Council for Scientific and Industrial Research aimed at reducing costs. At that stage the plant could have been relied upon to deliver 1,500,000 gallons per day of

525 p.p.m. TDS water, but at a somewhat higher cost than 30 cents per 1000 gallons.

As the mines buy their water at R 0.25 ($0.30) per 1000 gallons, they were not prepared to continue operating a plant producing water at a higher cost.

At the time of writing (November 1962) the future of the plant is under final review. As the amount of water from the mines has decreased to the point where the water can be evaporated from the existing surface evaporation dams, it is probable that the plant will be dismantled. If, in 1956, the geologists could have predicted the present water situation, the plant would probably not have been built.

Some of the difficulties experienced were expected. They were inherent in the decision to use large units after only limited prototype tests. These difficulties were largely mechanical and were particularly associated with the design, materials of construction, and fabrication of press components. Other difficulties, however, could have been found only by prolonged operation in the field; typical were difficulties relating to adequate removal of the suspended clay in the raw water, sludging of the membrane compartments with the clay, and failure after prolonged use of certain press components and piping.

Nevertheless, the plant has shown without doubt that the electrodialysis process can, under correct operating conditions, be very reliable; membrane packs of large dimensions and with large numbers of membranes (up to 200) can easily be assembled and handled; high voltages (450 to ground) can be used without mishap to operating staff, or causing excessive current leakage or corrosion of surrounding structures or equipment; and simple automatic control suffices where continuous, as against batch, desalting is used.

Some Basic Design Considerations

The Free State Geduld plant was based primarily on what is sometimes described as the sheet-flow, intermembrane spacer, or full-flow type of apparatus,

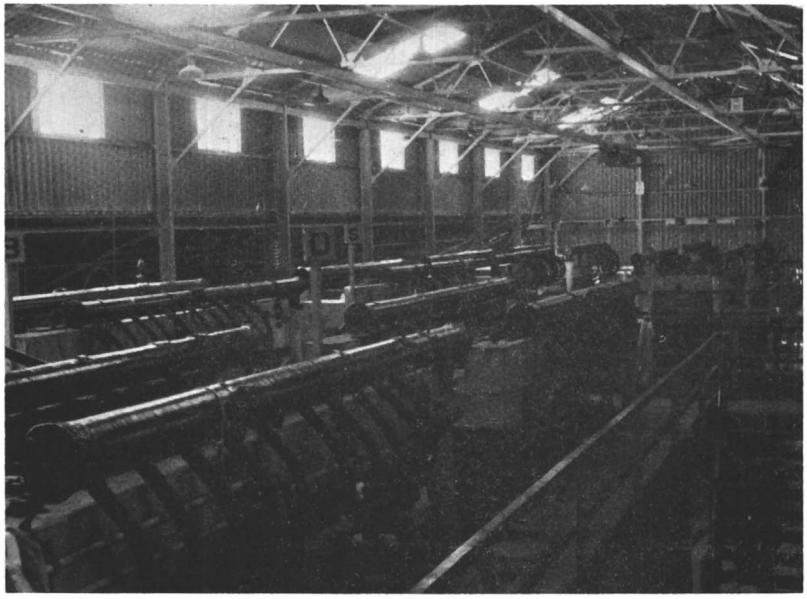

Figure 2. Section of electrodialysis presses

Figure 3. Top of electrodialysis units

as opposed to the tortuous path type. Considerations leading to the design of the plant are given by the South African Council for Scientific and Industrial Research (SACSIR) water desalting team (*9*); progress is reviewed by Wilson (*8*) and Volckman (*6*).

As a guide to sizes of existing sheet flow types of electrodialysis plants, Table I compares the membrane area of the FSG plant with those of the next largest commercial plants known to be in commercial operation in early 1961, and which were operating with multiple packs in a press.

In considering the design of the plant two related factors had to be considered very carefully.

The advantage, if any, of using a few large electrodialysis units rather than a multiplicity of smaller units (the term "unit" is here taken as a membrane press, whether consisting of one or a number of membrane packs). The plant uses the principle of multiple packs in each electrodialysis unit or "press."

The type of membranes that should be used, and the practical operating lifetime that could be expected from them (very few commercial membranes, especially of large size, had been extensively field-tested in 1956).

One of the severely limiting prerequisites of the plant was that the cost of desalting the water from 3000 p.p.m. NaCl (approximately 3100 p.p.m. TDS)

Table 1. Comparison of Free State Geduld Plant with Other Intermembrane Spacer Plants

	FSG	*A*	*B*
Over-all membrane dimensions, inches	$85^3/_4 \times 25^3/_4$	$59^1/_2 \times 15^3/_4$	$39^1/_2 \times 15^3/_4$
Over-all membrane area, sq. ft.	15.33	6.50	4.32
% effective membrane area	67	61	59.5
No. of electrodialysis presses on line (excluding spares)	8	1	1
No. of packs per press	10	1	1
No. of membranes per pack	200	200	100
Total membrane area of plant (excluding spare units), sq. ft.	245,290	1300	4320
Effective membrane area of plant (excluding spare units), sq. ft.	164,340	793	2570

A. Wm. Boby plant at Tobruk, N. Africa. B. S.O.D.E.M.I. installation, N. Africa.

to 500 p.p.m. NaCl (approximately 520 p.p.m. TDS) should not exceed R 0.25 per 1000 Imperial gallons (29 U. S. cents per 1000 U. S. gallons), including all pretreatment costs, and the complete plant and auxiliary facilities should be amortized over not more than 15 years.

Design and cost studies indicated that, so far as could be seen at that stage of development, the desired low costs of production of desalted water would be achieved only with a plant having a small number of presses taking large membranes of the order of 6 feet by 2 feet 6 inches. In this way, if the engineering difficulties associated with such large units could be overcome, capital and operating costs should be at an acceptable level.

The choice of size of unit was dependent not only on investment costs, but also on the availability of membranes of suitable size and price. Many other design and operating considerations had to be considered. These have been fully discussed (*9*).

The type of membrane to be used was ultimately decided on the basis of cost, possible life, mechanical suitability, and suitable electrochemical properties.

If the types of high quality membranes then available were to be used in units of the size considered desirable, a lifetime of at least 3 years was required to meet the desired desalted water cost, while for a plant with a larger number of relatively small units a considerably greater life would be required to break even on operating costs. There was, moreover, no guarantee that the numbers and sizes of high quality membranes required would be available with a guaranteed lifetime of 3 years or more. Under the circumstances, it was decided to base the design of the FSG plant on the use of SACSIR parchment-based membranes that had been used in the pilot plant. The estimated price of these was approximately 11 cents per sq. foot, with a 9-month proved life. Actual membrane prices for the plant were, in fact, almost double this figure, thus altering the price-lifetime relationship.

The parchment-type membranes were originally developed for the pilot plant work as a stopgap, when the membranes ordered could not be delivered in time. As experience was gained with the membranes, it was considered that they might have an application in the desalting of low salinity brackish waters (4000 p.p.m.), and that they were particularly suitable for the mine water problem. In the latter case, their cheapness was attractive, particularly where process difficulties might require long-life membranes to be discarded in large numbers before their useful life was ended. The parchment membranes, in their improved form, gave very satisfactory service in the plant; if it had not been possible to use them,

the FSG plant would probably not have been built, and no results on large plant operation would yet be available.

After it had been confirmed that SACSIR parchment membranes could be made and safely handled in sizes up to 72 × 28 inches over-all, tests were carried out on a prototype unit (*7*, *9*, *11*), taking membranes of an over-all size of 66 × $26^3/_4$ inches. Recalculation of the optimum operating conditions when using large membranes suggested the eventual size of unit taking membranes of $85^3/_4$ × $25^3/_4$ inches. This size was agreed on only after it had been confirmed that SACSIR-type parchment membranes of this larger size could also be made and safely handled.

Means to ensure even flow distribution in the individual $22^3/_4$-inch-wide compartments had to be considered carefully. It is important to obtain rather uniform flow distribution over the whole face of the membranes, if polarizing conditions and scale formation are to be avoided, particularly in the case of the FSG plant, which was designed to operate originally with mean compartmental flow rates only some 10% above the critical polarization value.

Experience in the pilot plant had shown that the ring distribution system from a single port (*9*) is not very effective with broad compartments. After a consider-

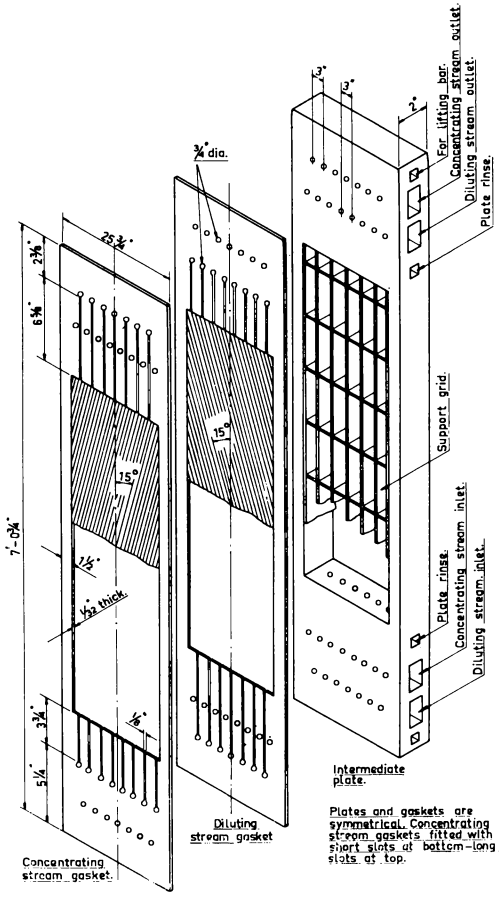

Figure 4. Electrode and intermediate plates, gaskets, and spacer design

able amount of experimentation on plates of the prototype size, the slot feeding distribution system (Figure 4) was decided on. It was always realized that there was danger of the membranes collapsing into the slots, particularly if pressures on the two sides of a membrane were considerably out of balance. Leakage from one compartment to the other could then take place (Figure 5). The dimensions of the slots were the largest that tests showed could be used without leakage. Unfortunately, these tests were carried out with fairly new membranes. In the plant the membranes gradually deformed with time, extensive leakage then taking place.

Operating Experience

The operation of the FSG plant for over 18 months has given the first opportunity for assessing the characteristics of a fully integrated plant designed for multimillion gallons per day output, using a sheet-flow type of electrodialysis apparatus.

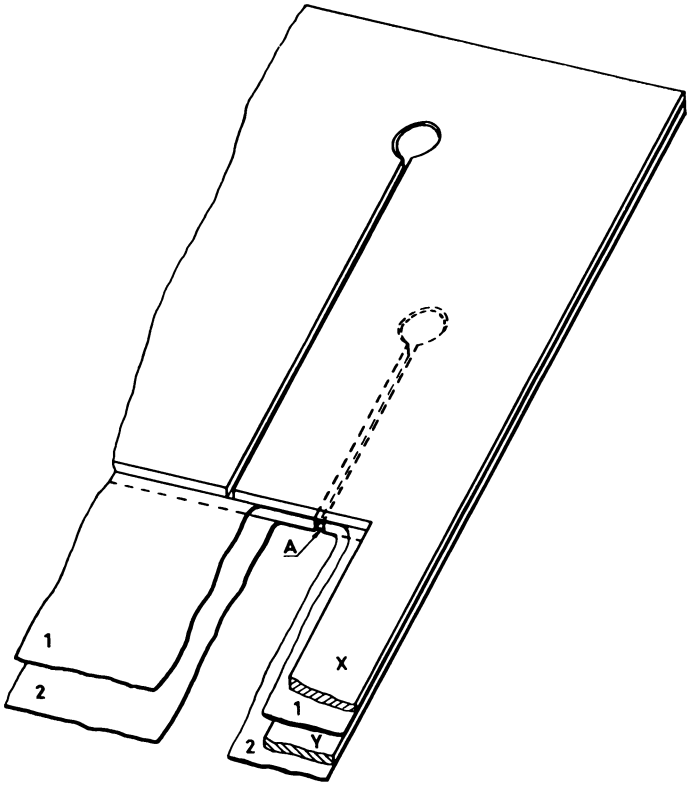

Figure 5. Mechanism of slot or intercompartmental leakage

Membrane 1, having pressure on top greater than pressure between membranes 1 and 2, is pressed down into slot at A at edge of gasket. Slot is in gasket Y, feeding compartment between membranes 1 and 2. Deformation at A progresses until liquid in compartment on top of membrane 1 can pass under gasket X into conduit feeding short slot as well as into the correct slot feeding long conduit. Spacer omitted for clarity

The plant underwent its first tests in November 1958, with one press on line. Commissioning tests continued until April 1959.

After the usual troubles experienced in starting up a new plant had been rectified as far as possible, the plant was put into routine operation under mine staff control in May 1959, with four of the eight presses on line. Delays in getting all eight presses into service were caused by very late delivery of some of the press intermediate plates.

In June 1959, the mining companies decided to operate the plant on a production basis to obtain income from the sale of water, although at this time the plant had not been brought into full production. Except for special tests in April 1960, this period lasted until October 1960, when a series of investigations was carried out to confirm certain ideas as to why the plant was not achieving its designed output.

From March 1960 to February 1961, a press with a single pack identical to those on the FSG plant was available at the SACSIR laboratories at Pretoria to check results obtained on the FSG plant, and to try out improvements in the design of pack components and methods of operation (*10*, *11*). The unit was also used to test, under carefully controlled conditions, packs sent from the FSG plant. The only difference between operation on the units at Pretoria and at the FSG plant was that the former was fed with synthetic brackish water from which the clay particles found in the FSG raw water were absent.

Table II. Data from Routine Operation

Period	Operating Time: Possible, hr.	Operating Time: Actual, hr.	Operating Time: On line, %	Units Operating per Stage	Production Rate: Mean U. S. g.p.h.	Production Rate: %[a]
1959						
3/29–4/25	672	590	87.8	1	8,338[c]	27.8
5/29–6/25	312	259.5	83.2	1	4,323[c]	14.4
	360	356.8	99.1	1	13,688[d]	45.7
6/26–7/25	720	631.8	87.8	1	13,040	43.4
7/26–8/25	744	585.5	78.7	2	30,080	50.0
8/26–9/25	744	714	96.0	2	35,300	58.8
9/26–10/25	720	661.7	91.9	3	40,960	45.5
10/26–11/25	744	627.2	84.3	3	45,000	49.9
11/26–12/25	672	644.2	95.9	3	43,954	48.8
1960						
12/26–1/25	744	637.7	85.7	3	38,971	43.3
1/26–2/24	715	645.8	90.3	3	48,153	54.6
2/25–3/24	561	541	96.4	3	53,420	59.4
3/25–4/24	442	438.7	99.3	3	64,260	71.4
4/25–5/24	226 (6 units)	201.5	89.2	3	51,766	57.5
	192 (8 units)	178	92.7	4	60,178	50.1
5/25–6/24	744	655.4	88.1	4	56,940	47.4
6/25–7/24	720	687.8	95.5	4	56,584	47.1
7/25–8/24	744	663.3	89.2	4	61,120	50.9
8/25–9/22	744	647	87	4	52,347	43.8

[a] % of designed capacity for section of plant actually in operation.
[b] Per electrode pair.
[c] Single diluting stream inlet connections to membrane packs.

The successful technical operation of an electrodialysis plant depends, among other things, upon the production of components to very close tolerances, precise assembly, ease of handling and assembly of components, mechanical reliability, freedom from corrosion, low electrical losses, freedom from liquid leakage from concentrating to diluting stream or *vice versa*, freedom from external liquid leakage, freedom from scaling, and safety of operation.

In the FSG plant difficulties were experienced in obtaining components having the necessary tolerances and intermediate pack plates having adequate mechanical strength and resistance to deterioration. Interstream leakage resulted in low electrical efficiencies and loss of output. Deposition of a clay sludge on the membranes proved troublesome; this was a problem peculiar to the particular mine water, but does emphasize the sensitivity of the electrodialysis process to the various substances that can be found in raw brackish waters, in particular membrane "poisons," scale-forming compounds, and suspended solids that can only with difficulty be coagulated or separated by filtration. In the latter case, the self-flushing characteristics of a particular design of plant can be important.

In spite of difficulties, the FSG plant has shown conclusively that large sheet flow-type units can be assembled and handled without difficulty, even when using relatively weak parchment-base membranes.

Operating reliability of the whole plant was of a high order in spite of defects developing in some of the pack plates. On-stream time over a continuous period

of Free State Geduld Electrodialysis Plant

Mean Electrical Conditions					*Coulomb Efficiency, %*					*Kw.-Hr./ 1000 U.S. Gal. Product*
Volts at 25° C.		*Amp.*[b]			*Mean*		*Max.*			
Stage I	*Stage II*	*Stage I*	*Stage II*	*Mean Temp., ° C.*	*Stage I*	*Stage II*	*Stage I*	*Stage II*	*25° C.*	*1000 p.p.m. TDS removed, 25° C.*
782	579	41	23	23.0	70	76	80	90	14.6	...
784	587	33	24	20.9	69	51	83	63	18.7	...
800	558	63	26	...	65	79	77	85	9.5	4.93
778	565	60	27	19.8	68	74	81	89	9.7	5.26
831	603	67	30	22.8	72	74	86	83	9.6	4.60
850	646	79	35	25.6	70	75	84	86	10.2	5.20
837	687	70	32	23.8	70	74	83	89	11.7	5.95
880.6	665.3	76.5	38.6	25.9	65	70	73	81	12.7	6.33
885.2	687.1	75.8	37.5	28.1	59	67	63	80	13.0	6.55
792.9	635.4	86.5	34.7	27.3	60	66	65	86	13.8	7.33
856.1	644	83.5	33.3	27.3	75	69	92	86	11.6	5.61
869.7	654.3	82.3	34.5	27.3	76	75	87	91	11.1	5.13
842.5	622.7	68.7	36.4	25.8	78	72	94	82	7.75	3.82
782.9	572.6	58.8	38.7	21.6	71	73	74	75	8.6	4.45
753.1	573.7	55.8	32.9	19.9	70	76	79	84	9.4	4.86
742.1	548.6	55.8	29.7	19.1	76	77	91	94	8.2	4.56
792.7	594.4	53.0	28.2	22.4	69	71	79	89	8.75	4.75
837	635.1	53.6	37.0	24.0	65	73	80	94	9.3	5.11

[d] Double diluting stream inlet connections to membrane packs for this and all subsequent periods of operation.

of 3 months was 93.6%, while for some individual months close on 100% was achieved (Table II).

Electrical short-circuiting was less than 2.5% of the maximum current; the plant was safely operated at voltages of 450 to ground.

The electrical resistance of the units in stage 1 increased by about 100% over a period of 10 to 15 days. This was due almost entirely to accumulation in the diluting compartments of a clay sludge from colloidal clay which was present in the treated raw water in amounts varying from 0.05 to 0.3 p.p.m., with an average of 0.25 p.p.m.

The complete removal of the colloidal clay particles found both in these mine waters and in surface waters over a large area in the region is a considerable water-treatment problem. Whereas residual suspended clay particles totaling 1.0 p.p.m. in a treated water will give domestic water of reasonable clarity, such amounts are unacceptable in the electrodialysis plant. Amounts not exceeding 0.05 p.p.m. are preferred, but this requires exceptionally good water treatment control and the use of a "polishing filter" of the precoat type in the final stage. No polishing filter was used in the FSG plant. To remove the accumulated sludge, the packs had to be scoured with a flush of compressed air and water every 7 to 10 days. The electrical resistance of the units was reduced to the original value in this way.

Membranes and graphite electrodes gave a little longer than the estimated service of 9 and 6 months' continuous use, respectively. A qualification is needed in the case of electrodes, as the plant operated for much of its time at well below the maximum designed current density, because the ohmic resistance of the packs, due to sludge formation and polarization, rose to approximately twice the designed value.

Labor requirements on the FSG plant were normally one operator per shift to check plant operation, plus three semiskilled operators employed for membrane pack assembly and overhaul, and general duties resulting from operating the plant partly on a development basis. On a routine basis two semiskilled operators on day work, instead of three, would be adequate. The plant was large enough to justify a full-time plant superintendent. Varying numbers of Africans were used for cleaning and miscellaneous unskilled duties.

Engineering and instrument maintenance was on a contract basis from the mine services.

For pack assembly and membrane replacement a minimum of two operators on day work was required. The operators were also required for unpacking, washing, trimming, and punching membranes, which were supplied to the plant as plain sheets slightly oversize. They also assisted the plant operator when a press was started up or shut down, and with filter plant and pretreatment plant operation, although this was not essential.

The human element in assembling packs should not be overlooked. This is particularly important in large plants, and could become an increasing problem the greater the number of packs and components in a plant. Thus, although there may be an argument in favor of using more cell pairs each of individually smaller area, instead of fewer units of larger individual membrane area, it must be realized that assembling membrane stacks is extremely monotonous, but nevertheless requires a certain degree of skill and attention to detail.

In the FSG plant, pack overhaul was determined largely by the life of the positive, or anion-selective, membranes. Their life was approximately 10 months, but for calculation purposes 9 months was allowed for. On this basis, approxi-

mately 110 membrane packs had to be opened up and serviced each year. In practice, the number could be slightly larger to allow for possible early failures.

Ideally, a plant of this size is started up in stages, so that replacement will be a continuous process. Membranes in all the 10 packs of a press are generally renewed at the same time. A reserve of 10 assembled packs can be kept in a water tank for immediate installation. If necessary, a single pack in a press can be renewed at any time, although this complicates the maintenance schedule. The reserve press on the plant, which could serve either stage I or stage II, was used when a press was being serviced.

On the basis of servicing 110 packs per year, approximately two packs a week would have to be repacked. Experience in the FSG plant showed the following schedule to be a conservative one:

Schedule[a]	*Replacement of All 10 Packs in Press at One Time, Min.*	*Replacement of Single Pack Only in Press, Min.*
1. Shut down press and drain packs	15	15
2. Remove hose connections and position pack clamps	80	80
3. Remove packs	60	10
4. Reposition new packs	60	10
5. Align packs and close press	45	15
6. Replace hose connections and start up	150	150
	6.8 hours	4.7 hours

[a] Schedules 2 and 6 could be considerably reduced for single-pack replacement if more flexible water-inlet hoses were fitted. The hoses used were rather inflexible and had to be removed before a press was opened.

Pack dismantling, checking of components, and reassembly took approximately 10 hours per pack. This time could be improved, but could not be maintained week after week while still maintaining the required standard of assembly.

The two pack assembly workers would therefore be occupied on day work throughout the year thus:

Presses to be serviced per annum, $8 \times \frac{12}{9}$	11 minimum
Packs to be serviced per annum	110 minimum
Hours per annum for servicing presses (allowing 1 day per press), say 11×8	88 minimum
Hours per annum for servicing packs, 110×10	1100 minimum
	1188 hours
Based on 40-hour week	29.7 weeks

Allowing for contingencies, approximately 32 weeks per annum would be required for press replacement and pack overhaul. The balance of 20 weeks is taken up by unpacking, soaking, trimming, and punching membranes, assisting with pretreatment plant operation, miscellaneous maintenance, statutory holidays, and leave. These other duties are highly desirable to relieve the workers of the monotony of pack assembly and to prevent mistakes that can be caused by it.

It is recommended that in any large plant using multipack presses, facilities be available for hydraulically and electrically testing packs after assembly and before installation in the presses.

Where very large plants are under consideration, the amount of labor required for membrane pack maintenance should be carefully examined. This will depend on membrane life, or other factors requiring packs to be dismantled, such as scale damage or membrane poisoning, the number and size of units employed, and the time required for removing the packs from the units and servicing them.

Integral membrane-spacer-gaskets were being developed by the SACSIR in

collaboration with an industrial firm, but this work, although promising, has been discontinued. Such spacer-gaskets might decrease handling time, but it is doubtful if any real advantage would accrue, as pack assembly workers would, in any case, have to be employed on a full-time basis. Damage to a gasket would also mean rejection of a spacer, and *vice versa.*

Apart from difficulties inherent in the scale-up from pilot plant to prototype, other difficulties arose when transferring from prototype tests on single-pack presses to multiple-pack presses. Thus, while single packs could be easily sealed, considerable difficulty was experienced in satisfactorily sealing the packs of the FSG presses. The friction between the gaskets and the membranes was relatively low, so that if the water pressure in a compartment was too high the gaskets tended to bow out and form a low resistance flow path between the edges of the gasket and spacer. This caused a lower than average water flow rate over the main area of the membrane, aggravating the risk of polarization in diluting compartments. In single-pack tests a small increase in sealing load can rectify leakage, whereas in large multiple-pack presses a considerable amount of friction is encountered when the packs move as they are squeezed up, so that a much larger force has to be applied to seal the unit.

From prototype tests it seemed that a net sealing load on the gaskets of as low as 30 p.s.i. would be adequate. In practice, the sealing load that had to be applied was 120 p.s.i., calculated on gasket area. The sealing load affects not only the amount of external leakage, but also the degree of internal leakage. If the pressure drop across a compartment (measured at the inlet and outlet manifolds) rises to 20 p.s.i., the minimum sealing load required on a single-pack assembly, calculated on gasket area, is 80 p.s.i. This is sufficient to ensure no external leakage, and, with adequate support for the membranes at the gasket slots, internal leakage can be kept down to approximately 0.2% of full flow.

Plant Operating Data

The operating history of the plant is given in Table II. At the start of the period shown the units on line had already operated for several months during preliminary testing.

From the beginning of February 1960 to the end of April 1960, membranes were gradually replaced in the units that had been on line for 9 months and more; the resulting progressive reduction in energy consumption per 1000 p.p.m. TDS removed is seen in the last column. [These values are given for comparison purposes, as the degree of desalting varied from time to time. In assessing the data presented it is important to realize that, unlike bore hole waters, there were wide variations in raw water salinity (depending on from which shafts water was being pumped) and from dilution by surface waters entering the holding dams during storms. Input concentration varied from 2780 p.p.m. maximum to 1954 p.p.m. minimum mean daily values.]

The production rate was below design because of intercompartmental leakage, and the desalting below design because of high cell electrical resistance due to excessive polarization. The current shown is the maximum that could be supplied at the maximum voltages obtainable from the rectifiers.

Capital Costs

Estimated and actual capital costs are given in Table III.

Table III. Capital Costs for Free State Geduld Electrodialysis Plant

	Estimate (1957), $	*Actual[a] (1959), %*
Pretreatment plant		
Plant items, pumps, lime and acid-dosing equipment, sand filters, etc.	73,500[b]	40,950[c]
Buildings	65,700	19,800
Piping, valves, and fittings		29,300[c]
Instrumentation		60,050[d]
Erection and site preparation	6,380	
Contingencies and overheads	7,270	
Subtotal	152,850	150,100
Electrodialysis plant		
Electrodialysis units, excluding piping and instrumentation, but including first charge of membranes and electrodes	179,000	282,000
Other items, H.T. and L.T. transformers, switch gear, rectifiers, pumps, storage reservoirs, etc.	276,400	191,000
Building, including laboratory and membrane pack assembly area (store and workshop under filter plant)	102,800	39,400
Piping, valves, and fittings	35,650	69,700[c]
Instrumentation	19,600	61,900[c]
Erection and site preparation	67,500	3,500[d]
Contingencies, overheads, and royalties	73,450	
Subtotal	754,400	647,500
Total	907,250	797,600

Prices converted to U. S. dollars at rate of R1.00 = $1.40.

[a] Values rounded off to nearest $50.
[b] Including piping, instrumentation, etc.
[c] Including erection.
[d] Excluding erection.

Production Costs

Table IV gives actual and estimated production costs for a number of conditions. Costs cannot be directly compared, as they are affected by plant output and the degree of desalting. In this particular case they can, however, be compared more nearly if calculated per 1000 gallons and per 1000 p.p.m. TDS removed.

The costs in column 2 are based on operation for the month of April 1960, in so far as output, degree of desalting, and chemical and electricity consumption are concerned. The other costs are based on average as accurately as could be ascertained. Averaging over a 15-year life, repairs and maintenance might be slightly higher. A membrane life of 9 months has been proved. No estimate of the ultimate life of the gaskets and spacers was possible. Experience indicated that they could be expected to last for many years in service. The allowances made in the estimates should be achieved in routine operation.

Column 3 of Table IV is extrapolated from the actual operating data used for column 2, for the plant operating with the fourth set of presses put in line, but still operating below design for the reasons given above.

Column 4 represents costs based on plant modifications enabling polarization and intercompartmental leakage to be eliminated, and full capacity and desalting to be achieved. The modifications would have involved additional work to the extent of $142,900. This cost has been added to the original costs in calculating amortization. No allowance has been made for credit for redundant equipment, or for the fact that these modifications if originally incorporated would actually have reduced the capital costs. Replacement and service costs are based on conservative values, as shown in the notes to the table. A mean coulomb efficiency of 75% throughout the plant has been allowed for, with membranes discarded

Table IV. Production Costs for Desalted Water from Free State Geduld Electrodialysis Plant

	Estimate, 1957	*F.S.G. Plant Operating at 71.4% Capacity per Unit, 1960*		*Modified for 100% Capacity, Calcd., 1961*
		Actual	*Calcd.*	
Units operating per stage	4	3	4	4
Desalted water, U.S.g.p.h.	120,000	64,260	85,500	120,000
Raw water concn., p.p.m. TDS	3,100	2,843	2,843	2,900[a]
Desalted water, p.p.m. TDS	525	813	813	525
A. Pretreatment	Costs in U. S. Cents/1,000 U. S. Gal. Produced[b]			
Chemicals	0.45	1.35	1.00	0.80
Electricity	0.13[c]		Included in B	
Labor			Included in B	
Repairs and maintenance	0.41		Included in B	
Interest and redemption[d]	1.54	2.74	2.06	1.47
Subtotal	2.53	...	...	...
B. Electrodialysis				
Replacements				
Membranes	3.66[e]	10.22[f]	10.22[f,g]	6.85[f,h]
Electrodes	0.29[i]	0.20[j]	0.20[j]	0.14[j]
Miscellaneous[k]	1.41	2.63	1.97	1.41
Electricity				
Electrodialysis[l]	5.89[m]	4.48[n]	4.48[n]	5.25[o]
Pumping, etc.[p]	0.49	1.70[q]	1.28[q]	1.18[q]
Labor and administration	4.38	5.00[q]	3.76[q]	3.22[q]
Repairs and maintenance	1.19	1.91[q,r]	1.43[q,r]	1.02[q,r]
Royalties	0.51	0.56	0.42	0.30
Interest and redemption[d]	7.31	11.86	8.91	8.04
Subtotal	25.13	...	...	...
Total cost				
Per 1000 U. S. gal. produced	27.7	42.65	35.73	29.7
Per 1000 U. S. gal. Per 1000 p.p.m. TDS removed	10.7	21.0	17.6	11.9
% TDS removed	83.3	71.4	71.4	82.1

[a] 2900 TDS was absolute maximum value expected from any mines serving plant at this date.

[b] Costs converted to U. S. currency at R1.00 (S.A) ± $1.40 (U. S.).

[c] 0.58 cent/kw.-hr.

[d] Redemption over 15 years; interest on capital 6.5% per annum payable quarterly = 10.3% per annum. For capital costs see Table III.

[e] SACSIR parchment membranes at $1.75 each delivered; 9-month life; 21,330 membranes per annum.

[f] $3.60 each delivered, including royalty; 9-month life; 16,000 membranes per annum.

[g] 21,330 membranes per annum.

[h] 8-month life and 16,000 membranes per annum.

[i] Graphite, 3-month life.

[j] Graphite, 6-month life.

[k] Including sundry spacer and gasket replacements, estimated.

[l] A.c. energy.

[m] A.c. energy at 0.58 cent/kw.-hr., 90% a.c./d.c. rectification efficiency.

[n] A.c. energy at 0.52 cent/kw.-hr., 90% a.c./d.c. rectification efficiency; 8.60 kw-hr. a.c. per 1000 U. S. gallons produced.

[o] A.c. energy at 0.52 cent/kw.-hr., 92% average a.c./d.c. rectification efficiency at higher loads possible. 10.1 kw-hr. a.c. per 1000 U. S. gallons produced at mean annual conditions of water temperature, membrane properties, and other plant operating conditions.

[p] A.c. energy at same prices as for electrodialysis; includes lighting and other miscellaneous services.

[q] Includes pretreatment plant.

[r] Supervisor R240.00 per month basic salary; chemist R167.00 per month; shift operator R3.97 per shift; packer R3.64 per shift; African laborer R20.00 per month, net.

when giving 65% instead of 60% coulomb efficiency, thus reducing membrane life from 9 to 8 months. This is achieved by a planned replacement of membranes in

Table V. Estimated Costs for Plant Based on OSW Standardized Estimating Procedure (3)

A. Capital costs[a]

	$
Special equipment (installed)	254,000
Standard equipment (installed)	84,000
Total PIE[b] (installed)	338,000
Erection and assembly	101,100
Instruments	13,500
Total essential plant costs	452,600
Raw water supply	18,000
Extra facilities	137,400
Product water storage	28,820
Service facilities and buildings	6,710
	643,530
Contingencies	64,200
	707,730
Engineering	72,400
Interest on investment during construction	31,200[c]
Site	8,640[c]
Total plant investment	819,970
Working capital	65,100
Total capital costs	885,070
Cost per U. S. gallon per day of production	0.307

B. Operating costs (Basis. 1 stream day and 330 operating days per annum)

	Cost per Stream Day, $	
Essential operating costs	I[d]	II[e]
Electric power	224.50	214.00
Chemicals	12.88	23.01
Membranes	105.80	197.20
Electrodes	8.40	4.04
Supplies and maintenance	12.31	13.70
Operating labor	224.00	224.00
Maintenance labor	12.31	35.65
Payroll extras	35.22[c]	38.94[c]
Total essential operating costs	635.42	750.54
Other operating costs		
General overhead and administration	81.50	89.58
Amortization	183.30	205.00
Taxes and insurance	49.20[c]	54.90[c]
Interest on working capital	7.00[c]	7.98[c]
Total operating costs for one stream day	956.42	1108.00
Cost per 1000 U. S. gallons of product	0.332	0.384
Approx. cost per 1000 U. S. gallons of product per 1000 p.p.m. TDS removed	0.133	0.160

[a] For plant as designed and erected. Actual prices used where available.
[b] Principal items of equipment.
[c] Not included in SACSIR estimates.
[d] Based on 1957 estimate values.
[e] Based on conditions applying to Table IV, col. 4.

the presses. The values allowed for coulomb efficiency are probably conservative, as efficiencies of membranes from the plant after 10 months' use still averaged 70% when used in a small laboratory electrodialysis cell.

The plant modification for costs in column 4 includes equipping each press with its own diluting and concentrating stream pumps, allowing for equal flow rates with 4.1 to 1 concentrating stream recycle, compartment flow rates of 40 U. S.

gallons per hour instead of 30, and 75 compartment pairs per pack instead of 100. Other conditions remain as before.

No allowance is made in the costs for taxation, cost of site, insurance, etc., as circumstances vary so greatly.

Estimated capital and operating costs, based on the Office of Saline Water standard procedure for cost estimating (3), are given in Table V. Agreement with Tables III and IV is good.

Estimates for a plant operating under conditions applying to column 4 of Table IV, but with very much simpler piping and control arrangements, would be possible only if plant operational data over a much greater time had been available. It would be premature to present an estimate at this stage, particularly as the question of plate fabrication has not been satisfactorily resolved.

Reduced Plant Capacity

As will be seen from Table II, the FSG plant did not operate much above about 55% of design output for any length of time, 71% being the highest value obtained and this only at the expense of some reduction in the degree of desalting.

The reasons for this reduced output are important from a design point of view.

1. The factor preventing the designed output from being obtained was the onset of polarizing conditions in the diluting compartments at average nominal linear liquid velocities across the compartments higher than expected from the pilot plant and prototype work.

The development of polarizing conditions was aggravated by the use of unequal flow rates in the diluting and concentrating compartments. This caused opening of the diluting compartments in spite of out-of-balance pressures being minimized by the application of a back-pressure on the concentrating compartments. Linear flow velocity in the diluting compartments was thus lower than that calculated for the compartment of designed thickness. A change in the intermembrane spacer corrugation angle used also contributed to a higher critical polarization velocity.

The sensitiveness of compartments to change in thickness from out-of-balance hydraulic pressures in adjacent compartments was much greater with the large areas of the FSG plant than with the pilot plant, where the membrane pack assembly was relatively rigid.

The polarization difficulties were overcome by using symmetrical flow systems and flow rates in both diluting and concentrating streams.

2. A contributory cause was the considerable leakage of the diluting stream into the concentrating stream, referred to as "intercompartmental leakage." This leakage was eventually held to 0.3% of the diluting stream flow, but before modifications were introduced (aimed at supporting the membrane at the feed slots in the gaskets), values were at times as high as 25%.

3. Another difficulty was a mechanical one regarding materials of construction for the pack, electrode, and intermediate plates, which were all of the same general design, differing only in details of liquid ports and conduits, etc. In particular, leakage from one stream to the other occurred in many of the timber plates because of opening up of the glued joints; this permitted interconnection from a main diluting stream conduit to a main concentrating stream conduit.

4. Some trouble was also experienced with the welds of 8-inch diameter high-density polyethylene pipe, which was later replaced by rubber-lined mild steel, or acrylonitrile-butadiene copolymers. The latter was used for all the smaller diameter piping, but was not available in the larger sizes (8-inch diameter and above), when the plant was being built.

Most of these difficulties occurred in transferring from pilot scale to full plant scale with only limited prototype work. The reasons for this have been stated above.

Electrodialysis Press Components and Effect on Operation

Intermediate and Electrode Pack Plates. The construction of reliable intermediate plates and electrode plates proved difficult. The general design of the plates is shown in Figure 4. Membrane support grids of design other than the form shown were also used.

The prototype plates were made from glass fiber–reinforced polyester resin and those on the pilot plant from glass fiber–reinforced epoxy resin. Although some distortion, surface rippling, and blow holes occurred on the prototype plates, the manufacturers were confident that the problems could be overcome and that rejects would be few. Just before the order for plates was due to be placed, the firm discontinued work in this field and the whole question of materials was thrown back to the beginning. It is only recently that satisfactory molding or casting techniques have been developed which might enable glass fiber–reinforced resin sections of the size required on the FSG plant to be reliably made. Even so, sections of the size and thickness required have not yet been made.

When the plant was being designed, typical alternative materials were rigid poly(vinyl chloride), rubber-lined steel, plastic-coated alloys, and timber. Rigid PVC was excluded on a cost basis; as it was available only in sections up to 1 inch thick, lamination would have been required and labor costs would have been considerable. Even so, as events have turned out, this might have ultimately been the cheaper solution. Rubber-lined steel was eliminated because of weight, extra size, and expense, and plastic-coated materials because of possible damage to thin plastic coatings and the, then, limited number of reliable coating techniques available in South Africa.

Work in Pretoria had shown that hardwoods like African kiaat and phenol-formaldehyde resin–impregnated European beech, glued with phenol-formaldehyde-resorcinol glues, could be expected to give reasonable service, and that weight and prices were reasonable.

The plant was equipped mainly with beech plates impregnated with phenol-formaldehyde and glued with a phenol-formaldehyde-resorcinol adhesive. Experience showed that unless extra special care is taken in selecting, curing, impregnating, and working the timber, reliable plates cannot be produced. Laminated beechwood plates made from material extensively used for electrical insulation in submerged conditions have shown no better results. Extensive warping and splitting of the material at the joints between laminates occurred and caused considerable difficulty in the plant. A few electrode plates were made of Perspex (Lucite). These suffered from incipient cracking, and, in any case, were expensive. They were used only to fill a gap before the main order for timber plates was completed.

Although kiaat plates gave good service over a long period of testing on the unit at Pretoria and were repeatedly dried out, timber plates cannot be recommended for mass production and plant use.

Experimental full-size plates of glass fiber–reinforced polyester resin, and also of a PVC or polyethylene-coated aluminum alloy have been made and tested. The plastic coating of the alloy plates was reparable on site. It was electrically tested for pinholes and was tested for abrasion, tear resistance, and resistance to stripping. The glass fiber–reinforced polyester plates needed considerable machining before being put into service. The plastic-coated aluminum alloy plates are the cheapest, but there is always danger of undetected damage of the lining.

Comparative costs for quantity production are approximately in the ratio of 1 to 4 for the aluminum alloy and the polyester plates, respectively.

In designing a large plant a balance must be struck among membrane, and hence plate, dimensions, available materials of construction, and their cost and workability. If fabrication costs are not important, rigid PVC is suitable. On the thick sections now available considerable machining is required. Glass fiber–reinforced resin plates are limited to sizes determined by production techniques. Plastic-coated cast metal plates are relatively cheap and lend themselves to large sizes, but suffer the disadvantage of all coated materials, that the coating may be damaged and the metal may then corrode. Timber does not seem a satisfactory material, even if impregnated with modern resins and bonded with modern waterproof marine glues.

From Figure 4 it will be seen that in the intermediate plates there were grids to support the membranes and yet permit electrical continuity. In starting or stopping the plant there was always the chance that the intermediate plate rinse stream might be started up after, or turned off before, the streams through the packs. If this happened, pressures up to 20 p.s.i., depending on outlet piping back pressures, could be exerted on the grids by expansion of the membrane pack. This had, on occasions, happened and been sufficient to break the grids and to damage the end membranes of a pack.

In the earlier plates breakage of the side stiles occurred due to the pressure of the rinse stream in the plates. Later modifications included insulated tie rods. Grids integral with the plate, which were used to strengthen the side frames of timber or Lucite plate, were also used. In this latter case, care had to be taken when building the packs that the tolerances of the components were such that the finished pack was substantially flat, or only slightly bowed outward. Excessive bulging could lead to breakage of the grids when the press was tightened up.

Where freely supported grids were fitted, a type made from strips of corrugated glass fiber PVC sheets placed end-on and solvent-welded to each other to form a honeycomb, was promising. It had considerable strength against deformation at right angles to its length or breadth.

Gaskets and Membrane Spacers. In considering tolerances of components, reference must be made to the gaskets and spacer material used in the FSG plant.

In all the early work it was considered advisable to use a gasket that was fairly rigid, would not suffer cold flow, would seal against the membranes at a reasonably low sealing pressure, and could be re-used repeatedly. Klingerit, a high quality steam jointing, fulfilled these requirements and also had a high degree of dimensional uniformity in thickness.

The same degree of uniformity was not achieved, however, with the corrugated perforated spacer material, the manufacturer averaging not better than ±0.004 inch on the stipulated thickness of 0.036 inch. Tolerances were fixed at ±0.002 inch.

This led to difficulty in assembling packs—the use of too much oversize spacer made it difficult to close the pack, while the use of too much undersize spacer led to inadequate support of the membranes. It is now considered that rather than trying to match the spacer thickness to the gasket, the reverse is to be preferred, as with a somewhat resilient gasket variations in spacer thickness can be accommodated and a firmer membrane assembly be obtained.

One reason for using more or less rigid gaskets of a uniform thickness was the desire to obtain a uniform mass flow rate in all the compartments of one type, particularly since the designed flow rate in the diluting compartments was fixed

rather closely to the critical polarization value. This feature, and the use of narrow compartments, were the result of having to design for optimum conditions.

Critical Polarization Velocities, Flow Distribution, and Pack Electrical Resistance. The critical polarization velocities allowed for were based on results from average packs in the pilot plant and some confirmatory testing on the prototype. It was considered that this would allow for normal flow variations from pack to pack and from compartment to compartment.

A method used in this laboratory to obtain a picture of the flow distribution in a pack (*11*) is based on the increase in resistance occurring as polarizing layers build up, and is a function of liquid velocity. In practice, platinum wires are inserted through the gaskets into the compartments and the voltage drop between a number of compartments is measured. The method can be extended to determine conditions in any portion of a compartment. Although actual velocities cannot easily be calculated from the data obtained, a general picture of flow distribution in a pack is given. Absolute flow rates and velocities relevant to the observed voltage drop can be obtained from studies on a single compartment, or a single cell pair. Figure 6 shows typical data so obtained for standard FSG-type packs. It shows also how the pack electrical resistance, as a whole, decreases as the flow rate is increased, the general flow distribution pattern remaining. Equality of distribution is dependent not only on uniformity of the components and accuracy in forming the conduits, but also on the manner in which the streams are introduced and taken from the packs—e.g., at one or both sides of a plate, or at one or both plates, and variations of this (*10*, *11*).

Critical polarization velocities were found to be some 25% higher than expected in the FSG plant, resulting in a pack resistance from 1.8 to 2.3 times higher than designed for at standard conditions of flow, concentration, and temperature (25° C.). This was eventually traced to the configuration of the spacer material used.

In the pilot plant maximum turbulence was desired in the diluting compartments, in which the corrugations of the spacer were placed at right angles to the direction of liquid flow (in the concentrating compartments they were placed parallel to the direction of flow). In the FSG plant the spacer material corrugations were arranged to be symmetrical in the compartments, so that identical conditions would exist when polarity was reversed. It was not possible to place the corrugations at right angles to the direction of liquid flow in every compartment, as the membranes might in time have deformed into the corrugations.

Preliminary tests with the corrugations set at 85° resulted in such a high back-pressure in the diluting stream relative to that in the concentrating stream, where the flow was one quarter of the diluting stream, that the membranes deformed into the grooves of the spacers. Corrugations were therefore set at 15° to the direction of flow (see Figure 4). This change in angle raised the critical polarization velocity to the extent mentioned above, but the effect was not observed on the prototype tests, possibly because, although the same angle was used, the material lacked uniformity.

For a given set of conditions the average ohmic resistance of a pack, expressed per cell pair, increased as the number of compartments increased, indicating possibly that with packs of large numbers of membranes there is considerably greater chance that one or more compartments will have a liquid velocity below the critical. This may, in part, be due to the inherent flexibility of large packs with large numbers of membranes.

These observations led to the necessity of increasing the flow rate per diluting

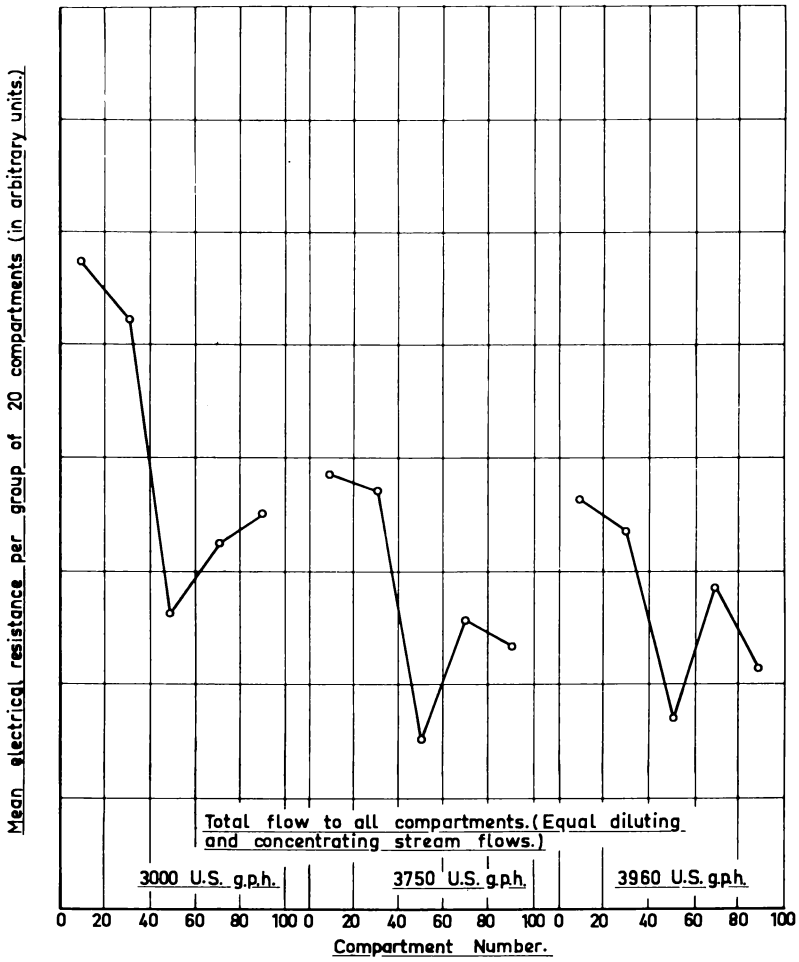

Figure 6. Distribution of electrical resistance across 100-compartment pack, and effect of over-all flow rate

compartment in the packs of the FSG plant from 25 Imperial gallons per hour (30 U. S. gallons per hour) to 33 Imperial gallons per hour (40 U. S. gallons per hour).

Intercompartmental Leakage. Intercompartmental leakage occurred by leakage across membranes behind the feed and outlet slots in the gaskets (see Figure 5). The plant was designed for a 4 to 1 ratio of flow rates across diluting and concentrating compartments, approximately equal pressures in the compartments being achieved by throttling the concentrating stream outlet to achieve a back-pressure at the pack inlet equal to that at the diluting stream inlet. Absolute equality of pressure is not possible, as is seen in Figure 7. This represents the approximate relative pressure conditions at designed flow rates. The slot feeding arrangement shown was chosen partly to balance pressure losses in adjacent compartments, and partly because the use of reversed polarity for scale control meant that the diluting compartments were used as concentrating compartments when polarity was reversed.

There is some doubt if the reversed polarity procedure on this plant was

justified. Normally, reversal was done daily, but scaling was not particularly serious, and the troublesome barium-strontium sulfate scale obtained from the mine water used in the pilot work was absent. Acid dosing of the brine to pH 4.5 to 5.0 controlled scale formation from calcium and magnesium carbonates in the water. Elimination of polarity reversal would obviate the switching and valve change-over arrangements, with the necessity for sizing all valves and piping for the diluting stream flow rates. This last point falls away, however, if the principle of equal flow rates with brine recycle is adopted.

The possibility of "slot leakage" was considered very carefully and investigated on the prototype unit. The dimensions of the slots used in FSG plant were the result of extended laboratory tests to check that the membrane would not collapse into the slot. Prolonged operation proved, however, that over a period of time the negative membranes deformed into the slots; the positive membranes also did this, but to a much lesser extent. The flow of liquid across the surface of the gasket at the leakage point led to softening of the gasket at that point. Once leakage started, it got rapidly worse.

Leakage seemed to be associated mostly with the negative membranes, which had a higher activity and degree of swelling. Whether or not this point is relevant has not been determined. The positive membranes showed a marked tendency to stick to the gaskets, and this sealing tendency may be of importance in preventing leakage.

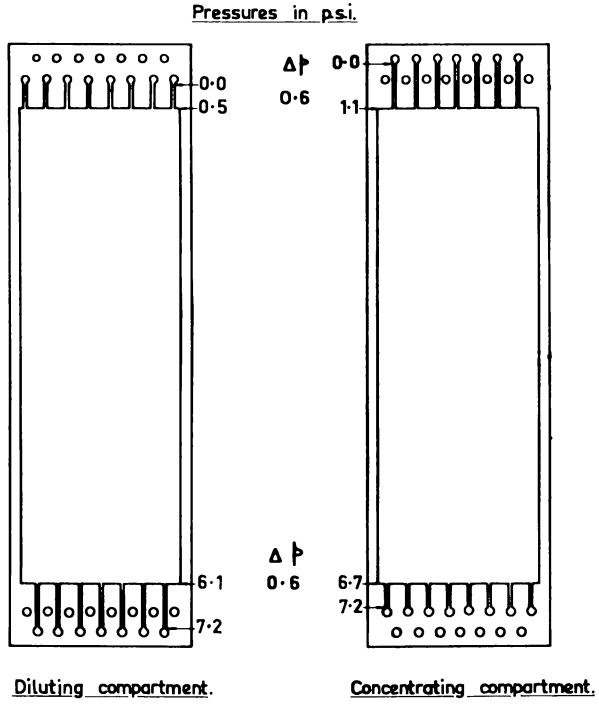

Figure 7. Pressure drop across and pressure differential between diluting and concentrating compartments for 30 U. S. gallons per hour per compartment

Absolute pressures in compartments are higher because of hydraulic resistance of outlet piping system

Even when only small pressure differences exist between adjacent compartments, considerable leakage can occur in packs of 100 membranes and over. Thus, with the slot feeding system as designed, a 25% difference of flow between adjacent compartments was sufficient to cause a difference of pressure at the inlet to the pack of 4 p.s.i., giving leakage of the order to 10% of the standard diluting stream flow rate. With a 4 to 1 ratio of diluting stream to concentrating stream and balanced outlet pressures it was not possible to achieve less than a 0.6-p.s.i. pressure difference at the inlet, which, with membranes that had been in use for some time, allowed an uneconomic degree of leakage.

By modifying the slots so that the membrane is supported (Figure 8), leakage at substantially equal flow rates can be held at less than 0.3% of the diluting stream flow rate.

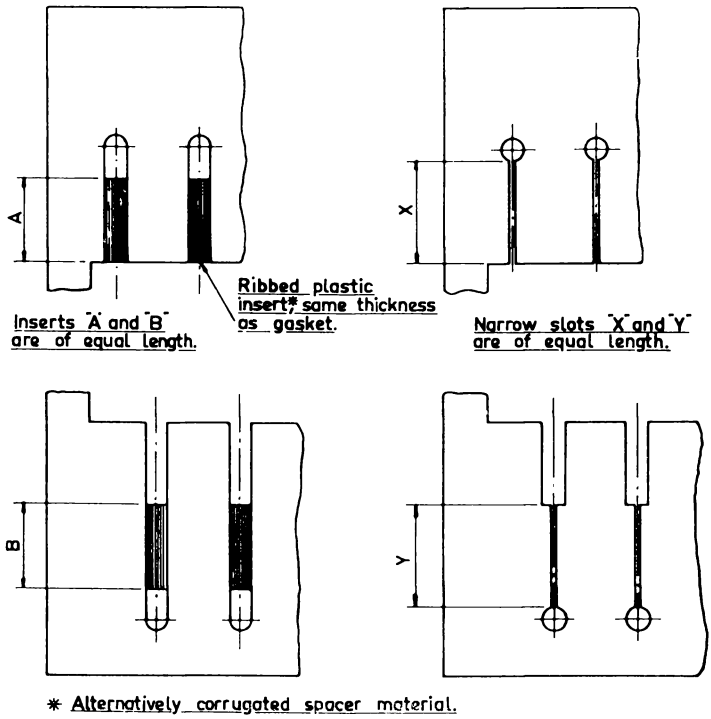

Figure 8. Alternative gasket slot feeding arrangement for equalizing pressure drop and supporting membrane

Plant Capacity

To bring the plant to full capacity would have required the elimination of polarizing conditions and of intercompartmental leakage. The former could have been achieved by increasing the diluting stream flow to 133.33% of design and the latter by using equal diluting and concentrating stream flow rates and adequate membrane support in the feed slots.

On increasing the diluting stream flow rate to 40 U. S. gallons per hour per compartment, the average pack electrical resistance fell to slightly below the designed values, thus enabling full designed current densities to be used. The

degree of desalting per pass was, however, reduced in proportion to the increase in mass flow rate. Recalculation of the plant design for the new flow conditions showed that the originally designed stage conditions of current density should be retained.

The required desalting could have been achieved at all times by allowing for a minimum average coulomb efficiency of 65% instead of 60%.

This value would have been possible instead of the 75% average coulomb efficiency mentioned above and used for column 4 of Table IV, because the salinity of the mine water was still decreasing and over the last 4 months of plant operation had approached 2700 p.p.m. TDS.

The total membrane area in the plant would be reduced to 75% of the original. Membrane life would be reduced from 300 days at a 60% minimum coulomb efficiency to 270 days at 65% efficiency. This is probably conservative, because plant membrane efficiencies as checked on small laboratory cells averaged 70% after 10 months' use. There is, thus, a net saving of approximately 17% on the annual requirement of membranes.

An additional safety margin is that the rectifiers were designed for maximum voltages at a minimum water temperature of 15° C. In fact, on only one day had the water temperature fallen to 17° C. The mean monthly minimum water temperature was 19.1° C. For most of the year temperatures ranged between 24° and 28° C. The temperature rise of the water in the plant did not exceed 2° C.

The use of equal flow rates would not have been a large complication, because most of the concentrating stream system was sized for the maximum flow rate of the diluting stream, to allow for reversed polarity.

The only remaining factor requiring extensive testing in the plant would have been the reliability of the revised scheme for maintaining intercompartmental leakage at or below 0.2% of the diluting stream flow.

External leakage could be kept well below 0.01% with plastic-covered plates or timber plates in good condition.

The proposed revised plant conditions are shown in Table VI.

Table VI. Proposed Revised Operating Conditions for Conditions Stated

Inlet water, U. S. gal./hr.	150,000 at 2700 p.p.m. TDS max.	
Desalted water, U. S. gal./hr.	120,000 at 525 p.p.m. TDS	
Concentrated water, U. S. gal./hr.	29,400 at 15,800 p.p.m. TDS	
No. of operating presses	8 (stage I, 4; stage II, 4)	
No. of packs per press	10	
No. of membranes per pack	150	
	Stage I	*Stage II*
Current density (max.), ma./sq. cm.	16	7
Desalted water, p.p.m. TDS	1,190	520
Concentrated water, p.p.p. in TDS	14,400	6360
Concentrated water, p.p.m. out TDS	15,800	7100
Flow rate per compartment, U. S. gal./hr.		
Diluting stream	40	40
Concentrating stream	40	40
Recycle on concentrating stream	4.1:1	

Membranes

Average values of membranes used are given in Table VII. The values for discarded membranes represent those for the original installed membranes, which were of appreciably lower quality than the ones later in use.

Table VII. Average Membrane Properties

	New		*As Discarded*[a]	
	Cationic	*Anionic*	*Cationic*	*Anionic*
Free electrolyte diffusion at 30° C. between distilled water and 15,000 p.p.m. NaCl, meq./sq. cm./sec.	0.55	0.95	2.5	4.6
Conductance, mmho/sq. cm. at 30° C.	79	176	51	13
Transport number, Na^+ in 0.3*N* NaCl at 25° C.	0.940	0.034	0.863	0.308

[a] Approximately 10-month equivalent continuous use.

Specifications required the following minimum properties (units as in Table VII):

Free electrolyte diffusion	Not more than 1.3
Conductance	Not less than 1.3
Transport number, t_+	<0.93 and >0.03
Mullen burst strength	Not less than 25 p.s.i.

Conclusions

Experience from 18 months' actual operation showed:

A large-scale sheet flow type of electrodialysis plant can be operated satisfactorily and reliably when large membranes and large presses are used.

Equal flow rates and balanced pressures in diluting and concentrating compartments are necessary when the slotted gasket distribution system is used.

If broad compartments are to be used, careful consideration must be given to the means of obtaining even flow distribution across a compartment and freedom from intercompartmental leakage.

Gaskets should be soft enough to permit their thickness to be adjusted to that of the intermembrane spacer.

In considering the size and number of units to be used, attention should be paid to the labor requirements for membrane replacement and pack maintenance.

The below-capacity performance of the FSG plant was due to operation too near the critical polarization velocity, excessive intercompartmental leakage, and inability to obtain components of the required standard in the limited time available for their development and manufacture.

Acknowledgment

The author is indebted to the South African Council for Scientific and Industrial Research, the Anglo American Corp. of South Africa, Ltd., the Anglo Transvaal Consolidated Investment Co., Ltd., Rand Mines, Ltd., Johannesburg Consolidated Investment Co., Ltd., New Consolidated Gold Fields, and Union Corp. for permission to publish this paper. Thanks are due to J. R. Wilson, who was responsible for the design of the FSG electrodialysis plant and for the commissioning program. Much of the subject matter has been drawn from his thesis and other unpublished work. Thanks are also due to the manager of the Free State Geduld Gold Mining Co., the staff of the Free State Geduld Water Demineralisation Plant, the staff of the Consulting Civil Engineering and Consulting Metallurgists Departments of the Anglo American Corp. of South Africa, Ltd., and the members of the Process Development Division of the National Chemical Research Laboratory.

Literature Cited

(1) Moyers, W. H., *Optima* (Anglo American Corp., Johannesburg) (September 1957).
(2) Moyers, W. H., Volckman, O. B., *Trans. So. African Inst. Civil Engrs.* **7**, 309–24 (1957).
(3) Office of Saline Water, "Standardized Procedure for Estimating Costs of Saline Water Conversion," March 1956.
(4) Rapson, W. S., *Optima* (June 1955).
(5) Volckman, O. B., *Brit. Chem. Eng.* **2**, 146 (1957).
(6) Volckman, O. B., "Electrodialysis Research and Development in South Africa," CCTA/CSA Specialist Conference on the Treatment of Water, Pretoria, Republic of South Africa, September 1960.
(7) Volckman, O. B., Moyers, W. H., Natl. Acad. Sci.–Natl. Research Council, Publ. **568**, 283–315 (1958).
(8) Wilson, J. R., CSIR Contract, Rept. **F. 31** (February 1960).
(9) Wilson, J. R., ed., "Demineralization by Electrodialysis," Butterworths, London, 1960.
(10) Wilson, J. R., "Depolarisation in Electrodialytic Demineralisation with Particular Reference to the 100,000 gph Electrodialysis Plant Erected at the Free State Geduld Mine, Welkom, Republic of South Africa," *Trans, Inst. Chem. Eng.* (*London*) **41**, 3 (February 1963).
(11) Wilson, J. R., "Design and Commissioning of the World's First Commercial Scale Electrodialysis Plant," SACSIR Contract Rept. **F. 31/1/60** (July 1960) and Supplement of March 1961, SACSIR Contract Rept. **CF. 31/1961.**

RECEIVED May 28, 1962.

11

Design of Medium-to-Large Electrodialytic Water Demineralizers

Several Hundred Thousand to Several Million Gallons per Day

WILLIAM E. KATZ
Ionics, Inc., Cambridge, Mass.

New data on a Mark III electrodialysis stack containing 550 18 × 40 inch membranes indicate capacity of 125,000 to 250,000 gallons per day with pressure drop of 12 to 40 p.s.i. A 650,000-gallon-per-day municipal water demineralizer is now in operation at Buckeye, Ariz., on a 2200-p.p.m. water, financed by a $305,000 revenue bond issue. Total costs range from 33 cents per 1000 gallons at 98% load factor to 51 cents at estimated actual annual load factor of 48%. Since water demand is four times as great in summer as in winter, the plant was designed with dual water pumps each taking half the load, and three two-stage "lines" of Mark III stacks, along with special instrumentation to allow operation without full-time attendance.

Electrodialytic water demineralizers, in which a direct electric current moves ions out of water through synthetic ion exchange membranes, have been under intensive development for more than a decade. The first public demonstration of a laboratory-scale "electrodialysis" unit operating on a saline water was held in Boston just over ten years ago (*6*).

The number and capacity of commercial electrodialysis plants increased slowly in the first years following their introduction, but installed plus committed capacity of demineralizers built by this company has increased at an average rate of over 60% per year in the past five years.

As of September 30, 1962, there are 24 commercial—i.e., nonexperimental—Ionics electrodialytic water demineralizers in operation in the United States, 44 overseas (mostly in North Africa and the Middle East), and 14 on order or under construction. These 82 units with an aggregate capacity of 2,300,000 gallons per day represent approximately 90% of the world's commercial installations almost 90% of the world's commercial capacity (*4*).

Until very recently, commercial electrodialysis plants were of relatively small capacity, and the largest was less than 100,000 gallons per day. In the last year, however, commercial units with capacities of several hundred thousand to several

million gallons per day have been constructed. One unit of 650,000-gallon-per-day capacity is now in operation at the town of Buckeye, Ariz. A 240,000-gallon unit for the Government of Kuwait is under construction.

An electrodialysis plant of 250,000-gallon capacity has been built for the U. S. Department of the Interior's Office of Saline Water at Webster, S. D., but actual operating data on this plant have not yet been reported.

The use of electrodialytic water demineralizers with daily capacity of several hundred thousand to several million gallons has been stimulated by the availability of a field-tested basic membrane stack of suitable size to form a logical building block for such plants. This stack, the Mack III stack, was first described two years ago (5). Since that time, field tests at Oxnard, Calif., have been completed, improvements have been made in stack production and characteristics, and commercial plants are now being designed. In this paper, we describe briefly the Oxnard field tests, present and discuss the revised characteristics of the Mark III stack, and describe certain aspects of the design and economics of the Buckeye unit as a typical example of a municipal electrodialysis plant.

Buckeye Electrodialysis Project

The nation's first saline water conversion plant to treat an entire municipal supply, built for the town of Buckeye, Ariz., went into operation early in September 1962. It has the capability to reduce water of 2200 p.p.m. total dissolved solids to 500 p.p.m., at a rate of 650,000 gallons per day. The plant was financed by a $305,000 issue of 25-year, $4^1/_2$% water revenue bonds sold at competitive bidding through normal municipal bond channels. No federal or state funds were utilized in the financing of this plant.

The town of Buckeye, Ariz., is a thriving agricultural community of 2500 people located on U. S. Highway 80 about 35 miles west of Phoenix. The town water supply is municipally owned and operated, with about 640 customers. Abundant water is derived from deep wells perforating various strata to 500 feet. The quality of the water is poor. Carefully drilled new wells have had total solids as low as 900 p.p.m., but on continued pumping over a period ranging from several months to several years, total solids have risen to at least 2000 and chlorides to at least 1000 p.p.m. Typical chemical analysis of the raw and treated water is shown in Table I. The poor quality of water leads to widespread use of hauled or bottled water for drinking, use of home softeners, softening agents, or waste of soap, and accelerated corrosion of plumbing, water-using appliances, and automobile radiators. In Buckeye, as in the other 1000 towns and cities of the U. S. and Canada which have highly mineralized municipal water supplies, the customer pays twice for his water. He pays the water department for the highly mineralized product and then he pays the plumber, the repairman, the softener man, the bottled water man, and others to avoid, to supplement, or to repair the ravages which the water caused. In Buckeye, where the average water bill was $5 to $6 per month, the additional "hidden" water expenses were estimated at $10 or more per month.

The advantages of "good" water were demonstrated to the citizens of Buckeye starting in May of 1961 through a public demonstration of a small demineralizer of 6000-gallon daily capacity. The effects of treated and untreated water were shown in dishwashers, home laundries, evaporative coolers, and drinking fountains. In an election in September 1961, 94% of the qualified voters of Buckeye turned out to approve a $305,000 bond issue and substantial water rate rise to demineralize their entire city supply.

Table I. Raw and Treated Water Analysis

	Raw Water Well No. 8		*Treated Water[b] Demonstration Plant*	*% Remaining*	*Treated Water Specifications (3)*
	A[a]	*B[b]*			
Sodium as Na	630	670	145	21.7	.....
Calcium as Ca	116	128	9	7.7	.....
Magnesium as Mg	15	16	1	6.0	.....
Total hardness as $CaCO_3$	345	385	24	6.2	.....
Chloride as Cl	1054	1120	207	18.5	250
Sulfate as SO_4	155	161	12	7.5	.....
Bicarbonate as HCO_3	78	66	22	33.0	.....
Nitrates as NO_3	9	4	1	..	.....
Fluorides as F	2	1.84	0.88	47.8	.....
Total dissolved solids (by summation)	2076	2165	398	18.3	500
pH	8.1	...	(7.3)[c]	..	Between 7.0 and 8.0
Silica	17	...	...	..	.....
Iron	0.0	0.05	0.05	..	.....
Manganese	Nil	0.05	0.05	..	.....

[a] Per specifications based on analysis by Valley Labs on June 22, 1961.
[b] Analysis by Arizona State Health Laboratory, June 1961, from samples treated in Ionics Model 152-C demineralizer (capacity 6000 gallons per day) during public demonstration in Buckeye.
[c] From sample done by another laboratory in June 1961. Arizona State Health Laboratory did not report pH.

Costs

Total operation, maintenance, and amortization costs at the estimated actual load factor for the first year of the Buckeye plant's operation (48% of theoretical full-load capability) will be 50.9 cents per 1000 gallons. Operation at 98% of theoretical full-load factor (the plant's maximum practical capability) would result in total costs of 33 cents per 1000 gallons (Table II). The 33 cent figure can be compared with previous cost estimates made by this company (*1*, *2*, *5*), the Office of Saline Water (*8*), or others (*9*), who have usually assumed full-load or virtually full-load operation in such calculations. Most of the factors making up this cost estimate have been guaranteed to the town of Buckeye. However, the 48% load factor is an estimate based on the historical demand pattern for untreated water around the year. It is difficult without actual experience over the next year or two to predict the effect, if any, of a substantial rate rise on the usage of water and the load factor.

In Table II, costs have been estimated for electrical energy, chemicals and filters, membrane replacement, replacement of other parts, operating and maintenance labor, and bond amortization and interest. This cost estimate is the first one for a saline water project of which we are aware which has an actual figure for capital amortization. No federal or state subsidy is involved, the project will be entirely self-liquidating, and the sale of the bond issue, which has already taken place, has provided a known upper limit for the capital budget and an actual interest rate obtained by competitive bidding in the free capital market. The actual average net interest cost to the city from the lowest of three bidders was 4.45%. The low bid for construction of the project was $297,741, submitted by the N. P. Van Valkenburg Co., general contractors, Phoenix, Ariz. Five construction bids were received, ranging from the low bid to approximately $340,000. Two bidders bid less than $300,000. The difference between the low bid and

Table II. Actual and Full Load Water Costs of Ionics Demineralizer

Basis. Estimated actual load, FY 1963 — 112,000,000 gallons annual delivery to system
Full load capacity — 233,000,000 gallons annual delivery to system

	Actual Load, 48%			*Full Load, 98%*		
	Cents per 1000 gal.		*Dollars per year*	*Cents per 1000 gal.*		*Dollars per year*
Operating costs						
Electrical energy[a,b]	14.0		15,700	13.8		32,200
Chemicals and filters	2.8		3,080	2.8		6,520
Total		16.8	18,780		16.6	38,720
Maintenance costs						
Membrane replacement, one fifth per year	8.8		9,900	4.2		9,900
Other parts replacement	3.8		4,200	1.8		4,200
Labor[c]	3.2		3,600	1.6		3,600
Total		15.8	17,700		7.6	17,700
Bond amortization and interest[d]		18.3	20,500		8.8	20,500
Total costs		50.9	$56,980		33.0	$76,920

[a] Electrical energy consumption varies from 8.2 to 12.0 kw.-hr. depending on plant load. Estimated weighted average at 48% load is 10 kw.-hr./1000 gallons; for 98% load it is 12 kw.-hr./1000 gallons.

[b] Cost of electrical energy from Arizona Public Service Co. (Schedule E-32-1) depends on amount used and load distribution around year. Pertinent weighted average costs are 1.4 cents per kw.-hr. for 48% load case and 1.15 cents per kw.-hr. for 98% load.

[c] 1500 hours per year at $2.40 per hour including overhead.

[d] Even payments to amortize 25 year, 4.5% $305,000 bond issue, calculated at 6.72% annually.

the proceeds of the bond issue (which was sold at a slight premium) is being utilized for engineering and fiscal agent fees and net interest during construction. Interest during construction was minimized by the relatively short construction time for the project, less than seven months from date of contract award.

Electrical energy, chemical and filter consumption, membrane replacement, and replacement of other parts are all guaranteed to the town. Initial operation of the unit, in September and October 1962, showed that immediately ascertainable values such as production rate, degree of demineralization, power consumption, and acid consumption were equal to or better than predicted values, and that operating variables were stable with time. More detailed actual operating results will be reported in a future paper and compared with the values predicted here.

The item for labor is crucial in any water conversion plant of this size. Total annual labor charges of $3600 are estimated, allowing 1500 hours per year. This estimate includes 2 hours per day, or a little over 700 hours per year of operating attendance, with the balance being available for maintenance of stacks and other items. Maintenance of each of the six stacks in the plant is estimated at four times per year, or 24 total stack disassemblies per year involving not more than 16 man-hours per disassembly.

Flowsheet

The major characteristics of the Buckeye plant are listed in Table III and a scale model is pictured in Figure 1.

Raw well water from a 100,000-gallon raw water storage tank is pumped by the pair of feed pumps visible in the lower right-hand corner of the building area

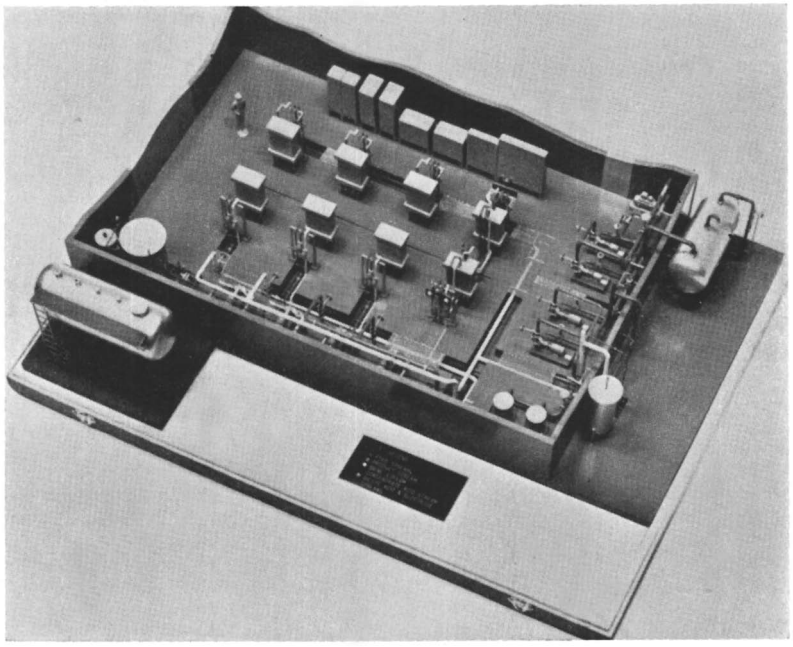

Figure 1. Model of 650,000-gallon-per-day Ionics electrodialysis desalting plant
First saline water conversion plant of any type to treat an entire municipal supply in the United States

in Figure 1 through replaceable, cartridge-type pressure filters visible in the extreme lower right-hand corner. These filters remove particulate matter (principally sand) which might be present in the deep well water and are of the woven cellulose type with a nominal rating of 10 microns. Filtered feed water at a full-load flow rate of approximately 600 gallons per minute is then split into two streams. One, of 450 gallons per minute, will become demineralized in the membrane stacks, and the other, of approximately 150 gallons per minute, will act as make-up to the recirculating brine stream which conducts water to and from the stacks to pick up the minerals removed.

One pair of pumps, called the product booster pumps, visible along the lower wall of the building area, pressurizes the product water and the other pair pressurizes the brine water. Both streams, pressurized to approximately 60 p.s.i., flow first through the bottom row of stacks and then through the top row without repumping. Three stacks in each row or "stage" are currently installed and the fourth pair will be added for expansion. A little over half the minerals are removed in the first stage and a little over half of the remaining minerals in the second stage to provide the necessary over-all demineralization. The demineralized product water flows in a pipe trench pictured just above the top row of stacks to the product transfer tank shown outside the building in the upper right-hand corner. This tank is vented to the atmosphere. From this tank, the product water is pumped into the town's 300,000-gallon treated water reservoir by the pair of product water transfer pumps visible in the upper right-hand corner of the building. The brine stream emerging from the second stage is also carried in the pipe trench. Of the 450 gallons per minute recirculating through the stacks in the brine stream, 300 gallons are returned to the suction of the brine-recirculating pump and 150 gallons are continuously wasted to the outside of the building and eventually through a sewer line to the town's sewage plant, where the water is mixed with the sewage plant effluent.

All electrical and control equipment, including separate d.c. rectifiers for the two stages, is mounted in a single row visible at the top of Figure 1. In the lower left-hand corner just outside the building can be seen a concentrated sulfuric acid tank suitable for tank truck deliveries of acid. This tank, having a capacity of approximately 3000 gallons, holds sufficient sulfuric acid for more than 100 days' operation at full load. Small quantities of sulfuric acid are fed by metering pumps in the lower left-hand corner to the brine-recirculating loop to maintain a pH of less than 5.8 and to the cathode stream to maintain a pH of less than 1.8.

Table III. Major Specifications of Water Demineralization Unit

Water treatment capacity, membrane stacks, gal./day	650,000[a]
Hydraulic and rectifier treatment capacity, gal./day	750,000
Blowdown rate	Not more than 25% of water fed
Raw water temperature (for ratings), ° F.	80
Pretreatment	Replaceable 10 micron-rated cellulose filter cartridges
Posttreatment	None required
Raw water storage tank, gal.	100,000
Membrane stacks	Six Ionics Mark III
Demineralization stages	Two, 3 stacks each
Product water storage, gal.	300,000, existing
Size of building, feet	40 × 60 feet
Peak running demand, kw.	330
Guaranteed electrical energy consumption at 650,000 gal./day, kw.-hr./1000 gal.	12
Guaranteed chemical consumption/1000 gal.	0.6 lb. H_2SO_4
Guaranteed annual membrane replacement cost	$9900
Guaranteed annual other parts replacement cost	$4200
Labor required (operation plus maintenance), hours/year	1500
Estimated annual water usage, fiscal 1963, gal.	112,000,000
Full-load plant capacity, gal.	233,000,000
Estimated annual load factor, fiscal 1962, %	48

[a] Must be expandable to 750,000 gallons per day by addition of more membranes or stacks only.

Design

The Buckeye plant is considered typical in many ways of medium-to-large electrodialysis plants for actual municipal use. A number of interesting design problems were encountered in the design phase of this project, which provide a useful guide for other such projects. The major problems include (1) a widely varying water demand around the year, which, in the case of Buckeye, is approximately four times as great in the peak summer month as in the minimum winter month, and which results in an annual load factor of 48%, (2) the necessity to allow for future expansion in several stages over the life of the bond issue, (3) requirement for simple operating and maintenance procedures with not more than part-time attendance of one man for daytime operation, no regular attendance overnight or on weekends, and no graduate technical personnel available for operation, maintenance, or supervision, and (4) the requirement for maximum operability and on-stream time without significant cost of standby or spare equipment.

To meet the widely varying water demand, dual water pumps have been installed for feed, concentrate booster, product booster, and product transfer duty, each pump capable of handling half the peak hydraulic demand. Thus, pump operation at less than about 50% of the pump rating has been avoided, yielding a higher average pump efficiency, a lower energy consumption, and the ability to operate the plant at about 50% of rated output in case of any pump failure (3). At periods of low load, further electric power and energy savings may be achieved

by simultaneous reduction of the flow rate and voltage applied to each line of stacks down to the minimum rated level for the full plant of about 385,000 gallons per day. By use of full plant membrane area at minimum throughput, guaranteed electrical energy consumption is reduced to 8.2 kw.-hr. per 1000 gallons from the full-rate energy consumption of 12 kw.-hr. per 1000 gallons.

The first plant expansion is expected to occur about 1965 and will increase plant capacity from 650,000 to 750,000 gallons per day by addition of two membrane stacks or of additional membranes to the present stacks (7). All necessary major hydraulic and electrical equipment for this expansion, except the membranes or stacks, has been installed in the original plant. The 750,000-gallon expanded plant is expected to be adequate until 1969. Further expansions will require new auxiliaries as well as new membrane area.

Operation and maintenance will be simplified through use of readily repaired, split-case, flexible-coupled water pumps of bronze construction and by extensive use of noncorrodible plastic pipe. Conductivity of feed, product, and waste water and pH of product, waste, and electrode streams will be recorded and the plant will automatically shut down with visual indication of the reason for shutdown if present limits of these variables are exceeded. The plant will be equipped with a traveling crane covering the entire 40 × 60 foot floor area for ease of handling pumps, motors, and membrane stack end plates. Membrane stacks are operated and serviced in the membrane-horizontal position and will not be moved from their operating position for most stack maintenance tasks. Hydraulic connections to membrane stacks are made through easily disconnected rigid PVC unions and electrical connections through quick disconnect d.c. connectors.

Minimum loss of plant production, due to component failure, or scheduled maintenance, is made possible by use of dual, high-reliability, long-lived pumps as noted above, automatic shutdown and alarm on acid failure or pH outside set limits, and a three-line design of the six stacks. Upon failure or scheduled shutdown of any stack, only one other stack need be shut down and two-thirds plant capacity can be maintained.

The Mark III Stack

The basic building block of an electrodialysis unit is the array of alternating anion and cation membranes (with interposed water-carrying spacers) called the membrane stack. The characteristics of an Ionics Mark III stack are described in Table IV.

The improved Mark III stack on which the Buckeye plant is based has a rated flow rate range of 125,000 to 250,000 gallons per day with corresponding pressure drop ranging from 12 to 40 p.s.i. Its maximum rated working pressure is 65 p.s.i.g. At flows in the neighborhood of 215,000 gallons per day and corresponding pressure drop of just under 30 p.s.i., two Mark III stacks can be used in series without interstage pumping as is done in the Buckeye plant.

The use of two stacks in series without interstage pumping has two important advantages:

Reduction of electrical energy consumption for pumping, and hence, cost of water produced.

Simpler flowsheet, reducing plant cost due to omission of interstage pumps and accessories.

Table IV. Design Characteristics of Ionics Mark III Membrane Stacks as of March 1962

Rated flow rate range, U. S. gal./day	
Rated full flow	250,000
Rated low flow	125,000
Rated flow rate range, U. S. gal./min.	
Rated full flow	175
Rated low flow	87.5
Stack pressure drop range, p.s.i.	
Rated full flow[a]	40[a]
Rated low flow	12
Number of membranes	550
Size of membranes, inches	18 × 40
Total area, all membranes, sq. feet	2750
% of total area available for transfer[b]	70[b]
Approximate weight, pounds	2300
Approximate over-all height (including legs), feet	6
Demineralization range per pass (standard conditions)[c], %	
Rated full flow	48
Rated low flow	57
Rated maximum working pressure, p.s.i.g.	65

[a] Reported in 1960 as 60 p.s.i., but improved to present reported value in 1961.
[b] Considering as unavailable only areas of adjacent membranes blocked by insulating spacer material touching both faces.
[c] Standard conditions. Feed water temperature, 70° F. Chemical composition of water, pure NaCl.

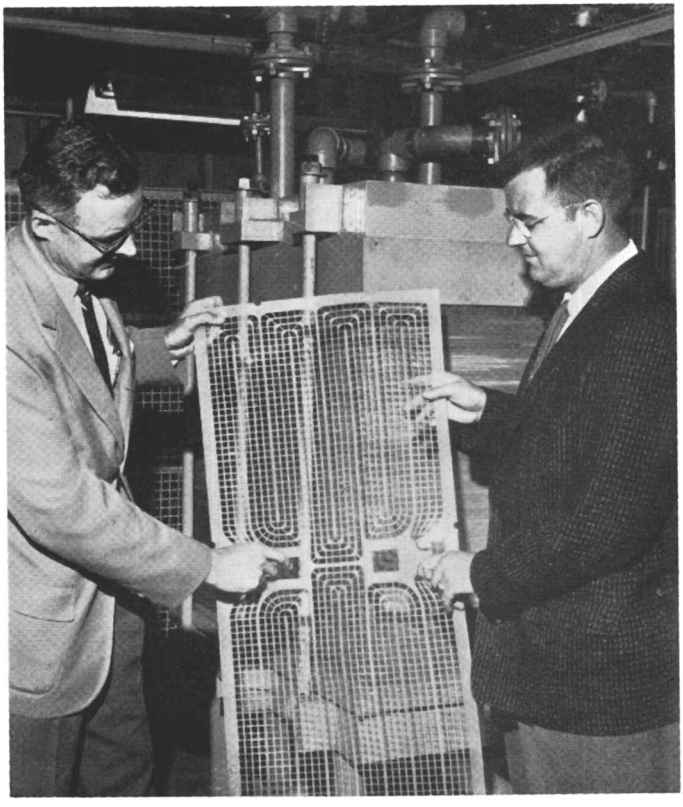

Figure 2. Mark III spacer

Oxnard Tests

A Mark III stack was first field-tested in cooperation with the city of Oxnard, Calif., during the summer of 1960. Figure 2 shows a Mark III spacer in detail. Several experimental conditions of operation were examined and the stack was frequently disassembled to maintain a careful record of membrane condition. An aggregate of approximately 2000 hours of electrical time was logged. Oxnard water with 1200 to 1300 p.p.m. of total dissolved solids contained very little sodium chloride and was high in calicum, magnesium, sulfate, and bicarbonate.

The Oxnard tests showed that a hydraulic flow rate of 175 gallons per minute could be continuously achieved at a stack pressure drop of about 51 p.s.i., as compared with the predicted value of 60 p.s.i. In the ensuing year, spacer manufacturing improvements led to a further reduction of pressure drop to 40 p.s.i. at 175 gallons per minute. The Oxnard tests showed that Mark III stacks in operation on a difficult natural water were sufficiently stable in performance so that overnight, unattended operation and unattended operation of 24 to 36 hours on weekends was feasible, and that a Mark III stack could be disassembled for inspection or repair and reassembled by one man in approximately 8 hours. A second man makes the task easier and is allowed in the Buckeye estimate of 16 man-hours per stack disassembly.

Conclusions

The annual demand on saline water conversion plants for full-flow municipal service is usually about 50% of total full-load capability, because the plant must meet peak summer demands.

Total costs per 1000 gallons for saline water conversion plants operating at about 50% annual load factor will be on the order of 50% higher than costs calculated on the basis of load factors in the 90 to 100% range.

Special hydraulic arrangements, such as the use of dual half-capacity pumps in parallel, are desirable to maintain good efficiency in medium-to-large plants which must operate over a hydraulic range of fourfold during the year.

In plants having capacities of several hundred thousand to a few million gallons per day, the actual number of operators to run the plant must be very small. For the Buckeye project, it is estimated that only 1500 man-hours per year will be required, which is equivalent to less than the time of one man working steadily on a 40-hour week basis.

Instrumentation and automatic control is desirable in plants of this size to allow for automatic shutdown and alarm in case events should occur during unattended periods which might be deleterious to the plant or the product water. Automatic startup, however, is not a requirement if there is adequate product water storage, if the startup procedure for the plant can be carried out in a short time, and if an operator is available on call.

Literature Cited

(1) Barnhill, K. G., *J. Am. Waterworks Assoc.* **54**, No. 5, 526–28 (1962).
(2) Barnhill, K. G., *Water and Sewage Works* **109**, 87 (1962).
(3) Carollo, J. A., "Contract Documents, Water Treatment Plant, Town of Buckeye, Arizona," Phoenix, Ariz., 1962.
(4) Ionics, Inc., Cambridge, Mass., Bull. **6** (1962).
(5) Katz, W. E., ADVAN. CHEM. SER., No. **27**, 232 (1960).
(6) Laurence, W. L., *New York Times*, p. 1 (Feb. 22, 1952).

(7) Town of Buckeye, Arizona, "Prospectus and Call for Bids, $305,000 Water Revenue Bonds, Series of 1961," Buckeye, Ariz., 1961.
(8) U. S. Dept. of Interior, Office of Saline Water, "250,000 GPD Electrodialysis Plant at Webster, S. D.," Specifications 212 (Sept. 20, 1960).
(9) Volckman, O. B., *Chem. Eng. News.* **39,** 66 (April 10, 1961).

RECEIVED June 21, 1962.

12

Economics of Demineralization by Electrodialysis

R. E. LACEY, E. W. LANG, and E. L. HUFFMAN

Southern Research Institute, Birmingham, Ala.

To determine the areas of research effort that will result in the largest reductions in the cost of demineralizing water, the cost data of Katz and Volckman were used to illustrate the approximate effects of membrane properties and operation conditions on the total cost of demineralizing water by electrodialysis. Reducing concentration polarization within the compartments is the most promising means of reducing the cost. Development of lower-cost membranes with longer operating lives and lower resistances would also reduce the cost, but not as much as might be expected. If the cumulative effect of all of the individual possibilities for cost reduction is considered, the cost of demineralization may be reduced from about $0.35 to about $0.20 per 1000 gallons.

To guide research and development efforts on electrodialysis processes for demineralization of water it is desirable to know the effects of certain technical factors and unit costs, such as polarization phenomena and cost of membranes, on the total cost of demineralization by electrodialysis.

Cary (*1*), Dankese (*5*), Katz (*7*), Strobel (*12*), Volckman (*2*, *13*), and Wilson (*14*) have published cost data and estimates of costs for demineralization by electrodialysis. Dankese and Katz presented estimates for large electrodialysis plants, based on extensive experience in field tests. Cary and Strobel presented cost data based on the first six months of operating experience with the 25,000-gallon-per-day electrodialysis plant at Coalinga, Calif. Volckman and Wilson presented cost data on operating experience with the 2,880,000-gallon-per-day plant at the Free State Geduld mine in South Africa.

The cost data of Katz and Volckman were used as a basis for illustrating the approximate effects of membrane polarization, limiting current density, cost, operating life, and resistance of membranes, and temperature on the over-all costs of demineralization of water with electrodialysis. The major objective was to pinpoint the problem areas needing greatest research effort and to show the probable effect of solving these problems upon the cost of demineralization.

The data of Cary, Dankese, and Strobel were not used in this study, because the data of Dankese have been superseded by those of Katz, and the data of Strobel and Cary are for a small installation not typical of costs for larger installations.

Certain revisions were made to place the cost data of Katz and Volckman on a comparable basis. All data and estimates were revised to be in accord with the standard cost procedure of the Office of Saline Water(8), with certain exceptions discussed later. The data of Katz were revised to apply to a 2800-p.p.m. feed water; the data of Volckman for a 2800-p.p.m. feed water were revised to apply to a 2,000,000-gallon-per-day capacity [p.p.m. is used for parts per million of total dissolved solids (TDS)].

Basic Cost Data and Revisions

The original cost data presented by Katz and the revised data based on Katz' estimates are shown in Table I. Katz' original estimate was based on a plant capacity of 2,000,000 gallons per day, an energy cost of 10 mills per kilowatt-hour, a membrane replacement rate of 1/5 per year, an amortization of 25 years with 5% interest, and the use of Ionics Mark III equipment. The major revisions to place his costs on the basis of the standard procedure used by the Office of Saline Water are shown at the top of Table I. Katz presented data for a 1000-, 2000-, and 4000-p.p.m. feed water. Graphical interpolation was used to obtain the approximate capital and energy costs for a 2800-p.p.m. feed. The major anion in the feed water was chloride, which was also the major anion in the water for the Volckman estimates. In Katz' original data the membranes cost $5 per sq. foot. This value was revised to $3 per sq. foot, the present cost for this thicker type of membrane (7). The membrane replacement rate was not revised, because Ionics, Inc., guarantees the replacement rate to be no more than 1/5 per year. The other revisions are explained in the footnotes to Table I.

Volckman's cost data (Table II) were based on a plant capacity of 2,880,000 gallons per day, an energy cost of 5.2 mills per kw.-hr., a membrane replacement rate of 1 1/3 per year with membranes that cost $0.20 per sq. foot, an amortization period of 15 years at 6.5% interest, and the use of the Free States Geduld electrodialysis presses. The major revisions were in capital cost, type of membranes, and amortization schedule.

It was assumed that a demineralizer of the "sheet flow" type used by Volckman would cost 20% more if built in the United States than if built in South Africa. An adjustment for reduced size of the plant was also made for the conventional process equipment by using the usual 0.6 power rule for capital cost applied to the 64% of the total capital cost that is for conventional process equipment. The cost of the dialysis presses, exclusive of membranes, was not reduced. However, the number of membranes required for the first charge was reduced by the ratio of throughputs.

The energy consumption estimated by Volckman was 10.1 kw.-hr. per 1000 gallons, but from an examination of the operating data (13) it seemed more realistic and more conservative to use 12 kw.-hr. per 1000 gallons in the revised estimates. The cost of energy was assumed to be 7 mills per kw.-hr. for the revised estimates.

It was assumed that the membranes used in the electrodialysis demonstration plant at Webster, S. D., would be used instead of those in Volckman's plant. The membranes used at Webster cost about $1 per square foot. The membrane

Table I. Estimated Costs for

(Revised from data of Katz)

Basis. Feed water temperature 85° F.
Demineralization range. Original, 4000 to 500 and 2000 to 500 p.p.m. TDS.
Revised, 2800 to 500 p.p.m. TDS
Anions predominantly chloride
Electrical energy cost. Original, 10 mills per kw.-hr.
Revised, 7 mills per kw.-hr.

	2,000,000 Gallons/Day	
	Original 2000-p.p.m. feed	*Original 4000-p.p.m. feed*
Number of stacks	16	24
Total capital cost[a]	$850,000	$1,300,000
Electrical energy[c]	$0.134	$0.260
Chemicals	0.025	0.025
Prefiltration[e]	0.030	0.030
Membrane replacement	0.060[b]	0.090[b]
Maintenance	0.018	0.027
Labor	0.013	0.017
Amortization	0.083	0.126
	$0.363	$0.575

[a] Estimated by plotting capital costs listed by Katz for feed concentrations of 1000, 2000, and 4000 p.p.m., and reading capital cost for 2800-p.p.m. feed from best line through points.

[b] In original estimate 55,000 sq. ft. of membrane used at $5.00/sq. ft. Adjusted capital cost figures reflect reduction in cost of original charge of membranes.

[c] Energy data from 1000-, 2000-, and 4000-p.p.m. feeds plotted, and value for 2800 p.p.m. read from graph. Katz lists d.c. stack energy for 3000-p.p.m feed as 9.5 kw.-hr. per 1000 gal. From this and total energy cost as interpolated, pumping cost may be inferred to be $0.08 to $0.10/1000 gal.

[d] To revise energy cost for 7-mill power: $\left(\frac{\$0.007}{\$0.010}\right)(\$0.190) = \$0.133.$

[e] Cost of prefiltration will vary considerably with amount and nature

replacement rate at Webster is less than 1/5 per year, but for the revised estimates shown in Table II a rate of 1/3 per year was assumed (the guaranteed replacement rate).

The original amortization conditions used by Volckman (15 years at 6.5% interest) reflect the high cost of money in South Africa. The revised amortization conditions are those suggested by the standard procedure of the Office of Saline Water—20 years at 4% interest.

One important assumption in both estimates is that the temperature of the feed water is fairly high (75° and 85° F). If it is lower, the resistance of the

Demineralization by Electrodialysis

Membrane replacement rates 1/5 per year
Membrane cost. $5 per sq. foot
Amortization basis. Original, 25-year, 5% int. (7.1% per year).
Revised, 20-year, 4% int. (7.4% per year).
Maintenance cost other than membranes. 1.5% capital per year
Operating days per year. Original, 365.
Revised, 330.

Interpolated for 2800-p.p.m. feed	*Revised Estimate (2800 P.P.M. Feed) with Membranes at*		
	$3.00/sq. ft.	*$2.50/sq. ft.*	*$2.00/sq. ft.*
20	20	20	20
$1,075,000	$965,000[b]	$938,000[b]	$910,000[b]
$0.190	$0.133[d]	$0.133[d]	$0.133[d]
0.025	0.025	0.025	0.025
0.030	0.030	0.030	0.030
0.072[b]	0.043[g]	0.036[g]	0.029[g]
0.021	0.019[h]	0.018[h]	0.018[h]
0.015	0.015	0.015	0.015
0.104[i]	0.098[j]	0.095[j]	0.092[j]
$0.457	$0.363	$0.352	$0.342

of suspended solids. Standard cost for prefiltration of $0.03 was assumed for all estimates.

[f] Cost of membranes in original estimate was $5/sq. ft.

[g] To revise for cheaper membranes: $\left(\frac{\$3.00}{\$5.00}\right)(\$0.072) = \$0.043$.

[h] To revise maintenance for changed capital cost: $\left(\frac{\$\ 965,000}{\$1,075,000}\right)(\$0.021) = \$0.019$.

[i] $\frac{\$1,075,000}{\$1,300,000}(\$0.126) = \$0.104$.

[j] Amortization revised for both reduced capital and change in amortization basis from 7.1 to 7.4% per year.

Example. $\frac{(\$965,000)\,(7.4\%)}{(365)\,(2000\text{ M gal./day})} = \$0.098/\text{M gal.}$

stacks is higher. The increase in resistance is about 2% per degree centigrade. Thus, at lower temperatures power costs will be higher. Another important factor in these estimates is that the anions are predominantly chloride. If large amounts of certain bivalent anions are present, power costs may be higher than those shown. The amortization cost may also be higher, if it is economically desirable to use a different current density (and thus a different capacity per stack) than the ones used for these cost estimates, or if the water to be treated has an appreciable quantity of calcium or magnesium, because polarization would limit the usable current densities to values less than the economic optimum.

Table II. Estimated Costs for Demineralization by Electrodialysis

(Revised from data of Volckman)

Basis. Feed water temperature 75 °F. (average)
Demineralization range. 2800 to 500 p.p.m. TDS
Anions predominantly chloride
Electrical energy cost. Original, 6 mills/kw.-hr.
Revised, 7 mills/kw.-hr.
Membrane replacement rate. Original, $1^1/_3$ per year with $0.20/sq. ft. membranes.
Revised, $^1/_3$ per year with membranes costing from $0.50 to $1/sq. ft.
Amortization basis. Original, 15-year at 6.5% int. (10.3% per year).
Revised, 20-year at 4.0% int. (7.4% per year).
Operating days per year. Original 365.
Revised 330.

	2,800,000 Gal./Day, Original	*2,000,000 Gal./Day Revised Estimate (2800 P.P.M. Feed) with Membranes at*		
		$1.00/sq. ft.[a]	*$0.75/sq. ft.*[b]	*$0.50/sq. ft.*[b]
Total capital cost	$797,000	$938,000[c]	$892,000[c]	$847,000[c]
Electrical energy	$0.0643	$0.084[d]	$0.084[d]	$0.084[d]
Chemicals	0.0080	0.025[e]	0.025[e]	0.025[e]
Prefiltration	0.0147	0.030[f]	0.030[f]	0.030[f]
Membrane replacement	0.0685	0.089[a]	0.067[a]	0.044[a]
Maintenance	0.0257	0.023[g]	0.022[g]	0.021[g]
Labor	0.0322	0.022[h]	0.022[h]	0.022[h]
Amortization	0.0834	0.098	0.093	0.088
	$0.2968	$0.371	$0.343	$0.314

[a] Assumed that membranes cost $1.00/sq. ft., cost of membranes for Webster, So. Dak., demonstration plant. Membrane replacement rate, $^1/_3$ per year. Seko (*10*) used a membrane life of 5 years in his estimates and guaranteed rate of replacement of membranes in Webster plant was $^1/_3$ per year.

[b] Two companies producing these thin membranes predicted that they could sell membranes for $0.50/sq. ft., or less, if production was large.

[c] From detailed breakdown of capital costs given by Wilson (*14*, p. 316), it was apparent that 64.4% of total capital cost was for conventional equipment and construction that is subject to the 0.6 power rule, and that plant cost would be somewhat higher in the United States than in South Africa. Accordingly, the total capital cost was divided into cost of conventional equipment [multiplied by 120% to allow for increased costs in the U. S. and then by $\left(\frac{2{,}000{,}000}{2{,}800{,}000}\right)^{0.6}$ to allow for change in size], cost of electrodialysis stacks (exclusive of membranes, but including cost of spacers, electrodes, and frames)—assumed to be same size as original, but increased by 20% to allow for increased cost in U. S.—and cost of first charge membranes (183,000 sq. ft. of membranes necessary).

[d] Values for energy consumption during actual tests of FSG electrodialysis unit varied from 8 to 13 kw.-hr. per 1000 gal. 10.1 kw.-hr. per 1000 gal. was used in original data (column 1). We used 12 kw.-hr./1000 gal. as a more conservative value.

[e] $0.025 chosen as standard, since demand for chemicals depends to large extent on composition of feed.

[f] Standard value of $0.030/1000 gal. used.

[g] Maintenance at 1.5% of capital cost.

[h] As explained by Volckman, major part of the labor charge is for periodic replacement of membranes. Membranes assumed that last 4 times longer than Volckman's. Cost of labor reduced to $^2/_3$ of Volckman's value to be on conservative side.

Effect of Polarization and Limiting Current Density on Operating Costs

Cook (*3*), Cowan (*4*) Rosenberg (*9*), Spiegler (*11*), and Wilson (*14*) have discussed polarization in electrodialysis. Because the transference number of the cation in the solution is lower than that in the cation-permeable membrane, the number of positive ions removed from the cathodic face of a cation-permeable membrane by electromigration through the solution is less than the number arriving at the face by electromigration through the membrane. Thus, the concentration of ions at the face increases until a concentration gradient is

established from the face of the membrane to the bulk of the solution such that all ions that migrate through the membrane by electromigration go into the bulk of the solution, by either electromigration or diffusion. The converse occurs at the anodic face, such that an ion-depleted layer is established. This phenomenon of concentration gradients at the interfaces between membranes and solutions is usually termed polarization.

As the current density is increased, the interfacial films that are being depleted of ions become more and more depleted in salt ions. At some value of current density, usually termed the limiting current density, the interfacial film is so depleted in salt ions that hydrogen and hydroxyl ions from the water compete with the salt ions in the electrical transport process. The onset of the limiting current density is accompanied by severe pH changes in the solutions and a change in the resistance of membrane cells. At the anodic face of anion-permeable membranes, the high pH that occurs when the limiting current is exceeded can cause precipitation of any ions that form sparingly soluble hydroxides. Carbonates can also precipitate because of the high pH, if bicarbonate anions are present in the water being treated. This precipitation of ions on and in the membranes can damage the membranes and block the narrow solution passages so that the electrodialysis unit becomes inoperable or inefficient. For this reason the operating current density should be kept less than the limiting current density.

If it were not for this limitation imposed by polarization, each stage of an electrodialysis unit could be designed to operate at the economic optimum current density. The curves of Figure 1 show the effect of current density on the costs of demineralization. The economic optimum current density is that which

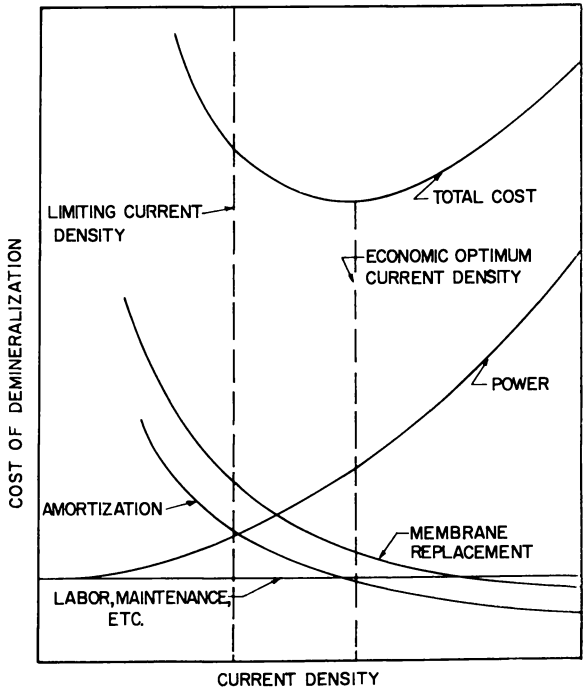

Figure 1. Factors making up total cost of demineralization by electrodialysis for a typical installation

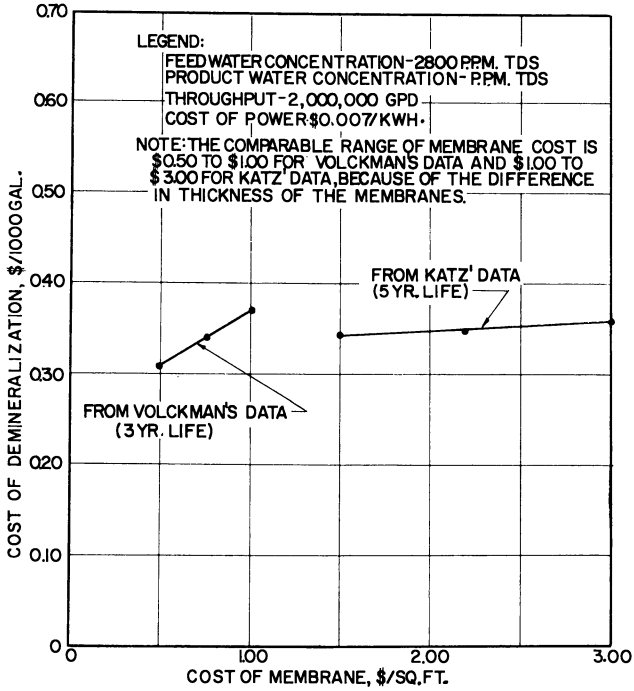

Figure 2. Effect of cost of membranes on cost of demineralization

gives the minimum in the curve for total costs. Because the size of the equipment and the area of membranes necessary become larger as current density is decreased, the membrane-replacement cost and the amortized capital cost vary inversely with current density. The power cost varies directly with current density, but costs of labor, maintenance, and chemicals are not affected greatly. Because of the way in which individual costs vary with current density, there is a minimum total cost of demineralization, which determines the optimum current density. In many electrodialysis plants the limiting current density is less than the optimum, and the cost of demineralization is higher than it would be if polarization could be overcome. This paper does not discuss methods of overcoming or minimizing polarization.

If the unit cost of power in Figure 1 is increased, the optimum current density will be lower than the one shown. Similarly, the unit cost of membranes, the resistance of the membranes, the average temperature of the feed, and other factors tend to shift the optimum current density, either higher or lower.

For the feed water assumed in Tables I and II little trouble was expected from polarization, and the current density used was close to the optimum. In the calculations of effect of unit costs on total costs, the current densities used in the original estimates were not changed to optimize them for each new cost condition. For this reason the changes in the total cost of demineralization with changes in unit costs or technical factors (Figures 2 to 5) should be viewed as only approximations. Use of a different operating current density (and therefore a different membrane replacement and amortization cost) would alter the slope of the various curves. However, the curves provide an approximate picture of the

cost reduction that can be obtained by solving technical problems, developing cheaper membranes, or developing membranes with longer lives.

Cost of Membranes

The direct variation in the total cost of demineralization with the cost of membranes is shown in Figure 2.

Doubling the unit cost of membranes (from \$1.50 to \$3 per square foot) increases the total cost of demineralization only \$0.02 per 1000 gallons [based on Katz' data (*6*)]. Doubling the unit cost for the data of Volckman (from \$0.50 to \$1) causes a \$0.06 increase.

Operating Life of Membranes

The effect of the operating life of the membranes is shown in Figure 3. The present membrane costs of \$1 to \$3 per square foot were assumed for the Volckman and the Katz data, respectively. In the Volckman unit doubling the life of the membranes to 6 years appreciably decreases cost, but increasing membrane life beyond 6 years decreases the cost of demineralization only by small increments. If the unit cost of membranes is less than \$1 and \$3 per square foot, the advantage of increasing the membrane life is less.

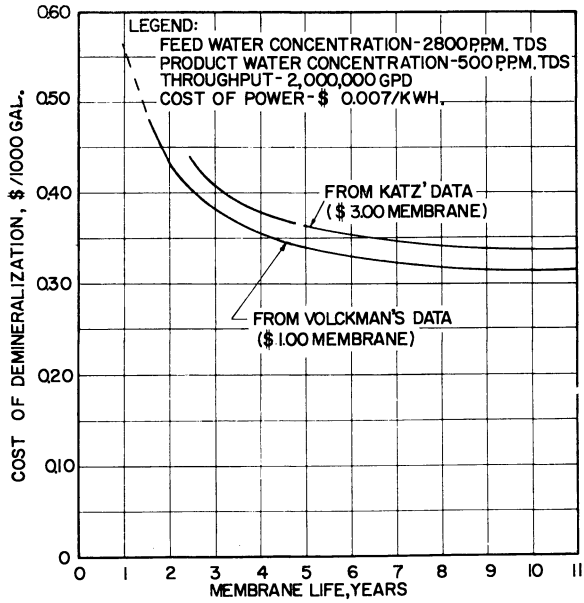

Figure 3. Effect of membrane life on cost of demineralization

Resistance of a Cell Pair

The influence of resistance on the cost of demineralization has been estimated. From the operating data of Katz, the average resistance per unit area of one cell pair or repeating unit—i.e., one cation- and one anion-permeable membrane plus

one depleting solution and one enriching solution—was calculated to be 118 ohm-sq. cm. In similar fashion the average resistance of a repeating unit was calculated to be 90 ohm-sq. cm., using the data of Wilson and Volckman.

The effect of the resistance of a repeating unit is shown in Figure 4. Reducing the resistance for either type of unit by one half reduces the cost of demineralization by about $0.04 per 1000 gallons.

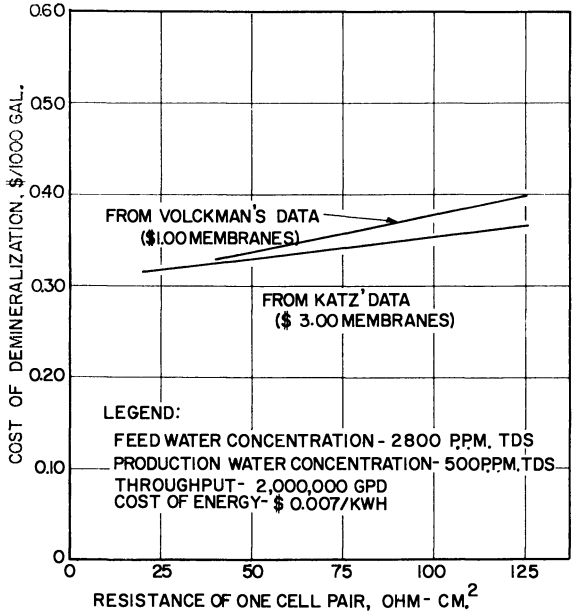

Figure 4. Effect of resistance of a cell pair on cost of demineralization

A larger reduction in over-all resistance can be obtained by finding means of reducing concentration polarization than by reducing the resistance of membranes. To illustrate, the resistance value of 118 ohm-sq. cm. for the repeating unit was calculated from operating data of Katz for an electrodialysis stack that used membranes having a resistance of 14 ohm-sq. cm. The resistance of the two solutions and the two membranes in a repeating unit would be only about 75 ohm-sq. cm., if no concentration polarization existed. If the resistance of membranes could be reduced to almost zero, the over-all resistance could be reduced another 25 ohm-sq. cm., to about 50 ohm-sq. cm.

Thus, minimizing polarization can effect a larger reduction in resistance and cost than developing low-resistance membranes.

Temperature

The influence of the temperature of the water on the cost of demineralization is shown in Figure 5. A 1° C. change in temperature will change the total resistance of an electrodialysis unit by about 2%, with a proportionate change in energy cost for the stacks. The energy necessary for pumping is not affected appreciably by small changes in temperature. Figure 5 shows that the cost of demineralizing water at 110° F. is about $0.03 per 1000 gallons less than at 65° F.

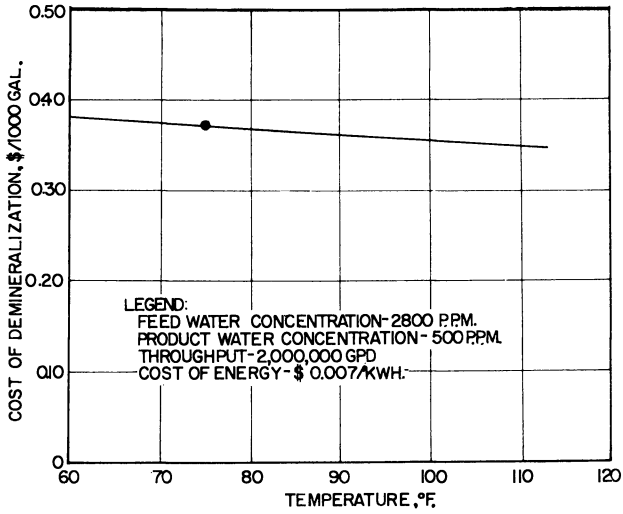

Figure 5. Effect of temperature on cost of demineralization

Conclusions

This analysis of individual costs making up the total cost of demineralization by electrodialysis helps to pinpoint the areas needing the greatest research effort. The costs are based on two published cost estimates, revised on a comparable basis for a 2,000,000-gallon-per-day plant. These studies indicate that development of methods to reduce concentration polarization within the compartments offers the best means of reducing the cost of demineralization by electrodialysis, not only because the limiting current density might be increased, but also because of the reduction in resistance that occurs when concentration polarization is eliminated.

The cost of demineralization can also be reduced by developing lower-cost membranes, since the cost of membranes is a major factor in amortization and membrane-replacement costs. Additional work is also needed to develop membranes that have an operating life of at least 5 years. If the useful life of membranes can be increased from 3 years to 5 years, the cost of demineralization can be reduced appreciably.

Literature Cited

(1) Cary, E. S., Ongerth, H. J., Phelps, R. O., *J. Am. Water Works Assoc.* **52,** 585 (1960).
(2) *Chem. Eng. News* **39,** 66 (April 10, 1961).
(3) Cooke, B. A., Volckman, O. B., Wilson, J. R., "Design Consideration in Electrodialysis Plant for Saline Water Demineralization," "Salinity Problems in the Arid Zones," Proceedings of Teheran Symposium, **353,** United Nations Educational, Scientific, and Cultural Organization, Paris, 1961.
(4) Cowan, D. A., Brown, J. H., *Ind. Eng. Chem.* **51,** 1445 (1959).
(5) Dankese, J. A., Kirkham, T. A., *et al.*, Office of Saline Water Research and Development, Progr. Rept. **11** (December 1956).
(6) Katz, W. E., ADVAN. CHEM. SER., No. **27,** 333 (1960).
(7) Katz, W. E., Ionics, Inc., private communication.
(8) Office of Saline Water, Washington, D. C., "Standardized Procedure for Estimating Costs of Saline Water Conversion," 1956.
(9) Rosenberg, N. W., Tirrell, C. E., *Ind. Eng. Chem.* 49, 781 (1957).

(10) Seko, M., "Large Scale Brackish Water Conversion Electrodialysis Demonstration plant at Webster, South Dakota," First European Symposium on Fresh Water from the Sea, Athens, Greece, June 1, 1962.
(11) Spiegler, K. S., ADVAN. CHEM. SER. No. 38, 179 (1963).
(12) Strobel, J. J., *Chem. Eng. Progr.* **57**, 41 (1961).
(13) Volckman, O. B., ADVAN. CHEM. SER., No. 38, 133 (1963).
(14) Wilson, J. R., ed., "Demineralization by Electrodialysis," Chap. 8, Butterworths, London, 1961.

RECEIVED May 14, 1962.

Saline Water Conversion Research in Israel

K. S. SPIEGLER[1]

Department of Chemistry, Technion-Israel Institute of Technology, Haifa, Israel

Electrodialysis of brackish water is being studied at the Negev Institute for Arid Zone Research to develop techniques to retard formation of scale on membranes. In the "pulse method," short intense pulses of reverse current passed through the electrodialysis unit at regular intervals reduce the formation of hard scale and cause formation of a soft sludge. The degree of success depends on the nature of the water treated and electrodialysis conditions. Fundamental studies of polarization phenomena on membrane surfaces provide insight into changes of cell resistance on passage of a constant current. The equation describing buildup of the polarization layer is discussed and results of polarization studies in the laboratory are described. Measurements are reported of the transport of bicarbonate ions across three commercial electrodialysis membranes in contact with mixed sodium bicarbonate-sodium chloride solutions. Pilot plant studies of desalting by direct freezing have been made.

Research and development in salt water purification in Israel have concentrated on two methods: electrodialysis of brackish water and freezing-evaporation of sea water. In the field of electrodialysis, laboratory work on basic membrane properties has been carried out at the Technion-Israel Institute of Technology, Haifa, and the Negev Institute for Arid Zone Research, Beer Sheva. The work at the latter institute also relates to membrane preparation, design of electrodialysis units, and pilot plant studies in an installation of about 5000 gallons per day capacity (rated on brackish water containing 2500 p.p.m. of dissolved salts). This work has led to a better understanding of polarization and scale formation phenomena in electrodialysis, the development of a new method of scale control (*10*) and a household unit using this method. Development work on freezing processes is carried out by Water Desalination Plants, Ltd., Tel Aviv, and is based on the original work of Zarchin (*17*).

[1] Present address, Pratt & Whitney Aircraft, East Hartford, Conn.

Research on specific distillation problems at the Israel Institute of Technology is in its first stages and is not reported here. This work deals with heat transfer in flash distillation units with particular reference to annuli. Older work on solar distillation and ion exchange demineralization of moderately brackish waters was done at the Weizmann Institute of Science (*14*).

Electrodialysis and Membrane Phenomena

Polarization Studies. In the electrodialysis of most brackish ground waters, scaling of the membrane surfaces is common (*15*). The source of this troublesome phenomenon must be sought in the concentration changes occurring in the vicinity of the membranes when electric current flows. The concentration profiles in the solution are schematically shown in Figure 1. The basic assumption is made that the current has been flowing long enough to ensure steady state, although certain oscillations of the potential differences across the membranes after continuous passage of a constant current have been reported (*8*).

Since the transport number of the cation in the solution is lower than in the cation exchange membrane, the amount of positive ions transported by the electrical current from the solution to the face of this membrane (left, Figure 1) is not sufficient to make up for the positive ions removed through the membrane. The balance is made up by diffusion of ions from the solution to the membrane surface. At the other membrane surface, more positive ions arrive by electromigration than are carried away by this mechanism. The concentration remains constant, because the excess of ions is removed into the solution by diffusion. An analogous situation prevails near the anion exchange membrane.

In an electrodialysis cell, the solutions flow past the membranes and a continuous velocity gradient extends from the membrane face to the center of the channel. It is customary, however, to describe the situation by a simplified model. It is assumed that there is a completely stationary layer close to the surfaces and

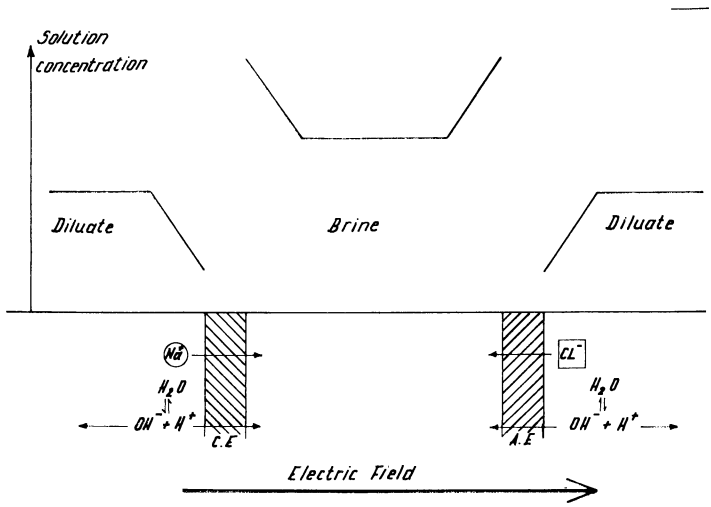

Figure 1. Steady-state concentration profiles near membrane surfaces in electrodialysis

C. E, A.E. Cation and anion exchange membrane surfaces

beyond this layer there is complete mixing. Within the layer, all transport processes occur by diffusion and electromigration only.

If this assumption is made, the solution concentration profiles in the steady state are composed of straight lines, as shown in Figure 1. But irrespective of the assumptions about the structure of the boundary layer, the electrolyte concentration near the membrane surfaces is low in the diluate compartments and high in the brine compartments. The lower the concentration of the boundary layers in the diluate compartments, the higher the voltage necessary to maintain constant current, for the concentration changes cause a membrane potential opposing the applied voltage. Also, the effect of the electrolyte depletion in the diluate compartments on the resistance outweighs the opposite effect of the increased concentration near the boundaries facing the brine compartments. The phenomenon described here is known as concentration polarization (*2–4*).

At high current densities, an additional effect is important. In this case, there are not enough ions of the electrolyte in the vicinity of the membrane, and hence hydrogen and hydroxyl ions, derived from water, pass through the cation and anion exchange membranes, respectively, to maintain constant current. This phenomenon is well known and is referred to as "water splitting."

Both concentration polarization and water splitting have a profound influence on the scale-forming tendency. Most brackish waters in the Negev and other arid regions contain appreciable amounts of calcium and bicarbonate ions. The concentrations of these ions near the membrane surfaces in the brine compartments can exceed the solubility limit. Moreover, the pH in the anion exchange membrane–brine surface boundary layer is high because of the influx of OH^- ions. This region is therefore the main danger zone for the precipitation of calcium carbonate scale. Indeed, when scaling occurred in the experiments, the deposits were always found in or near this surface.

Fortunately, calcium carbonate scale does not always precipitate immediately when the solubility product is exceeded. A considerable degree of supersaturation can be tolerated for a while. In fact, the method of "contact stabilization" (*11*) for preventing scale in sea water stills is based on this fact. If supersaturation conditions near the membrane are not allowed to prevail long enough, scale will not form there. Thus it becomes very important to study the process of

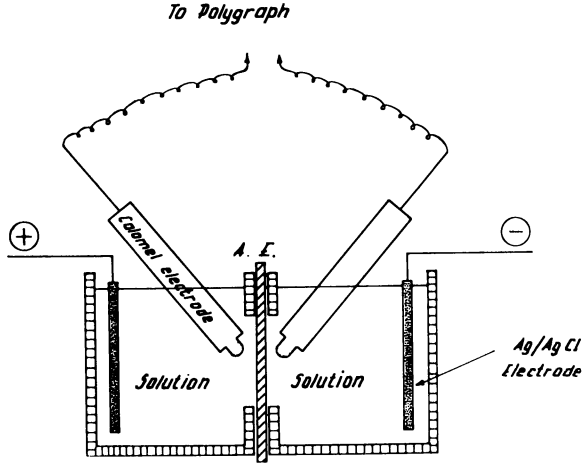

Figure 2. Polarization voltage measurement

concentration buildup near the membrane surfaces—i.e., the concentration profiles before the steady state is reached—and to take remedial steps against too high concentrations prevailing for too long periods.

The theoretical and laboratory polarization studies have been concerned mainly with relatively simple systems containing only one membrane and a solution of potassium or sodium chloride. The experimental arrangement is shown in Figure 2 (9). Current from a constant current source was passed for a specified period between two large silver–silver chloride electrodes placed in two compartments separated by an anion exchange membrane. The potential difference between two calomel electrodes placed about 1 mm. from the two membrane surfaces was measured by a Polygraph, Model 5 (Grass Co.), which records changes of voltage with a response time of the order of 0.1 second.

The solutions were 0.01*N* KCl or 0.01*N* NaCl. The membrane was supplied by T.N.O., The Hague, Netherlands. Its exposed area was about 1 sq. cm. and the current density in the different experiments was varied up to 25 ma. per sq. cm. The experiments were carried out at room temperature without stirring. Under these conditions concentration polarization and water splitting may be expected to occur to a larger extent and hence be more readily observed than in a flow compartment of an electrodialysis stack.

The results of a typical experiment with 0.01*N* KCl solutions in both compartments and a current density of 5 ma. per sq. cm. are shown in Figure 3. The electrical potential drop between the calomel electrodes rises to a maximum voltage, then drops slowly and reaches a constant value, the working voltage. When the current is shut off, the potential difference does not drop to zero immediately. A certain residual voltage remains, which decreases slowly. The time necessary for the residual voltage to disappear is called the decay time.

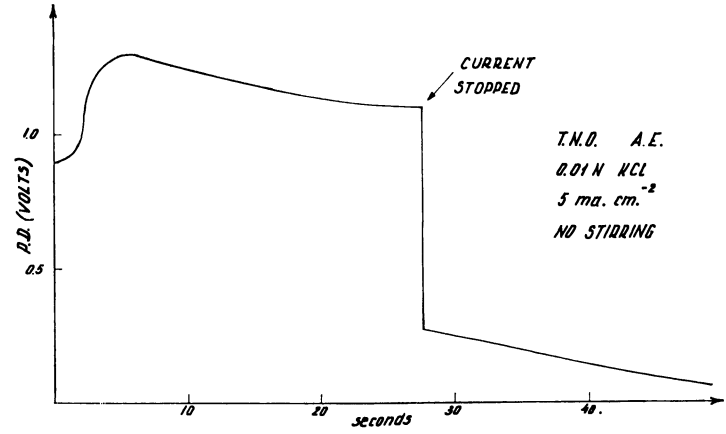

Figure 3. Electric potential drop across membrane vs. time
Anion exchange membrane (T.N.O., The Hague, Netherlands)
Solution 0.01 N KCl. Current density 5 ma. per sq. cm. No stirring.
Experiment carried out in apparatus shown in Figure 2

Both the residual voltage and the decay time provide some indication of the degree of polarization. If the current is stopped at an earlier stage, the residual voltage and the decay time are smaller, as shown in Figure 4. In these experiments it took almost 30 seconds to reach a constant residual voltage and the decay time had not reached a maximum even after this period.

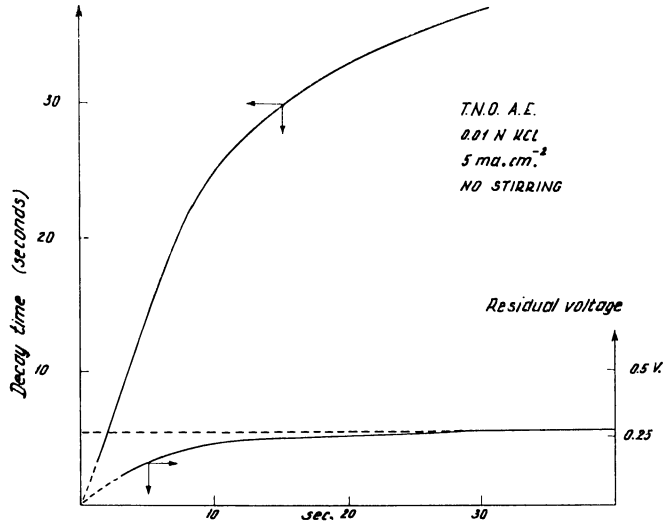

Figure 4. Decay time and residual voltage vs. current time
Materials and conditions as described in Figure 3

Experiments at higher current densities and also with 0.01*N* NaCl solutions showed qualitatively similar results, although the actual values of the potential drop, the time needed to reach the maximum voltage, the residual voltage, and the decay time were different.

To explain these phenomena, it is necessary to consider the transient solutions of the ion flux equations for constant current. For simplicity we assume perfect solution laws (ion activity coefficients unity), a completely anion-selective membrane (transport number of anions in the membrane unity), and constant temperature, and neglect electro-osmotic water transport. We also assume linear geometry and a stationary diffusion layer of thickness δ close to the membrane, beyond which the concentration remains essentially constant. Convection in the diffusion layer (2–4) is assumed to be negligible.

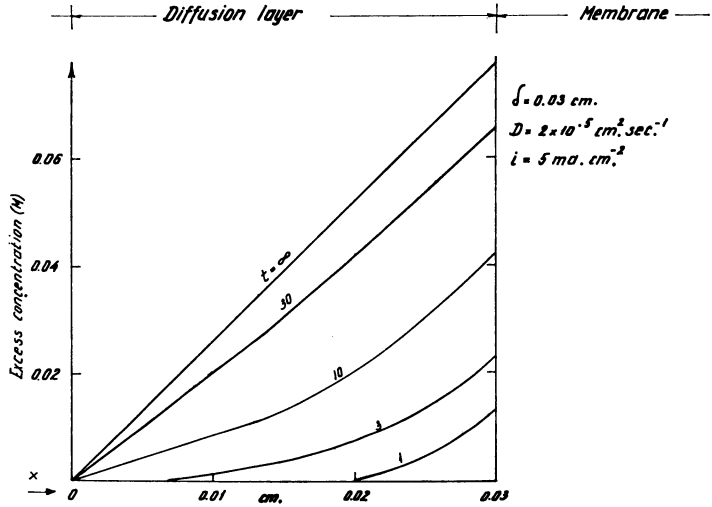

Figure 5. Concentration profile in boundary layer

For each ion there exists a mass balance equation of the form

$$-\frac{\partial \phi}{\partial x} = \frac{\partial c}{\partial t} \tag{1}$$

where Φ is the ion flux (moles per sq. cm. per second), c is the concentration (moles per cc.), x is the distance from the solution-diffusion layer boundary (cm.), and t is the time (seconds).

The basic flux equation for each ion in the solution is

$$\Phi = -D_i \left(\frac{\partial c}{\partial x} + \frac{zF}{RT} c \frac{\partial E}{\partial x} \right) \tag{2}$$

where D_i is the ionic diffusion coefficient (sq. cm. per second), E the electric potential (volt), and z the ion valence (positive for cations, negative for anions). F is Faraday's constant (coulombs per mole), R the gas constant (watt sec. mole^{-1} degree^{-1}), and T the absolute temperature (*13*).

Combining Equations 1 and 2 for cations (subscript$_+$) and anions (subscript$_-$), we obtain:

$$\frac{\partial^2 c_+}{\partial x^2} + \frac{F}{RT} \frac{\partial}{\partial x} \left(c_+ \frac{\partial E}{\partial x} \right) - \frac{1}{D_+} \frac{\partial c_+}{\partial t} = 0 \tag{3}$$

$$\frac{\partial^2 c_-}{\partial x^2} - \frac{F}{RT} \frac{\partial}{\partial x} \left(c_- \frac{\partial E}{\partial x} \right) - \frac{1}{D_-} \frac{\partial c_-}{\partial t} = 0 \tag{4}$$

Because of electroneutrality the following relation holds at any time and place in the solution:

$$c_+ = c_- = c \tag{5}$$

where c is the electrolyte concentration (moles per cc.).

Since we know the flux of anions, $\Phi = i/F$ in the membrane, it is convenient to consider Equation 4 only, which refers to the anions (i is the current density, amperes per sq. cm.) In the case of electrolytes like KCl, in whose aqueous solutions there is no diffusion potential, the second term in this equation is zero, for the current is, by Ohm's law, the product of the potential gradient, $\partial E/\partial x$ and the conductance (mho). The latter, in turn, is assumed to be proportional to the concentration, c. Since the current is the same at any x, so is the product, $c\ \partial E/\partial x$, and hence the second term in Equation 4 is zero.

Thus for KCl solutions, Equation 4 reduces to

$$\frac{\partial^2 c}{\partial x^2} - \frac{1}{D_-} \frac{\partial c}{\partial t} = 0 \tag{6}$$

Here, the ionic diffusion coefficient of Cl^-, D_-, is equal to the ionic diffusion coefficient of K^+, D_+, and hence to the electrolyte diffusion coefficient, D of KCl.

The boundary conditions for the solution of Equation 6 are

$$\text{At } x = \delta,\ \Phi = -i/F \tag{7}$$

The negative sign results because the (negative) ion current flows opposite to the (positive) electric current.

$$\text{At } x = 0,\ c = c_0 \text{ (a constant)} \tag{8}$$

These boundary conditions prevail at any time.

Moreover, we assume that the solution concentration is uniform at the start:

$$\text{At } t = 0,\ c = c_0 \text{ for any } x \tag{9}$$

This problem is analogous to the problem of heat flow in a slab of thermal conductivity κ, with constant temperature at $x = 0$ and constant heat flux, F_0, at $x = \delta$. The solution of this problem has been published, but seems to have received less attention (*6, 7*) than the solution for the boundary conditions:

$$\text{At } x = \infty, \text{ temp.} = 0; \text{ at } x = 0, F_0 = \text{const.} \tag{10}$$

which leads to different temperature gradients or concentration profiles.

If we write the ionic diffusion coefficient, D_-, instead of the thermal conductivity, κ (sq. cm. per second), concentrations instead of temperatures, and $-\Phi/D_-$ instead of the ratio F_0/κ of the heat flux, F_0, (cal. per sq. cm. per second) at the boundary $x = \delta$ and the thermal conductivity κ, of the slab (cal. cm.$^{-1}$ deg.$^{-1}$ sec.$^{-1}$), the heat flow equation is transformed into the ion flow equation in the boundary layer:

$$c - c_0 = \frac{2\Phi_-}{D}\sqrt{Dt}\sum_{n=0}^{\infty}(-1)^n\left[\text{ierfc}\,\frac{(2n+1)\delta - x}{2\sqrt{Dt}} - \text{ierfc}\,\frac{(2n+1)\delta + x}{2\sqrt{Dt}}\right] \tag{11}$$

where ierfc x is defined as

$$\text{ierfc}\,x = \int_x^{\infty}(1 - \text{crf}\,\mu)\mathrm{d}\mu \tag{12}$$

and erf designates the error function (*5*).

The calculated concentration profiles in a KCl solution–anion exchange membrane boundary layer at different times after the start of a constant current of density 5 ma. per sq. cm. are plotted in Figure 5. The diffusion coefficient of KCl in the solution was taken as 2.0×10^{-5} sq. cm. per second and the thickness of the diffusion layer as 0.03 cm.

It is seen that the electrolyte concentration in the vicinity of the membrane increases gradually. The concentration change spreads into the whole diffusion layer until a linear concentration gradient is obtained. It is important that, for the conditions chosen here, this transient stage takes more than 10 seconds.

The concentration profile on the other side of the membrane is of exactly the opposite sign. It is obtained by turning the graph (Figure 5) 180° around both the x and the concentration axes. Instead of excess concentration, we have a concentration depletion on that side, which can, of course, not be larger than the original concentration. The electrolyte concentration close to the membrane surface may approach zero before a constant concentration profile with linear concentration gradient is reached. (In the case described in Figure 5 this will be true for KCl solutions less than 0.078*N*.) If i and δ remain constant, water splitting will then begin and a rather complicated concentration distribution in the membrane and solution will result.

The results of the experiments described in Figures 3 and 4 can be interpreted in terms of these findings. The total potential difference measured between the calomel electrodes is the sum of the *IR* drop and the membrane potential, both of which increase with the buildup and depletion of the electrolyte concentration on the two faces of the membrane, respectively (I = current, R = resistance). Hence the total potential difference (Figure 3) and the residual voltage, which contains the membrane potential, rise initially. When the ions produced by water splitting account for an appreciable part of the current, the *IR* drop decreases because of the high mobility of H^+ and OH^- ions in the solution

and the membrane. The sum of these opposing effects leads to a maximum in the curve of potential difference *vs.* time.

Since the source of the scale is in the diffusion layer and the development of a stable concentration gradient in this layer takes considerable time, it seemed practically feasible to upset the concentration buildup by reversing the current. At first sight it might seem that one would have to reverse polarity for a period about equal to the period of current passage in the forward direction, for the complete elimination of the excess concentrations should take about as long as their buildup. However, it was surprisingly found that even brief reverse pulses have a marked effect on scale formation, provided they occur at short intervals. It seems that supersaturation can exist for a certain period in the boundary layer and if, as a result of the pulses, it is periodically and temporarily relieved, calcium carbonate precipitation on the membranes is greatly reduced (*10*). Precipitation occurs then as a sludge in the brine compartment. This sludge is largely carried along with the brine, although some of this loose material can get caught in the spacer meshwork.

The pulse method of scale control has undergone extensive pilot plant tests with very encouraging results. The analysis of the raw water which was made up synthetically to resemble that of a typical Negev brackish water well is shown in Table I. This water contains much temporary and permanent hardness. In the following, data are reported for the first long run. The pilot plant program is continuing and since this run was finished, additional work has been in progress. A summary of the results will be available when additional runs have been completed.

Table I. Composition of Yotvata (Negev) Water

(P.p.m.)

Na^+	308	SO_4^{-2}	803
Ca^{+2}	254	Cl^-	600
Mg^{+2}	146	HCO_3^-	250
	Total dissolved solids	2388	
	pH	7.58	

The main purpose of the first series of runs was to determine the effectiveness of the pulse system for scale reduction, and determination of the shutdown time. This run lasted for 1560 hours and the average reduction of salinity for 13 weeks was 1762 p.p.m. The production rate of the pilot plant was 5200 gallons per day. Almost no adherent scale deposited on the membrane. However, part of the soft sludge was held back by the expanded plastic spacer material and caused a slow increase of voltage. When the over-all voltage reached 125% of the mean operating value, reversed polarity was applied for 1 or 2 hours. This procedure was adopted in addition to the short cycle pulse system.

From these preliminary results it may be concluded that the pulse treatment represents a distinct advance, since it reduces the problem of a hard adherent scale to a question of removal of a soft sludge. It is believed that this latter difficulty can be resolved by adequate spacer design.

Ion and Water Transport through Membranes. The quantitative interpretation of experiments on the influence of pulses is complicated by the fact that even in originally pure KCl solutions, there are four ionic species in the polarization layers—viz., K^+, Cl^-, H^+, and OH^-. In natural waters the number of ionic species is still larger. Since there are no experimental methods to determine the

concentrations of each species at any time and any point in the diffusion layer, one might wish to compute these concentrations from the flux equations using appropriate boundary conditions; at least for ions that affect scale formation—e.g., Ca^{+2}, CO_3^{-2}, OH^-, and HCO_3^-. However, many basic data on the transport of these ions in membranes are still lacking.

A start has been made in determining these data by measuring the ion and water transport in various commercial anion exchange membranes separating solutions of sodium chloride and sodium bicarbonate, either separately or mixed (*1*). Silver–silver chloride electrodes were used for the passage of a constant current, while the solutions were stirred vigorously. The membrane surface area was about 10 sq. cm. The total solution concentration was 0.05*N*, but the ratio of the concentrations of chloride and bicarbonate in the cathode compartment was varied while the anode compartment contained only 0.05*N* NaCl solution. The concentrations changed somewhat during the experiments. The current densities used were 4 and 8 ma. per sq. cm. and there was no difference between the results at these two current densities (Table II).

Table II. Ion and Water Transport through Three Commercial Anion Exchange Membranes (*1*)

Membrane	*Permutit 3148*	*AMF 101*	*Asahi Anionic*
Manufacturer	Permutit, Inc., New York, N. Y.	American Machine and Foundry Co., Springdale, Conn.	Asahi Chemical Co., Tokyo, Japan
Transport number of chloride[a]	0.66	0.71	0.64
Water content, wet, chloride form			
Weight %	17	17	25
Per exchange group	15–16	6–7	13–14
Electro-osmotic water transport, moles H_2O			
With chloride ion	6.5	3	4
With bicarbonate ion	9.5	5.7	6.5

[a] When solution in cathode compartment is 0.025*N* with respect to NaCl and 0.025 with respect to $NaHCO_3$.

Over the whole range of variation of the Cl^-: HCO_3^- ratio in the cathode compartment, the transport number of chloride was somewhat higher than the molar ratio of chloride in the solution. In other words, in all the three membranes tested chloride ion transport is favored over bicarbonate ion transport. This fact is not unrelated to the data on water transport. The electro-osmotic water transport with chloride ions is smaller than with bicarbonate ions. It is known that, other factors being equal, low water transport and high mobility of ions in a membrane–as measured, for instance, by electrical conductivity–are correlated (*13, 16*).

Freezing–Evaporation

This method has been under intensive pilot plant study for a number of years. The pilot plant, with a designed capacity of about 6000 gallons per day, was planned by A. Zarchin and built and operated with funds of the Israel Ministry of Development. The results of the pilot runs encouraged continuation and extension of this work. In 1959, Fairbanks Morse Co., a subsidiary of Fairbanks

Whitney Corp., New York, entered into a partnership with the Government of Israel to develop the process and the special equipment needed for it. As a result of pilot experiments, it was decided to build a moderately sized plant for the Red Sea port of Eilat, where the only water resources are sea water or highly brackish ground water, the latter in limited quantities. This plant is to have a total capacity of 250,000 gallons of fresh water per day and is to consist of four units, the first of which has been completed.

The process utilizes the direct freezing method, in which a portion of the sea water is frozen by self-evaporation without use of an additional refrigerant (Figure 6). The ice is separated from the brine and the vapor is adiabatically compressed and brought in contact with the ice, producing fresh water. The brine and fresh water are withdrawn through separate conduits in a heat exchanger which precools the incoming raw water. During the last few years, several modifications of the process have been described in periodicals and the patent literature, summarized by Spiegler (*12*). The latent heat of fusion of ice at 0° C. is 143.5 B.t.u. per pound (79.71 cal. per gram) and the heat of vaporization 1072 B.t.u. per pound (595.4 cal. per gram)—i.e., about 7.5 times higher. The freezing temperature depends on the concentration of the brine, but at any practical freezing temperature the evaporation of 1 pound of water causes the freezing of over 7 pounds of ice. When the compressed vapor condenses on the ice, in the melting section, it gives up its latent heat of vaporization to the ice, in addition to the heat of adiabatic compression. Hence more heat than is required to melt the ice isothermally is exchanged and some auxiliary refrigeration is required to maintain the cycle. There is also a purge system not shown in the diagram.

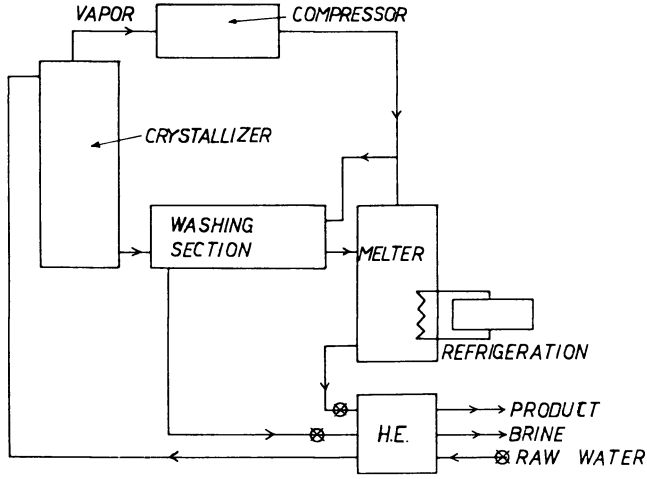

Figure 6. Block diagram of freezing evaporation pilot plant

The major engineering problems are the production of large, readily washable crystals, development of an efficient washing process, and construction of a suitable compressor for the very large volumes of low pressure water vapor that have to be transferred from the crystallizing to the melting section of the apparatus. The degree of success of the present engineering solution will be accurately known only when a full set of operating data of the units of the present plant is available.

Some data from a pilot plant series covering a wide salinity range, listed in Table III, illustrate the approximate scope of the pilot plant development work. The experiment described is neither one of the most nor of the least successful. The units for the Eilat plant were designed by combining the conclusions from the data of the runs in the Israeli pilot plant with the experience of the American partner in component and process design in other fields of chemical engineering.

Table III. Operating Data for One Run of Freezing-Evaporation Pilot Plant

Daily capacity, gal.	6000	Crystallizer temperature, ° F.	28.4
Raw water salinity, p.p.m.	28,000	Crystallizer pressure, mm. Hg	3.9
Product salinity, p.p.m.	450	Compression,[b] mm. Hg	1.3
Brine salinity, p.p.m.	32,000[a]	Wash water, % of product	8

[a] At entrance to rinsing section.
[b] Differential pressure across compressor.

In the run described slightly diluted sea water was used. Its salinity was reduced from 28,000 to 450 p.p.m. with a loss of 8% of product for rinse water. It would be very interesting to have reliable estimates for the energy consumption of the process, but the pilot plant energy requirements would lead to grossly exaggerated results, because the components were overdesigned. Meaningful experimental figures can be reported only when full sets of data on the Eilat units are available. The company hopes to release final figures based on the full operation of the commercial plant in the near future.

Literature Cited

(1) Block, M., M.Sc. thesis, Department of Chemistry, Technion-Israel Institute of Technology, Haifa, 1961.
(2) Cooke, B. A., *Electrochim. Acta* **3,** 307 (1961).
(3) *Ibid.*, **4,** 179 (1961).
(4) *Ibid.*, **5,** 216 (1961).
(5) Carslaw, H. S., Jaeger, J. C., "Conduction of Heat in Solids," 2nd ed., p. 113, Oxford University Press, London, 1959.
(6) Delahay, P., "New Instrumental Methods in Electrochemistry," Interscience, New York, 1954.
(7) Dewhurst, D. J., *Trans. Faraday Soc.* **56,** 599 (1960).
(8) Forgacs, C., *Nature* **190,** 339 (1961).
(9) Forgacs, C., private communication.
(10) Israel, State of, Israel Patent **13,242** (March 23, 1961).
(11) Langelier, W. F., Caldwell, D. H., Lawrence, W. B., *Ind. Eng. Chem.* **42,** 126 (1950).
(12) Spiegler, K. S., "Salt Water Purification," Wiley, New York, 1962.
(13) Spiegler, K. S., *Trans. Faraday Soc.* **54,** 1408 (1958).
(14) Spiegler, K. S., Juda, W., Carron, M., *J. Am. Water Works Assoc.* **44,** 80 (1952).
(15) Wilson, J. R., ed., "Demineralization by Electrodialysis," Butterworth, London, 1960.
(16) Winger, A. G., Ferguson, R., Kunin, R., *J. Phys. Chem.* **60,** 556 (1956).
(17) Zarchin, A., Brit. Patent **806,727** (Dec. 31, 1958).

RECEIVED May 14, 1962.

14

Properties of the Hydrates of Fluorocarbons 142b and 12B1

Comparison of Six Agents for Use in the Hydrate Process

FREDERICK A. BRIGGS[1] **and ALLEN J. BARDUHN**
Department of Chemical Engineering, Syracuse University, Syracuse, N. Y.

Thermodynamic data on the systems F-142b (CH_3CClF_2)–H_2O–NaCl and F-12B1 ($CClF_2Br$)–H_2O–NaCl include pressure-temperature phase diagrams, heats of formation, hydrate compositions, and the temperature depressions due to NaCl. Both hydrating agents have properties which appear useful in the hydrate process for desalting sea water. Six hydrating agents are compared by calculating the energy requirements and total heat exchanger surface required for each process when producing 1,000,000 gallons per day of fresh water. The agents considered are propane, F-21($CHCl_2F$), F-12B1, F-142b, methyl bromide, and F-31(CH_2ClF) in order of increasing critical formation temperature. High temperature hydrating agents have a distinct advantage with respect to energy requirements and capital costs of heat exchangers. Energy requirements lower than 20 kw.-hr. per 1000 gallons appear easily possible.

The hydrate process for demineralizing sea water has been described and discussed in several publications (*2*, *3*, *6*). The development of the process is in its beginning stages, the first such work having been started at Syracuse University and at the Koppers Co. in 1959. Among the problems needing solution is that of choosing the most economical hydrating agent. To make such a decision requires a rather large amount of information on the properties of each possible agent and its hydrate. A preliminary screening can be made, however, on the basis of the hydrate critical decomposition temperature and pressure only, since a lower temperature limit of about 5° C. can be set, so that the process will have a significant advantage over freezing and an upper pressure limit of around 5 to 6 atm. can be set to keep the process equipment cost at a reasonable value. These are not firm limits, but they exclude many substances.

[1] Present address, E. I. du Pont de Nemours & Co., Inc., Waynesboro, Va.

On the basis of the pressure and temperature limits thus specified the number of hydrating agents which have any reasonable chance of becoming important can be reduced to about 12, shown in Table I. Further work has been reported on F-31, methyl bromide, and F-21 (2) and on propane (6); and this paper presents thermodynamic data on F-142b and F-12B1. Except for chlorine, similar data can probably be predicted for the remaining six agents with sufficient accuracy for economic evaluation studies (1).

Table I. Promising Hydrating Agents for Desalination

	Temperature		*Pressure*	
Hydrating Agent	*° C.*	*° F.*	*Mm.*	*P.s.i.g.*
Chlorine	28.7	84	4570	74
Methyl chloride	21	70		(60) est.
F-31(CH_2ClF)	17.9	64	2147	27
F-152a(CH_3CHF_2)	15.3	60	3382	51
Methyl bromide	14.7	58	1151	8
F-142b(CH_3CClF_2)	13.1	56	1743	19
F-12(CCl_2F_2)	12.1	54	3435	52
F-12B1($CClBrF_2$)	9.9	50	1272	10
F-22B1($CHBrF_2$)	9.9	50	2012	24
F-21($CHCl_2F$)	8.7	48	760	0
F-11(CCl_3F)	8.0	46	419	−7
Propane	5.7	42	4141	65

It is not impossible, but it seems improbable, that any new hydrating agents will be discovered that are superior to those listed in Table I, since a rather systematic search has been made among the hydrocarbons and their halogenated derivatives, and no other class of compounds seems as likely to form hydrates and simultaneously to have the properties useful in desalting (1, 3).

Many properties other than those presented will determine the eventual worth of an agent in a desalting process. Among these are the stability in water, the solubility in water and salt solutions, the rates of nucleation and growth and the nature of the hydrate crystals, and the cost of the agent.

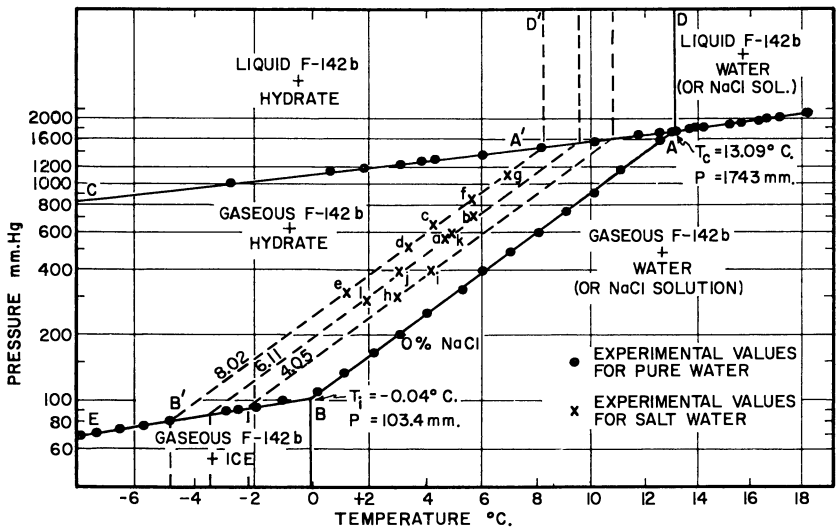

Figure 1. Experimental phase diagram for F-142b–water–NaCl system

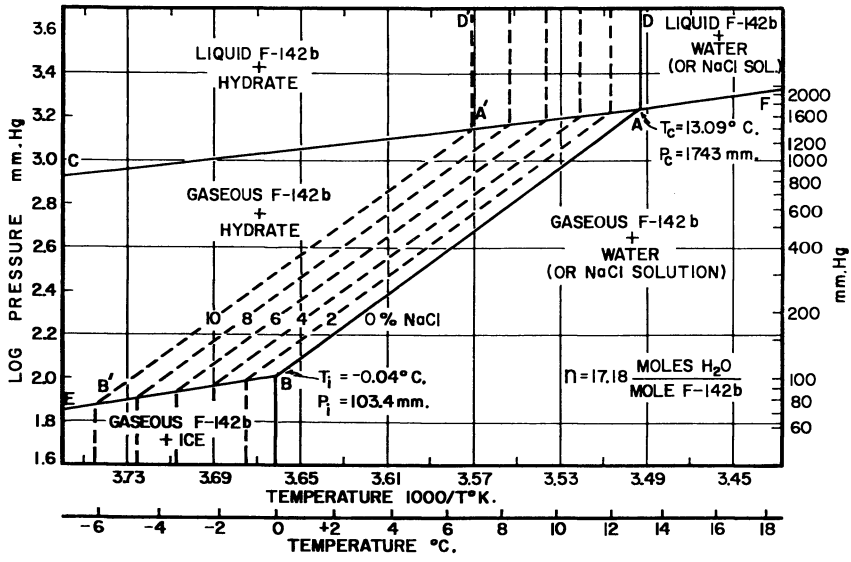

Figure 2. Calculated phase diagram for F-142b–water–NaCl system

Hydrates of F-142b and F-12B1

The pressure-temperature phase diagrams for these two substances with H_2O and NaCl are presented in Figures 1 to 4 and the data are tabulated in Tables II to V. From these data have been calculated heats of formation, hydrate compositions, and the depression of the formation temperature due to NaCl. The important measured and derived quantities for both systems are summarized in Table VI.

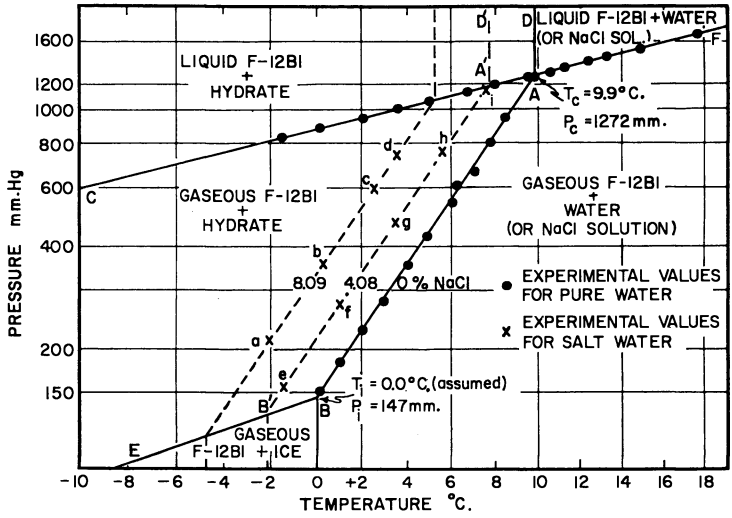

Figure 3. Experimental phase diagram for F-12B1–water–NaCl system

Table II. Experimental Phase Equilibrium Data for the System F-142b–Water

CH_3CClF_2 (Gas), Water Hydrate		CH_3CClF_2 (Gas + Liq.), Hydrate	
t°, C.	P, mm.	t, °C.	P, mm.
		Below t_c	
0.19	110.5	−2.80	1000.5
1.09	135.4	0.63	1148.0
2.12	167.7	1.80	1181.5
3.07	203	1.83	1184.5
4.00	252.8	3.06	1234
5.26	329.6	3.82	1267
6.00	397.8	4.38	1290
7.00	485.5	6.00	1367
8.03	599.4	8.10	1459.5
9.03	746.3	10.10	1569.5
10.09	911.2	11.71	1679
11.06	1168	12.50	1720
12.51	1588	12.95	1736
		Above t_c	
CH_3CClF_2 (Gas), Ice, Hydrate		13.10	1748
		13.60	1779
−7.78	69.2	13.87	1816
−7.24	71.2	14.17	1830
−5.73	76.6	15.15	1904
−4.85	82.5	15.18	1891
−2.98	89.6	15.62	1906
−2.56	91.1	16.25	1967
−1.96	93.1	16.59	2004
−1.04	101.5	17.10	2031.5
		18.11	2105
		18.17	2101

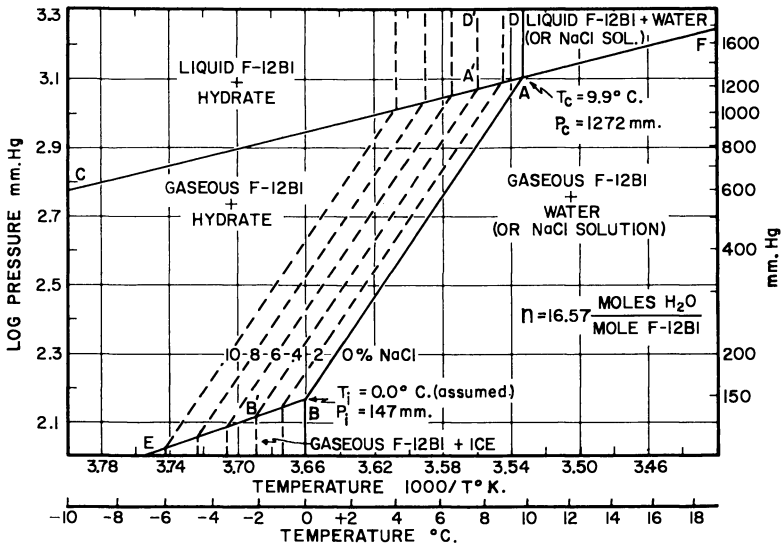

Figure 4. Calculated phase diagram for F-12B1–water–NaCl system

Figures 1 and 3 show the original experimental data points and Figures 2 and 4 are calculated from the data on heats of formation and hydrate compositions and are so constructed as to be more useful in engineering design.

The experimental apparatus and techniques have been described (*4*, *5*, *7*), as have the methods of calculation (*2*).

Table III. Experimental Phase Equilibrium Data for the System F-142b–Water–Sodium Chloride

Point (Fig. 1)	*W, Wt.% NaCl*	*t, ° C.*	P_1[a]	P_2[b] *(No Salt)*	*n*[c]
a	6.12	4.66	559.4	293.0	17.58
b	6.05	5.69	706.9	366.6	18.01
c	8.13	4.24	635.4	267.4	17.14
d	8.11	3.34	515.5	219.4	17.03
e	8.01	1.22	306.0	137.1	16.29
f	7.98	5.58	835.9	357.9	17.06
g	7.86	6.90	1082.0	475.8	16.72
h	3.99	2.95	300.9	201.4	17.32
i	4.11	4.15	398.1	262.1	17.38
j	6.19	2.98	396.3	202.7	17.96
k	6.25	4.91	587.2	309.5	16.99
l	5.93	1.88	286.1	158.8	16.64
					Av. 17.18 ±0.40 (av. dev.)

[a] P_1. Experimental equilibrium pressure for given temp. and % NaCl in mm.
[b] P_2. Calculated pressure for given temp. but with no salt present in mm. See 5a, Table VI.
[c] *n*. Calculated moles of water per mole of agent in hydrate using P_1 and P_2 with Miller and Strong equations (*2*).

Table IV. Experimental Phase Equilibrium Data for the System F–12B1–Water

$CClBrF_2$(Gas), Water, Hydrate		*$CClBrF_2$(Gas + Liq.), Hydrate*	
t, ° C.	*P, mm.*	*t, ° C.*	*P, mm.*
0.08	153.3	*Below t_c*	
1.02	186.1	−1.51	834.3
2.02	229.9	0.13	890.4
2.95	278.8	2.04	947.3
4.06	354.9	3.60	1033.0
4.89	431.8	5.03	1067.5
6.05	541.2	6.77	1134.0
6.50	611.7	8.03	1185.5
7.09	667.3	9.59	1251.0
8.49	955.2	*Above t_c*	
9.73	1267	10.60	1295.5
		11.27	1334.0
		12.40	1387.0
		13.30	1434.5
		14.93	1513.5
		17.74	1663.0

Table V. Experimental Phase Equilibrium Data for the System F-12B1–Water–Sodium Chloride

Point (Fig. 3)	*W, Wt.% NaCl*	*t, ° C.*	P_1	P_2*(No Salt)*	*n*
a	8.14	−2.04	214.1	92.4	16.82
b	8.12	0.28	355.9	156.6	16.44
c	8.09	2.55	594.8	260.0	16.49
d	8.02	3.55	742.2	324.2	16.63
e	4.15	−1.44	158.3	106.0	16.72
f	4.11	1.00	271.3	184.1	16.22
g	4.09	3.53	475.3	322.9	16.45
h	4.05	5.65	762.8	513.0	17.03
i	4.01	7.61	1152	782.2	16.32
					Av. 16.57 ± 0.21 (av. dev.)

Table VI. Critical Decomposition Constants, Heat of Reaction, Compositions, and Temperature Depressions Due to Salts for F-142b and F-12B1

(M = agent, W = water, H = hydrate)

		F-142b	*F-12B1*
1.	Hydrate compn., moles H_2O/mole agent, n	17.18	16.57
2.	Critical decompn. temp.		
	° C.	13.09	9.9
	° F.	55.56	49.8
3.	Critical decompn. pressure		
	Mm. Hg	1743	1272
	P.s.i.a.	33.7	24.5
4.	Invariant point with ice		
	Temp., ° C.	−0.04	0.0 (assumed)
	Pressure, mm. Hg	103.4	147
5.	Constants in equation		
	log $P_{mm} = A\text{-}B/(t + 273.16)$		
	a. M(g) + nW(1) = H (Figs. 1 and 3, AB)		
	A	28.78541	28.95234
	B	7311.8	7316.6
	b. M(g) + H = M(1) + H (Figs. 1 and 3, AC)		
	A	7.33942	7.48253
	B	1173.0	1239.3
	c. M(g) + nW (ice) = H (Fig. 1, BE)		
	A	8.00995	...
	B	1637.5	...
6.	Compressibility factor of M(g) at crit. temp. and press., Z	0.930	0.952
7.	Heats of reaction ($-\Delta H$ = 4.574BZ)		
	a. M(g) + nW(1) = H(kcal./mole)	31.11	31.86
	b. M(g) + H = M(1) + H(kcal./mole)	4.99	5.40
	c. M(g) + nW(ice) = H(kcal./mole)	7.492	...
	d. M(1) + nW(1) = H(B.t.u./lb. H_2O)	152	159.7
8.	Depression of critical decompn. temp. by NaCl, ° C.		
	2% (by weight)	1.10	1.04
	4%	2.27	2.15
	6%	3.49	3.32
	8%	4.77	4.54
	10%	6.22	5.92
9.	Depression of critical decompn. temp. by 6% sea salt solution, ° F.	5.82	5.53
10.	Hydrate reactor operating conditions allowing 3° F. for driving force in 6% sea salt solution		
	Temp., ° F.	46.74	41.3
	Pressure, p.s.i.g.	13.9	6.1

Calculated Energy and Heat Exchanger Requirements for Hydrate Processes

Adequate data are now available to estimate the energy requirements for converting sea water to fresh water by the hydrate process, using the hydrating agents F-21, F-12B1, 142b, methyl bromide, and F-31. In addition, calculations have been made for comparison purposes on the propane hydrate process and on the direct contact freezing process, using n-butane as the refrigerant.

Energy requirements are calculated for the primary and secondary compressors and estimated for the feed, recycle, and cooling water pumps for a plant producing 1,000,000 gallons of fresh water per day. The areas of the feed-product exchangers and secondary refrigerant condensers are also calculated.

The general flowsheet used is shown in Figure 5. Any work or heat required for stripping of products or deaerating of feed is presumed small and is not considered. Power for lighting, various small pumps, instruments, and other miscellaneous uses is ignored also. Energy requirements for agitation in the reactor beyond that supplied by the brine recirculation would also increase the given figures.

The assumptions used to make the calculations are listed in Table VII.

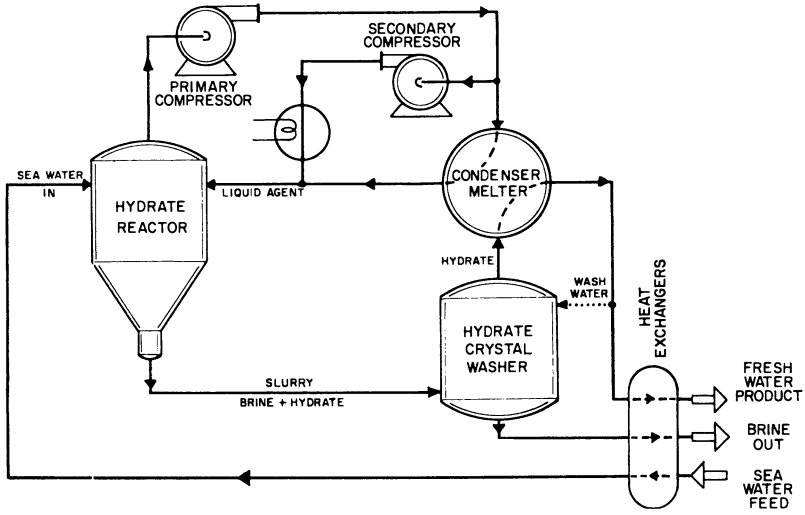

Figure 5. Flowsheet of hydrate process for desalting sea water

The results of the calculations are summarized in Table VIII, in which the hydrating agents are arranged in order of increasing critical decomposition temperatures. The following items in this summary are worthy of comment.

1. The energy requirement for the primary compressor is practically independent of the hydrating agent used and averages 700 hp., with a maximum variation of 3%. This is due partly to the identical nature of all reversible heat pumping processes and partly to the fact that the driving forces in the reactor and melter have been assumed at 3° and 2° F. for all agents. The 3° F. driving force in the reactor is based on Koppers' work on propane, and assuming the same value for the other hydrates, may be overly liberal or overly conservative. Without more kinetic data, however, the accuracy of this assumption cannot be judged. The 2° F. driving force in the condenser-melter is based on the work of Carrier and of Blaw-Knox on ice and is probably applicable indiscriminately to hydrates, since the process is physical and not chemical in nature.

2. The work required of the secondary compressor decreases regularly with increasing operating temperature of the reactor. It would be reduced to zero for a hydrate such as chlorine hydrate, for which the reactor would operate above the ambient temperature assumed. If the sea water feed were at about 55° F. no secondary compressor would be needed for F-31, since the excess vapor could be condensed with sea water with no compression.

The amount of heat to be rejected to the atmosphere is fairly constant. It is the work required to pump it to the rejection temperature that decreases with increased operating temperature levels. Thus the secondary refrigerant condenser has a fairly fixed area also.

The work required in this cycle is due mainly to incomplete heat exchange, but a small fraction is due to the work input of the compressors and pump. Heat leakage is negligible, although it has been included.

3. The feed-product heat exchanger areas decrease regularly with increased operating temperature and they may be eliminated completely for F-31. This would represent a very substantial saving in initial plant cost, since these ex-

Table VII. Assumptions Used for Estimating Operating Conditions in Hydrate Process

Sea water feed — 3.5% total salts — Temp. 70° F.

Reactor conditions
- Brine out = 6% salts
- Slurry out = 5% hydrate solids
- Temp. = crit. decompn. temp. − (depress. due to 6% sea salts + 3° F. for driving force)
- Press. = vapor press. of agent at operating temp.

Primary compressor
- Suction press. = reactor press.
- Discharge press. = vapor press. of agent at (crit. decompn. temp. + 2° F.)
- Adiabatic eff. = 80%
- Driver eff. = 90%

Secondary compressor
- Suction press. = critical decompn. press. of hydrate
- Discharge press. = agent vapor press. at 80° F.
- Adiabatic eff. = 80%
- Driver eff. = 90%

Heat exchangers
- Feed *vs.* products
  - Temp. of both products out = 62.5°F. (7.5° F. approach)
  - Over-all heat transfer coefficient = 200 B.t.u./hr. sq. ft.° F.
- Secondary refrig. condenser
  - Over-all heat transfer coefficient = 125 B.t.u./hr. sq. ft.° F.
  - Sea water in at 70° F. and out at 74° F.

Secondary refrig. load
- Heat added to system due to
  - Incomplete feed-product heat exchange
  - All work input to both compressors
  - Work input of recycle brine pumps
  - Heat leakage = 10,000 (75 − $t_{crit.}$), B.t.u./hr. for 1,000,000 gal./day product

Wash water
- Water for ice washing = 5% of net fresh water product

Pumps

All pumps	89% efficiency
All motors	90% efficiency
Recycle pumps	Operating press. difference = 10 p.s.i.
Cooling water pumps	20 hp. per mgd. product
Feed pumps	Operating press. difference = reactor gage press. + 15 psi.
	No allowance made for energy recovery from product streams

changers alone represent 10 to 15% of the initial plant investment for the lower temperature processes.

In the case of F-31, two possibilities for heat exchange between feed and products have been considered. In case I no such exchange is used and in case II heat is exchanged between the feed and brine out only. The fresh water product temperature is too near the feed temperature to exchange heat when a 7.5° F. approach is assumed.

The addition of 1600 sq. feet of feed-brine exchangers reduces the energy required by 7% and the secondary refrigerant condenser area by 29%, for a net decrease in total required exchanger area of 15%.

4. The inlet volumes to the compressors depend mainly on the reactor operating pressures, the high pressure agents giving the lower volumes, since the moles of gas going to each compressor is substantially constant, with a variation of only about 10%.

5. Since the main contribution to the secondary refrigeration cycle load is the incomplete heat exchange between the feed and products, the energy required for this cycle may be varied at the expense of feed-product heat exchanger area.

Table VIII. Calculated Operating Conditions for the Hydrate and Freezing Process Using Various Agents

Basis. 1,000,000 gallons of fresh water product per day

	n-Butane + Ice	*Propane*	*F-21*	*F-12B1*	*F-142b*	*Methyl Bromide*	*F-31*	
							Case I, no feed-prod. exchg.	*Case II, feed-brine exchg. only*
Critical decompn.								
Temp., °F.	32	42.3	47.6	49.8	55.6	58.5	64.2	64.2
Press., p.s.i.g.	0.3	65.3	0.0	9.9	19.3	7.6	26.8	26.8
Reactor conditions								
Temp., °F.	23	33.2	39.0	41.4	46.8	49.4	56.1	56.1
Press., p.s.i.g.	−2.3	55.0	−2.5	6.1	13.9	4.0	21.0	21.0
Feed-product exchanger areas, sq. ft.								
Brine	10,750	8,200	6,700	5,910	4,400	3,790	0	1,600
Water	7,100	4,950	3,580	3,100	1,675	910	0	0
Total	17,850	13,150	10,280	9,010	6,075	4,700	0	1,600
Primary compressor								
Horsepower (80% eff.)	677	715	708	725	720	710	704	680
Inlet volume, cu. ft./min.	43,000	10,000	45,600	29,300	21,600	33,000	18,600	17,900
Secondary compressor								
Horsepower (80% eff.)	448	363	284	263	223	183	166	118
Inlet volume, cu. ft./min.	5,710	1,345	5,200	3,430	2,580	3,500	2,430	1,730
Secondary refrig. cond. heat load, M^2B.t.u./hr.	9.2	9.1	8.85	8.80	8.65	9.1	10.7	7.6
Area, sq. ft.	9,350	9,300	9,000	9,000	8,800	9,300	10,900	7,700
Major pumps, total hp.	111	184	140	169	158	176	177	176
Compressor and pump, energy totals								
Horsepower	1,236	1,262	1,132	1,157	1,101	1,069	1,047	974
Kw.-hr./1000 gal. (incl. 90% driver eff.)	24.6	25.1	22.5	23.0	21.9	21.2	20.8	19.4

A 7.5° F. approach temperature was assumed for these calculations. A 5° F. approach would increase the exchanger area and reduce the secondary compressor load, and a 10° F. approach would do the opposite. An economic balance will eventually determine how best to apportion these variables.

With direct contact heat exchangers in which a recirculating immiscible fluid is alternately exchanged against a hot stream and a cold stream, it appears that temperature differences may be reduced to about 3° F. economically. In the hydrate process the obvious immiscible agent to use is the hydrating agent. In the exchange between the feed water and cold agent the feed will be cooled and simultaneously saturated with agent. This may reduce the required reactor volume somewhat. In the exchange between cold products and warm agent, little agent will dissolve, since the products will be saturated on entering these exchangers. Such systems have been studied by Woodward (9).

6. The total energy requirement for pumps and compressors decreases fairly regularly from 25.1 kw.-hr. per 1000 gallons for propane hydrate to 19.4 kw.-hr. per 1000 gallons for F-31 hydrate, a reduction of 23%. The advantage of the F-31 hydrate process over the freezing process is 21% in this regard.

By reducing the approach temperatures in the heat exchangers and/or reducing the feed water temperature below 70° F. the energy requirement for F-31 hydrate process can be reduced to 17 kw.-hr. per 1000 gallons.

The energy requirements may be expressed in units other than kilowatt-hours per 1000 gallons and it is interesting to convert these figures to foot-pounds of energy per pound of water, which is numerically equal to the number of feet that water can be elevated vertically with 100% efficiency. The conversion factor is 1 kw.-hr. per 1000 gallons = 319 foot elevation. Thus a requirement of 20 kw.-hr. for making 1000 gallons of fresh water from the sea is equivalent to raising the water at least 6380 feet vertically. This gives a visual comparison of the energy required to desalt sea water with that required to pump it uphill, and tells us that from the energy standpoint it is equally disadvantageous to be without fresh water at sea level and to have fresh water available several thousand feet below you.

7. The total heat exchange surface decreases regularly from 22,450 sq. feet for propane to 9300 for F-31 hydrate, a reduction of 58%. The advantage of F-31 over freezing is a 66% reduction of this quantity.

These calculations point out clearly the two main advantages of a high temperature hydrate process over the freezing process or a low temperature hydrate process—namely, the substantial reductions possible in both heat exchanger investment and energy requirements. The energy advantage has been commented on by Wiegandt (8).

Acknowledgment

This research was sponsored by the Office of Saline Water, to which appreciation is expressed. Theodore Kulpa and Richard Collette made most of the calculations for Table VIII.

Literature Cited

(1) Barduhn, A. J., Hu, Y. C., Briggs, F. A., Ann. Rept. 2 to Office of Saline Water (December 1961).
(2) Barduhn, A. J. Towlson, H. E., Hu, Y. C., *A.I.Ch.E. J.* **8**, 176–83 (1962).
(3) Barduhn, A. J., Towlson, H. E., Hu, Y. C., Research and Dev. Progr. Rept. 44 to Office of Saline Water (September 1960).
(4) Briggs, F. A., "Gas Hydrates of F-142b and F-12B1," thesis, Syracuse University, 1962.
(5) Hu, Y. C., "Determination of Gas Hydrate Compositions by Thermodynamic Methods," thesis, Syracuse University, 1961.
(6) Knox, W. G., Hess. M., Jones, G. E., Smith, H. B., *Chem. Engr. Progr.* **57**, 66–71 (1961).
(7) Towlson, H. E., "Gas Hydrates," thesis, Syracuse University 1960.
(8) Wiegandt, H. F., Division of Water and Waste Chemistry, 139th Meeting, ACS, St. Louis, Mo., March 1961.
(9) Woodward, T., *Chem. Engr. Progr.* **57**, 52 (1961).

RECEIVED June 21, 1962.